Supporting Information

Aryl Amination Using Soluble Weak Base Enabled by a Water-Assisted Mechanism

Sii Hong Lau,[†] Peng Yu,[†] Liye Chen,[†] Christina B. Madsen-Duggan,[¶] Michael J. Williams,[¶] and Brad P. Carrow [†,*]

[†]*Department of Chemistry, Princeton University, Princeton, NJ 08544, United States*

[¶]*Chemical Process Development, Bristol Myers Squibb, 556 Morris Avenue, Summit, NJ 07902, United States*

*Email: bcarrow@princeton.edu

General Remarks

All reactions were performed inside a dry nitrogen filled glovebox or using standard Schlenk techniques unless otherwise noted. Solvents (tetrahydrofuran, toluene, diethyl ether, dichloromethane, *n*-pentane, *tert*-amyl alcohol (*t*-AmOH), cyclopentyl methyl ether (CPME), and anisole) were purified in a solvent purification system by percolation through neutral alumina under positive pressure of nitrogen or purchased from Millipore Sigma in Sure/Seal® containers. Deuterated solvents (chloroform-d_3, benzene-d_6, tetrahydrofuran-d_8) were stored over 4 Å molecular sieves. All chemicals purchased from commercial suppliers were used as received unless otherwise noted. PAd_3,[1] $Pd(PAd_3)(4\text{-}FC_6H_4)Br$ (**1**),[2] and $[Pd(PAd_3)(4\text{-}FC_6H_4)]^+ BF_4^-$ (**33**)[3] were prepared according to literature. ^1H, ^{13}C (^1H decoupled), $^{19}F\{^1H\}$, and $^{31}P\{^1H\}$ nuclear magnetic resonance spectra (NMR) were obtained on a Bruker Avance III 500 MHz, Bruker NanoBay 400 MHz or Bruker NanoBay 300 MHz spectrometers recorded in ppm (δ), referenced to residual solvent ($CHCl_3$, $CHDCl_2$, etc.).[4] Spin-spin coupling is described as singlet (s), doublet (d), triplet (t), quartet (q), quintet (quint), heptet (hept), broad (br) or multiplet (m); coupling constants (*J*) are reported in Hz. Purity values were utilized from commercial sources or determined via ^1H NMR spectroscopy (300 MHz, delay = 30 s) implementing 1,3,5-trimethoxybenzene as the internal standard. All analysis was performed on a mixture of accurately weighed (0.01 mg) standard and substrate in deuterated solvents. HR-MS was obtained from either Agilent 6320B LC TOF-MS with 0.01 M ammonium acetate in 95:5 and 5:95 mixtures of acetonitrile and water as mobile phases or Waters GCT Premier Spectrometer using the desorption chemical ionization probe (DCI) with methane as CI reagent gas. UPLC analysis was performed on a Waters I-Class instrument (MP-A: 0.05% TFA in 95:5 water:acetonitrile; MP-B: 0.05% TFA in 95:5 acetonitrile:water; Column: Agilent Zorbax Eclipse C18+ (2.1 x 50 mm; 1.8 μm); Temperature: 40 °C; flow: 0.8 mL/min; wavelength: specified for experiment; and gradient: 100 % MPA to 100% MPB over 1.2 min, hold at 100% MPB for 0.4 min, and return to initial conditions). Measurement of pH was accomplished using a Mettler Toledo Seven Excellence meter (with pH electrode) and calibrated using commercially available buffer standards (pH = 4, 7, and 10; slope ≥ 99%).

Methodology Optimization

General procedure for high-throughput screening. A 96-well aluminum microvial plate (Analytical Sales & Services cat. no. 96973) was equipped with 1 mL microvials (Analytical Sales & Services cat. no. 884001). In all reactions, stock solutions of reactants were used. In cases where reactants were only partially soluble, slurry additions were employed. Catalyst $Pd(PAd_3)(4\text{-}C_6H_4F)Br$ **1** (0.2 μmol, 0.004 M) was loaded by one of two methods: (*i*) a THF solution (50 μL) was transferred to all vials in the reaction plate then the plate was evaporated to dryness using a Genevac, at RT, 15 min, 20 Torr, or (*ii*) a solution/slurry of **1** (50 μL) using the appropriate solvent choice for each well depicted in Figure S1 was transferred to the reaction plate last after all other reagents and solvent were charged. For reactant dosing in method *i*, stock solutions containing 4-chloro-1,1'-biphenyl (20 μmol, 0.2 M), 4-nitroaniline (24 μmol, 0.24 M), and and 4-propyl-1,1'-biphenyl (internal standard, 2 μmol, 0.04 M) in the indicated solvent were each dispensed into the appropriate wells (100 μL), as shown in Figure S1. For reactant dosing in method *ii*, stock solutions containing 4-chloro-1,1'-biphenyl (20 μmol, 0.4 M), 4-nitroaniline (24 μmol, 0.48 M), and and 4-propyl-1,1'-biphenyl (internal standard, 2 μmol, 0.08 M) in the indicated solvent were each dispensed into the appropriate wells (50 μL), as shown in Figure S1. To the left half of the plate (wells A1:A6, B1:B6, C1:C6, D1:D6, E1:E6, F1:F6, G1:G6, H1:H6) additional solvent (50 μL) was added to the appropriate well. Degassed water (50 μL) was added to the same left half of the plate (wells A1:A6, B1:B6, C1:C6, D1:D6, E1:E6, F1:F6, G1:G6, H1:H6), (solvent / H_2O (3:1) = 150 μL solvent, 50 μL water total added per well). Degassed water (100 μL) was also added to the right half of the plate (wells A7:A12, B7:B12, C7:C12, D7:D12, E7:E12, F7:F12, G1:G12, H7:H12), (solvent / H_2O (1:1) = 100 μL solvent, 100 μL water total added per well). The organic bases (40 μmol) were added neat, as diagrammed in Figure S1, the microvial plate was sealed, removed from the glovebox and shaken at 1000 rpm for 16 h at 60 ^oC on an Eppendorf Thermomixer C with plate adapter. After aging, the reactions were diluted with MeCN: DMSO: H_2O (3:1:1) with 1% HOAc (0.5 mL) and the plate was sealed and shaken at 1000 rpm an additional 15 minutes at RT. Aliquots of the quenched reaction mixtures (30 μL) were diluted into 750 μL of 2:1 MeCN:water. The plate was filtered and analyzed on Acquity I-class plus, Zorbax Eclipse plus C18, 2.1 x 50 mm, 1.8 μm, TFA, 2 mins methods, 284 nm.

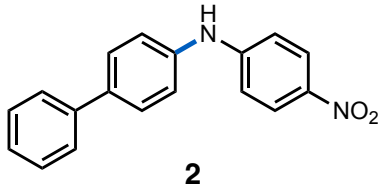

2

Reaction mixture from wells in columns B1:H1, B2:H2, B7:H7, B8:H8 and B10:H10 in the HTE screen were pooled and diluted with EtOAc (7 mL) and brine (7 mL) and transferred to a separatory funnel. Layers were split and the organics were collected, and solvents evaporated. The solid residue was redissolved in CH_2Cl_2 and the mixture was purified via silica, eluted with 0-40 % EtOAc/heptanes. Evaporation of solvent, followed by drying under vacuum, provided an analytical sample of **2**, as a yellow solid.

^{1}H NMR (500 MHz, DMSO-d_6) δ 9.41 (s, 1H), 8.13–8.10 (m, 2H), 7.71–7.65 (m, 4H), 7.48–7.44 (m, 2H), 7.36–7.32 (m, 3H), 7.15–7.11 (m, 2H).

^{13}C NMR (126 MHz, DMSO-d_6) δ 150.5, 139.6, 139.5, 138.1, 134.9, 128.9, 127.6, 127.1, 126.2, 126.2, 120.8, 113.7.

HRMS (ESI+) Calcd. for [$C_{18}H_{15}N_2O_2^+$] (M+H), 291.1128; Found, 291.1130.

HPLC (Zorbax Eclipse plus C18, 2.1 x 50 mm, 1.8 µm, TFA, 2 mins methods, 284 nm): 1.184 mins

96 total reaction conditions (6 bases x 8 solvents x 2 solvent / H_2O ratios)

Bases: Et_3N, DIPEA, DBU, MTBD, NMM, TMG

Solvents: MeCN, Anisole, IPAc, DMF, DME, 2-MeTHF, t-AmOH, MEK

Solvent / H_2O ratios: (3:1) and (1:1)

	MTBD	DBU	TMG	DIPEA	Et_3N	NMM	MTBD	DBU	TMG	DIPEA	Et_3N	NMM
MeCN												
toluene												
IPAc	**Left half of screen**						**Right half of screen**					
DMF	Solvent / H_2O (3:1)						Solvent / H_2O (1:1)					
DME	20 µmol / reaction						20 µmol / reaction					
2-MeTHF	200 µL scale in microvials						200 µL scale in microvials					
t-AmOH												
MEK												

Figure S1. Plate design for HTE screening of soluble base and solvent combinations at two different solvent/water ratios.

Table S1. Tabular reaction conversions (%) for HTE screen shown in Figure 1 using catalyst loading method *i*.[a]

		Solvent / H_2O (3:1)						Solvent / H_2O (1:1)					
		MTBD	DBU	TMG	DIPEA	Et_3N	NMM	MTBD	DBU	TMG	DIPEA	Et_3N	NMM
		1	2	3	4	5	6	7	8	9	10	11	12
MeCN	A	4	0	0	12	13	0	17	3	5	40	37	14
toluene	B	46	3	5	15	36	15	79	8	9	32	50	25
IPAc	C	64	6	15	37	54	26	55	24	14	53	65	35
DMF	D	14	3	5	41	49	14	49	11	14	71	76	33
DME	E	21	8	4	37	34	6	51	17	26	75	82	26
2-MeTHF	F	62	4	3	42	39	15	76	15	10	57	72	26
t-AmOH	G	13	27	19	55	66	21	55	27	38	74	84	41
MEK	H	25	6	7	34	47	7	38	6	17	58	72	24

Conversion (%):	10	20	30	40	50	60	70	80

[a]Normalized conversions, versus 4-propyl-1,1'-biphenyl as internal standard, are reported as a single run.

Table S2. Tabular reaction conversions (%) for HTE screen using catalyst loading method *ii*.[a]

		Solvent / H_2O (3:1)						Solvent / H_2O (1:1)					
		MTBD	DBU	TMG	DIPEA	Et_3N	NMM	MTBD	DBU	TMG	DIPEA	Et_3N	NMM
		1	2	3	4	5	6	7	8	9	10	11	12
MeCN	A	4	0	0	9	5	2	13	4	3	52	45	16
anisole	B	49	0	0	56	67	26	65	1	5	62	71	38
IPAc	C	66	21	34	46	58	39	57	37	35	59	69	39
DMF	D	17	3	4	50	60	14	38	11	9	50	57	16
DME	E	30	9	7	49	58	9	54	18	22	84	82	32
2-MeTHF	F	37	0	0	60	70	48	70	5	7	72	82	57
t-AmOH	G	32	21	26	59	66	26	44	23	34	81	87	41
MEK	H	39	3	17	41	54	10	52	9	22	62	72	24

Conversion (%):	10	20	30	40	50	60	70	80	90

[a]Normalized conversions, versus 4-propyl-1,1'-biphenyl as internal standard, are reported as a single run.

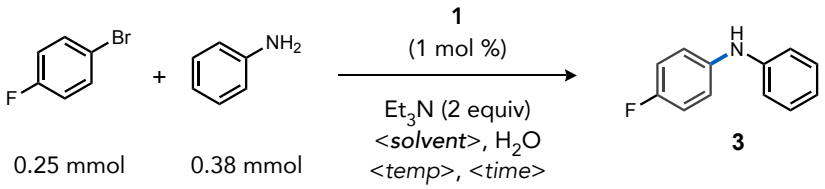

Representative procedure for non-parallel reaction optimizations. In a nitrogen filled glovebox, to an oven-dried 4 mL scintillation vial equipped with a stir bar was charged with 1-bromo-4-fluorobenzene (27 µL, 0.25 mmol, 1.0 equiv), aniline (34 µL, 0.375 mmol, 1.5 equiv), triethylamine (70 µL, 0.50 mmol, 2.0 equiv), trifluorotoluene (internal standard, 10 µL, 0.083 mmol, 0.33 equiv), Pd(PAd$_3$)(4-C$_6$H$_4$F)Br (**1**) (1.8 mg, 2.5 µmol, 1 mol %) and solvent. The vial was capped with a puncturable PTFE-lined cap and taken out of the glovebox. Under N_2 atmosphere, degassed deionized water was injected into the vial and the reaction mixture was left stirring at a certain temperature for the desired time period. After cooling down to room temperature, the mixture was diluted with $CDCl_3$ (1 mL) and the organic layer was separated for NMR characterization. The yield of **3** was obtained from the relative ^{19}F resonance integration of product and standard.[5]

Table S3. Effect of water on C–N coupling yield.

Entry	Variation from standard conditions[a]	Yield (%)
1	1:2 tol:H_2O	>99
2	No water (1.0/0.0 mL)	0
3	25:1 tol:H_2O (1.0/0.04 mL)	5
4	10:1 tol:H_2O (1.0/0.1 mL)	18
5	2:1 tol:H_2O (1.0/0.5 mL)	50
6	1:1 tol:H_2O (1.0/1.0 mL)	55
7	0:1 tol:H_2O (0.0/1.0 mL)	>99

[a]Conditions: toluene (0.5 mL):H_2O (1 mL), 60 ºC, 24 h.

Table S4. Effect of base, additive, and electrophile identity on the C–N coupling yield.

Entry	Variation from standard conditions[a]	Yield (%)
1	None (1:4 tol:H_2O (0.25/1.0 mL))	61
2	1:2 toluene:H_2O	92
3	NCy_2Me instead of NEt_3	25
4	Triethanolamine instead of NEt_3	33
5	With 1.1 equiv LiI as additive	11
6	*p*-F-C_6H_4OTf instead of *p*-F-C_6H_4Br	3

[a]Conditions: toluene (0.5 mL):H_2O (1 mL), 60 ºC, 6 h.

Table S5. Effect of solvent choice on the C–N coupling yield.

Entry	Variation from standard conditions[a]	Yield (%)
1	None	59
2	THF instead of toluene	52
3	Dioxane instead of toluene	44
4	2-MeTHF instead of toluene	53
5	DMF instead of toluene	45
6	DMA instead of toluene	35
7	K Phosphate Buffer pH 7.0 (0.1 M) instead of water, no NEt_3	0
8	K Phosphate Buffer pH 6.0 (0.1 M) instead of water	44
9	K Phosphate Buffer pH 7.0 (0.1 M) instead of water	46
10	K Phosphate Buffer pH 8.0 (0.1 M) instead of water	26

[a]Conditions: toluene (0.25 mL):H_2O (1 mL), 60 ºC, 1 h.

Catalyst screen. Complex **1** was compared against other selected palladium catalysts[6] for Buchwald-Hartwig amination using three substrate combinations:

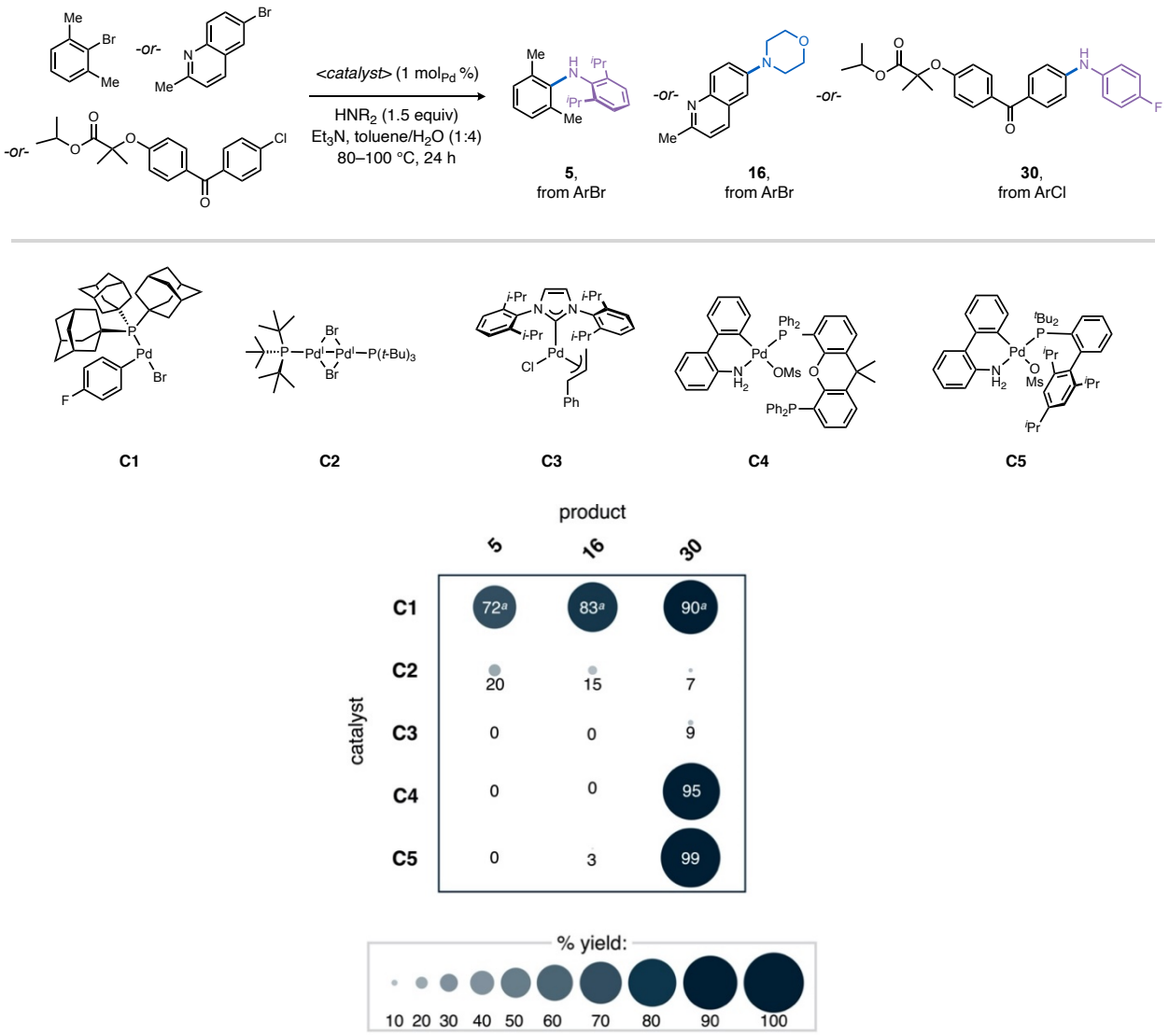

Figure S2. Survey of alternative Pd catalysts to form products **5** or **16** using procedure A on 0.25 mmol scale, or **30** using procedure B on 0.25 mmol scale. Yields were determined by ^{1}H or ^{19}F NMR using 1,3,5-$(CF_3)_3C_6H_3$, 1,3,5-$(MeO)_3C_6H_3$, or $CF_3C_6H_5$ as internal standard for **5**, **16**, or **30**, respectively. [a]Isolated yield.

Comparison of 1 to commercial precatalyst. Into separate 4 mL vials equipped with stir bar and PTFE septa in a nitrogen filled glovebox were added either **1** (1.8 mg, 2.5 µmol, 1 mol %) or (2'-amino-1,1'-biphenyl-2- yl)methanesulfonatopalladium(II) dimer, CAS [1435520-65-2] (0.924 mg, 1.250 µmol, 0.5 mol %) and PAd_3 (1.092 mg, 2.500 µmol, 1 mol %). Toluene (0.25 mL) was charged into each vial and the mixture was capped and stirred for approximately 10 min. 4-Chloro-1,1'-biphenyl (0.047 g, 0.25 mmol, 1.0 equiv) and 4-nitroaniline (0.052 g, 0.375 mmol, 0.375 mmol, 1.5 equiv) were then added to each vial. Additional toluene (0.25 mL) was added to the vial containing **1**. Triethylamine (70 µL, 0.50 mmol, 2.0 equiv) was added to each vial, then they were sealed with a puncturable PTFE-lined cap and taken out of the glovebox. Degassed deionized water (1 mL) was injected into the vials and the reaction mixture was heated and stirring at 80 °C overnight. After cooling down to room temperature, the mixtures were each transferred and diluted into a 100 mL volumetric flask with THF (5 mL), MeCN (60 mL), water (20 mL) and DMSO (15 mL) whereupon conversion (%) and solution yield (%) were determined for each of the reactions using calibrated UPLC analysis.

Table S6. Effect of $(Ad_3P)Pd$ precatalyst on the C–N coupling yield.

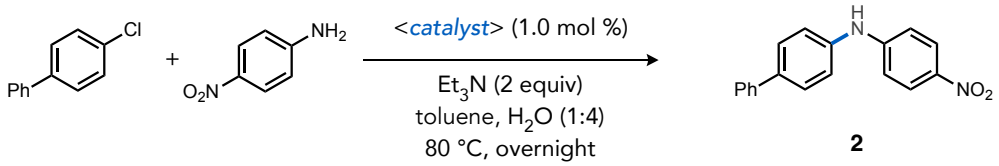

Entry	Catalyst	Conversion (%)	Yield (%)
1	**1**	99.3	95
2	PAd_3-Buchwald-G3 [a]	87.5	86

[a]Generated *in situ* by the admixture of PAd_3 and (2'-amino-1,1'-biphenyl-2- yl)methanesulfonatopalladium(II) dimer (CAS [1435520-65-2]) in 2:1 ratio.

General procedures for C–N coupling reactions

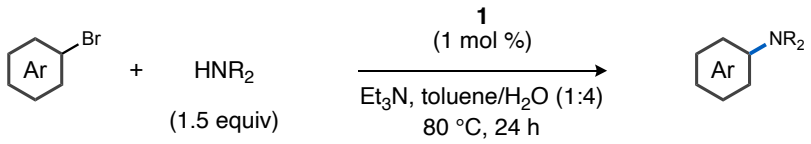

Procedure A (bromoarenes). To an oven-dried 20 mL scintillation vial equipped with a stir bar was charged with Pd(PAd$_3$)(4-C$_6$H$_4$F)Br (**1**) (5.4 mg, 7.5 μmol, 1 mol %), aryl bromide (0.75 mmol), amine nucleophile (1.13 mmol, 1.5 equiv), triethylamine (0.20 mL, 1.5 mmol, 2.0 equiv), and toluene (0.75 mL) under nitrogen (a 4 mL scintillation vial was used as reaction vessel for reactions conducted on 0.05 or 0.25 mmol-scale). The vial was capped with a puncturable PTFE-lined cap and taken out of the glovebox.[a] Degassed deionized water (3.0 mL) was injected into the vial *via* a syringe. The reaction mixture was stirred at 80 °C for 24 h. After cooling to room temperature, the mixture was extracted with dichloromethane (3 x 5 mL) and the organic layer was dried over Na_2SO_4. After evaporation, the crude product was purified by column chromatography.

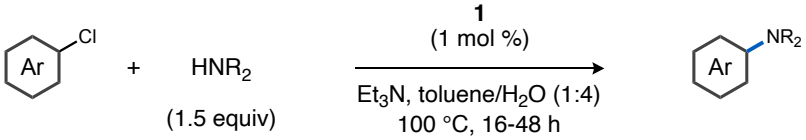

Procedure B (chloroarenes). To an oven-dried 4 mL scintillation vial equipped with a stir bar was charged with Pd(PAd$_3$)(4-C$_6$H$_4$F)Br (**1**) (1.8 mg, 2.5 μmol, 1 mol %), aryl chloride (0.25 mmol), amine nucleophile (0.38 mmol, 1.5 equiv), triethylamine (70 μL, 0.50 mmol, 2.0 equiv), and toluene (0.25 mL) under nitrogen. The vial was capped with a puncturable PTFE-lined cap and taken out of the glovebox.[a] Degassed deionized water (1.0 mL) was injected into the vial via a syringe. The reaction mixture was left stirring at 100 °C for the indicated time. After cooling to room temperature, the mixture was extracted with dichloromethane (3 x 5 mL) and the organic layer was dried over Na_2SO_4. After evaporation, the crude product was purified by column chromatography.

[a]Note that reaction preparation in a glove box was convenient but unnecessary. A benchtop procedure has also been demosrated. See scaled synthesis of **30** on pS29 for details.

Compound Characterization:

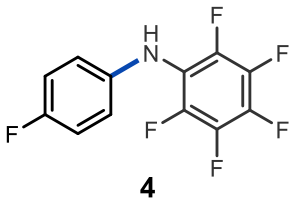

4

General procedure A was used, except using water (3.0 mL) as the only solvent, on 0.75 mmol scale, and 191 mg of **4** (92%) was obtained as a pink solid.

^{1}H NMR (500 MHz, $CDCl_3$) δ 7.07–6.96 (m, 2H), 6.83–6.81 (m, 2H), 5.37 (s, 1H).

^{13}C NMR (126 MHz, $CDCl_3$) δ 158.6 (d, J = 241.4 Hz), 141.0 (m, only $^{1}J_{CF}$ = 246.3 Hz is well-resolved), 138.4 (m, only $^{1}J_{CF}$ = 250.2 Hz is well-resolved), 138.2 (d, J = 2.5 Hz), 137.0 (m, only $^{1}J_{CF}$ = 249.6 Hz is well-resolved), 118.8 (d, J = 8.1 Hz), 118.4–118.2 (m), 116.0 (d, J = 22.9 Hz).

^{19}F NMR (376 MHz, $CDCl_3$) δ -121.3 (m, 1F), -150.5 – -150.6 (m, 2F), -162.7 (td, J = 21.8, 5.3 Hz, 2F), -164.3 (tt, J = 21.8, 3.4 Hz, 1F).

HRMS (DCI) Calcd. for [$C_{12}H_5F_6N$] (M), 277.0326; Found, 277.0338.

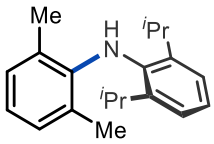

5

General procedure A was used on 0.75 mmol scale, and 152 mg (72%) of **5** was obtained as a colorless liquid.

^{1}H NMR (500 MHz, $CDCl_3$) δ 7.16–7.10 (m, 3H), 6.94 (d, J = 7.5 Hz, 2H), 6.72 (t, J = 7.5 Hz, 1H), 4.79 (s, 1H), 3.15 (hept, J = 7.0 Hz, 2H), 1.98 (s, 6H), 1.12 (d, J = 7.0 Hz, 12H).

^{13}C NMR (126 MHz, $CDCl_3$) δ 144.3, 143.3, 138.9, 129.6, 125.7, 124.9, 123.4, 119.7, 28.2, 23.6, 19.5.

HRMS (ESI+) Calcd. for [$C_{20}H_{28}N^{+}$] ($M+H^{+}$), 282.2216; Found, 282.2222.

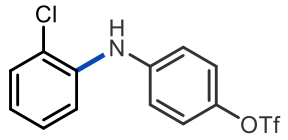

6

General procedure A was used, except using water (3.0 mL) as the only solvent, on 0.75 mmol scale, and 219 mg (83%) of **6** was obtained as a colorless liquid.

^{1}H NMR (500 MHz, $CDCl_3$) δ 7.40 (dd, *J* = 8.0, 1.5 Hz, 1H), 7.30 (dd, *J* = 8.0, 1.5 Hz, 1H), 7.22–7.13 (m, 5H), 6.91 (td, *J* = 7.5, 1.5 Hz, 1H), 6.14 (s, 1H).

^{13}C NMR (126 MHz, $CDCl_3$) δ 143.9, 142.3, 139.0, 130.2, 127.7, 123.0, 122.6, 122.1, 119.8, 118.9 (q, *J* = 321.3 Hz), 117.2.

HRMS (ESI+) Calcd. for [$C_{13}H_{10}ClF_3NO_3S^+$] ($M+H^+$), 352.0017; Found, 352.0020.

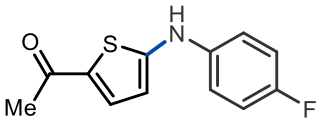

7

General procedure B was used on 0.25 mmol scale (48 h reaction time), and 26.5 mg (45%) of **7** was obtained as a grey solid.

^{1}H NMR (500 MHz, $CDCl_3$) δ 7.45 (d, *J* = 4.0 Hz, 1H), 7.18–7.16 (m, 2H), 7.04 (t, *J* = 9.0 Hz, 2H), 6.50 (s, 1H), 6.39 (d, *J* = 4.0 Hz, 1H), 2.46 (s, 3H).

^{13}C NMR (126 MHz, $CDCl_3$) δ 189.6, 159.0 (d, *J* = 243.2 Hz), 158.4, 137.5 (d, *J* = 2.6 Hz), 134.2, 130.3, 120.5 (d, *J* = 7.8 Hz), 116.5 (d, *J* = 22.9 Hz), 109.3, 25.7.

^{19}F NMR (376 MHz, $CDCl_3$) δ -119.2.

HRMS (DCI) Calcd. for [$C_{12}H_{11}FNOS^+$] (M+H), 236.0545; Found, 236.0536.

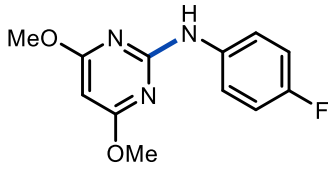

8

General procedure B was used on 0.25 mmol scale (16 h reaction time), and 56 mg (90%) of **8** was obtained as a white solid.

^{1}H NMR (500 MHz, $CDCl_3$) δ 7.58–7.54 (m, 2H), 7.03–6.99 (m, 2H), 6.97 (s, 1H), 5.58 (s, 1H), 3.90 (s, 6H)

^{13}C NMR (126 MHz, $CDCl_3$) δ 172.1, 158.4 (d, J = 240.0 Hz), 157.5, 135.8 (d, J = 2.5 Hz), 120.83 (d, J = 7.5 Hz), 115.5 (d, J = 21.3 Hz), 81.2, 54.0.

^{19}F NMR (282 MHz, $CDCl_3$) δ -121.1.

HRMS (ESI+) Calcd. for [$C_{12}H_{13}FN_3O_2^+$] ($M+H^+$), 250.0986; Found, 250.0995.

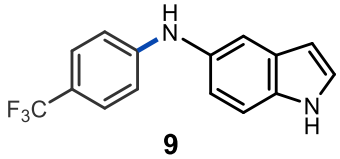

9

General procedure A was used on 0.75 mmol scale, and 174 mg (84%) of **9** was obtained as a brown solid.

^{1}H NMR (500 MHz, $CDCl_3$) δ 8.17 (s, 1H), 7.47 (d, J = 2.5 Hz, 1H), 7.40 (t, J = 8.5 Hz, 3H), 7.25 (d, J = 3.0 Hz, 1H), 7.05 (dd, J = 8.5, 2.0 Hz, 1H), 6.88 (d, J = 9.0 Hz, 2H), 6.53 (t, J = 2.0 Hz, 1H), 5.87 (s, 1H).

^{13}C NMR (126 MHz, $CDCl_3$) δ 149.6, 133.5, 133.3, 128.7, 126.7 (q, J = 3.8 Hz), 125.4, 125.0 (q, J = 270.6 Hz), 120.0 (q, J = 32.6 Hz), 119.5, 115.5, 113.6, 112.0, 102.8.

HRMS (ESI+) Calcd. for [$C_{15}H_{12}F_3N_2^+$] ($M+H^+$), 277.0947; Found, 277.0955.

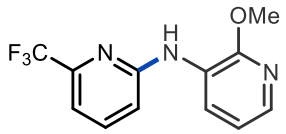

10

General procedure A was used on 0.25 mmol scale, and 61.2 mg (91%) of **10** was obtained as a white solid.

^{1}H NMR (500 MHz, $CDCl_3$) δ 8.71 (dd, *J* = 7.9, 1.7 Hz, 1H), 7.78 (d, *J* = 1.7 Hz, 1H), 7.65 (t, *J* = 8.0 Hz, 1H), 7.17 (s, 1H), 7.14 (d, *J* = 7.3 Hz, 1H), 6.94 (dd, *J* = 7.8, 5.0 Hz, 1H), 6.91 (d, *J* = 8.4 Hz, 1H), 4.05 (s, 3H).

^{13}C NMR (126 MHz, $CDCl_3$) δ 155.06, 153.04, 146.36 (q, *J* = 34.3 Hz), 138.36, 138.01, 124.91, 124.30, 121.68 (q, *J* = 274.1 Hz), 117.54, 113.99, 111.62, 53.81.

^{19}F NMR (376 MHz, $CDCl_3$) δ -68.64.

HRMS (ESI+) Calcd. for [$C_{12}H_{11}F_3N_3O^+$] ($M+H^+$), 270.0849; Found, 270.0858.

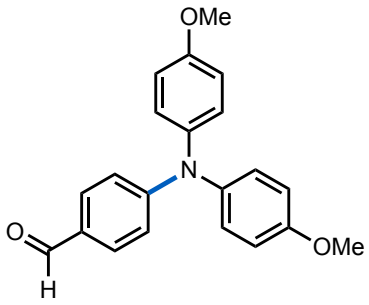

11

General procedure A was used on 0.75 mmol scale, and 228 mg (91%) of **11** was obtained as a yellow oil.

^{1}H NMR (500 MHz, $CDCl_3$) δ 9.76 (s, 1H), 7.64–7.62 (m, 2H), 7.14–7.12 (m, 4H), 6.91–6.84 (m, 6H), 3.82 (s, 6H).

^{13}C NMR (126 MHz, $CDCl_3$) δ 190.43, 157.43, 154.19, 138.94, 131.56, 128.20, 127.89, 116.87, 115.18, 55.64.

HRMS (ESI+) Calcd. for [$C_{21}H_{20}NO_3^+$] ($M+H^+$), 334.1438; Found, 334.1445.

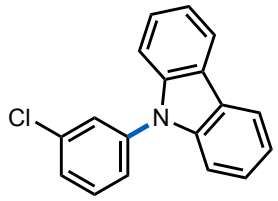

12

General procedure A was used on 0.75 mmol scale, and 165 mg (79%) of **12** was obtained as a yellow oil.

^{1}H NMR (500 MHz, $CDCl_3$) δ 8.15 (d, *J* = 8.0 Hz, 2H), 7.60 (t, *J* = 2.0 Hz, 1H), 7.55 (t, *J* = 8.0 Hz, 1H), 7.50 – 7.48 (m, 1H), 7.47 – 7.44 (m, 1H), 7.44 – 7.41 (m, 4H), 7.33 – 7.29 (m, 2H).

^{13}C NMR (126 MHz, $CDCl_3$) δ 140.7, 139.1, 135.5, 131.0, 127.7, 127.4, 126.3, 125.4, 123.6, 120.5, 120.5, 109.8.

HRMS (ESI+) Calcd. for [$C_{18}H_{13}ClN^+$] ($M+H^+$), 278.0731; Found, 278.0737.

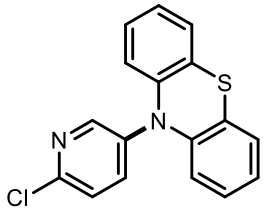

13

General procedure A was used on 0.25 mmol scale, and 67.6 mg (87%) of **13** was obtained as a white solid.

^{1}H NMR (500 MHz, $CDCl_3$) δ 8.40 – 8.39 (m, 1H), 7.66 (dd, *J* = 8.5, 3.0 Hz, 1H), 7.49 – 7.47 (m, 1H), 7.18 – 7.16 (m, 2H), 7.04 – 7.00 (m, 2H), 6.99 – 6.95 (m, 2H), 6.48 – 6.46 (m, 2H).

^{13}C NMR (126 MHz, $CDCl_3$) δ 148.6, 143.0, 138.2, 127.8, 127.4, 125.8, 124.5, 124.3, 118.8, 118.8.

HRMS (ESI+) Calcd. for [$C_{17}H_{12}ClN_2S^+$] ($M+H^+$), 311.0404; Found, 311.0411.

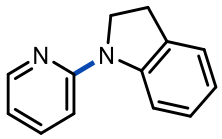

14

General procedure A was used, except using water (3.00 mL) as the only solvent and 3 mol % **1**, on 0.75 mmol scale, and 119 mg (81%) of **14** was obtained as an off-white solid.

^{1}H NMR (500 MHz, $CDCl_3$) δ 8.37 – 8.35 (m, 1H), 8.22 – 8.19 (m, 1H),), 7.61 – 7.56 (m, 1H), 7.21 – 7.17 (m, 2H), 6.87 (t, *J* = 9.0 Hz, 1H), 6.79 – 6.76 (m, 2H), 4.04 (t, *J* = 10.5 Hz, 2H), 3.21 (t, *J* = 10.5 Hz, 2H).

^{13}C NMR (126 MHz, $CDCl_3$) δ 155.6, 148.1, 145.0, 137.4, 131.5, 127.4, 124.7, 120.5, 114.5, 113.4, 108.7, 49.5, 27.8.

HRMS (ESI+) Calcd. for [$C_{13}H_{13}N_2^+$] ($M+H^+$), 197.1073; Found, 197.1080.

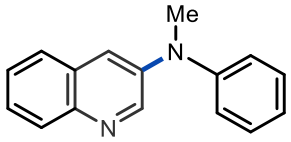

15

General procedure A was used on 0.25 mmol scale, and 57.4 mg (98%) of **15** was obtained as a yellow oil.

^{1}H NMR (500 MHz, $CDCl_3$) δ 8.69 (d, *J* = 3.0 Hz, 1H), 7.99 (d, *J* = 8.5 Hz, 1H), 7.67 (dd, *J* = 8.0, 2.0 Hz, 1H), 7.52 – 7.50 (m, 2H), 7.49 – 7.46 (m, 1H), 7.36 – 7.33 (m, 2H), 7.16 – 7.13 (m, 2H), 7.11 – 7.08 (m, 1H), 3.44 (s, 3H).

^{13}C NMR (126 MHz, $CDCl_3$) δ 148.2, 146.4, 143.3, 142.6, 129.8, 129.1, 129.1, 127.1, 126.7, 126.6, 123.4, 122.3, 119.6, 40.6.

HRMS (ESI+) Calcd. for [$C_{16}H_{15}N_2^+$] ($M+H^+$), 235.1230; Found, 235.1233.

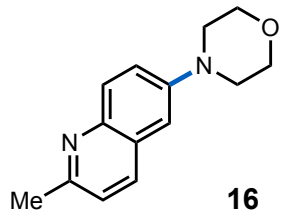

16

General procedure A was used on 0.25 mmol scale, and 47.4 mg (83%) of **16** was obtained as an orange solid.

^{1}H NMR (500 MHz, $CDCl_3$) δ 7.91 (dd, *J* = 9.0, 3.0 Hz, 2H), 7.45 (dd, *J* = 9.0, 3.0 Hz, 1H), 7.22 (d, *J* = 8.0 Hz, 1H), 7.01 (d, *J* = 7.5 Hz, 1H), 3.93–3.91 (m, 4H), 3.28 – 3.26 (m, 4H), 2.70 (s, 3H).

^{13}C NMR (126 MHz, $CDCl_3$) δ 156.4, 148.9, 143.7, 135.2, 129.6, 127.5, 122.5, 122.1, 109.4, 67.0, 49.8, 25.2.

HRMS (ESI+) Calcd. for [$C_{14}H_{17}N_2O^+$] (M+H^+), 229.1335; Found, 229.1343.

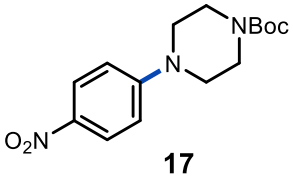

17

General procedure A was used on 0.75 mmol scale, and 205 mg (89%) of **17** was obtained as an orange solid.

^{1}H NMR (500 MHz, $CDCl_3$) δ 8.14 (d, *J* = 9.5 Hz, 2H), 6.82 (d, *J* = 9.0 Hz, 2H), 3.61 – 3.59 (m, 4H), 3.43 – 3.41 (m, 4H), 1.49 (s, 9H).

^{13}C NMR (126 MHz, $CDCl_3$) δ 154.8, 154.7, 138.9, 126.1, 113.0, 80.5, 47.0, 28.5.

HRMS (ESI+) Calcd. for [$C_{15}H_{22}N_3O_4^+$] (M+H^+), 308.1605; Found, 308.1606.

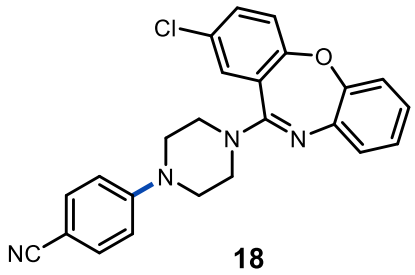

18

General procedure A was used (48 h reaction time) on 0.25 mmol scale, and 63.3 mg (61%) of **18** was obtained as an off-white solid.

^{1}H NMR (500 MHz, $CDCl_3$) δ 7.53 (d, *J* = 9.0 Hz, 2H), 7.42 (d, *J* = 9.0, 3.0 Hz, 1H), 7.36 (d, *J* = 3.0 Hz, 1H), 7.21 (d, *J* = 8.5 Hz, 1H), 7.18 – 7.16 (m, 1H), 7.12 – 7.09 (m, 2H), 7.04 – 7.01 (m, 1H), 6.91 (d, *J* = 8.5 Hz, 2H), 3.69 (s, 4H), 3.46 (s, 4H).

^{13}C NMR (126 MHz, $CDCl_3$) δ 159.5, 158.9, 153.4, 151.9, 139.9, 133.7, 133.0, 130.6, 129.0, 127.3, 126.0, 125.1, 124.9, 123.0, 120.3, 120.0, 114.7, 101.1, 47.2.

HRMS (ESI+) Calcd. for [$C_{24}H_{20}ClN_4O^+$] ($M+H^+$), 415.1320; Found, 415.1326.

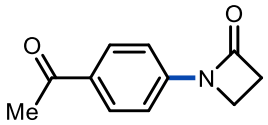

19

General procedure A was used on 0.25 mmol scale, and 42.1 mg (89%) of **19** was obtained as an off-white solid.

^{1}H NMR (500 MHz, $CDCl_3$) δ 7.96 (d, *J* = 9.0 Hz, 2H), 7.41 (d, *J* = 8.5 Hz, 2H), 3.70 (t, *J* = 4.5 Hz, 2H), 3.18 (d, *J* = 4.5 Hz, 2H), 2.58 (s, 3H).

^{13}C NMR (126 MHz, $CDCl_3$) δ 196.9, 164.9, 142.3, 132.7, 130.1, 115.9, 38.4, 36.7, 26.6.

HRMS (ESI+) Calcd. for [$C_{11}H_{12}NO_2^+$] ($M+H^+$), 190.0863; Found, 190.0870.

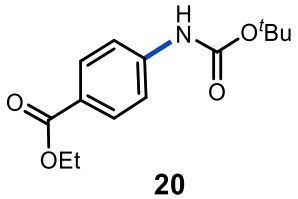

20

General procedure A was used on 0.75 mmol scale, and 193 mg (97%) of **20** was obtained as a white solid.

^{1}H NMR (500 MHz, $CDCl_3$) δ 7.98 (d, *J* = 9.0 Hz, 2H), 7.42 (d, *J* = 8.5 Hz, 2H), 6.66 (s, 1H), 4.35 (d, *J* = 7.0 Hz, 2H), 1.53 (s, 9H), 1.38 (t, *J* = 7.0 Hz, 3H).

^{13}C NMR (126 MHz, $CDCl_3$) δ 166.4, 152.3, 142.7, 131.0, 124.9, 117.4, 81.3, 60.9, 28.4, 14.5.

HRMS (ESI+) Calcd. for [$C_{14}H_{20}NO_4^+$] ($M+H^+$), 266.1387; Found, 266.1391.

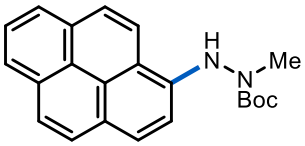

21

General procedure A was used (48 h reaction time) on 0.25 mmol scale, and 59.8 mg (69%) of **21** was obtained as an off-white solid.

^{1}H NMR (500 MHz, $CDCl_3$) δ 8.12 – 8.06 (m, 3H), 8.05 – 7.99 (m, 2H), 7.98 – 7.93 (m, 2H), 7.87 (d, *J* = 9.0 Hz, 1H), 7.43 (d, *J* = 8.4 Hz, 1H), 7.02 (s, 1H), 3.40 (s, 3H), 1.35 (s, 9H).

^{13}C NMR (126 MHz, $CDCl_3$) δ 156.2, 141.0, 132.0, 131.3, 127.6, 126.6, 126.0, 125.9, 125.7, 125.6, 125.3, 124.6, 124.5, 124.0, 119.3, 117.1, 109.9, 81.3, 37.7, 28.2.

HRMS (ESI+) Calcd. for [$C_{22}H_{23}N_2O_2^+$] ($M+H^+$), 369.1573; Found, 369.1580.

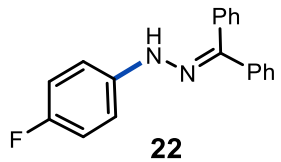

22

General procedure A was used on 0.25 mmol scale, and 58.1 mg (80%) of **22** was obtained as a brown solid.

^{1}H NMR (500 MHz, $CDCl_3$) δ 7.60 – 7.56 (m, 4H), 7.54 – 7.51 (m, 1H), 7.42 (s, br, 1H), 7.34 – 7.29 (m, 5H), 7.04 – 7.01 (m, 2H), 6.97 – 6.94 (m, 2H).

^{13}C NMR (126 MHz, $CDCl_3$) δ 157.4 (d, J = 237.8 Hz), 144.5, 141.1 (d, J = 2.1 Hz), 138.4, 132.8, 129.8, 129.4, 129.2, 128.3, 128.2, 126.6, 115.9 (d, J = 22.6 Hz), 113.9 (d, J = 7.7 Hz).

HRMS (ESI+) Calcd. for [$C_{19}H_{16}FN_2^+$] ($M+H^+$), 291.1292; Found, 291.1305.

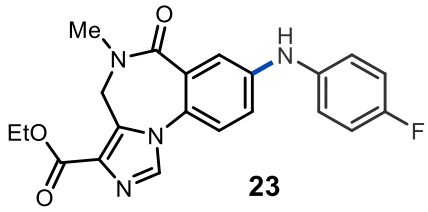

23

General procedure A was used on 50 μmol scale, and 17.7 mg (90%) of **23** was obtained as an off-white solid.

^{1}H NMR (500 MHz, $CDCl_3$) δ 7.84 (s, 1H), 7.52 (d, J = 2.7 Hz, 1H), 7.26 (d, J = 8.6 Hz, 1H, obscured by chloroform-d_6 peak), 7.17 – 7.10 (m, 3H), 7.08 – 7.02 (m, 2H), 5.93 (s, 1H), 5.25-5.07 (m, 1H), 4.51 – 4.29 (m, 3H), 3.23 (s, 3H), 1.45 (t, J = 7.2 Hz, 3H).

^{13}C NMR (126 MHz, $CDCl_3$) δ 166.6, 163.3, 159.4 (d, J = 242.9 Hz), 145.2, 136.9 (d, J = 2.9 Hz), 135.5, 134.8, 130.4, 128.3, 124.2, 123.3, 123.2 (d, J = 8.1 Hz), 118.7, 118.0, 116.6 (d, J = 22.6 Hz), 61.1, 42.6, 36.0, 14.6.

^{19}F NMR (376 MHz, $CDCl_3$) δ -118.8.

HRMS (ESI+) Calcd. for [$C_{21}H_{20}FN_4O_3^+$] ($M+H^+$), 395.1514; Found, 395.1521.

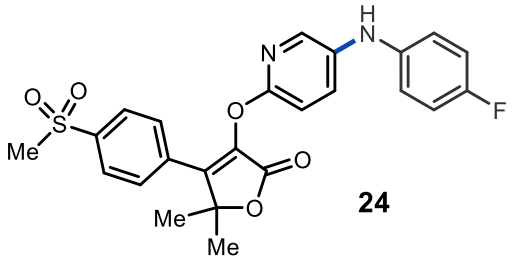

24

General procedure A was used on 50 μmol scale, and 21.3 mg (91%) of **24** was obtained as a green oil.

^{1}H NMR (500 MHz, $CDCl_3$) δ 8.03 – 7.97 (m, 2H), 7.83 – 7.81 (m, 1H), 7.80 – 7.76 (m, 2H), 7.40 (dd, J = 8.7, 2.8 Hz, 1H), 7.01 – 6.89 (m, 6H), 3.07 (s, 3H), 1.76 (s, 6H).

^{13}C NMR (126 MHz, $CDCl_3$) δ 165.9, 158.2 (d, J = 240.8 Hz), 155.6, 147.6, 141.2, 138.7, 138.1, 137.4, 136.4, 135.1, 129.7, 129.0, 127.9, 120.0 (d, J = 7.6 Hz), 116.2 (d, J = 22.6 Hz), 111.6, 84.3, 44.4, 26.5.

HRMS (ESI+) Calcd. for [$C_{24}H_{22}FN_2O_5S^+$] ($M+H^+$), 469.1228; Found, 469.1233.

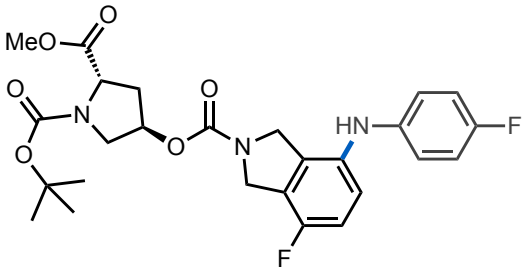

25

General procedure A was used on 50 μmol scale, and 24.3 mg (94%) of **25** was obtained as an orange solid. Note that the starting aryl bromide (X4 in Merck informer library) is supplied as a mixture of diastereomers. Flash chromatography did not separate the diastereomers of **25**, and spectral data are reported for the mixture as a result.

^{1}H NMR (500 MHz, $CDCl_3$) δ 7.01 – 6.84 (m, 6H), 5.36 – 5.26 (m, 1H), 5.18 (d, J = 28.1 Hz, 1H), 4.81 – 4.77 (m, 1H), 4.72 (s, 1H), 4.59 (s, 1H), 4.56 – 4.53 (m, 1H), 4.49 – 4.30 (m, 1H), 3.78 – 3.72 (m, 4H), 3.78 – 3.59 (m, 1H), 2.52 – 2.37 (m, 1H), 2.29 – 2.16 (m, 1H), 1.49 – 1.39 (m, 9H).

^{13}C NMR (126 MHz, $CDCl_3$) δ 173.2, 173.1, 172.9, 172.8, 159.0, 158.9, 157.1, 157.0, 154.4, 154.4, 154.1, 154.0, 153.9, 153.8, 153.7, 153.7, 152.1, 152.1, 151.9, 139.1, 139.1, 139.0, 139.0, 134.8, 134.7, 134.7, 134.6, 134.6, 129.7, 129.7, 129.5, 129.5, 129.3, 129.2, 124.7, 124.5, 124.4, 124.4, 124.3, 124.2, 119.7, 119.7, 119.6, 119.5, 119.5, 118.8, 116.2, 116.2, 116.0, 116.0, 115.4, 115.3, 115.3, 115.2, 115.2, 115.1, 80.6, 73.8, 73.8, 73.2, 73.2, 58.1, 58.0, 57.7, 57.6, 52.8, 52.7, 52.5, 52.4, 52.2, 51.5, 51.0, 51.0, 50.3, 49.8, 37.0, 37.0, 36.1, 36.0, 28.4, 28.3.

HRMS (ESI+) Calcd. for [$C_{26}H_{30}F_2N_3O_6^+$] ($M+H^+$), 540.1917; Found, 540.1925.

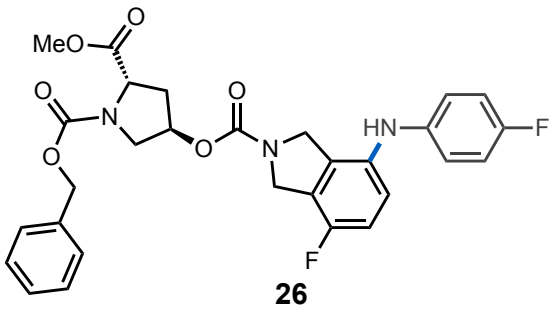

26

General procedure A was used on 50 μmol scale, and 26.1 mg (98%) of **26** was obtained as an orange solid. Note that the starting aryl bromide (X8 in Merck informer library) is supplied as a mixture of diastereomers. Flash chromatography did not separate the diastereomers of **26**, and spectral data are reported for the mixture as a result.

^{1}H NMR (500 MHz, $CDCl_3$) δ 7.38 – 7.28 (m, 5H), 7.18 (t, J = 7.8 Hz, 1H), 7.07 – 6.92 (m, 5H), 6.86 – 6.77 (m, 1H), 5.38 – 4.96 (m, 4H), 4.74 (s, 1H), 4.69 – 4.42 (m, 4H), 3.93 – 3.73 (m, 4H), 3.56 (d, J = 5.2 Hz, 1H), 2.56 – 2.45 (m, 1H), 2.32 – 2.19 (m, 1H).

^{13}C NMR (126 MHz, $CDCl_3$) δ 172.7, 172.7, 172.5, 172.5, 159.4, 159.4, 157.5, 157.5, 154.9, 154.9, 154.3, 153.9, 153.7, 139.3, 139.3, 138.2, 138.1, 138.1, 138.0, 138.0, 137.9, 137.9, 136.3, 136.3, 136.3, 136.2, 129.1, 128.5, 128.1, 128.1, 127.9, 127.9, 125.0, 124.8, 124.8, 124.7, 121.5, 121.4, 121.3, 121.3, 116.2, 116.0, 114.9, 114.8, 114.8, 114.8, 114.4, 114.2, 114.1, 73.6, 73.0, 72.9, 67.4, 58.1, 58.1, 57.8, 57.8, 53.1, 53.0, 53.0, 52.8, 52.7, 52.7, 52.5, 52.3, 51.0, 50.6, 50.5, 37.2, 37.1, 36.1, 36.1.

HRMS (ESI+) Calcd. for [$C_{29}H_{29}FN_3O_6^+$] ($M+H^+$), 534.2035; Found, 534.2038.

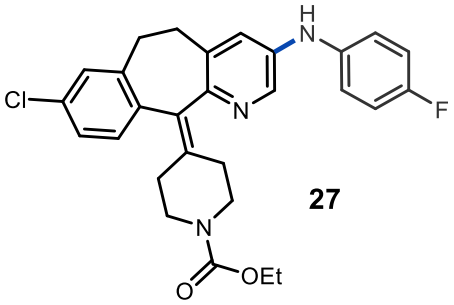

27

General procedure A was used on 50 μmol scale, and 18.7 mg (76%) of **27** was obtained as an orange solid.

^{1}H NMR (500 MHz, $CDCl_3$) δ 8.10 (d, *J* = 2.7 Hz, 1H), 7.20 – 7.07 (m, 3H), 7.06 – 6.96 (m, 5H), 5.63 (s, 1H), 4.13 (q, *J* = 7.1 Hz, 2H), 3.82 (d, *J* = 16.1 Hz, 2H), 3.41 – 3.31 (m, 1H), 3.31 – 3.20 (m, 1H), 3.18 – 3.04 (m, 2H), 2.85 – 2.68 (m, 2H), 2.55 – 2.44 (m, 1H), 2.43 – 2.35 (m, 1H), 2.35 – 2.28 (m, 2H), 1.25 (t, *J* = 7.1 Hz, 3H).

^{13}C NMR (126 MHz, $CDCl_3$) δ 158.5 (d, *J* = 241.5 Hz), 155.5, 148.6, 139.7, 139.3, 138.5, 137.7 (d, *J* = 2.9 Hz), 137.2, 136.0, 133.8, 133.6, 132.7, 130.2, 128.7, 126.2, 123.8, 121.2 (d, *J* = 7.9 Hz), 116.2 (d, *J* = 22.6 Hz), 61.3, 44.9, 44.9, 32.0, 31.5, 30.8, 30.6, 14.7.

HRMS (ESI+) Calcd. for [$C_{28}H_{28}ClFN_3O_2^+$] ($M+H^+$), 492.1849; Found, 492.1855.

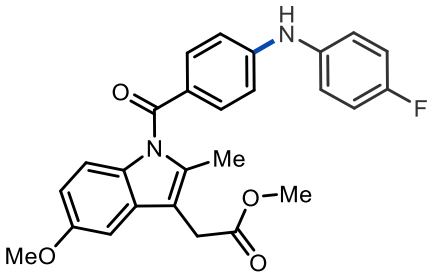

28

General procedure A was used on 0.25 mmol scale, and 100 mg (90%) of **28** was obtained as a brown solid.

^{1}H NMR (500 MHz, $CDCl_3$) δ 7.62 (d, *J* = 9.0 Hz, 2H), 7.18 – 7.15 (m, 2H), 7.07 – 7.03 (m, 2H), 6.98 – 6.96 (m, 2H), 6.88 (d, *J* = 8.5 Hz, 2H), 6.67 (dd, *J* = 9.0, 2.5 Hz, 1H), 6.14 (s, 1H), 3.84 (s, 3H), 3.70 (s, 3H), 3.68 (s, 2H), 2.47 (s, 3H).

^{13}C NMR (126 MHz, $CDCl_3$) δ 171.8, 168.9, 159.5 (d, *J* = 242.5 Hz), 155.7, 149.5, 136.3, 136.3, 132.9, 131.3, 130.3, 125.3, 123.9 (d, *J* = 7.5 Hz), 116.5 (d, *J* = 22.5 Hz), 114.8, 113.9, 111.5, 111.1, 101.0, 55.9, 52.2, 30.4, 13.0.

^{19}F NMR (282 MHz, $CDCl_3$) δ -118.2.

HRMS (ESI+) Calcd. for [$C_{26}H_{24}FN_2O_4^+$] ($M+H^+$), 447.1715; Found, 447.1720.

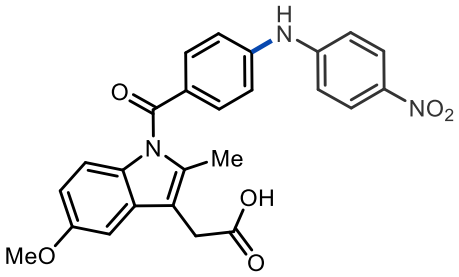

29

General procedure B was used (48 h reaction time), except using 2 mol % **1**, on 0.25 mmol scale, and 58.6 mg (51%) of **29** was obtained as a yellow solid.

^{1}H NMR (500 MHz, DMSO-d_6) δ 9.78 (s, 1H), 8.18 (d, *J* = 9.5 Hz, 2H), 7.65 (d, *J* = 8.5 Hz, 2H), 7.36 (d, *J* = 9.0 Hz, 2H), 7.31 (d, *J* = 9.0 Hz, 2H), 7.03 (d, *J* = 2.5 Hz, 1H), 6.93 (d, *J* = 9.0 Hz, 1H), 6.71 (dd, *J* = 9.0, 3.0 Hz, 1H), 3.76 (s, 3H), 3.67 (s, 2H), 2.28 (s, 3H).

^{13}C NMR (126 MHz, DMSO-d_6) δ 172.3, 168.1, 155.2, 148.6, 145.5, 139.7, 135.3, 131.9, 130.5, 130.4, 127.6, 126.0, 117.8, 116.0, 114.2, 112.5, 111.2, 101.4, 55.4, 29.6, 12.9.

HRMS (ESI+) Calcd. for [$C_{25}H_{22}N_3O_6^+$] ($M+H^+$), 460.1503; Found, 460.1505.

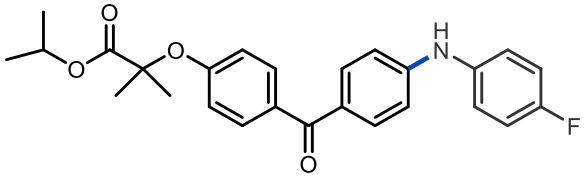

30

General procedure B was used (36 h reaction time) on 0.25 mmol scale, and 98.0 mg (90%) of **30** was obtained as a white solid.

^{1}H NMR (500 MHz, $CDCl_3$) δ 7.71 – 7.69 (m, 4H), 7.17 – 7.14 (m, 2H), 7.05 – 7.01 (m, 2H), 6.90 (d, *J* = 10 Hz, 2H), 6.85 (d, *J* = 10 Hz, 2H), 6.21 (s, 1H), 5.08 (hept, *J* = 6.5 Hz, 1H), 1.65 (s, 6H), 1.20 (d, *J* = 6.5 Hz, 6H).

^{13}C NMR (126 MHz, $CDCl_3$) δ 194.2, 173.4, 159.2 (d, *J* = 241.3 Hz), 159.0, 148.7, 136.8 (d, *J* = 2.5 Hz), 132.6, 131.7, 131.7, 128.9, 123.4 (d, *J* = 7.5 Hz), 117.3, 116.3 (d, *J* = 22.5 Hz), 113.8, 79.4, 69.4, 25.5, 21.6.

^{19}F NMR (282 MHz, $CDCl_3$) δ -118.9.

HRMS (ESI+) Calcd. for [$C_{26}H_{27}FNO_4^+$] ($M+H^+$), 436.1919; Found, 436.1907.

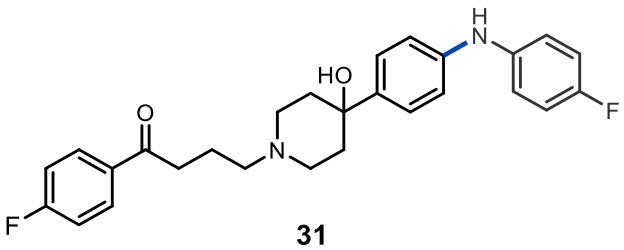

31

General procedure B was used (48 h reaction time), except using 2 mol % **1**, on 0.25 mmol scale, and 65.3 mg (58%) of **31** was obtained as a white solid. The yield of **31** was 60% as determined by ^{19}F NMR analysis versus internal standard. The product is poorly soluble in common deuterated solvents.

^{1}H NMR (500 MHz, DMSO-*d*$_6$) δ 8.13 (s, 1H), 8.09 – 8.07 (m, 2H), 7.37 (t, *J* = 9.0, 2H), 7.30 (t, *J* = 8.5, 2H), 7.06 (d, *J* = 6.5, 4H), 6.99 (d, *J* = 8.5, 2H), 6.98 (brs, 1H), 3.36 – 3.17 (m, 10H), 2.02 (s, 2H), 1.72 (s, 2H).

^{13}C NMR (126 MHz, DMSO-*d*$_6$) δ 197.6, 165.0 (d, *J* = 251.7 Hz), 156.2 (d, *J* = 236.0 Hz), 142.4, 140.0, 133.4, 130.9 (d, *J* = 9.6 Hz), 125.6, 118.4 (d, *J* = 7.7 Hz), 115.8, 115.7 (d, *J* = 21.9 Hz), 115.7 (d, *J* = 22.2 Hz), 68.2, 48.5, 35.4, 21.0.

^{19}F NMR (376 MHz, CD_2Cl_2) δ -107.1, -123.2.

HRMS (ESI+) Calcd. for [$C_{27}H_{29}FNO_4^+$] ($M+H^+$), 451.2192; Found, 451.2193.

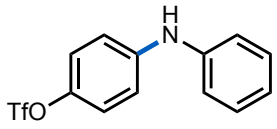

S1

General procedure A was used on 0.25 mmol scale, and 72 mg (91%) of **S1** was obtained as a colorless liquid.

^{1}H NMR (400 MHz, $CDCl_3$) δ 7.34–7.30 (m, 2H), 7.15–7.09 (m, 4H), 7.06–7.01 (m, 3H), 5.80 (s, 1H).

^{13}C NMR (101 MHz, $CDCl_3$) δ 143.9, 142.8, 141.8, 129.7, 122.7, 122.4, 119.5, 118.9 (d, J = 319.3 Hz), 117.4.

^{19}F NMR (376 MHz, $CDCl_3$) δ -72.8.

HRMS (ESI+) Calcd. for [$C_{13}H_{11}F_3NO_3S^+$] ($M+H^+$), 318.0406; Found, 318.0408.

Table S7. Attempted reactions with primary aliphatic amines.

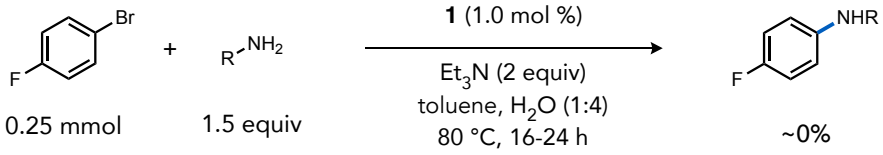

0.25 mmol 1.5 equiv ~0%

Entry	R group	Yield (%)
1	CPh_3	0
2	1-adamantyl	0
3	CH_3CF_3	0
4	cyclohexyl	0
5	benzyl	0
6	*n*-butyl	trace

Conditions: General Procedure A. Yields determined by ^{19}F NMR versus internal standard.

Scale-Up of Synthesis of Fenofibrate Derivative 30:

Reaction Conversion Calibration Curve. To 4 x 8 mL vials was charged fenofibrate (MW 360.83 g/mol; measured purity 98%) and **30** (MW 435.495 g/mol; measured purity 99.5%) according to the values in the Table S6. The mixtures were then dissolved in EtOAc (7 mL), sampled (30 uL in 1.5 mL of 2:1 acetonitrile:water), and assayed via UPLC analysis. The resulting areas of each peak were measured at 304 nm and conversion (%) values were compared to the actual mass conversion values (%).

Table S8. Tabular data for detector response for substrate and product analytes.

Entry	Compound	Wt. (mg)	Corrected wt. (mg)		mmol	Measured Area (304 nm)
	fenofibrate	159.4	156.212		0.4329	333319.00
1	**30**	44.9	44.6755		0.103	77607
				conversion:	19%	19%
	fenofibrate	84.2	82.516		0.228	183257
2	**30**	116	115.42		0.265	203654
		-	-	conversion:	54%	53%
	fenofibrate	25.7	25.186		0.0697	58840
3	**30**	194.0	193.03		0.4432	323089
				conversion:	86%	85%
	fenofibrate	5.4	5.292		0.014	16690
4	**30**	226.8	225.666		0.5181	382633
		-	-	conversion:	97%	96%

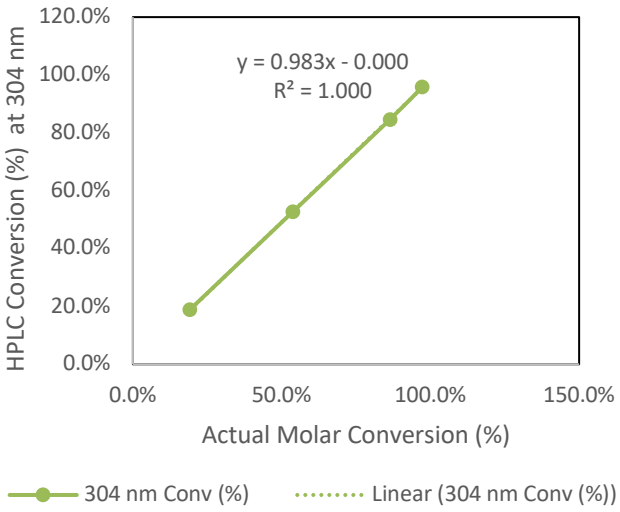

Figure S3. Calibration curve of measured versus actual conversion of fenofibrate to **30**.

Optimization of solvent and temperature in synthesis of 30. To 8 x 20 mL vials with stir bars outside of the glovebox was charged isopropyl 2-(3-(3-chlorobenzoyl)phenoxy)-2-methylpropanoate (fenofibrate) (530 mg, 1.44 mmol, 98% purity), 4-fluoroaniline (245 mg, 2.16 mmol, 1.5 equiv, 98% purity), and **1** (9.39 mg, 0.013 mmol, 0.9 mol %). The vials were then brought into the glovebox and charged with solvent (1.5 mL), degassed water (6 mL), and triethylamine (405 uL, 2.88 mmol, 2 equiv, 99% purity). The vials were sealed, removed from the glovebox, and placed into a pre-heated hotplate at the specified temperatures and aged for 21 h with vigorous stir bar agitation. Upon cooling, aliquots (50 uL) were taken with continued agitation, diluted into 2:1 acetonitrile:water (7 mL), and assayed for reaction completion using UPLC-MS analysis at 304 nm.

Table S9. Results of Temperature and Solvent Variation During Synthesis of 30.

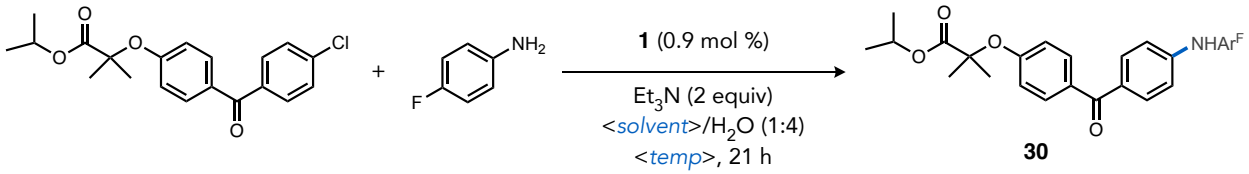

Entry	Solvent	Temperature (°C)	Conversion (%)
1	anisole	98	89
2	CPME	98	98
3	*t*-AmOH	98	96
4	toluene	98	97
5	anisole	80	74
6	CPME	80	71
7	*t*-AmOH	80	94
8	toluene	80	83

Monitoring aqueous pH at initial reaction time. To a 20 mL vial with stir bar was charged isopropyl 2-(3-(3-chlorobenzoyl)phenoxy)-2-methylpropanoate (fenofibrate**)** (1.00 g, 2.72 mmol, 98% purity), 4-fluoroaniline (462 mg, 4.07 mmol, 1.5 equiv., 98% purity), *tert*-amyl alcohol (3 mL), degassed water (9 mL), and triethylamine (765 µL, 5.43 mmol, 2 equiv., 99% purity). The vial was agitated for ~10 min where upon the initial pH measurement was obtained (pH = 11.9) using the pH meter, electrode, and calibration procedure (*vide supra*).

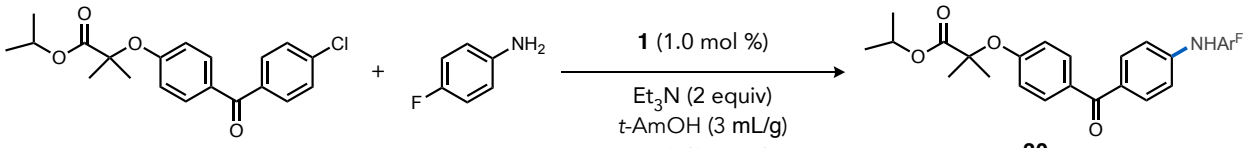

30

97% solution yield
80% Isolated yield (7.0 g)
Final pH = 8.5

Synthesis of 30 on 20-mmol Scale. To a 100 mL 2-piece EasyMax vessel fitted with reflux condenser, pitched blade impeller, and nitrogen inlet was charged isopropyl 2-(3-(3-chlorobenzoyl)phenoxy)-2-methylpropanoate (fenofibrate) (7.36 g, 20.0 mmol, 98% purity) and 4-fluoroaniline (3.40 g, 30.0 mmol, 1.5 equiv, 98% purity). The vessel was sealed and purged with N_2. Degassed water (66 mL, 9 mL/g), *t*-Amyl alcohol (22 mL, 3 mL/g, commercially available anhydrous solvent from Millipore Sigma), and degassed triethylamine (5.63 mL, 40.0 mmol, 2 equiv, 99% purity) were charged to the reactor via syringe (inert handling) while keeping the internal temperature at 25 °C with agitation set at 600 RPM. To the reactor was then charged complex **1** (144 mg, 200 µmol, 1 mol %) as a solid under nitrogen purge. The reaction was then ramped to 85 °C over 15 min at 600 RPM agitation rate, aged for 12 h, sampled (50 µL in 7 mL of 2:1 acetonitrile:water), and deemed complete (100% conversion). The reaction mixture was cooled to 25 °C, EtOAc (37 mL, 5mL/g) was charged, and the mixture was transferred to a separatory funnel with additional EtOAc (37 mL, 5 mL/g). The resulting biphasic solution was separated (aqueous layer loss <0.1%, pH = 8.5), and the organic layer assayed (solution yield = 97%). The resulting dark organic phase was concentrated to a near oil on the rotary evaporator (70-80 mm Hg, 40 °C), and then diluted with EtOAc (37 mL, 5× vol.). To the organic mixture was then charged heptanes (22 mL, 3 mL/g), then compound **30** seed crystals (~50 mg), and the resulting slurry was allowed to age (~30 min). Additional heptanes (29 mL, 4 mL/g) was charged to the dark slurry over ~ 20 min. The resulting mixture was allowed to further age (30 min) whereupon it was filtered through at disposable polypropylene filter funnel (10 µm). The wet cake was slurry washed two times with 20% EtOAc in heptanes (22 mL, 3 mL/g), and the cake was allowed to dry overnight at room temperature under vacuum and a stream of N_2 to yield **30** as a light gray solid (7.02 g, 16.0 mmol, 80% yield at 99% purity by ^{1}H wt/wt NMR).

HRMS (ESI+) Calcd. for [$C_{26}H_{27}FNO_4^+$] ($M+H^+$), 436.1919; Found, 436.1938.

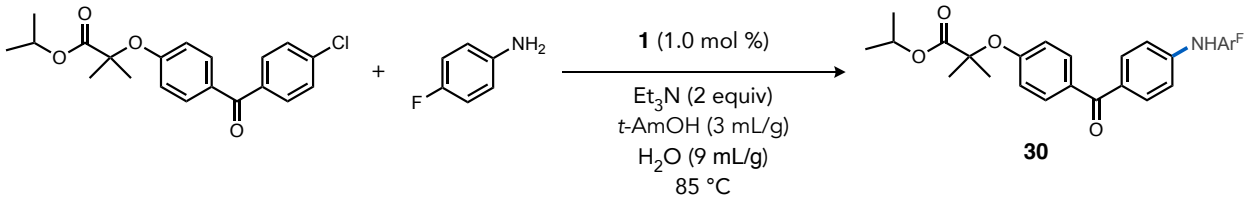

Kinetic Profile of Reaction on 20-mmol Scale. To a 100 mL 2-piece EasyMax vessel fitted with reflux condenser, pitched blade impeller, nitrogen inlet, and EasySampler (Fitted with the following solvent lines: Reaction = degassed water; Quench and Diluent = 2:1 acetonitrile:water – non-degassed; Dilution Factor = 350) was charged isopropyl 2-(3-(3-chlorobenzoyl)phenoxy)-2-methylpropanoate (fenofibrate) (7.36 g, 20.0 mmol, 98% purity) and 4-fluoroaniline (3.40 g, 30.0 mmol, 1.5 equiv., 98% purity). The vessel was sealed and purged with N_2. Degassed water (66 mL, 9 mL/g), *t*-Amyl alcohol (22 mL, 3 mL/g - commercially available anhydrous solvent from Millipore Sigma), and degassed triethylamine (5.63 mL, 40.0 mmol, 2 equiv., 99% purity) were charged to the reactor via syringe (inert handling) keeping the internal temperature at 25 °C with agitation set at 600 RPM. To the reactor was then charged complex **1** (144 mg, 0.200 mmol, 1 mol %) as a solid under nitrogen purge. The sampling times (min), temperature ramp (°C in min), and reaction conversion (%) are tabulated below.

Table S10. Tabular Data for 20-mmol Scale Amination of Fenofibrate.

Entry	Temp Ramp Time (min)	Temp (°C)	Sampling Time (min)	Compound **30** area (304 nm)	starting material area (304 nm)	Conv. (%)	Comment
1	0	25	2	13272	240538	5%	Sampling delay of ~2 min
2	15	25	17	104215	219975	32%	Sampled after 17 min at 25 °C
3	30	85	32	448567	24593	95%	Sampled 2 min after reaching 85 °C
4	45	85	47	476641	0	100%	Sampled 17 min after reaching 85 °C
5	60	85	62	421346	0	100%	Sampled 32 min after reaching 85 °C
6	120	85	122	442854	0	100%	Sampled 1h after reaching 85 °C

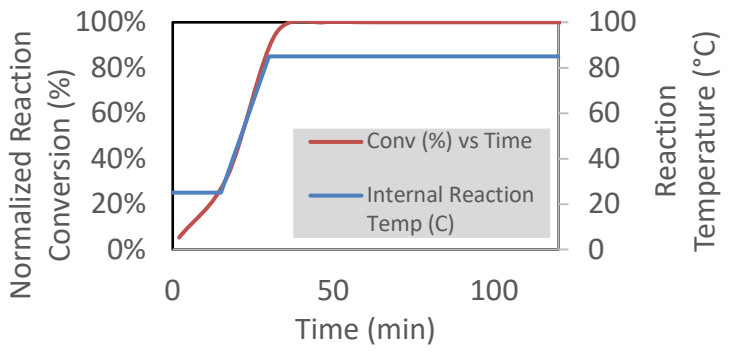

Figure S4. Reaction conversion (left-axis) and temperature (right-axis) of fenofibrate to **30** (20-mmol scale) versus time.

Synthesis of 2 on 17.5-mmol Scale. To a 100 mL 2-piece EasyMax vessel fitted with reflux condenser, pitched blade impeller, and nitrogen inlet was charged 4-bromo-1,1'-biphenyl (4.16 g, 17.5 mmol, 98% purity), and 4-Nitroaniline (3.70 g, 26.3 mmol, 1.5 equiv, 98% purity). The vessel was sealed and purged with N_2 for at least 10 minutes. Degassed water (70 mL), toluene (15 mL, commercially available anhydrous solvent from Millipore Sigma), and degassed triethylamine (4.93 mL, 35.0 mmol, 2 equiv, 99% purity) were charged to the reactor via syringe (inert handling) with agitation set at 800 RPM. The reactor was then heated to an internal temperature of 80 °C. To a 4 mL vial with PTFE septum and magnetic stir bar was charged complex **1** (126 mg, 0.175 mmol, 1.0 mol %). The vial was then inerted with N_2, and toluene (2.5 mL) was charged via syringe (inert handling). The slurry was allowed to stir and age (~5 min) whereupon it was charged to the reactor via syringe (inert handling), and the syringe was rinsed with the reactor contents two times. The contents of the reactor were aged (6 h) after which it was deemed complete by UPLC analysis (100% conversion @ 238 nm), cooled to 20 °C and stirred overnight. The resulting orange biphasic slurry was quantitatively transferred to a vessel with EtOAc (150 mL) and *tert*-butylmethylether (100 mL) where the biphasic solution was decanted from the solids, and the top organic layer collected. The remaining orange solids were dissolved in acetone (100 mL), the organic layers were combined, dried over $MgSO_4$, filtered through a plug of Silica gel, and concentrated on a rotovap (40 °C) to yield an a crude orange solid. The resulting solid was dissolved in acetone (100 mL) after stirring for several minutes in a water bath (40 °C). To the resulting orange solution was charged water (30 mL) whereupon an orange solid crystallized from solution. Additional water (20 mL) was added to the slurry, allowed to age at room temperature (approximately 10 minutes), filtered, slurry washed two times with 1:1 water:acetone (20 mL) and then toluene (20 mL). The orange wetcake was dried overnight at room temperature with vacuum to yield 4.83g of **2** (94% yield, 99wt% as determined by ^{1}H NMR) as a bright orange solid. NMR spectroscopic data matched those for a reference sample of **2** (*vide supra*).

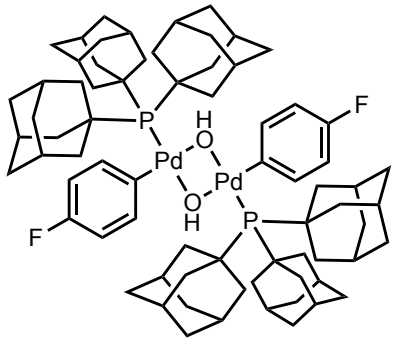

32

***anti*-[Pd(PAd$_3$)(4-C$_6$H$_4$F)(μ-OH)]$_2$ (32).** To an oven-dried 100 mL Schlenk flask equipped with a magnetic stir bar was charged with Pd(PAd$_3$)(4-C$_6$H$_4$F)Br (**1**) (90 mg, 0.13 mmol) and dichloromethane (30 mL). A solution of sodium hydroxide (50 mg, 1.3 mmol, 10 equiv) in water (30 mL) was injected into the reaction mixture. The resulting biphasic solution was stirred vigorously for 30 min at room temperature. The aqueous layer was then separated, the organic layer was concentrated, and resulting was washed with *n*-hexane (3 x 5 mL), filtered and dried under reduced pressure to afford 64 mg (78%) of **32** an off-white solid.

^{1}H NMR (500 MHz, CD_2Cl_2) δ 7.40 (t, J = 7.1 Hz, 4H), 6.63 (t, J = 9.2 Hz, 4H), 2.42 (s, 36H), 1.88 (s, 18H), 1.72 - 1.57 (m, 36H), -2.19 (d, J = 3.2 Hz, 2H).

^{13}C NMR (126 MHz, CD_2Cl_2) δ 160.91 (d, J = 238.0 Hz), 139.96, 138.68, 112.48 (d, J = 18.5 Hz), 48.83 (d, J = 5.1 Hz), 42.02, 36.97, 29.84 (d, J = 7.5 Hz).

^{19}F NMR (470 MHz, CD_2Cl_2) δ -125.2.

^{31}P{^{1}H} NMR (202 MHz, CD_2Cl_2) δ 67.1.

HRMS (ESI) m/z calculated for $C_{38}H_{52}FNPPd$ (M/2−OH+MeCN), 678.28562, found 678.28588.

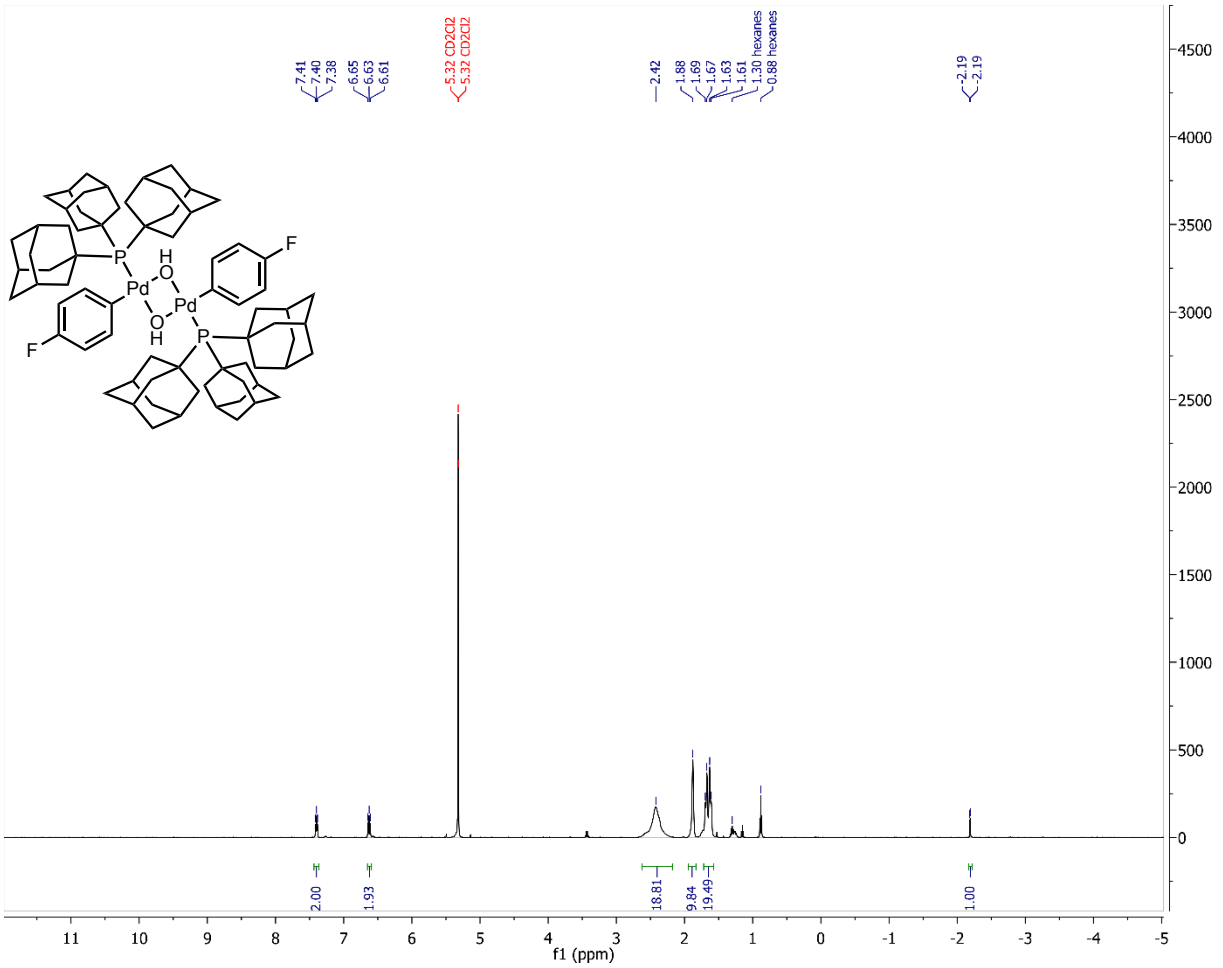

Figure S5. ^{1}H NMR spectrum (CD_2Cl_2, 500 MHz) of **32**.

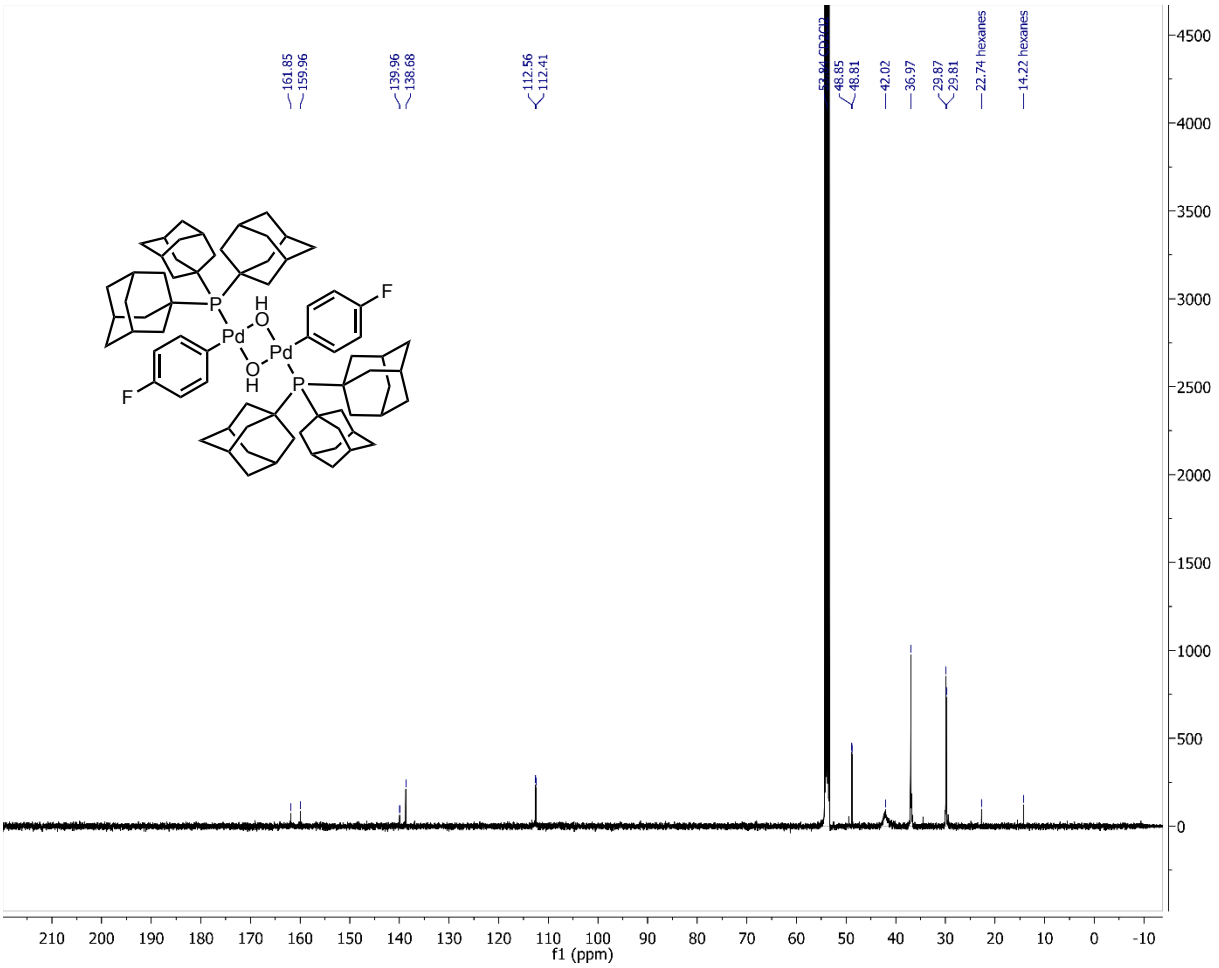

Figure S6. ^{13}C NMR spectrum (CD_2Cl_2, 126 MHz) of **32**.

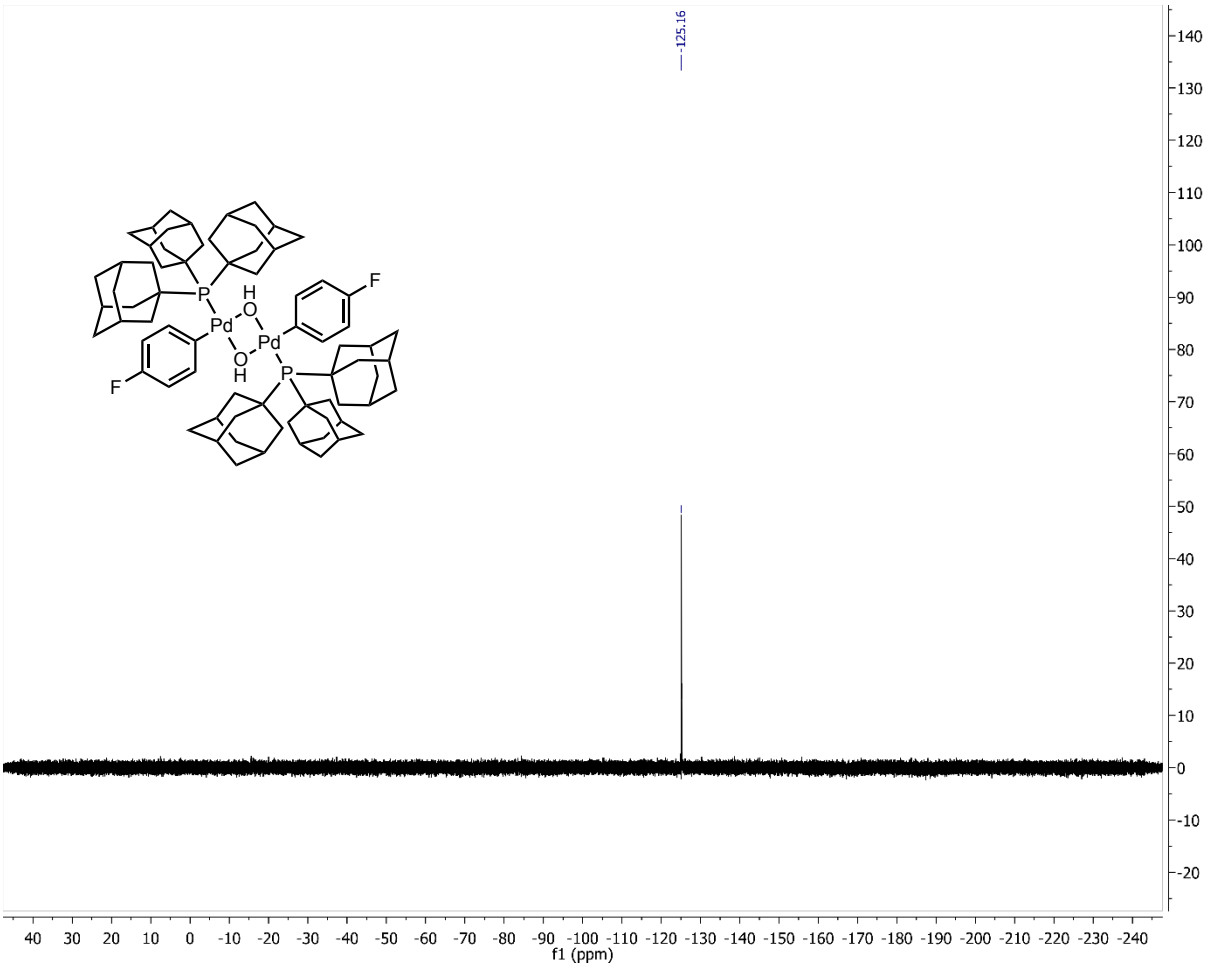

Figure S7. ^{19}F NMR spectrum (CD_2Cl_2, 470 MHz) of **32**.

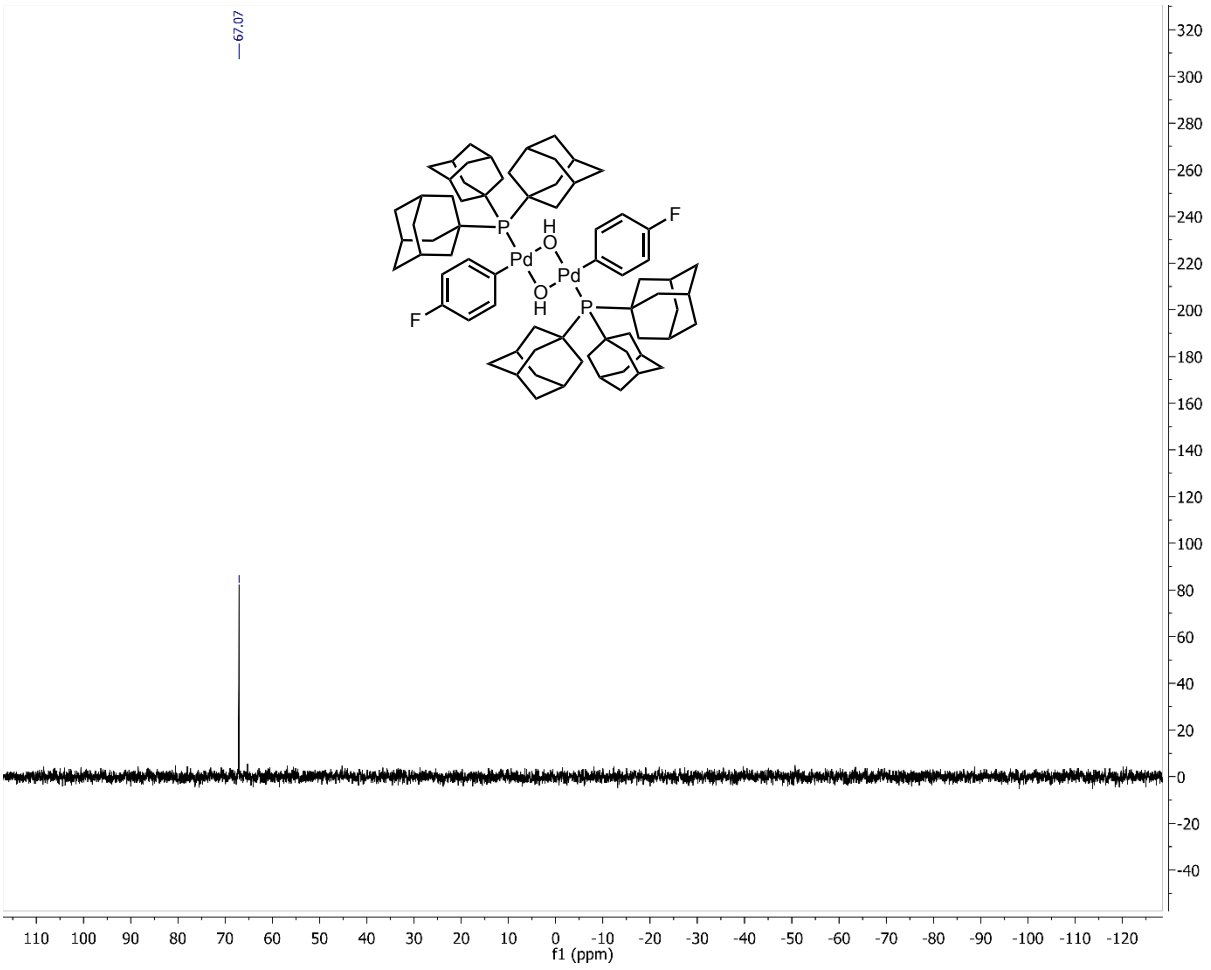

Figure S8. $^{31}P\{^{1}H\}$ NMR spectrum (CD_2Cl_2, 202 MHz) of **32**.

Stoichiometric Mechanistic Experiments:

Independent route to **32** under catalytically-relevant conditions. A solution of $Pd(PAd_3)(4\text{-}C_6H_4F)Br$ (**1**) (1.8 mg, 2.5 μmol) in toluene (1.0 mL) was transferred to an NMR tube capped with a rubber septum. Triethylamine (50 μL, 359 μmol, 143 equiv) and water (1.0 mL) were injected and the reaction mixture was shaken gently for 1 min at room temperature. A $^{31}P\{^1H\}$ spectrum of the resulting solution indicated complete consumption of **1**, and **32** was cleanly formed. Analogous reactions that omitted water or triethylamine showed no conversion of **1**.

$^{31}P\{^1H\}$ NMR (202 MHz, toluene) δ 66.9.

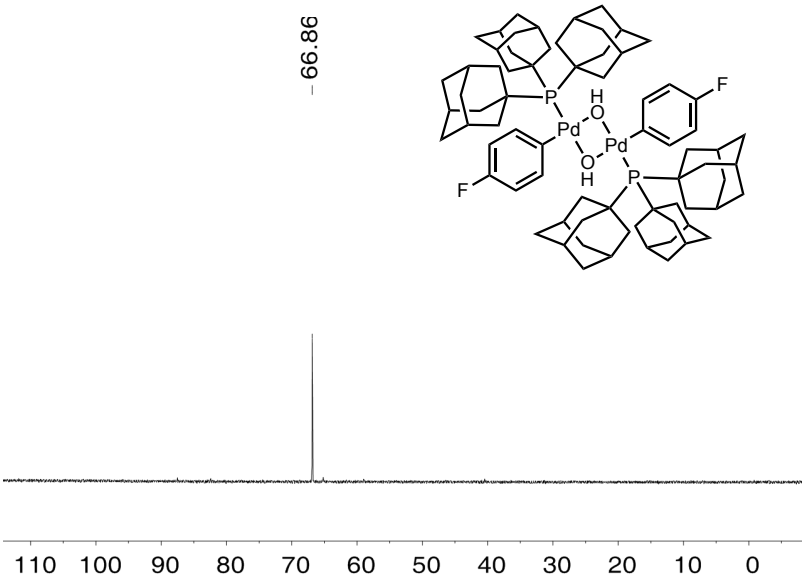

Figure S9. $^{31}P\{^1H\}$ NMR spectrum (202 MHz, toluene) of reaction of 1 with Et_3N and water in toluene after 1 min at RT.

Independent route to 32 from an independently prepared cationic aryl-Pd complex:

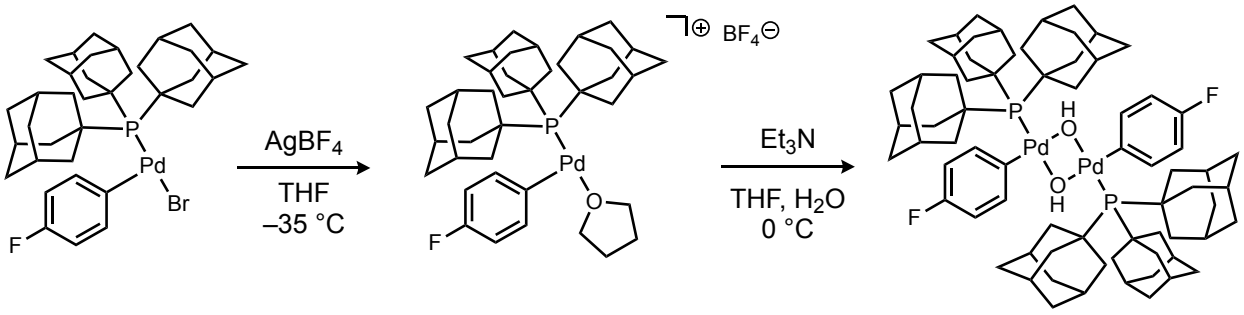

33 **32**

Generation of [Pd(PAd$_3$)(4-FC$_6$H$_4$)]$^+$ BF$_4^-$ (33). The generation of **33** was adapted from a published procedure.[3] Pd(PAd$_3$)(*p*-FC$_6$H$_4$)Br **1** (9.0 mg, 12.5 μmol) was dissolved in THF (2.5 mL). Separately, AgBF$_4$ (20 mg, 0.10 mmol) was dissolved in THF (2 mL). Both solutions were chilled at -35 °C (MeOH/H$_2$O dry ice bath). The latter solution (AgBF$_4$, 2.5 μmol, 50 μL) was then added to an aliquot of the solution of **1** (2.5 μmol, 0.5 mL) in a 4 mL vial at -35 °C. The mixture (0.55 mL) was quickly shaken, left in the cooling bath for 10 min, and transferred under nitrogen into an NMR tube capped with a rubber septum. Generation of **33** was confirmed by ^{31}P{^{1}H} spectrum at -25 °C before proceeding to the next step.

Generation of 32 from 33. Triethylamine (10 μL, 72 μmol, 29 equiv) and water (68 μL) were injected into the solution of **32** and the resulting mixture was shaken gently for 1 min at 0 °C. A ^{31}P{^{1}H} spectrum was acquired at 0 °C, which showed full conversion of **33** and clean formation of **32**.

^{31}P{^{1}H} NMR (202 MHz, THF, 0 °C) δ 66.2.

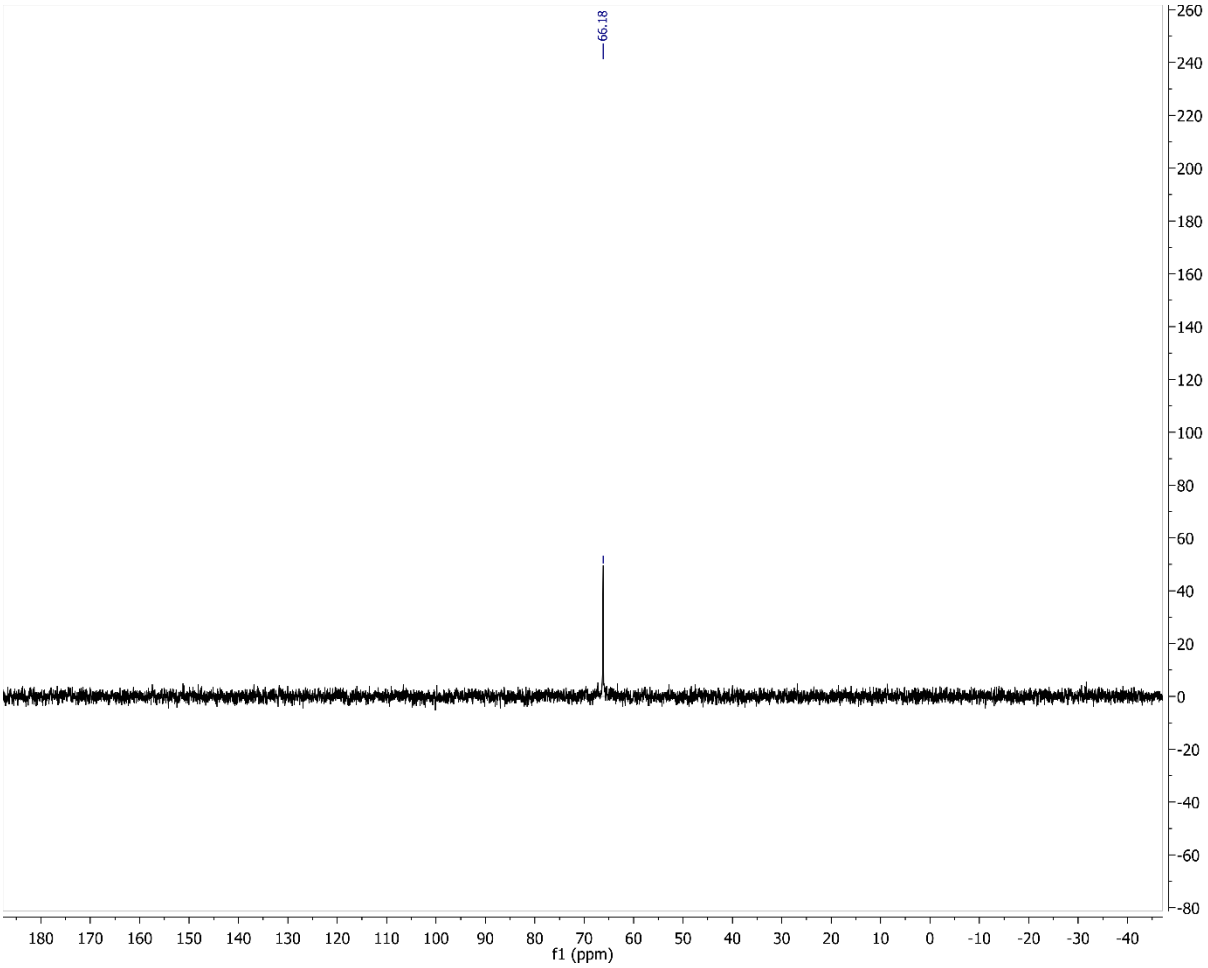

Figure S10. $^{31}P\{^{1}H\}$ NMR spectrum (202 MHz, THF, 0 °C) of the reaction of **33** with Et_3N and H_2O in THF.

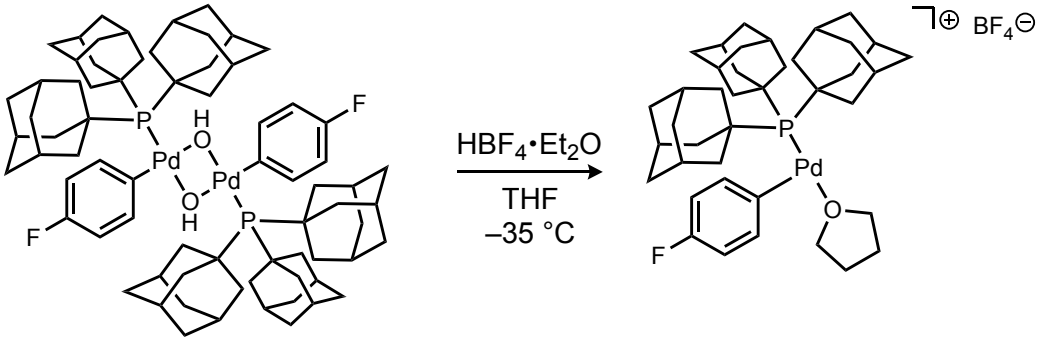

32 **33**

Conversion of 32 to 33. A solution of **32** (1.8 mg, 1.34 μmol) in THF-d_8 (0.5 mL) was transferred to an NMR tube capped with a rubber septum. Tetrafluoroboric acid diethyl ether complex (0.5 μL, 3.7 μmol, 1.3 equiv to Pd) was injected and the reaction mixture was shaken gently for 1 min at -35 °C. ^{1}H, ^{19}F, and ^{31}P{^{1}H} NMR spectra acquired at -25 °C, which indicated full conversion of **32** and clean formation of **33**.[3]

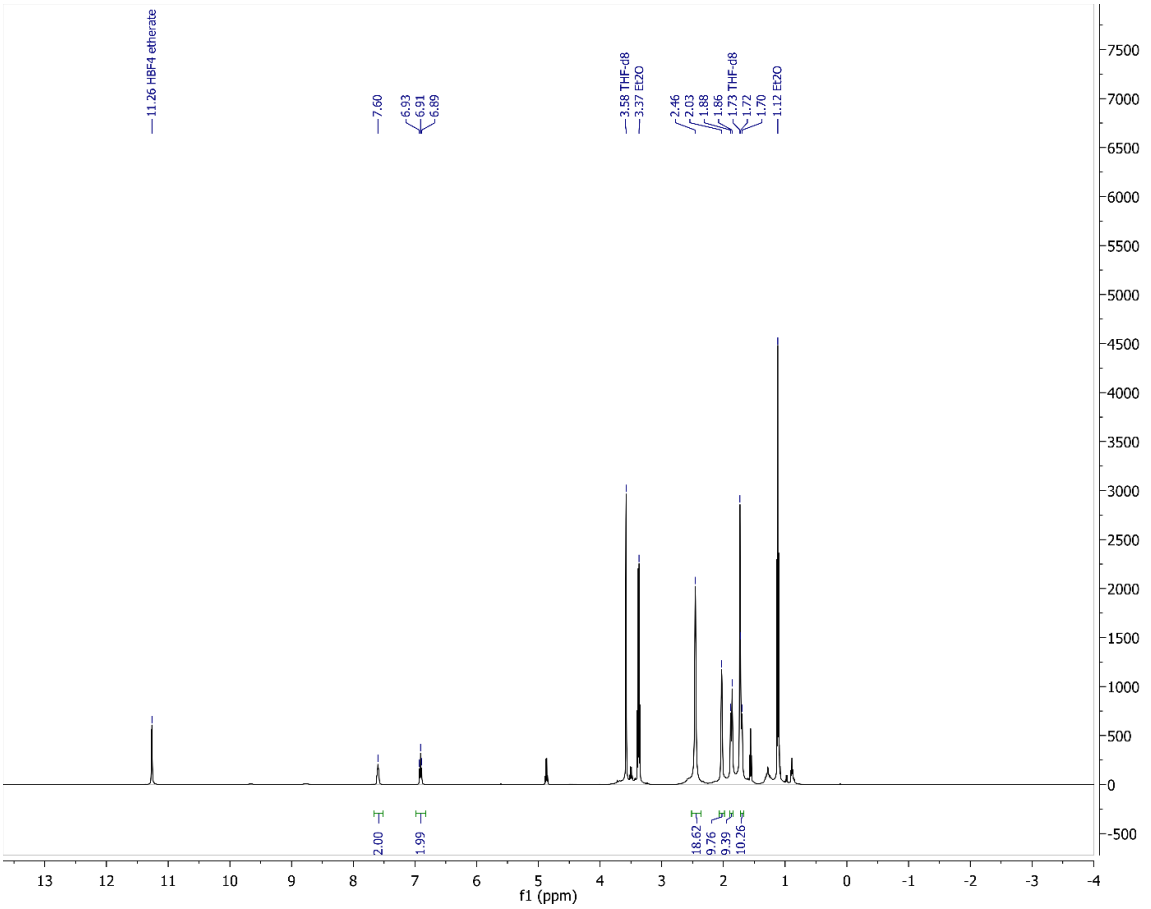

Figure S11. ^{1}H NMR spectrum (500 MHz, THF-d_8) of the mixture generated by reaction of **32** with $HBF_4{\cdot}Et_2O$ in THF at –35 °C.

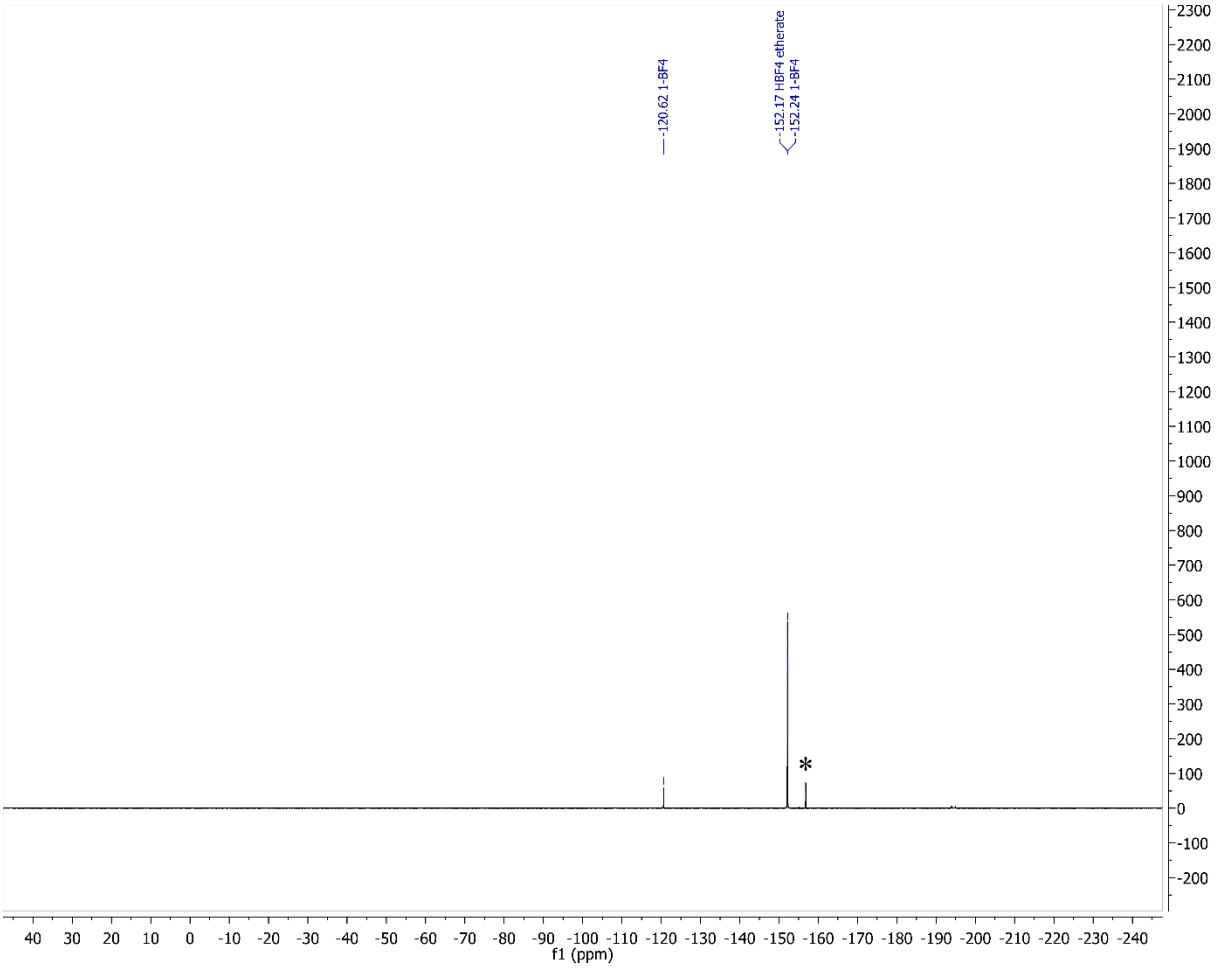

Figure S12. ^{19}F NMR spectrum (470 MHz, THF-d_8) of the mixture generated by reaction of **32** with $HBF_4 \cdot Et_2O$ in THF at –35 °C (* = unidentified).

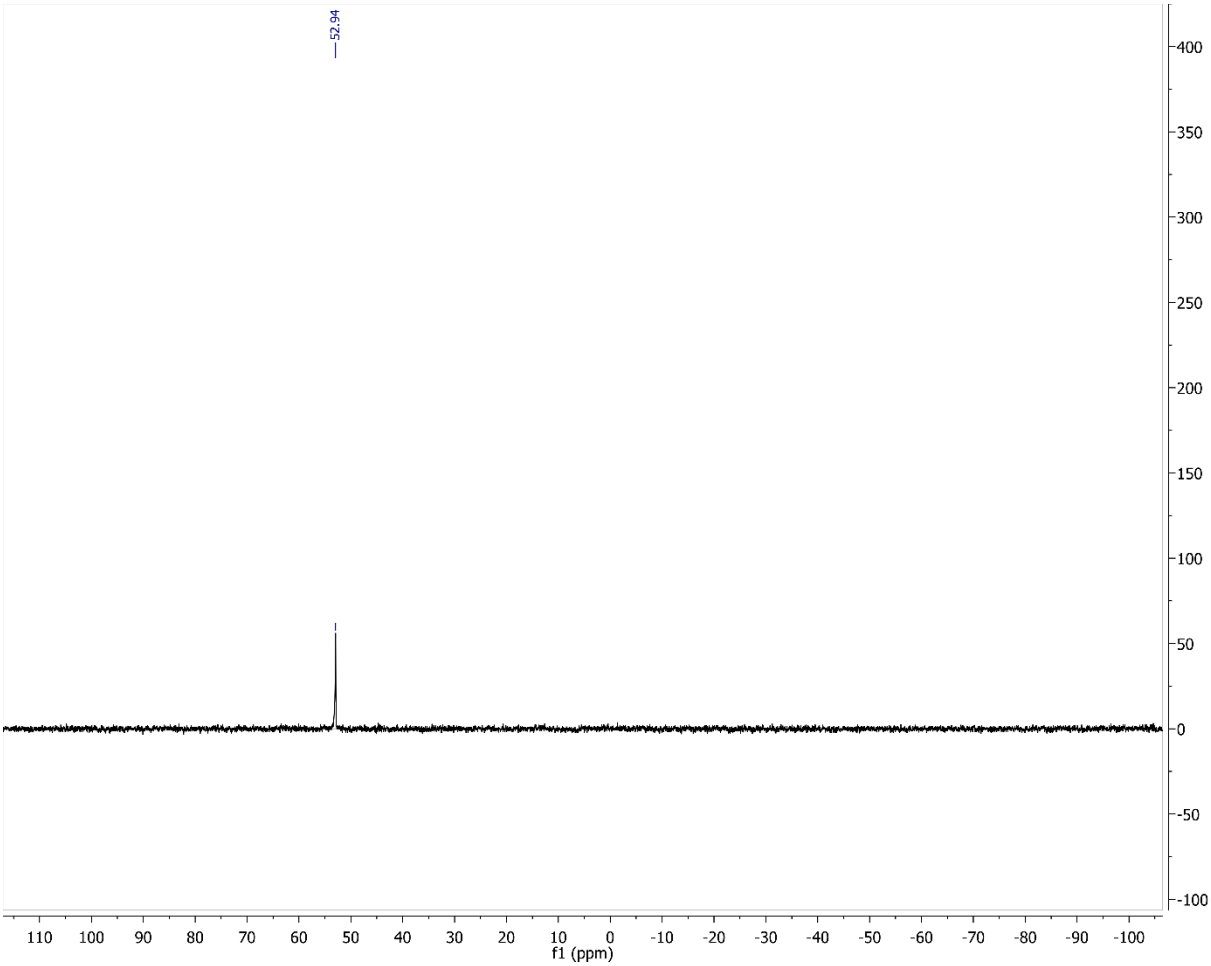

Figure S13. $^{31}P\{^{1}H\}$ NMR spectrum (202 MHz, THF-d_8) of the mixture generated by reaction of **32** with $HBF_4{\cdot}Et_2O$ in THF at –35 °C .

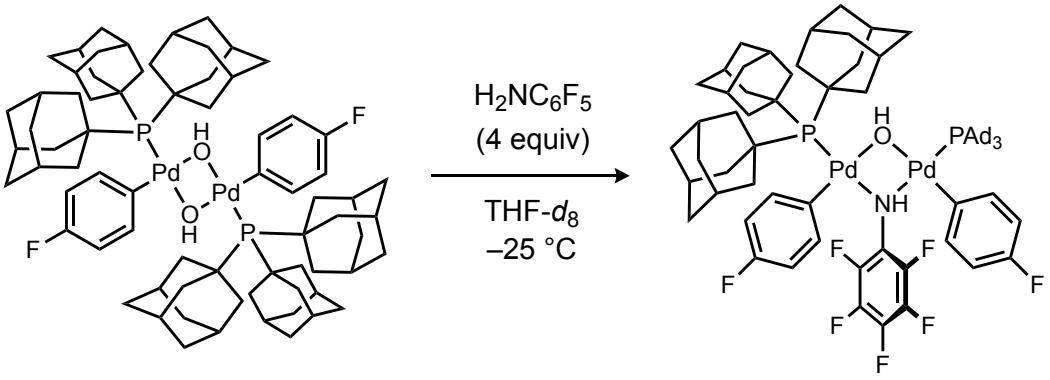

32 **34**

Synthesis and characterization of catalyst resting state, *syn*-[Pd$_2$(PAd$_3$)$_2$(4-C$_6$H$_4$F)$_2$(μ-OH)(μ-NH$_2$C$_6$F$_5$)] (34). A solution of **32** (4.9 mg, 3.8 μmol) in THF-*d*$_8$ (0.5 mL) was transferred to an NMR tube under nitrogen and capped with a rubber septum. Separately, pentafluoroaniline (2.8 mg, 15 μmol, 4 equiv) was dissolved in THF-*d*$_8$ (0.1 mL) in a 4 mL vial, and the resulting solution was added to the solution of **32** via a 1 mL syringe at low temperature (acetone/dry ice bath). The NMR tube was then shaken gently for 1 min. ^{1}H, ^{19}F, and ^{31}P{^{1}H} NMR spectra acquired at –25 °C indicated full conversion of **32** and clean formation of **34**. An EXSY NMR analysis indicated exchange between free $C_6F_5NH_2$ and the μ-anilido ligand in **34** during NMR time scale suggesting formation of **34** can occur reversibly.

^{1}H NMR (500 MHz, THF-*d*$_8$) δ 7.33 (t, *J* = 7.2 Hz, 2H), 6.51 (td, *J* = 8.9, 3.1 Hz, 2H), 6.46 (t, *J* = 7.6 Hz, 2H), 6.20 (td, *J* = 8.7, 3.1 Hz, 2H), 2.74 (s, 2H), 2.70 – 2.53 (m, 36H), 2.46 – 2.27 (m, 18H), 2.03 – 1.58 (m, 36H, partly obscured by THF residual peak), -3.84 (s, 1H).

^{19}F NMR (470 MHz, THF-*d*$_8$) δ -125.09 (2F), -147.73 (1F), -158.18 (1F), -170.71 (1F), -171.42 (1F), -176.06 (1F).

^{31}P{^{1}H} NMR (202 MHz, THF-*d*$_8$) δ 58.8.

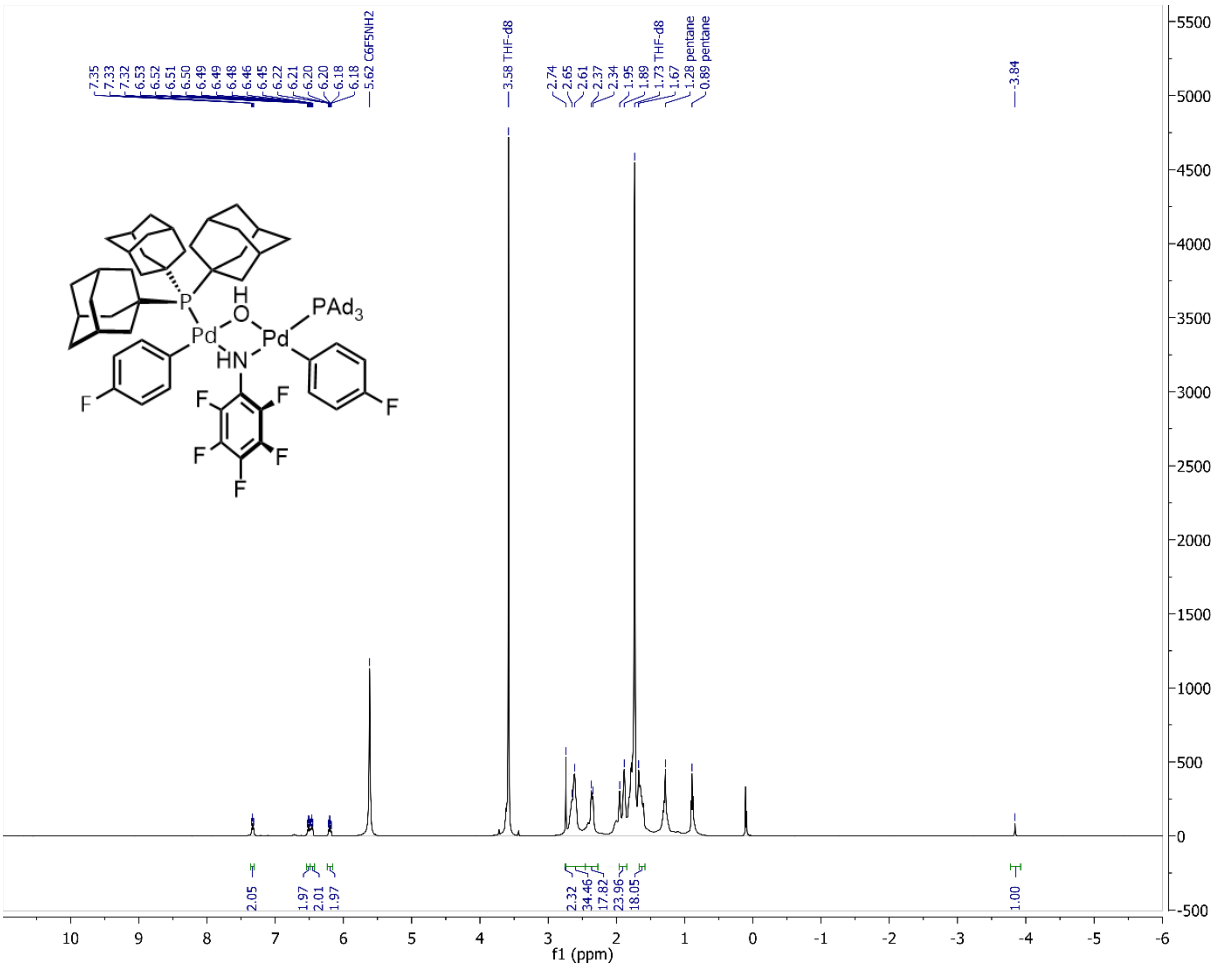

Figure S14. ^{1}H NMR spectrum (500 MHz, THF-d_8) of **34**.

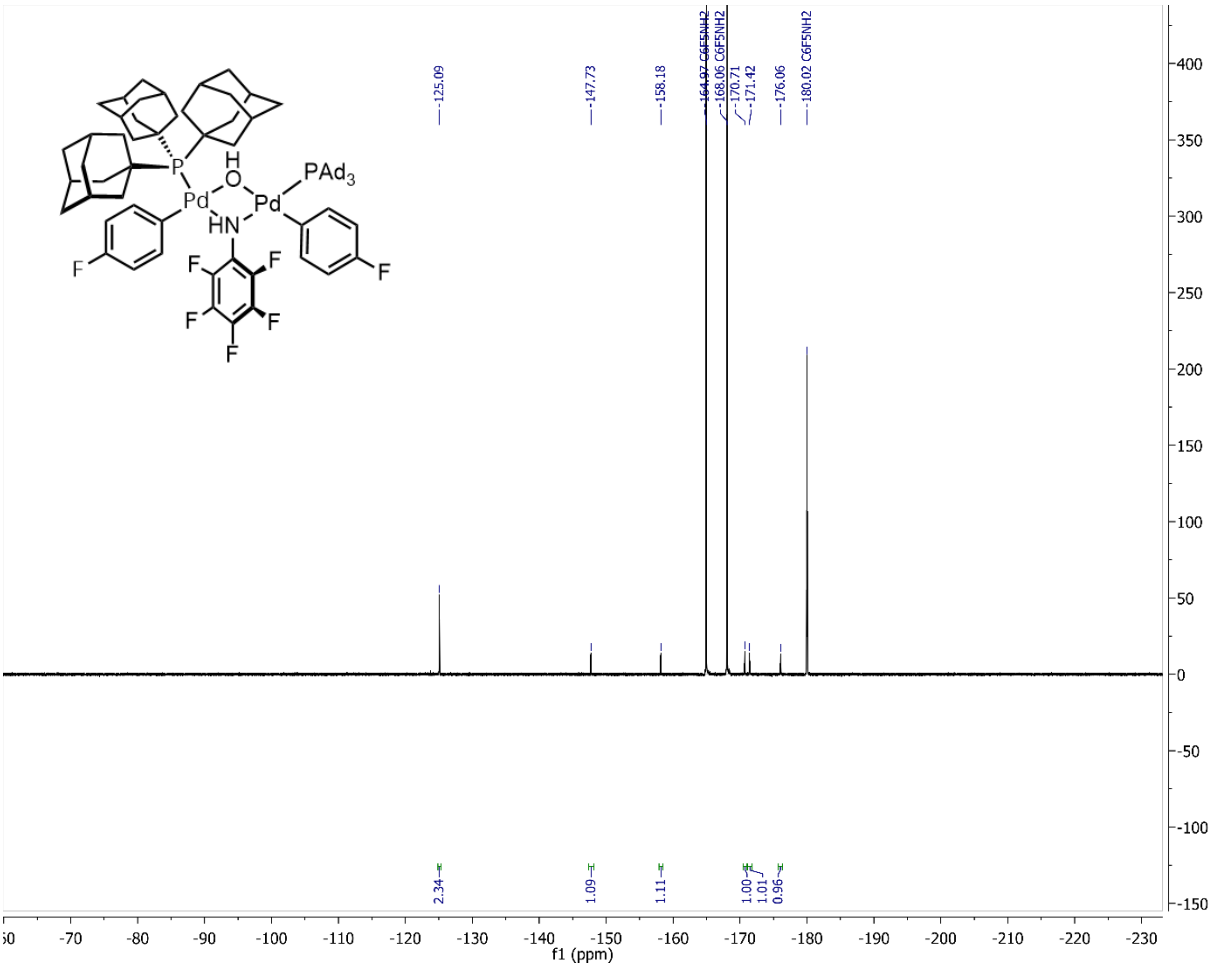

Figure S15. ^{19}F NMR spectrum (470 MHz, THF-d_8) of **34**.

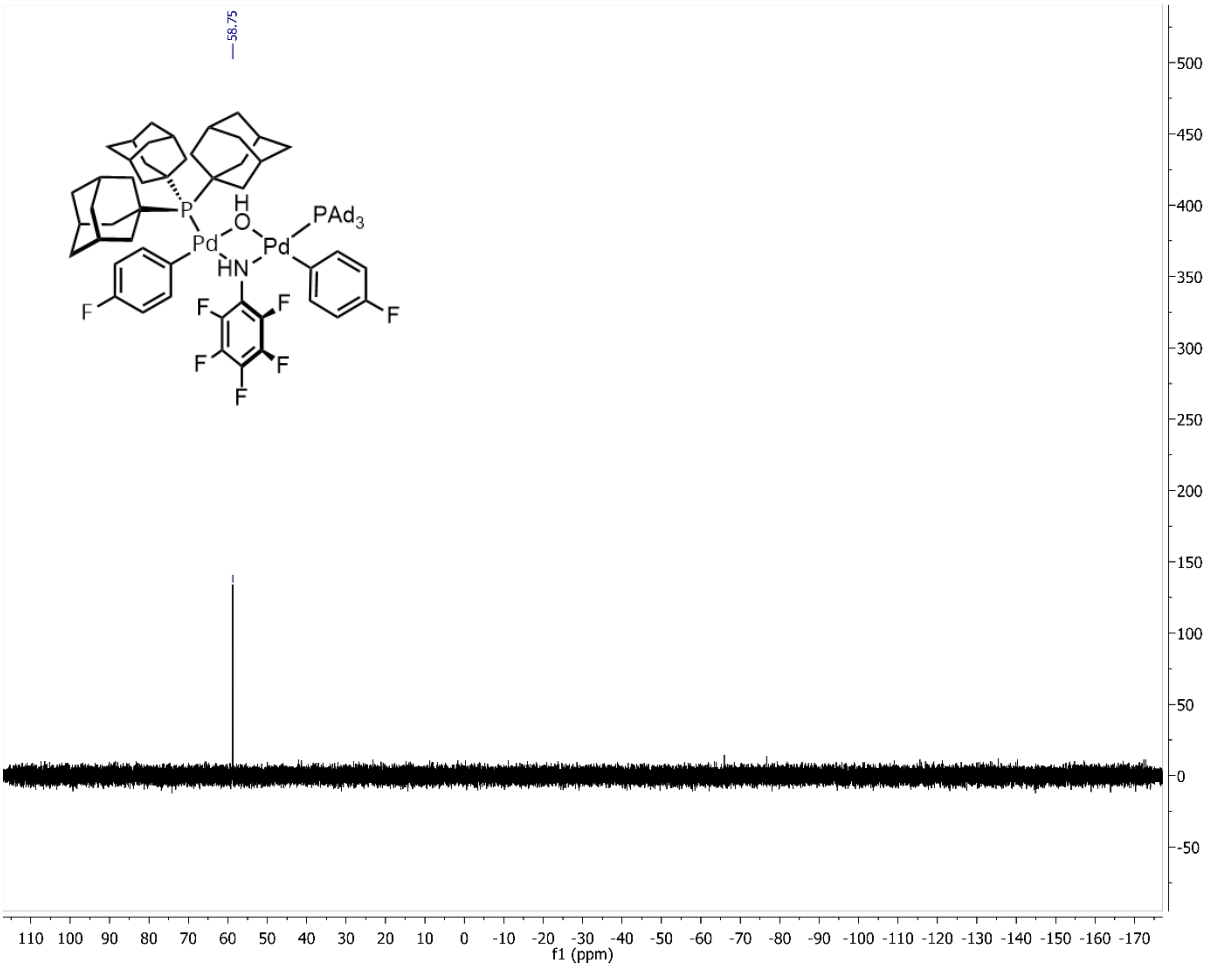

Figure S16. $^{31}P\{^{1}H\}$ NMR spectrum (202 MHz, THF-d_8) of **34**.

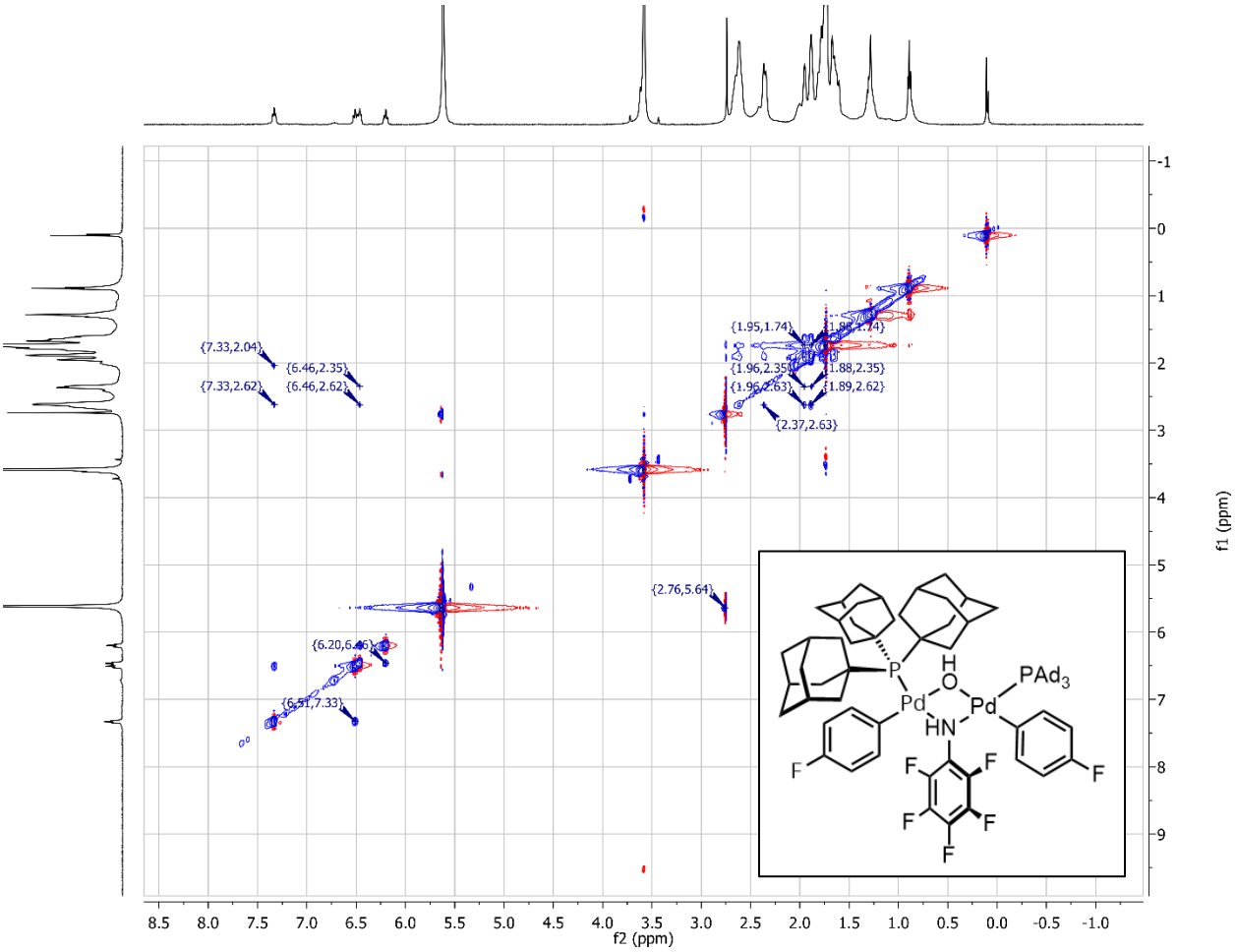

Figure S17. ^{1}H-^{1}H NOESY/EXSY NMR spectrum (500 MHz, THF-d_8) of **34**.

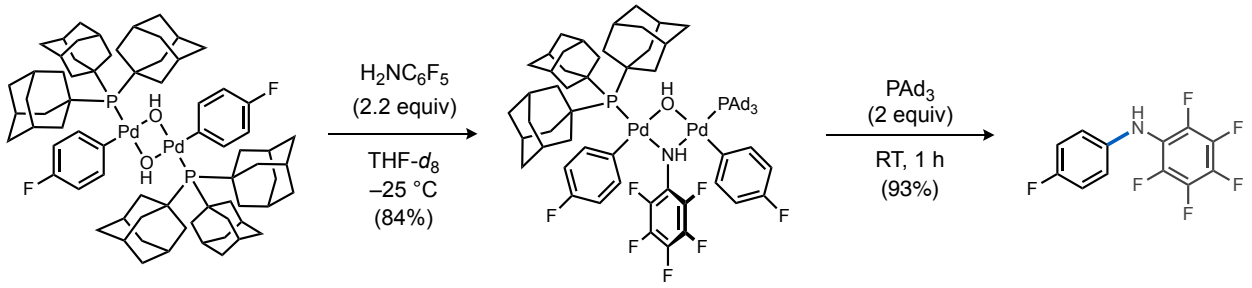

32 **34** **4**

Stoichiometric C–N bond formation from resting state complex 34. In a glove box, **32** (3.3 mg, 2.5 μmol) and octafluorotoluene (internal standard, 15 μL, 106 μmol) were dissolved in THF (0.5 mL) in a 4 mL vial. The resulting solution was transferred into an NMR tube capped with a rubber septum. Separately, pentafluoroaniline (10 mg, 55 μmol) was dissolved in THF (1 mL) in a 4 mL vial, and the resulting solution (0.1 mL, 5.5 μmol, 2.2 equiv) was drawn into a 1 mL syringe. A solution of PAd_3 (4.4 mg, 10 μmol) in THF (0.2 mL) was drawn into another 1 mL syringe. The syringe needles were sealed by insertion into a rubber septum to prevent exposure to air. Both the NMR tube and syringes were taken out of the box, and the $C_6F_5NH_2$ solution was then injected into the NMR tube cooled in an acetone/dry ice bath. The NMR tube was shaken gently for 1 min after the addition. ^{19}F and $^{31}P\{^1H\}$ NMR spectra acquired at –25 °C, which confirmed full conversion of **32** and formation of **34** (84%). Next, the PAd_3 solution (to stabilize $(Ad_3P)Pd^0$) was injected into the NMR tube at -78 °C, and the mixture was warmed up to room temperature. ^{19}F and $^{31}P\{^1H\}$ NMR spectra acquired after 1 h, which indicated full conversion of **34** and formation of **4** in 93% yield.

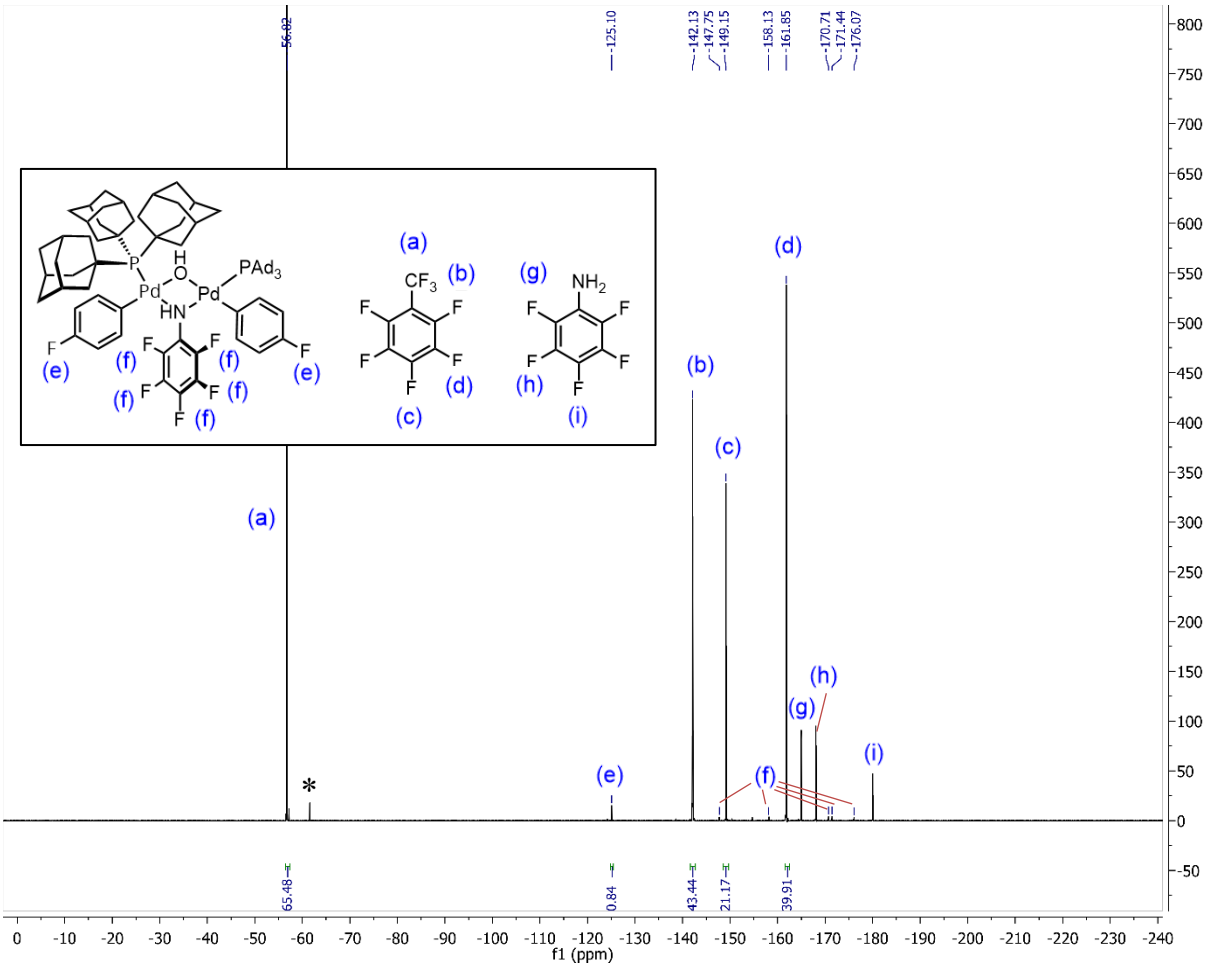

Figure S18. ^{19}F NMR spectrum (470 MHz, THF) of **34** generated in presence of internal standard (* = unidentified).

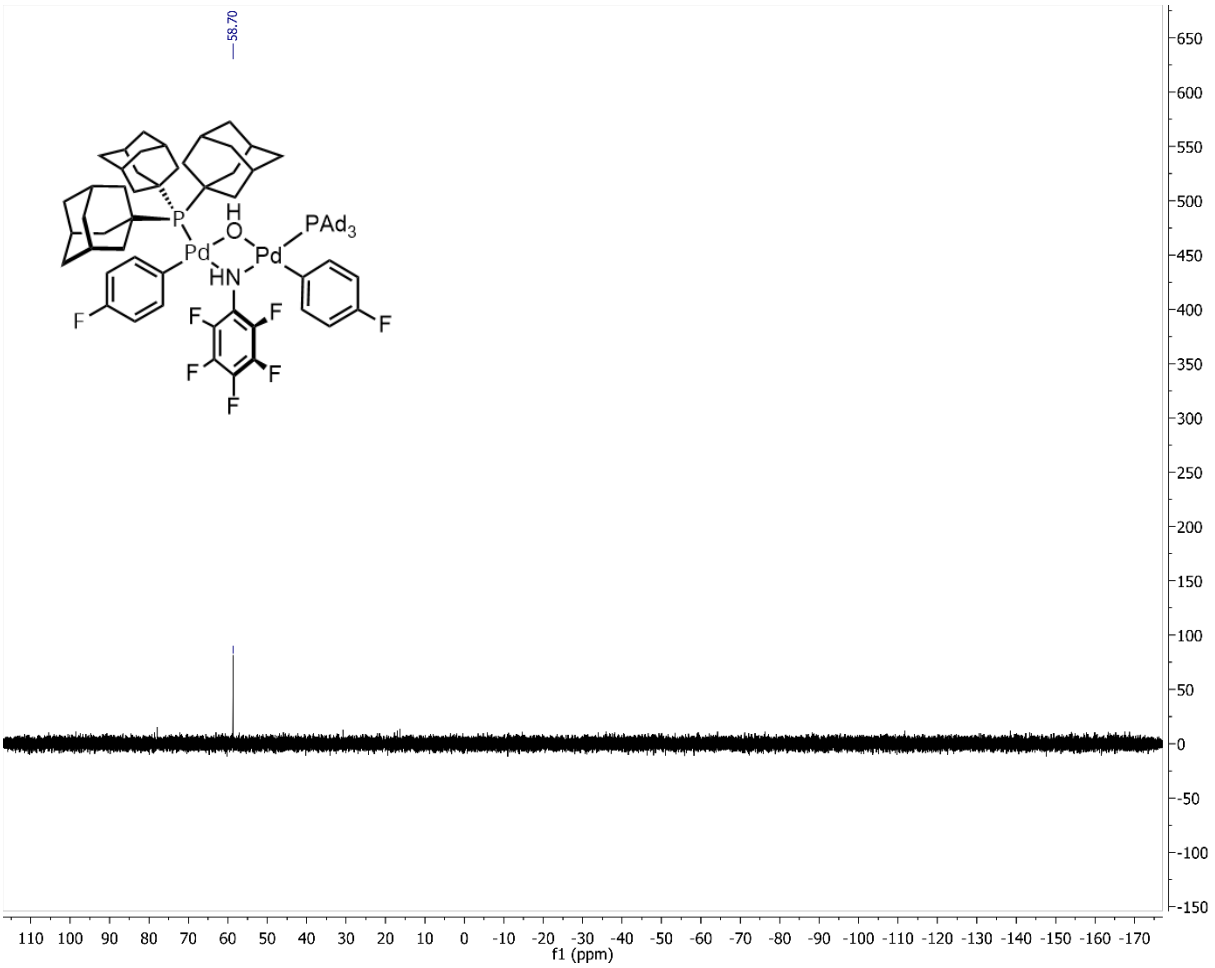

Figure S19. $^{31}P\{^{1}H\}$ NMR spectrum (202 MHz, THF) of **34**.

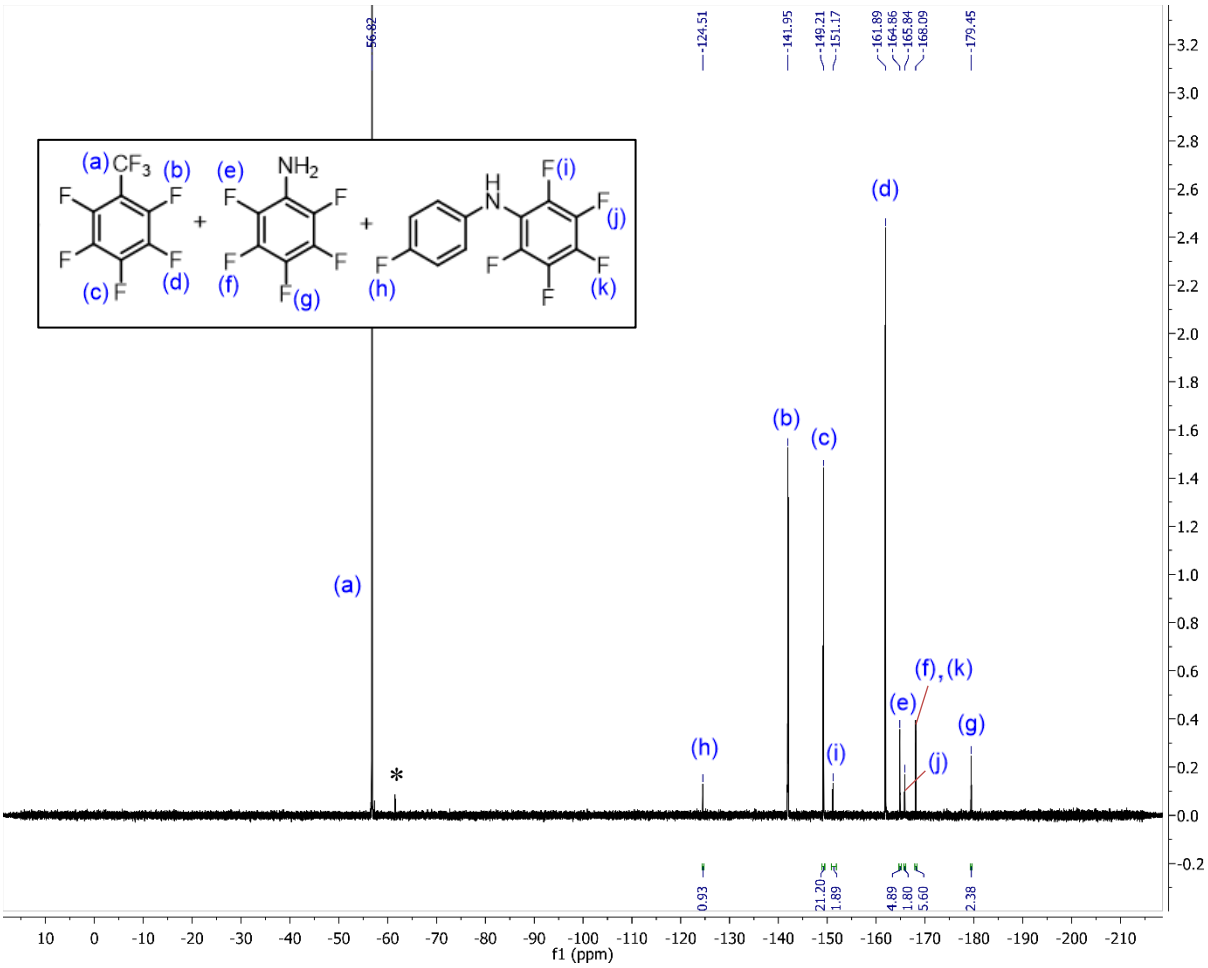

Figure S20. ^{19}F NMR spectrum (470 MHz, THF) of **4** generated upon warming a solution of **34** (* = unidentified).

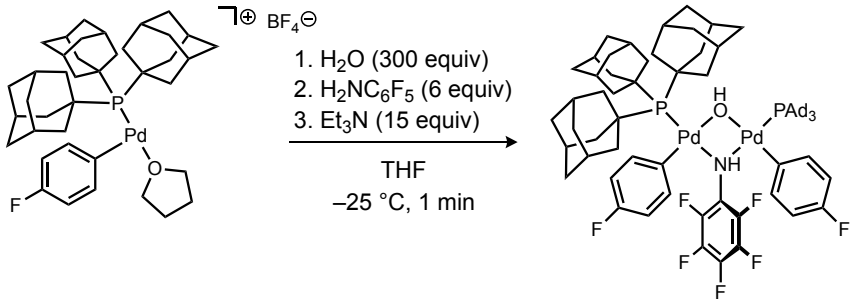

33 **34**

Independent synthesis of 34 from 33 in the presence of H_2O. The generation of $[Pd(PAd_3)(4\text{-}FC_6H_4)]^+$ BF_4^- (**33**) was adapted from a known procedure.[3] $Pd(PAd_3)(4\text{-}FC_6H_4)Br$ (**1**) (9.0 mg, 12.5 μmol) was dissolved in THF (2.5 mL). Separately, $AgBF_4$ (20 mg, 0.10 mmol) was dissolved in THF (2 mL). Both solutions were chilled at -35 °C ($MeOH/H_2O$ dry ice bath). The latter solution ($AgBF_4$, 2.5 μmol, 50 μL) was then added to the solution of **1** (2.5 μmol, 0.5 mL) in a 4 mL vial at -35 °C. The mixture (0.55 mL) was quickly shaken, left in the cooling bath for 10 min, and transferred into an NMR tube capped with a rubber septum. Next, degassed deionized water (14 μL, 0.75 mmol, 300 equiv), pentafluoroaniline (0.1 mL from a 15 mM stock solution in THF, 15 μmol, 6 equiv), and triethylamine (5 μL, 38 μmol, 15 equiv) were injected into the NMR tube sequentially at -78 °C. The reaction mixture was shaken gently for 1 min, then a $^{31}P\{^1H\}$ NMR spectrum was acquired at -25 °C, which indicated clean formation of **34**.

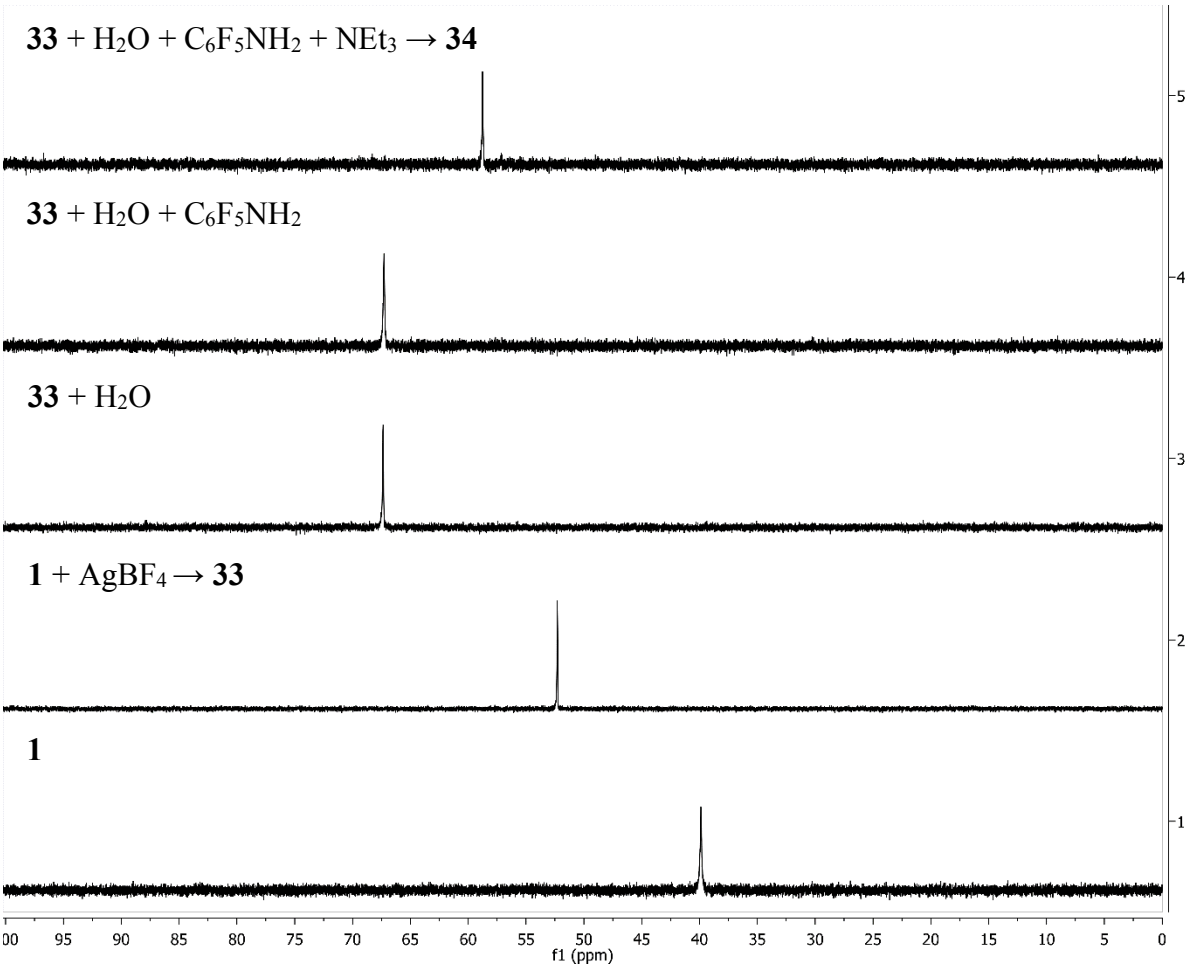

Figure S21. Stacked $^{31}P\{^{1}H\}$ NMR spectra (202 MHz, THF) for generation of **34** from **1** (via **33**) by sequential addition of (top to bottom) $AgBF_4$, water, pentafluoroaniline, then Et_3N.

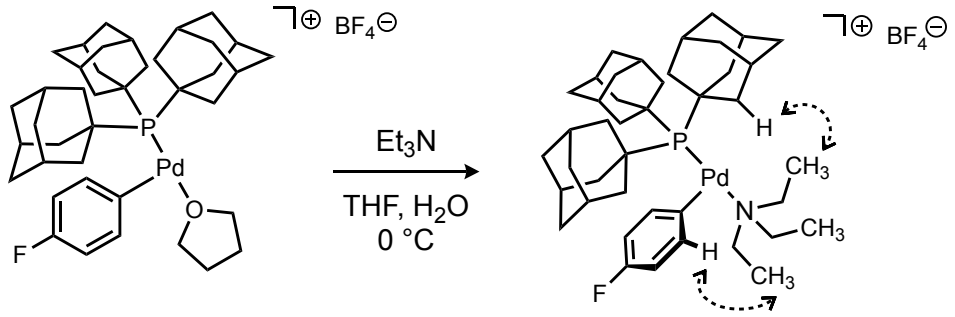

33 **35**

Synthesis and characterization of [Pd(PAd$_3$)(4-FC$_6$H$_4$)(NEt$_3$)]$^+$ BF$_4^-$ (35). The generation of [Pd(PAd$_3$)(4-FC$_6$H$_4$)]$^+$ BF$_4^-$ (**33**) was adapted from a known procedure.[3] Pd(PAd$_3$)(4-FC$_6$H$_4$)Br **1** (5.4 mg, 7.5 μmol) was dissolved in THF-*d*$_8$ (1.5 mL). Separately, AgBF$_4$ (9.8 mg, 50 μmol) was dissolved in THF-*d*$_8$ (1 mL). Both solutions were chilled at -35 °C (MeOH/H$_2$O dry ice bath). The latter solution (AgBF$_4$, 2.5 μmol, 50 μL) was then added to the solution of **1** (2.5 μmol, 0.5 mL) in a 4 mL vial at -35 °C. Octafluorotoluene (internal standard, 0.3 μL, 1.9 μmol) was added to the solution. The mixture (0.55 mL) was quickly shaken, left in the cooling bath for 10 min, and transferred into an NMR tube capped with a rubber septum. ^{1}H, ^{19}F, and ^{31}P{^{1}H} NMR spectra were acquired at -25 °C to confirm clean formation of **33** prior to proceeding to the next step. Next, triethylamine (5.0 μL, 38 μmol, 15 equiv) was injected and the reaction mixture was shaken gently for 1 min at -35 °C. ^{1}H, ^{19}F, and ^{31}P{^{1}H} NMR spectra were acquired at -25 °C, which indicated formation of a new complex (**35**) in 74% yield along with an unidentified side product (19%). Analysis by EXSY NMR indicated exchange between free and Pd-bound NEt$_3$ on the NMR time scale; signals corresponding to the 4-fluorophenyl group on **35** and the unidentified side product supports an equilibrium process involving the two compounds. NOE correlations (dashed lines) between the 4-fluorophenyl on Pd and coordinated Et$_3$N, and also between PAd$_3$ resonances and coordinated Et$_3$N, support the structure assignment of **35** shown above.

^{1}H NMR (500 MHz, THF-*d*$_8$) δ 7.55 – 7.49 (m, 2H), 6.96 (t, *J* = 8.7 Hz, 2H), 2.47 (6H, obscured by NEt$_3$ peak), 2.43 (18H, obscured by NEt$_3$ peak), 2.07 (br, 9H), 1.87 – 1.69 (m, 18H, obscured by THF peak), 1.51 (br, 9H).

^{19}F NMR (470 MHz, THF-*d*$_8$) δ 120.5, 153.8

^{31}P{^{1}H} NMR (202 MHz, THF-*d*$_8$) δ 41.5.

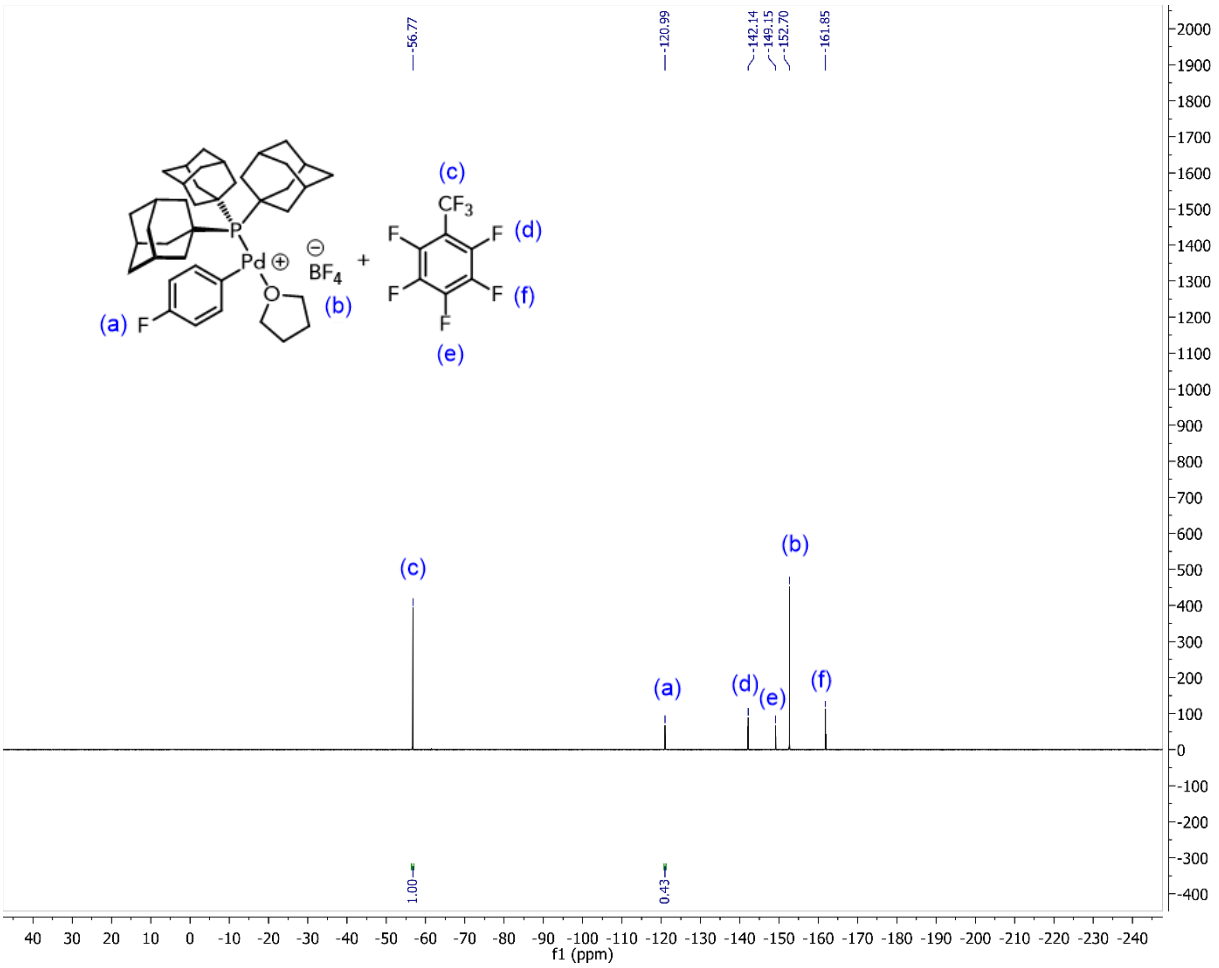

Figure S22. ^{19}F NMR spectrum (470 MHz, THF-d_8) of **33** generated prior to addition of Et_3N and formation of **35**.

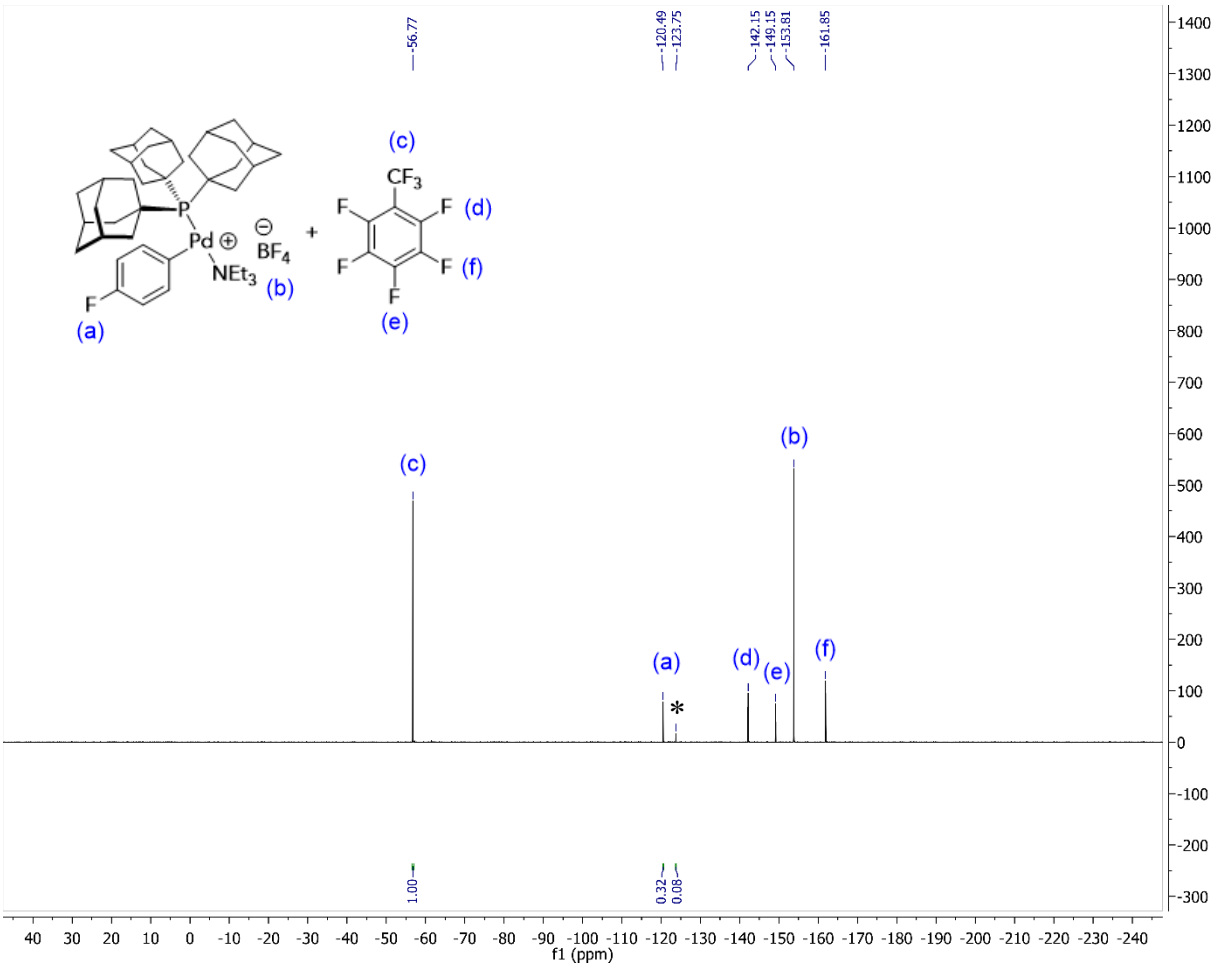

Figure S23. ^{19}F NMR spectrum (470 MHz, THF-d_8) of **35** (* = unidentified).

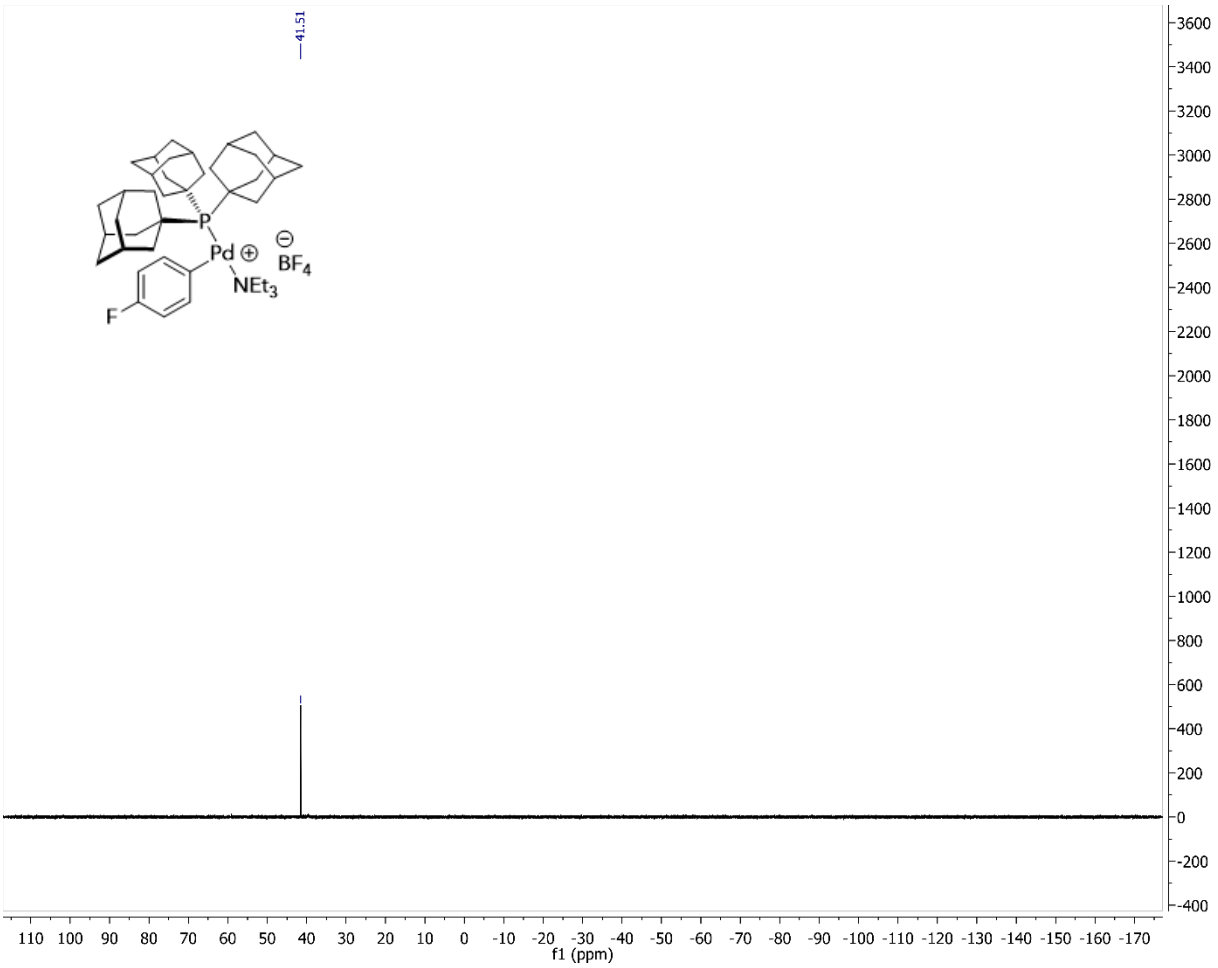

Figure S24. $^{31}P\{^{1}H\}$ NMR spectrum (202 MHz, THF-d_8) of **35**.

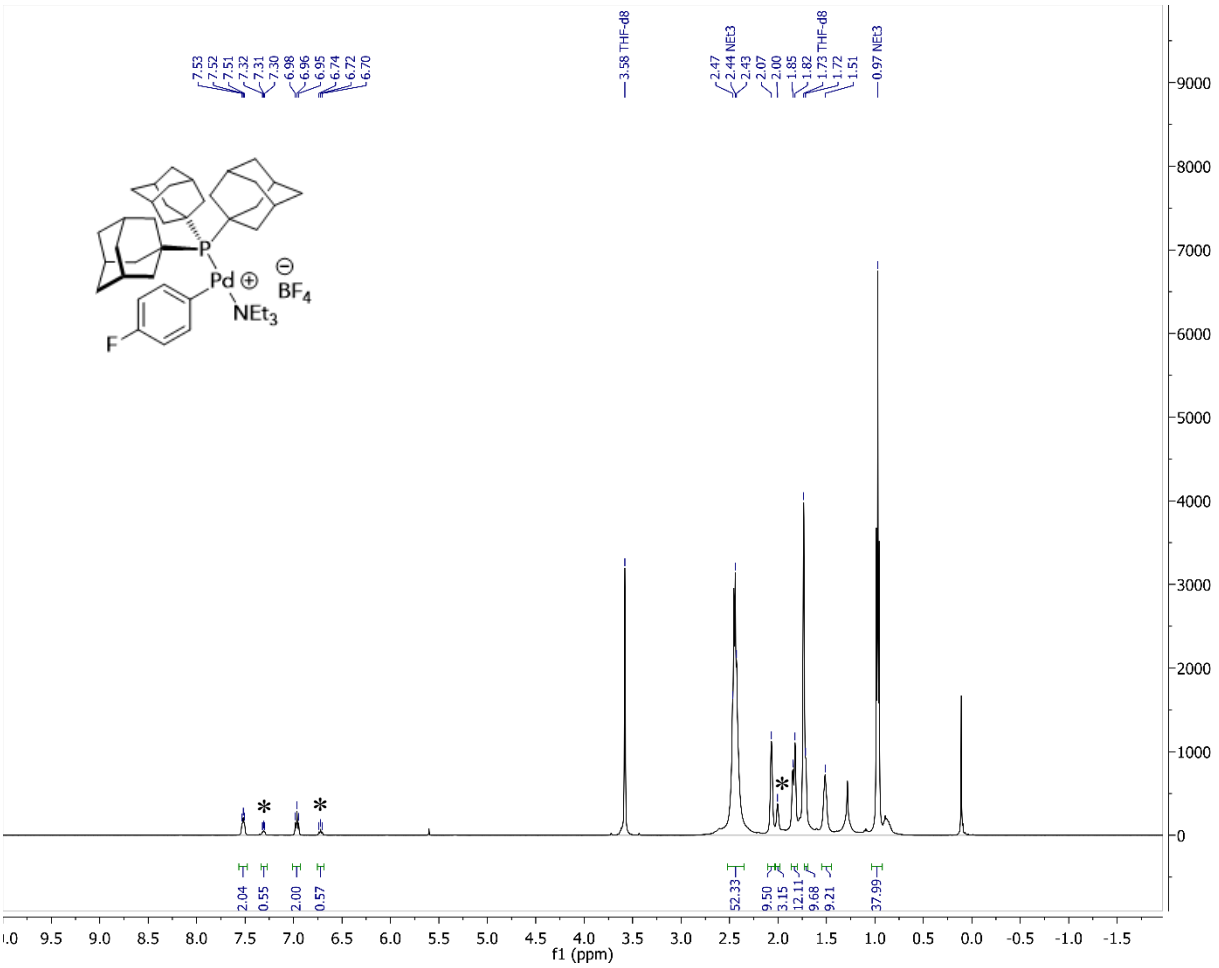

Figure S25. ^{1}H NMR spectrum (500 MHz, THF-d_8) of **35** (* = unidentified).

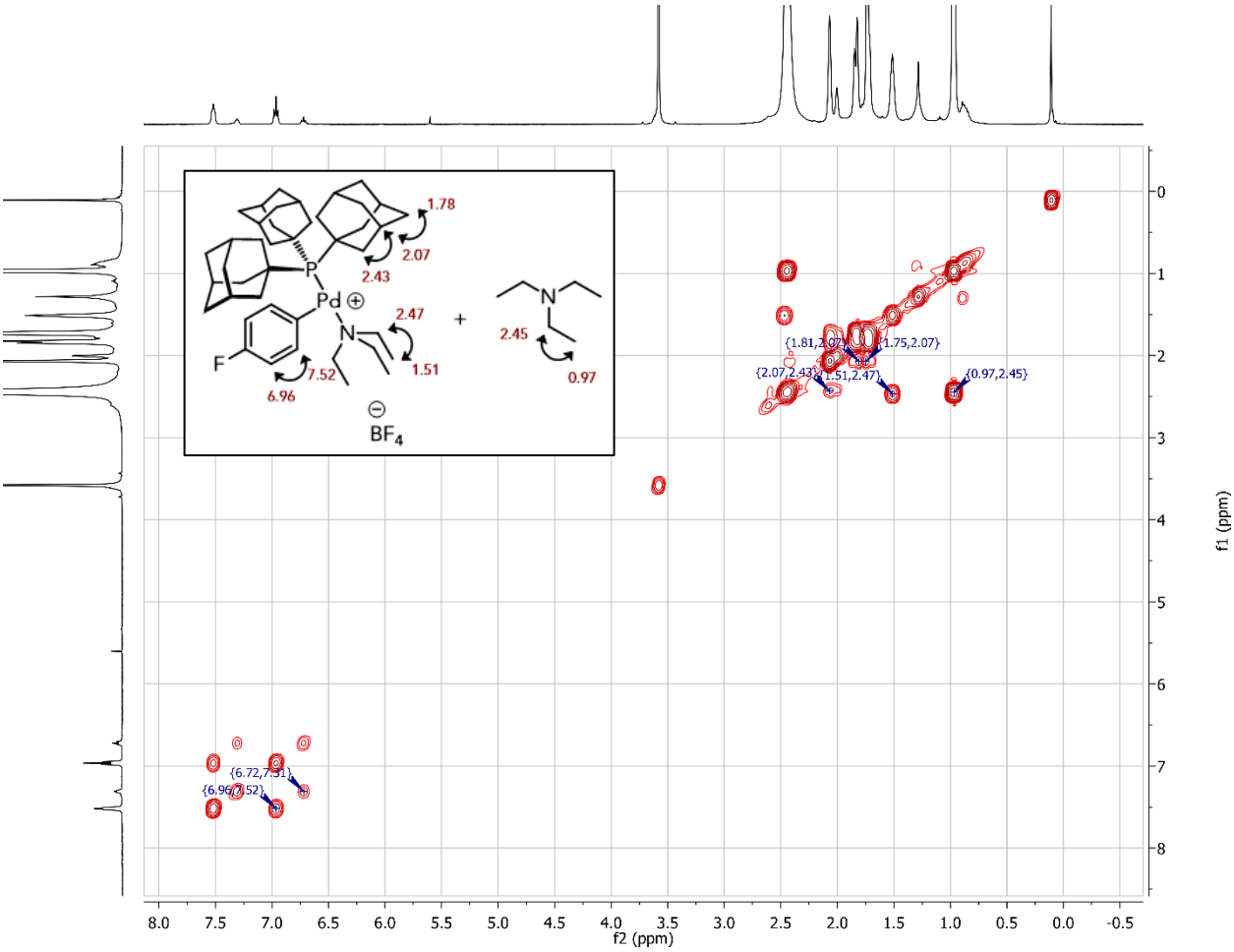

Figure S26. ^{1}H-^{1}H COSY NMR spectrum (500 MHz, THF-d_8) of **35**.

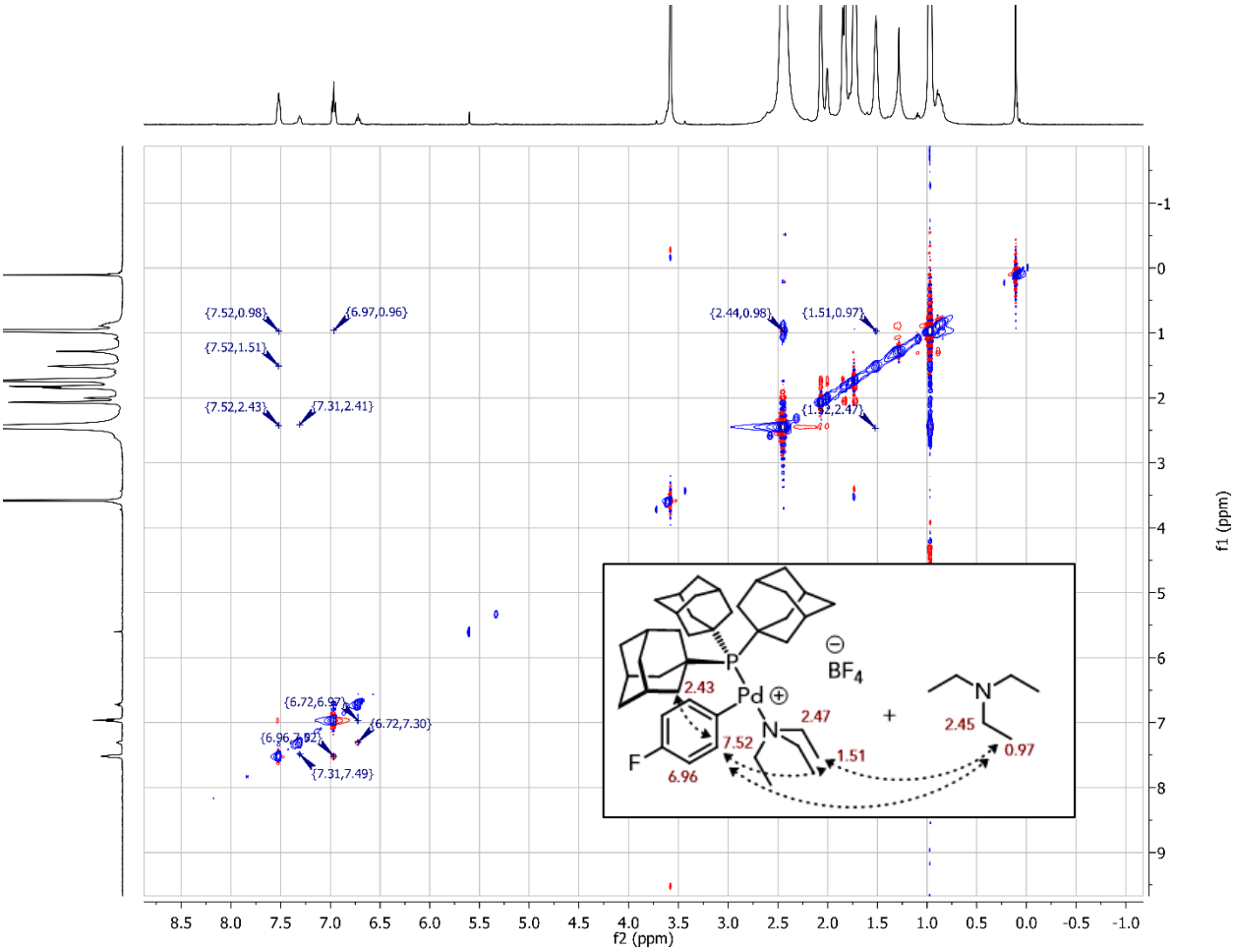

Figure S27. ^{1}H-^{1}H NOESY/EXSY NMR spectrum (500 MHz, THF-d_8) of **35**.

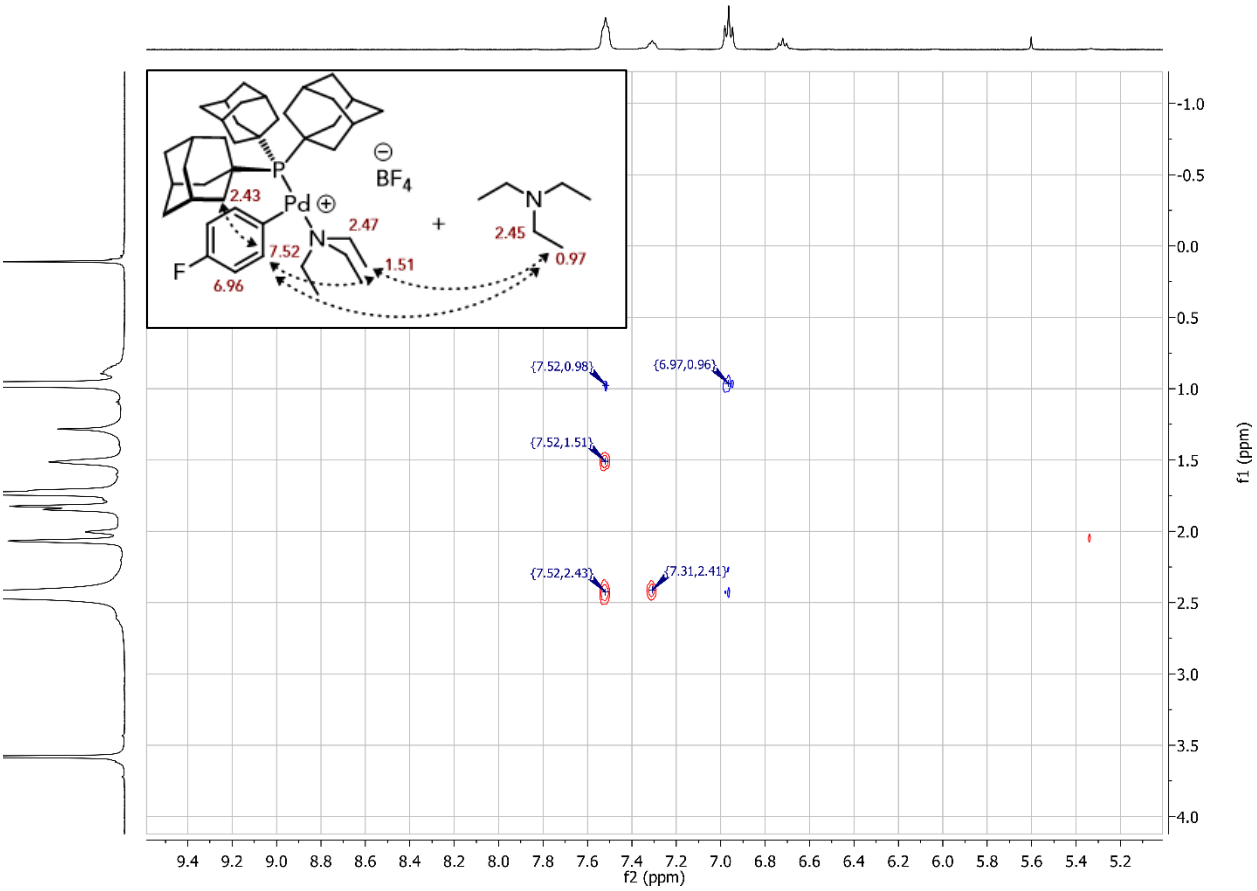

Figure S28. Inset of ^{1}H-^{1}H NOESY/EXSY NMR spectrum (500 MHz, THF-d_8) of **35**.

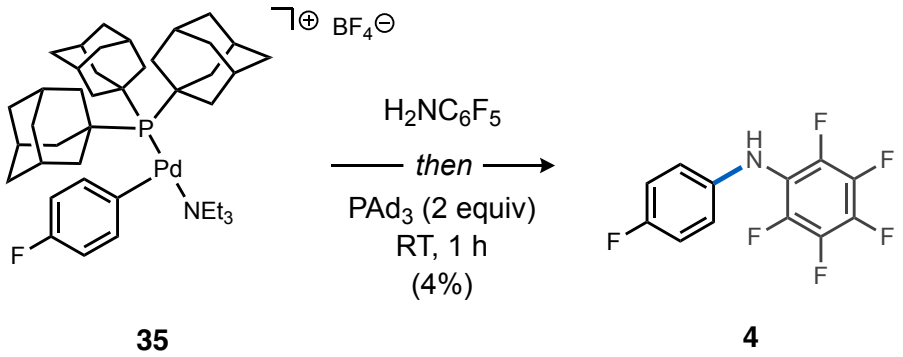

35 **4**

Attempted conversion of 35 into 4 in the absence of water. The generation of $[Pd(PAd_3)(4\text{-}FC_6H_4)]^+ BF_4^-$ (**33**) was adapted from a known procedure.[3] $Pd(PAd_3)(4\text{-}FC_6H_4)Br$ **1** (5.4 mg, 7.5 μmol) and trifluorotoluene (internal standard, 1 μL, 8.2 μmol) were dissolved in THF-d_8 (1.5 mL). Separately, $AgBF_4$ (10 mg, 50 μmol) was dissolved in THF-d_8 (1 mL). Both solutions were chilled at -35 °C (MeOH/H_2O dry ice bath). The latter solution ($AgBF_4$, 2.5 μmol, 50 μL) was then added to the solution of **1** (2.5 μmol, 0.5 mL) in a 4 mL vial at -35 °C. The mixture (0.55 mL) was quickly shaken, left in the cooling bath for 10 min, and transferred into an NMR tube capped with a rubber septum. Next, pentafluoroaniline (0.1 mL from a 15 mM stock solution in THF, 15 μmol, 6 equiv), and triethylamine (5 μL, 37.5 μmol, 15 equiv) were injected into the NMR tube sequentially at -78 °C. The reaction mixture was shaken gently for 1 min then a $^{31}P\{^1H\}$ NMR spectrum was acquired at -25 °C confirming formation of **35** (77%). Finally, a solution of PAd_3 (2.2 mg, 5.0 μmol, 2 equiv) in THF (0.1 mL) was injected into the NMR tube and the mixture was warmed to room temperature. After 1 h, ^{19}F and $^{31}P\{^1H\}$ NMR spectra were acquired that showed formation of only a trace of **4** (4%).

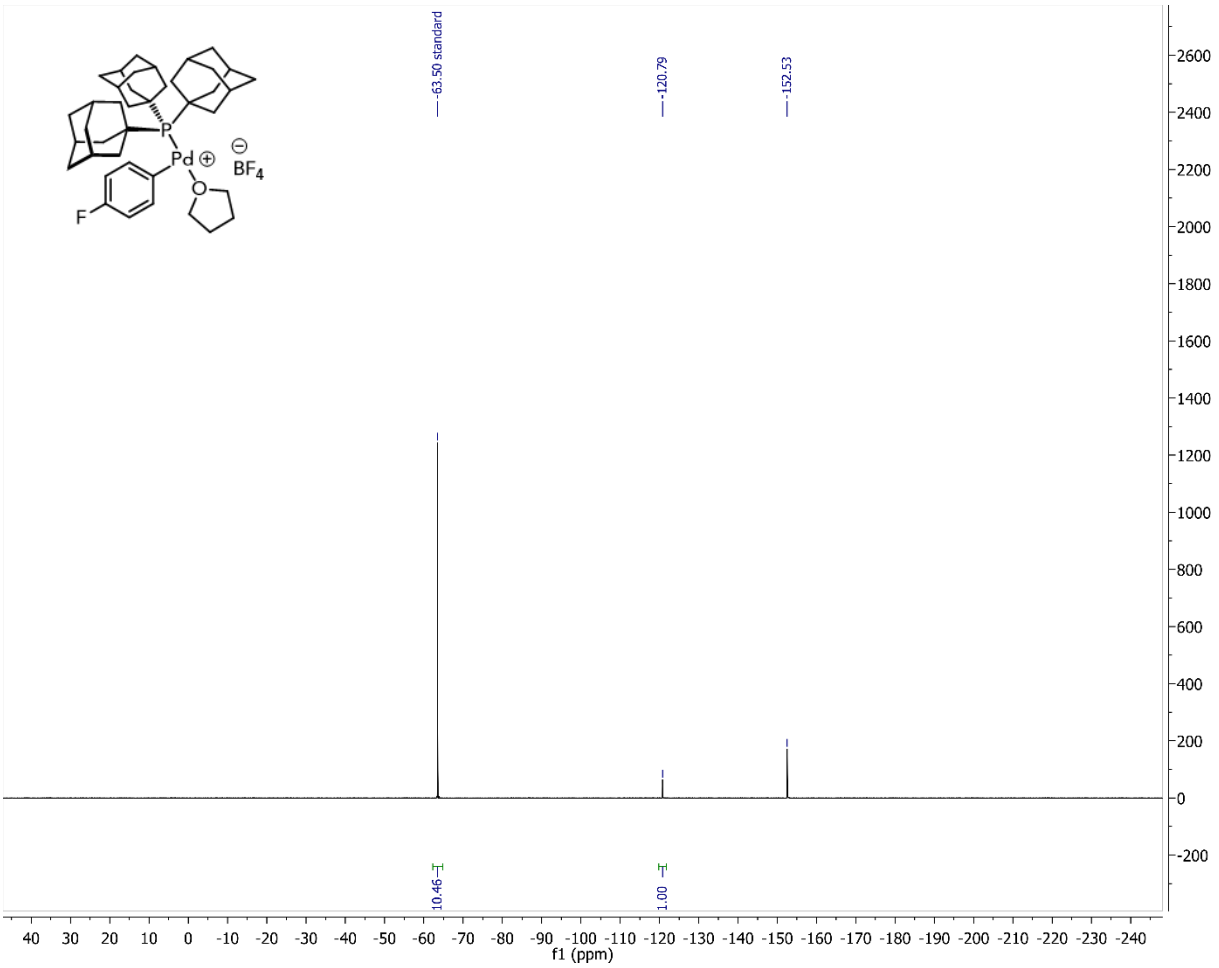

Figure S29. ^{19}F NMR spectrum (470 MHz, THF) of **33** prior to addition of Et_3N and formation of **35**.

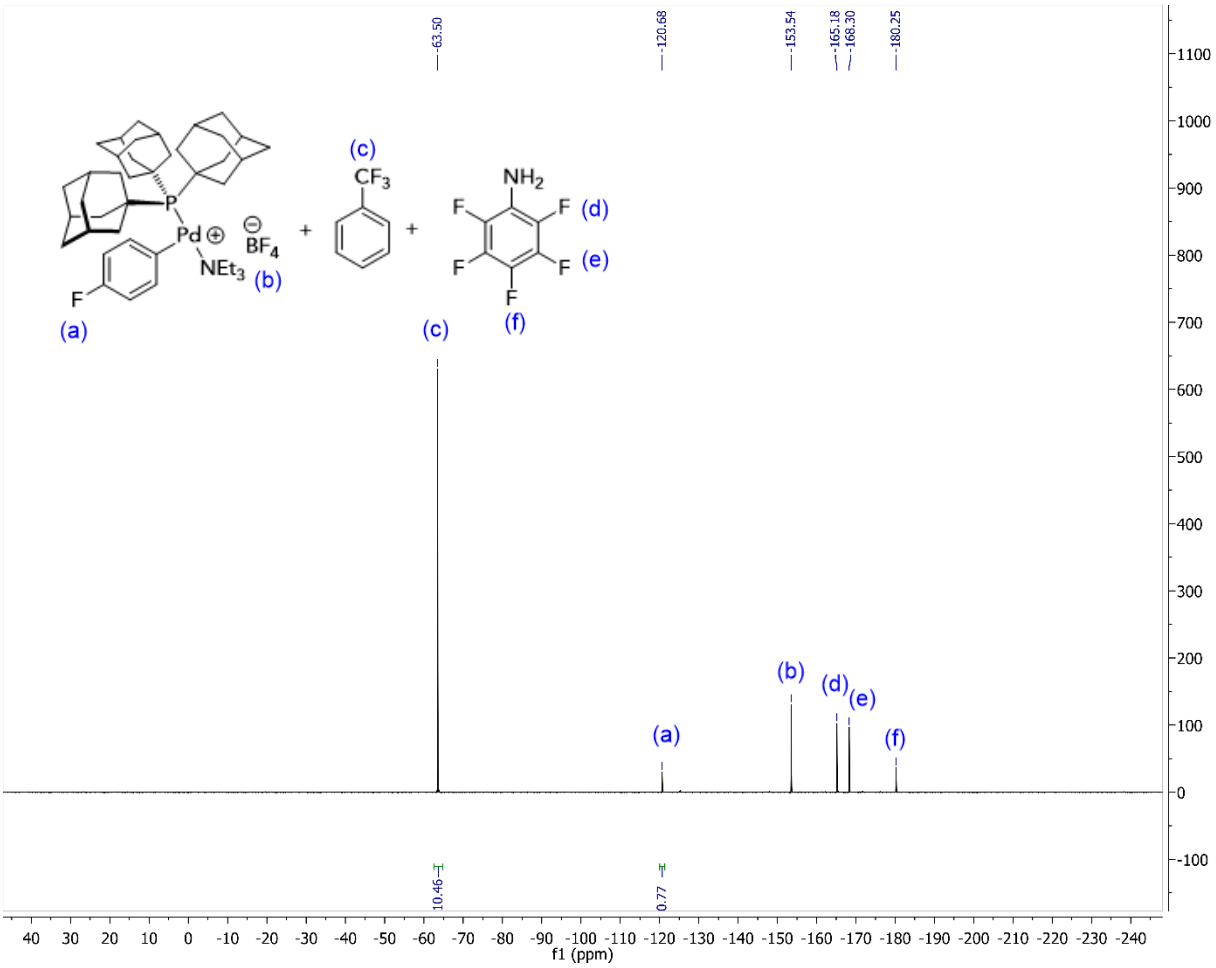

Figure S30. ^{19}F NMR spectrum (470 MHz, THF) of **35** in the presence of pentafluoroaniline, indicating the preference for coordination of Et_3N to Pd.

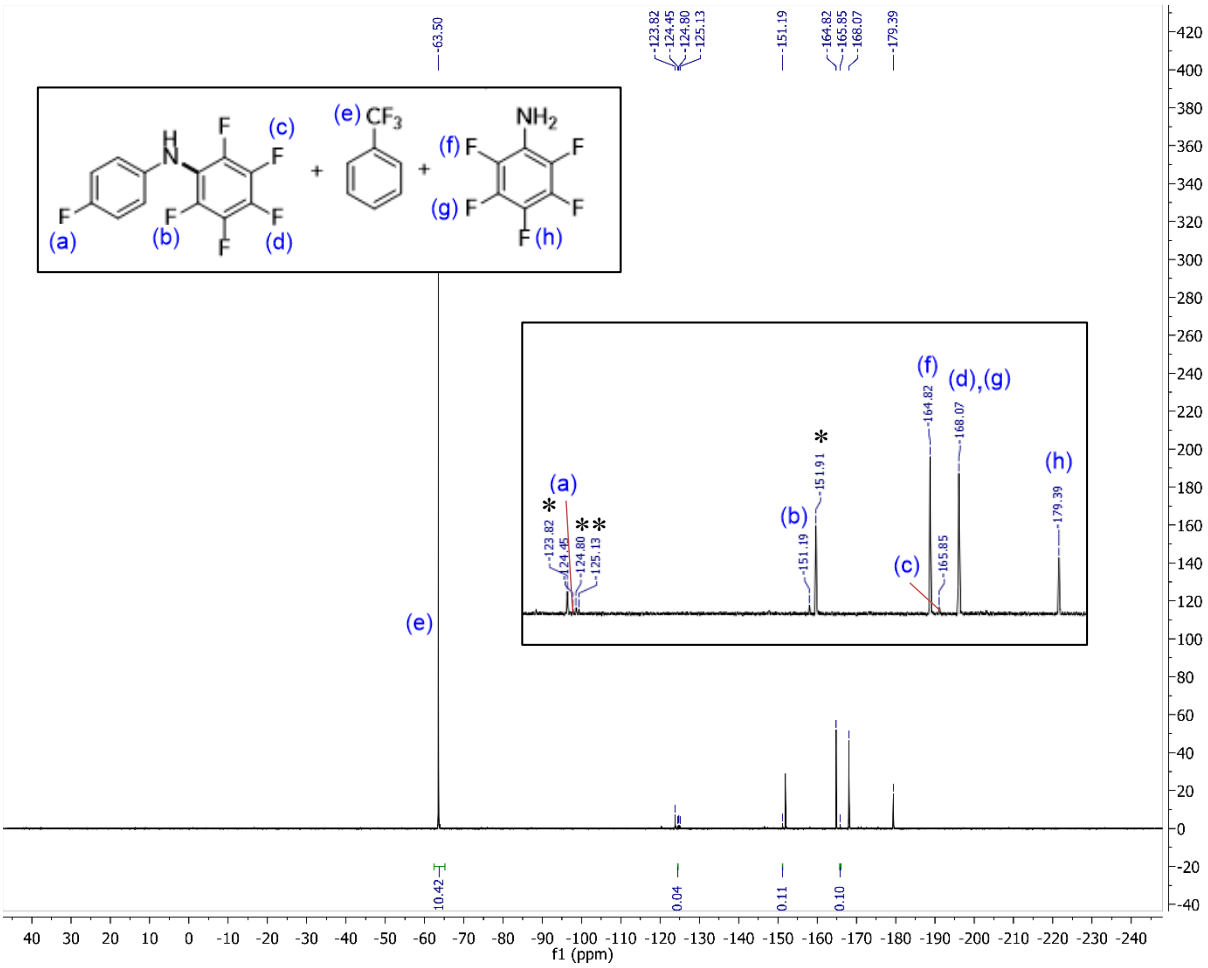

Figure S31. ^{19}F NMR spectrum (470 MHz, THF) of **35** after warming to RT for 1 h (* = unidentified).

Rapid conversion of 35 into 32 in the presence of water. The sequential conversion of **1** (7.5 µmol scale) to **33** then to **35** was repeated according to the procedure described above. Water (1 µL, 75 µmol, 10 equiv) was injected into the solution of **35** and the resulting mixture was shaken gently for 1 min at 0 °C. A $^{31}P\{^{1}H\}$ spectrum (Figure S31) was then acquired at -25 °C, which showed consumption of **35** and formation of **32** as the only new species.

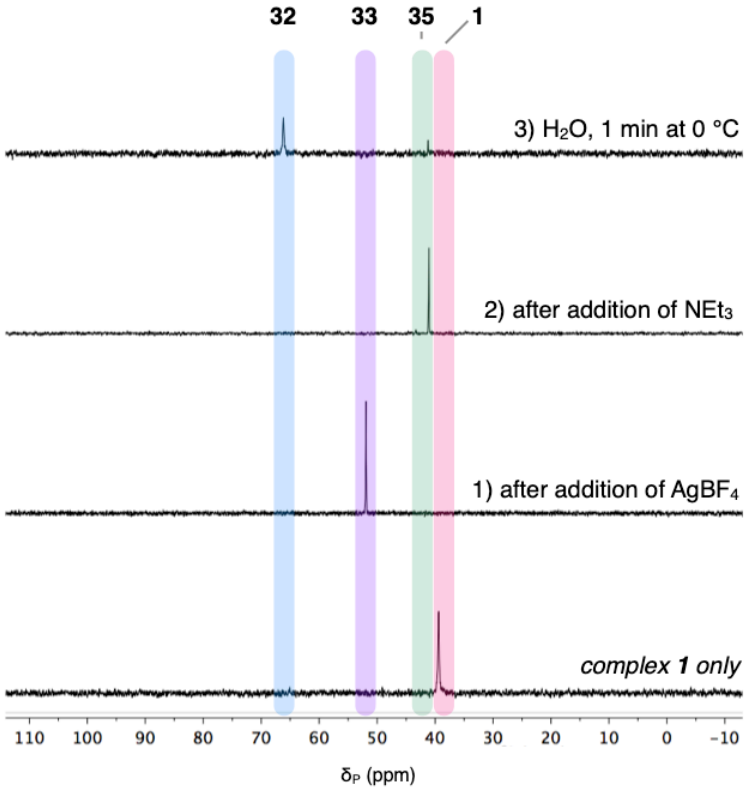

Figure S32. ^{19}F NMR spectrum (470 MHz, THF) of **35** after warming to RT for 1 h (* = unidentified).

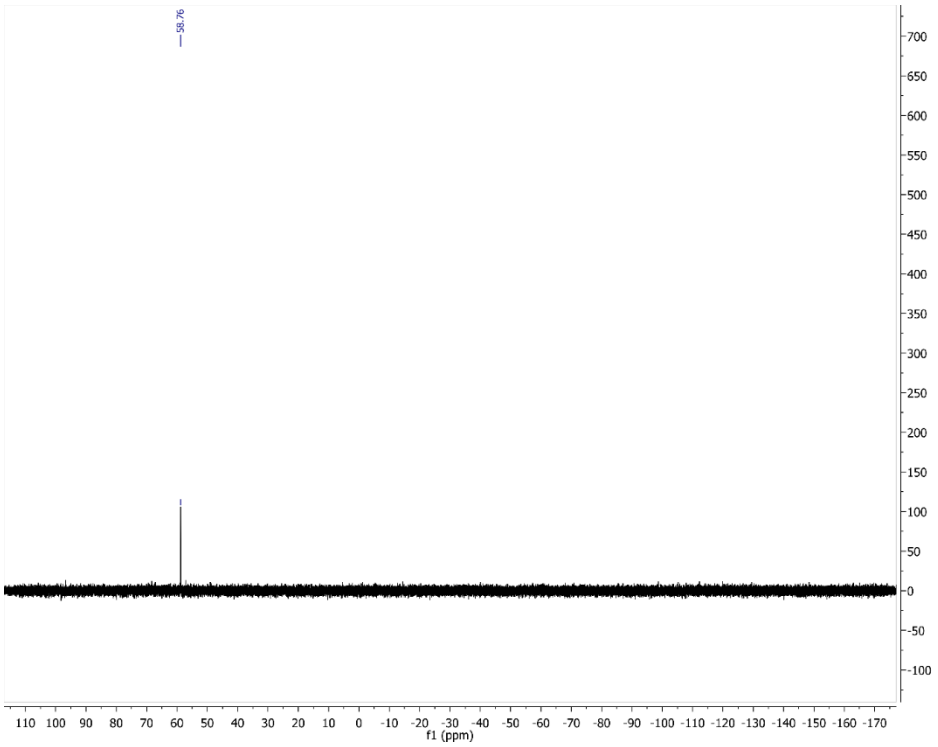

Figure S33. Untruncated ^{31}P NMR spectrum of inset in Figure 7, top.

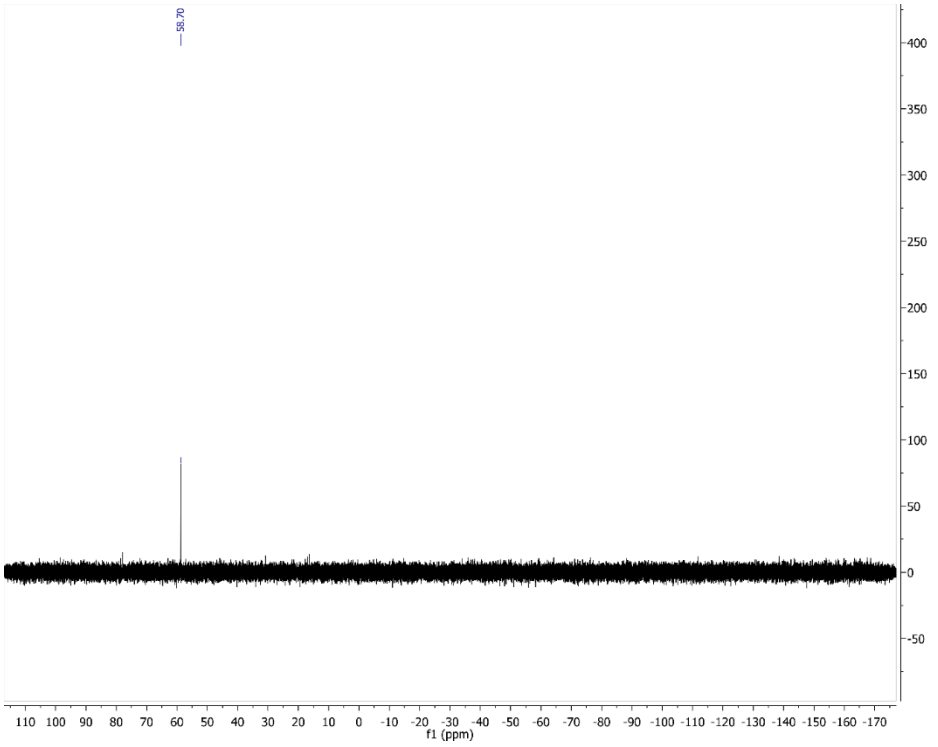

Figure S34. Untruncated ^{31}P NMR spectrum of inset in Figure 7, second from top.

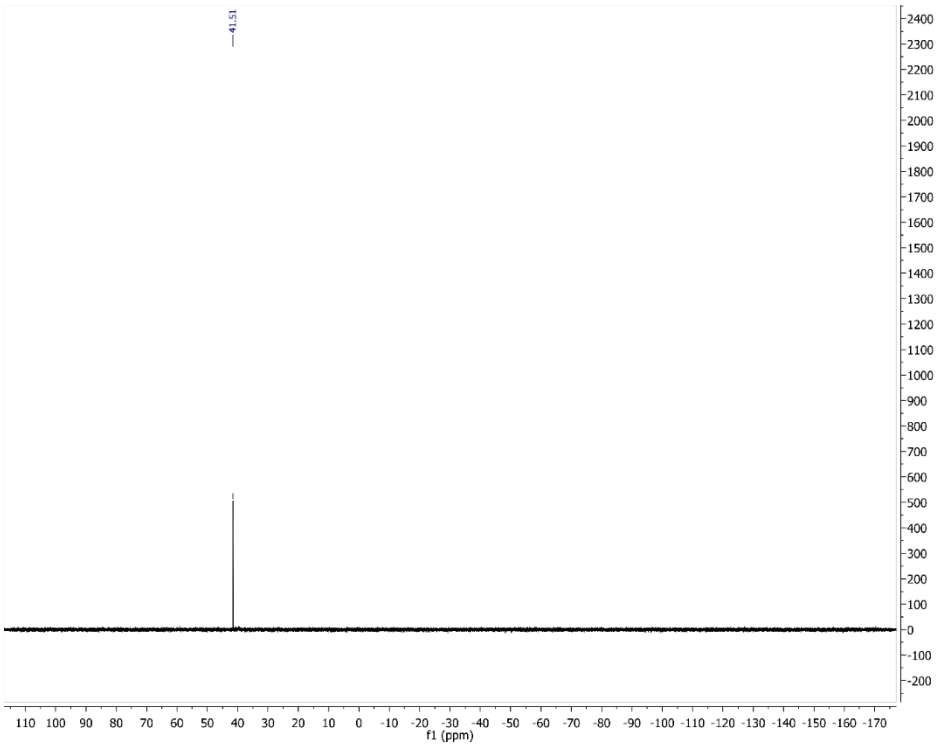

Figure S35. Untruncated ^{31}P NMR spectrum of inset in Figure 7, second from bottom.

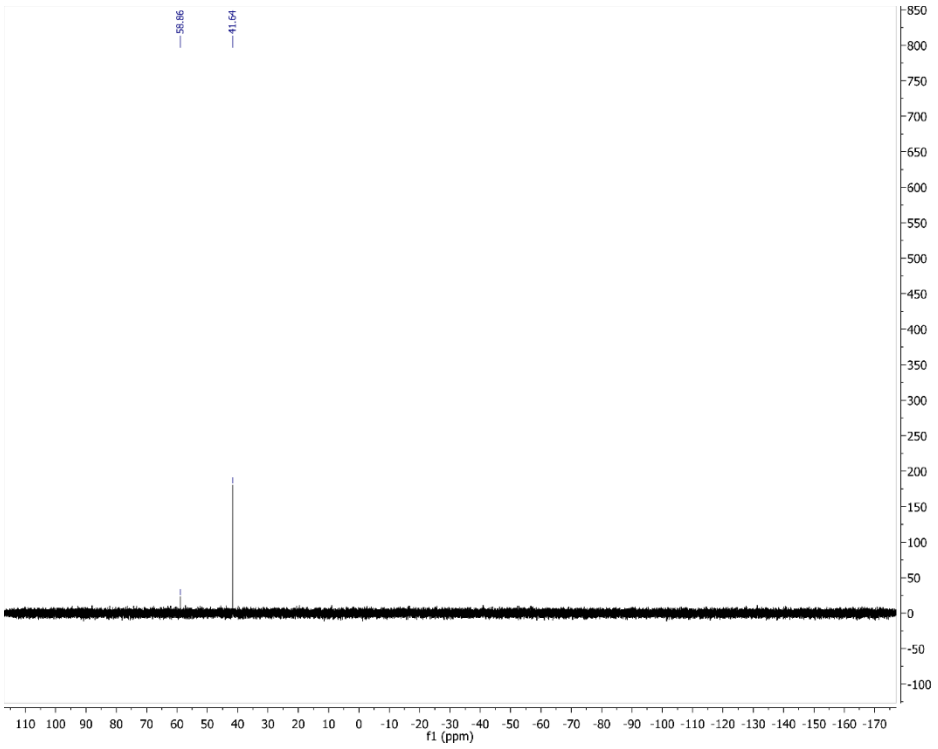

Figure S36. Untruncated ^{31}P NMR spectrum of inset in Figure 7, bottom.

Kinetic studies:

General procedure for determination of the rate dependence on [4-FC$_6$F$_4$Br]. The method of variable time normalization analysis (VTNA) was used to interpret kinetic data.[7] To an oven-dried 4 mL scintillation vial equipped with a stir bar was charged with 1-bromo-4-fluorobenzene (0.125 or 0.25 mmol), aniline (34 µL, 0.38 mmol), triethylamine (70 µL, 0.5 mmol), trifluorotoluene (internal standard, 10 µL, 83 µmol), **1** (1.8 mg, 2.5 µmol) and toluene (0.5 mL). The vial was capped with a puncturable PTFE-lined cap and was taken out of the glovebox. Under N_2 atmosphere, degassed deionized water (3 mL) was injected into the vial and the reaction mixture was left stirring vigorously at 80 °C for 160 minutes. Aliquots (20 µL) were taken at 5, 10, 20, 40, 80, and 160 min and were quenched by dilution in $CDCl_3$ (0.6 mL) at RT in an NMR tube. The yields were determined by ^{19}F NMR using a quantitative, single-scan experiment (acquisition time of 1.46 s and recycle delay time (d1) of 10 s). Both [**3**] vs. Σ([4-F-C$_6$F$_4$Br]^0*Δt) and [**3**] vs. Σ([4-F-C$_6$F$_4$Br]^1*Δt) were plotted where time (t) is in units of min, and the best overlay of data points was found for the zeroth-order plot with respect to the dependence of the rate on [4-F-C$_6$F$_4$Br]^n. Note that for the reaction using 0.25 mmol 4-F-C$_6$F$_4$Br, data were not plotted beyond 20 min because yield of **3** at this time was 94%.

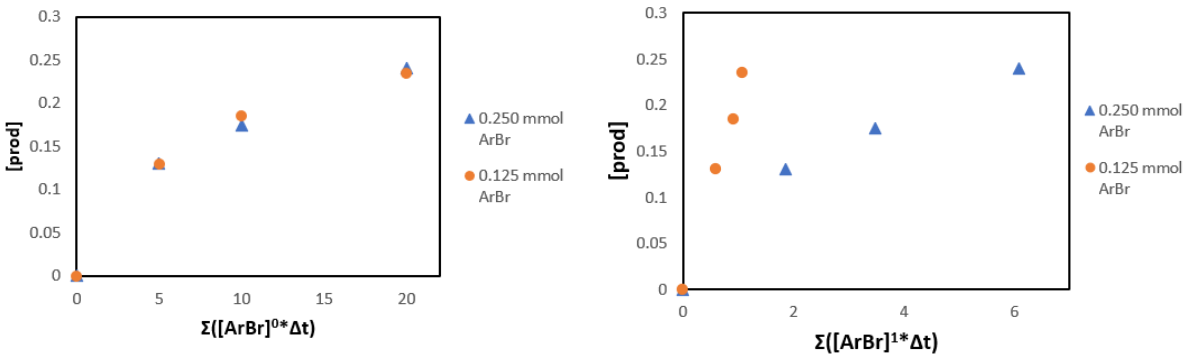

Figure S37. Variable time normalization analysis (VTNA) of reactions conducted at varying [4-F-C$_6$F$_4$Br].

General procedure for determination of the rate dependence on [$PhNH_2$]. The method of variable time normalization analysis (VTNA) was used to interpret kinetic data.[7] To an oven-dried 4 mL scintillation vial equipped with a stir bar was charged with 1-bromo-4-fluorobenzene (27 µL, 0.25 mmol, 1.0 equiv), aniline (0.38 mmol or 0.75 mmol), triethylamine (70 µL, 0.5 mmol), trifluorotoluene (internal standard, 10 µL, 83 µmol), **1** (1.8 mg, 2.5 µmol) and toluene (0.5 mL). The vial was capped with a puncturable PTFE-lined cap and was taken out of the glovebox. Under N_2 atmosphere, degassed deionized water (3 mL) was injected into the vial and the reaction mixture was left stirring vigorously at 80 °C for 160 minutes. Aliquots (20 µL) were taken at 5, 10, 20, 40, 80, and 160 minutes and were quenched by dilution into $CDCl_3$ (0.6 mL) at RT in an NMR tube. The yields were determined by ^{19}F NMR using a quantitative, single-scan experiment (acquisition time of 1.46 s and recycle delay time (d1) of 10 s). Both [**3**] vs. $\Sigma([PhNH_2]^0*\Delta t)$ and [**3**] vs. $\Sigma([PhNH_2]^1*\Delta t)$ were plotted where time (t) is in units of min, and the better overlay of data points was found for the zeroth-order plot with respect to the dependence of the rate on $[PhNH_2]^n$.

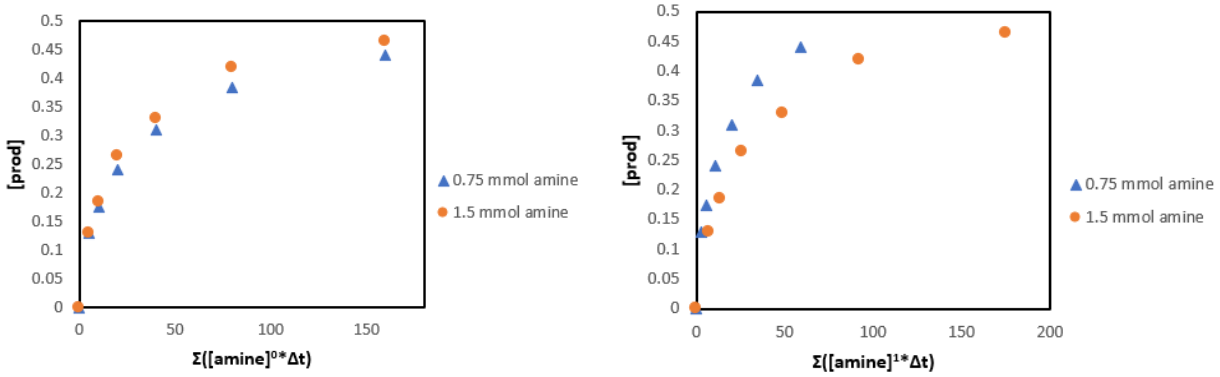

Figure S38. Variable time normalization analysis (VTNA) of reactions conducted at varying [$PhNH_2$].

General procedure for determination of the rate dependence on [Et_3N]. The method of variable time normalization analysis (VTNA) was used to interpret kinetic data.[7] To an oven-dried 4 mL scintillation vial equipped with a stir bar was charged with 1-bromo-4-fluorobenzene (27 µL, 0.25 mmol, 1.0 equiv), aniline (34 µL, 0.38 mmol), triethylamine (0.5 mmol or 1.0 mmol), trifluorotoluene (internal standard, 10 µL, 83 µmol), **1** (1.8 mg, 2.5 µmol) and toluene (0.5 mL). The vial was capped with a puncturable PTFE-lined cap and was taken out of the glovebox. Under N_2 atmosphere, degassed deionized water (3 mL) was injected into the vial and the reaction mixture was left stirring vigorously at 80 °C for 160 minutes. Aliquots (20 µL) were taken at 5, 10, 20, 40, 80, and 160 minutes and were quenched by dilution into $CDCl_3$ (0.6 mL) at RT in an NMR tube. The yields were determined by ^{19}F NMR using a quantitative, single-scan experiment (acquisition time of 1.46 s and recycle delay time (d1) of 10 s). Both [**3**] vs. $\Sigma([NEt_3]^0*\Delta t)$ and [**3**] vs. $\Sigma([NEt_3]^1*\Delta t)$ were plotted where time (t) is in units of min, and the better overlay of data points was found for the zeroth-order plot with respect to the dependence of the rate on $[Et_3N]^n$.

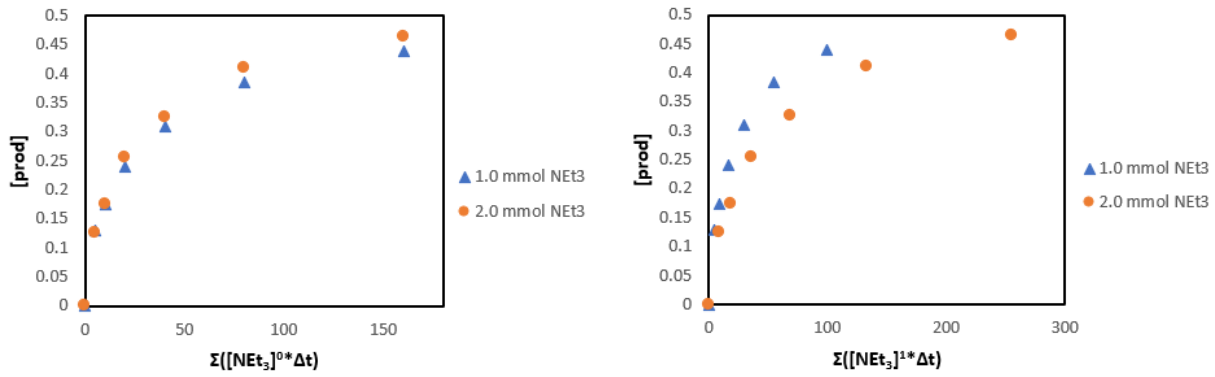

Figure S39. Variable time normalization analysis (VTNA) of reactions conducted at varying [Et_3N].

General procedure for determination of the rate dependence on [1] by initial rates. The method of initial rates was used. To an oven-dried 4 mL scintillation vial equipped with a stir bar was charged with 1-bromo-4-fluorobenzene (27 µL, 0.25 mmol), aniline (34 µL, 0.375 mmol), triethylamine (70 µL, 0.5 mmol), trifluorotoluene (internal standard, 10 µL, 83 µmol), **1** (2.5 µmol or 5.0 µmol) and toluene (0.5 mL). The vial was capped with a puncturable PTFE-lined cap and was taken out of the glovebox. Under N_2 atmosphere, degassed deionized water (3 mL) was injected into the vial and the reaction mixture was left stirring vigorously at 80 °C. Aliquots (20 µL) were taken at 2, 4, 6, 8, and 10 minutes and were quenched by dilution into $CDCl_3$ (0.6 mL) at RT in an NMR tube. The yields at each time were determined by ^{19}F NMR using a quantitative, single-scan experiment (acquisition time of 1.46 s and recycle delay time (d1) of 10 s). Data were fit by linear regression analysis of plots of [**3**] vs. time at conversions of ≤30% yield. The dependence of the initial rate on [**1**] was calculated according to the following equations:

$$\left(\frac{[Pd]_2}{[Pd]_1}\right)^x = \left(\frac{slope\ 2}{slope\ 1}\right)$$

$$(2)^x = \left(\frac{0.028}{0.015}\right)$$

$$x = 0.90$$

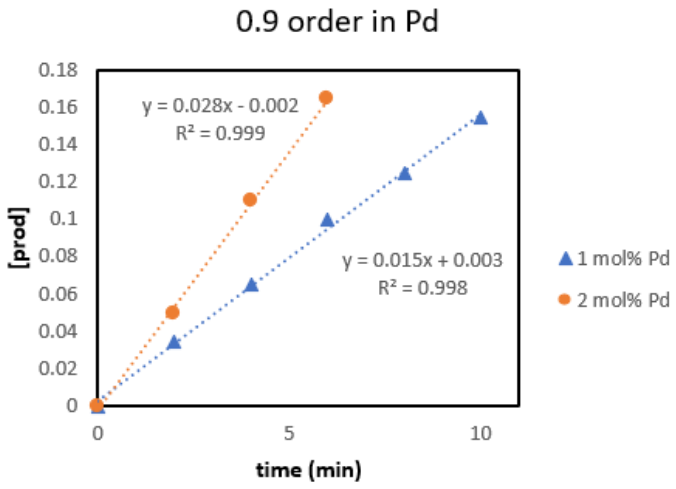

Figure S40. Initial rates during reactions conducted with either 2.5 µmol or 5.0 µmol of catalyst **1**.

General procedure for determination of the rate dependence on [Pd] by VTNA. The method of variable time normalization analysis (VTNA) was used to interpret kinetic data. To an oven-dried 4 mL scintillation vial equipped with a stir bar was charged with 1-bromo-4-fluorobenzene (27 µL, 0.25 mmol, 1.0 equiv), aniline (34 µL, 0.38 mmol), triethylamine (70 µL, 0.5 mmol), trifluorotoluene (internal standard, 10 µL, 83 µmol), **1** (2.5 µmol or 7.5 µmol) and toluene (0.5 mL). The vial was capped with a puncturable PTFE-lined cap and was taken out of the glovebox. Under N_2 atmosphere, degassed deionized water (3 mL) was injected into the vial and the reaction mixture was left stirring vigorously at 80 °C for 160 minutes. Aliquots (20 µL) were taken at 5, 10, 20, 40, 80, and 160 minutes and were quenched by dilution into CDCl3 (0.6 mL) at RT in an NMR tube. The yields were determined by ^{19}F NMR using a quantitative, single-scan experiment (acquisition time of 1.46 s and recycle delay time (d1) of 10 s). Both [**3**] vs. $[Pd]_0^{0.9}$*t and [**3**] vs. $[Pd]_0^{0.5}$*t were plotted where time (t) is in units of min, and the better overlay of data points was found for the 0.9 order plot with respect to the dependence of the rate on $[Pd]^n$.

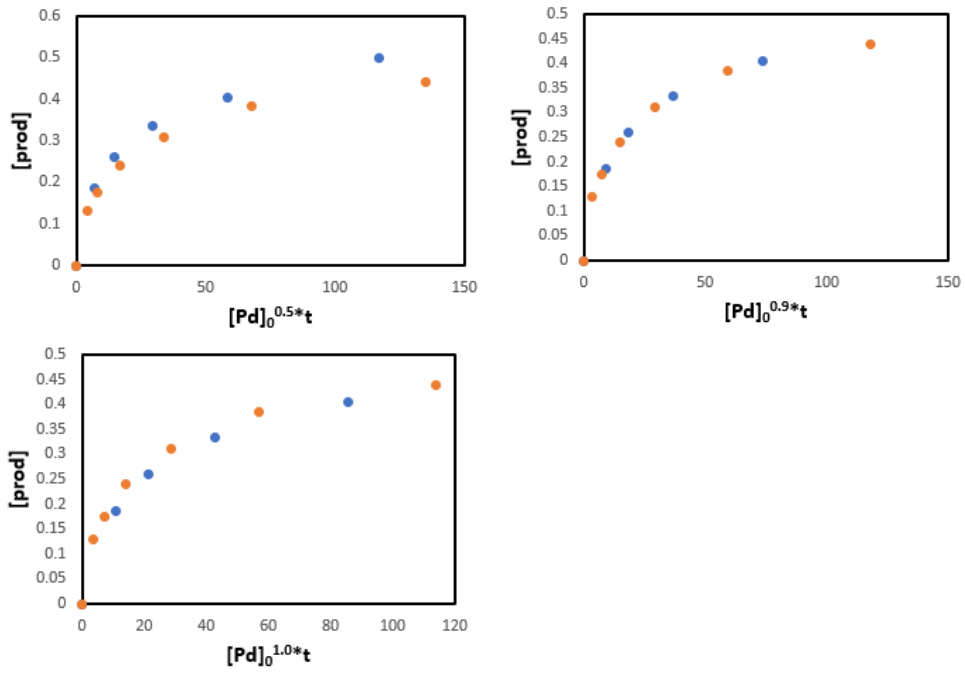

Figure S41. Variable time normalization analysis (VTNA) of reactions conducted with either 2.5 µmol or 5.0 µmol of catalyst **1**.

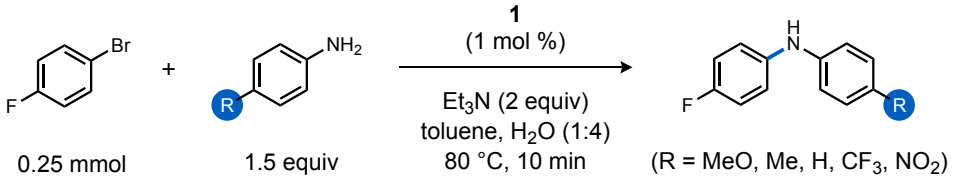

Linear free-energy relationship (LFER) studies with respect to *para*-substituted anilines. Five parallel reactions were performed using a *para*-substituted aniline (*p*-R-$C_6H_4NH_2$; R = MeO, Me, H, CF_3, or NO_2). To an oven-dried 4 mL scintillation vial equipped with a stir bar was charged with 1-bromo-4-fluorobenzene (27 µL, 0.25 mmol, 1.0 equiv), aniline (0.38 mmol), triethylamine (70 µL, 0.5 mmol), trifluorotoluene (internal standard, 10 µL, 83 µmol), **1** (1.8 mg, 2.5 µmol, 1 mol %), and toluene (0.5 mL). The vial was capped with a puncturable PTFE-lined cap and was taken out of the glovebox. Under N_2 atmosphere, degassed deionized water (3 mL) was injected into the vial and the reaction mixture was left stirring vigorously at 80 °C. Aliquots (20 µL) were taken at 2, 4, 6, 8, and 10 minutes and were quenched by dilution into $CDCl_3$ (0.6 mL) at RT in an NMR tube. The yields at each time were determined by ^{19}F NMR using a quantitative, single-scan experiment (acquisition time of 1.46 s and recycle delay time (d1) of 10 s). Data were fit by linear regression analysis of plots of [product] vs. time at conversions of ≤30% yield.[5,8] A Hammett analysis was performed using the initial rates and corresponding substituent constants (σ_P).[9] A ρ value of +0.3 was determined from the slope of this plot.

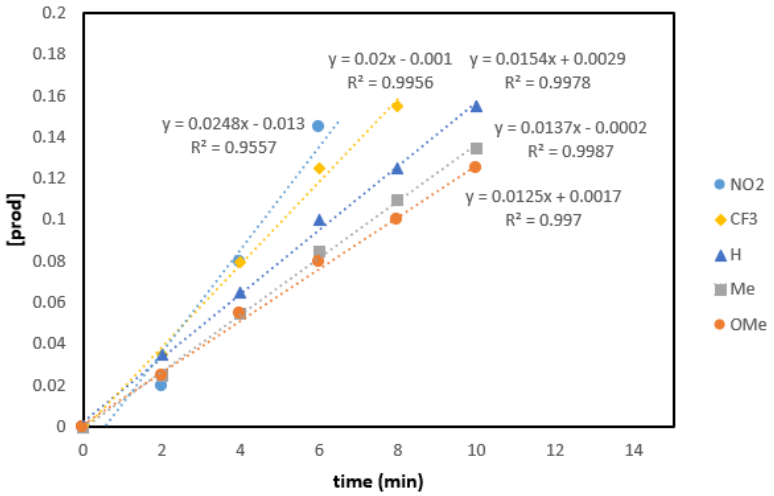

Figure S42. Determination of the initial rate of reactions between 4-FC_6H_4Br and a *para*-subsituted aniline under the conditions noted above.

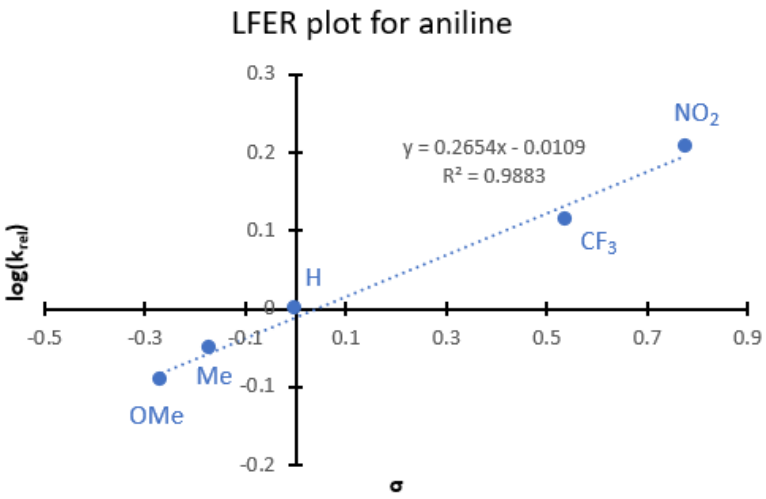

Figure S43. Hammett plot determined from initial rates of reactions between 4-FC_6H_4Br and a *para*-subsituted aniline under the conditions noted above.

$C_6H_5ND_2$. To a 20 mL scintillation vial equipped with a stir bar was charged with aniline (0.5 mL, 5.5 mmol), D_2O (5.0 mL, 0.28 mol, 51 equiv), and DCM (2 mL). The mixture was stirred at room temperature for 3 min. The organic layer was extracted with DCM and washed with D_2O (3 mL x 2), dried over sodium sulfate, and concentrated under reduced pressure. ^1H NMR taken in $CDCl_3$ indicated the absence of NH_2 resonances.

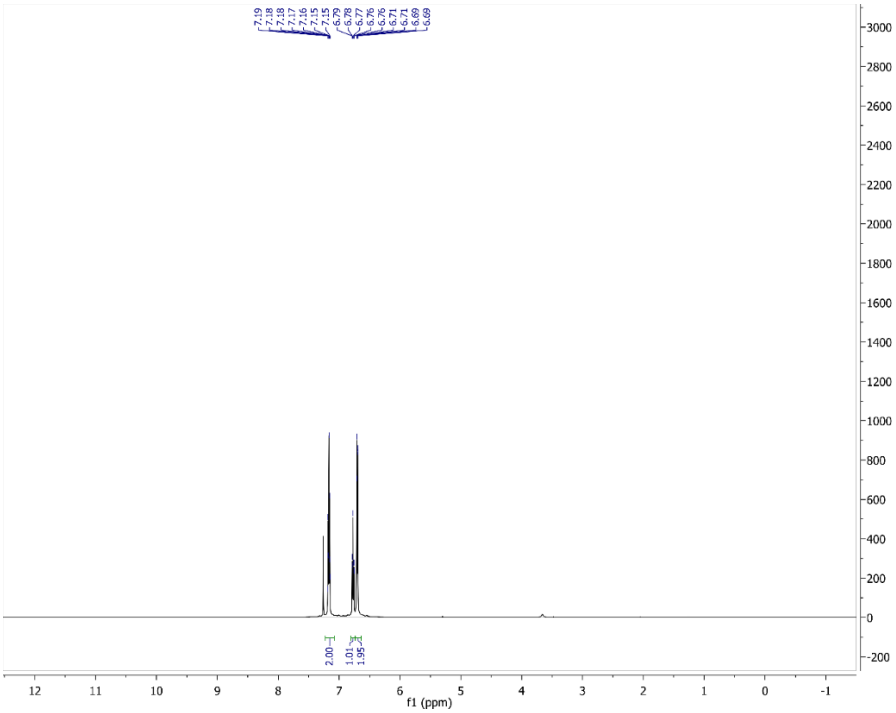

Figure S44. ^1H NMR spectrum (500 MHz, $CDCl_3$) of $C_6H_5ND_2$.

Kinetic isotope effect (KIE) experiments. To an oven-dried 4 mL scintillation vial equipped with a stir bar was charged with 1-bromo-4-fluorobenzene (27 µL, 0.25 mmol, 1.0 equiv), $C_6H_5NH_2$ (0.38 mmol), triethylamine (70 µL, 0.5 mmol), trifluorotoluene (internal standard, 10 µL, 83 µmol), **1** (1.8 mg, 2.5 µmol, 1 mol %), and toluene (0.5 mL). The vial was capped with a puncturable PTFE-lined cap and was taken out of the glovebox. Under N_2 atmosphere, degassed deionized water (3 mL) was injected into the vial and the reaction mixture was left stirring vigorously at 80 °C. Aliquots (20 µL) were taken at 2, 4, 6, 8, and 10 minutes and were quenched by dilution into $CDCl_3$ (0.6 mL) at RT in an NMR tube. The yields at each time were determined by ^{19}F NMR using a quantitative, single-scan experiment (acquisition time of 1.46 s and recycle delay time (d1) of 10 s). Data were fit by linear regression analysis of plots of [**3**] vs. time at conversions of ≤30% yield. The experiment and data analysis were repeated with substitution of $C_6H_5ND_2$ for $C_6H_5NH_2$ and D_2O for H_2O. The KIE was calculated according to the equation:

$$KIE = \frac{k_H}{k_D} = \frac{0.154}{0.127} = 1.2$$

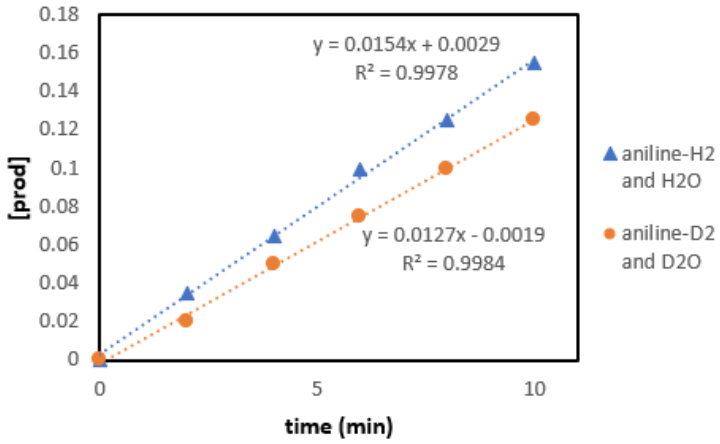

Figure S45. Plot of product (**3**) formation versus time during reacitons with aniline isotopologues.

Kinetic simulations. A rate law was derived for the catalytic cycle below involving the proposed formation of off-cycle species **C·D** (e.g., **34**).

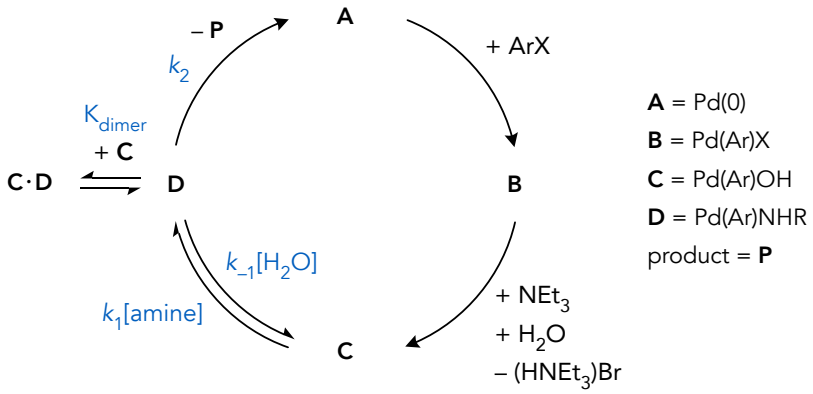

Expressions for [**C**] (eq S1) and [**C·D**] (eq S2) using the steady-state approximation:

$$\frac{d[\mathbf{D}]}{dt} = k_1[\mathbf{C}][\text{amine}] - k_{-1}[H_2O][\mathbf{D}] - k_2[\mathbf{D}] = 0$$

$$[\mathbf{C}] = \left(\frac{k_{-1}[H_2O] + k_2}{k_1[\text{amine}]}\right)[\mathbf{D}] \quad \text{(S1)}$$

$$\frac{d[\mathbf{C{\cdot}D}]}{dt} = k_{dimer}[\mathbf{C}][\mathbf{D}] - k_{-dimer}[\mathbf{C{\cdot}D}] = 0$$

$$[\mathbf{C{\cdot}D}] = K_{dimer}[\mathbf{C}][\mathbf{D}] \quad \text{(S2)}$$

An expression for the mass balance of kinetically relevant catalyst species, stipulating that [**A**] and [**B**] are approximately zero based on kinetic data in Figures S38 and S40:

$$[\text{Pd}]_{total} \cong [\mathbf{C}] + [\mathbf{D}] + 2[\mathbf{C{\cdot}D}] \quad \text{(S3)}$$

Combining eqs S1 and S2 with eq S3 gives:

$$[\text{Pd}]_{total} = \left(\frac{k_{-1}[H_2O] + k_2}{k_1[\text{amine}]}\right)[\mathbf{D}] + [\mathbf{D}] + 2K_{dimer}\left(\frac{k_{-1}[H_2O] + k_2}{k_1[\text{amine}]}\right)[\mathbf{D}]^2 \quad \text{(S4)}$$

The expression for the rate of product formation is given in eq S5:

$$\frac{d[P]}{dt} = k_2[\mathbf{D}] \quad \text{(S5)}$$

Substituting for [**D**], which was determined by quadratic factoring of eq S4,[10] in eq S5 gives:

$$r = \frac{2k_2[\mathrm{Pd}]_{\mathrm{total}}}{(1+f) + \{(1+f)^2 + 8K_{\mathrm{dimer}} f [\mathrm{Pd}]_{\mathrm{total}}\}^{1/2}} \qquad \text{where } f = \left(\frac{k_{-1}[\mathrm{H_2O}] + k_2}{k_1[\mathrm{amine}]}\right) \tag{S6}$$

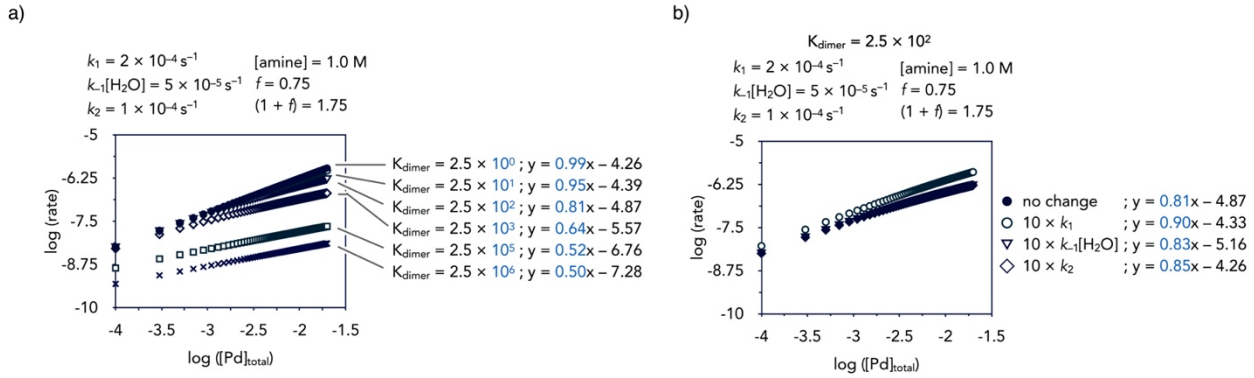

Figure S46. Kinetic simulations to determine the change in catalyst order from (a) variation of K_{dimer}, or (b) variation of other elementary rate constants by 10× at fixed $K_{dimer} = 2.5 \times 10^2$.

Simulated kinetic data were calculated using eq S6. Values for elementary rate constants were selected arbitrarily with relative magnitudes estimated to be $k_2 < k_1 >> k_{-1}$ based on the results of stoichiometric reactions. The order in catalyst was determined by the slope of linear regression analysis of calculated plots of log(rate) versus log($[Pd]_{total}$ shown in Figure S48a. The experimentally determined value for the order in catalyst of 0.9 is thus consistent with the predicted fractional values for $[Pd]_{total}$ at moderate values of K_{dimer}. Adjusting the arbitrary elementary rate constant values (Figure S48b) does influence the calculated catalyst order but to a lesser extent than a comparable change to the dimerization equilibrium at moderate values of K_{dimer} (e.g., $K_{dimer} = 10^2$–10^4). These data also suggest catalyst orders approaching the upper boundary of 1 can occur even when the off-cycle mixed dimer **C·D** (i.e., **34**) is thermodynamically favored (e.g., K_{dimer} = 2.5–25).

$$\chi([\mathbf{D}]) = \frac{r}{k_2[\mathrm{Pd}]_{\mathrm{total}}} \tag{S7}$$

$$\chi([\mathbf{C}]) = \frac{f\,[\mathbf{D}]}{[\mathrm{Pd}]_{\mathrm{total}}} \tag{S8}$$

$$\chi([\mathbf{C}\cdot\mathbf{D}]) = \frac{2K_{\mathrm{dimer}}\,[\mathbf{C}][\mathbf{D}]}{[\mathrm{Pd}]_{\mathrm{total}}} \tag{S9}$$

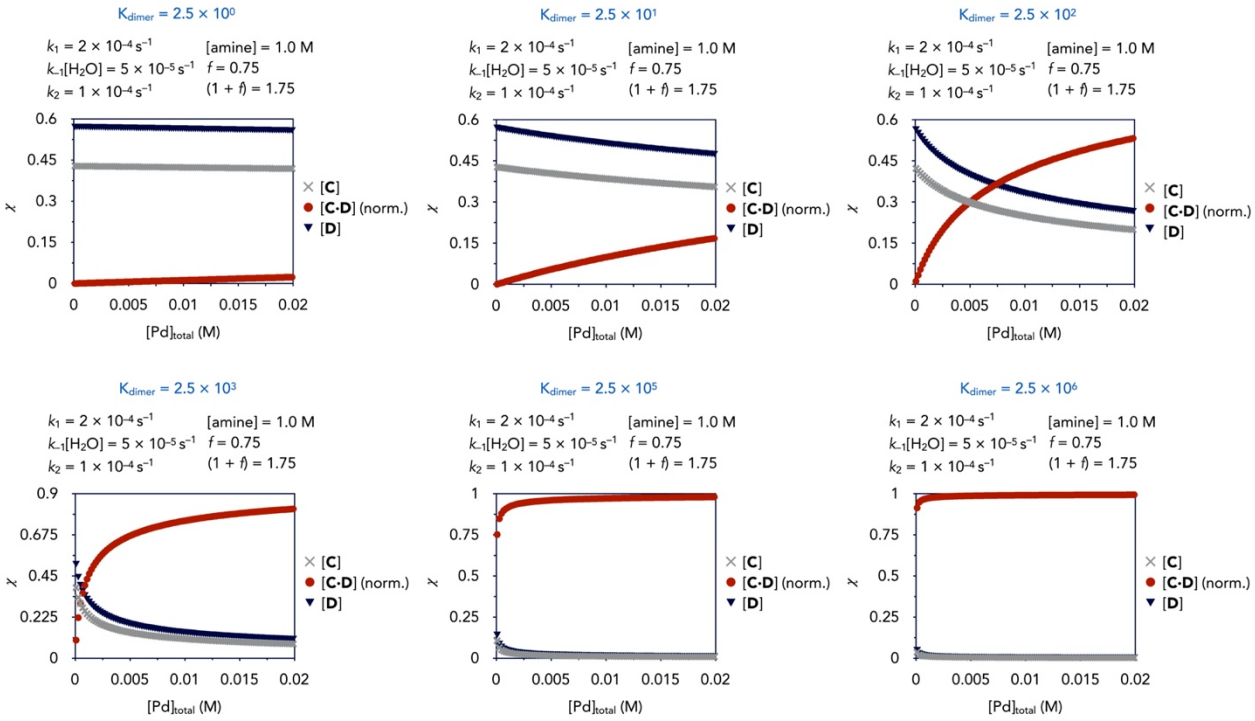

Figure S47. Simulations of catalyst speciation between **C**, **C·D** (normalized, 2× versus **C** or **D**), and **D** at different K_{dimer} values and the specified elementary rate constants as using eqs S7–S9.

Data shown in Figure S49 illustrate the relative mol fraction (χ) of catalytic intermediates at different catalyst loadings and different values of K_{dimer}. The possibility for the off-cycle aggregate **C·D** to comprise a significant or even major propotion of the total Pd mass balance is apparent even when the catalyst order falls toward the upper boundary (e.g., $K_{dimer} = 2.5 \times 10^2$), which supports **C·D** as a reasonable resting state species under catalytic conditions giving rise to an experimental order in [**1**] of 0.9.

Test for byproduct inhibition. To a 100 mL 2-piece EasyMax vessel fitted with reflux condenser, pitched blade impeller, nitrogen inlet, and EasySampler probe (Note: Easysampler is fitted with the following solvent lines and reagents: Reaction = degassed H_2O; Quench = acetone, non-degassed; Diluent = 2:1 MeCN:H_2O, non-degassed; 450× dilution) was charged 4-bromo-1,1'-biphenyl (4.16 g, 17.5 mmol, 98% purity), 4-nitroaniline (3.70 g, 26.3 mmol, 1.5 equiv, 98% purity) with or without triethylammonium bromide (1.626 g, 8.75 mmol, 0.5 equiv, 98% purity). The vessel was sealed and purged with N_2 for at least 10 minutes. Degassed H_2O (70 mL), toluene (15 mL, commercially available anhydrous solvent from Millipore Sigma), and degassed triethylamine (4.93 mL, 35.0 mmol, 2 equiv, 99% purity) were charged to the reactor via syringe (inert handling) with agitation set at 800 RPM. The reactor mixture was then heated to an internal temperature of 60 °C. To a 4 mL vial with PTFE septum and magnetic stir bar was charged complex **1** (63 mg, 0.088 mmol, 0.5 mol %). The vial was then inerted with N_2, and toluene (2.5 mL) was charged via syringe (inert handling). The slurry was allowed to stir and age (~5 min) whereupon it was charged to the reactor via syringe (inert handling). The syringe was rinsed with the reactor contents (2x's) and sampling was initiated using the Easysampler.

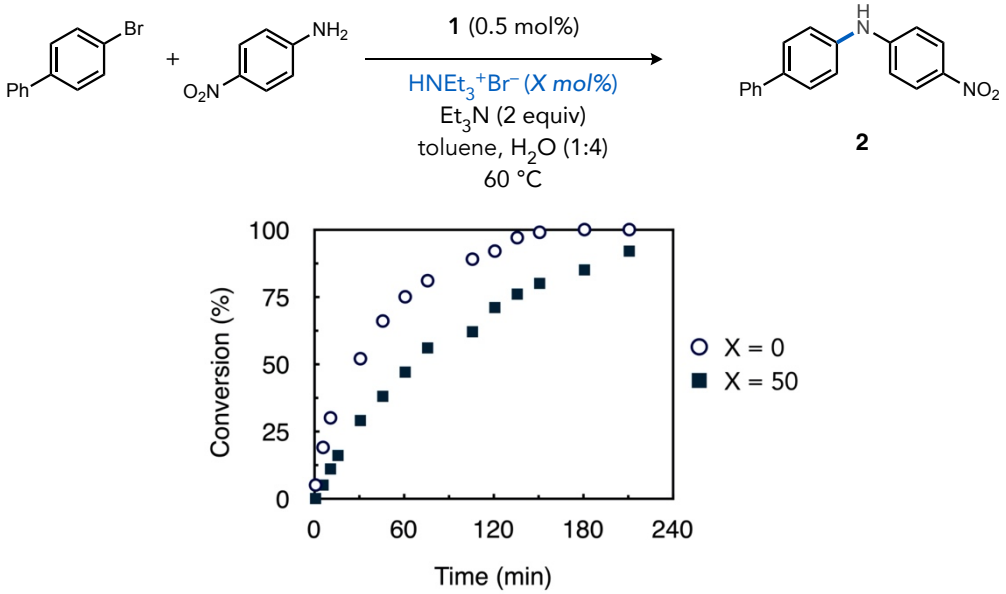

Figure S48. Reaction profile for formation of **2** from 4-bromobiphenyl in the presence or absence of added $(HNEt_3)^+Br^-$ (50 mol %) under conditions of general procedure A, expect with 0.5 mol % catalyst at 60 °C to modulate the rate for ease of data sampling.

The modest inhibitory effect of the rate with added exogenous bromide could indicate reversibility in the ionization equilibrium converting $(Ad_3P)Pd(Ar)X$ (X = Br, Cl) intermediates to $[(Ad_3P)Pd(Ar)(OH_2)]^+$ species in the proposed catalytic mechanism. However, exogenous halide salts may also induce inhibitory effects during catalysis due to other potential effects on catalyst speciation between active and inactive states. For leading references on this topic, see ref. 11. Either rationalization seems plausible and further study required to differentiate unambiguously.

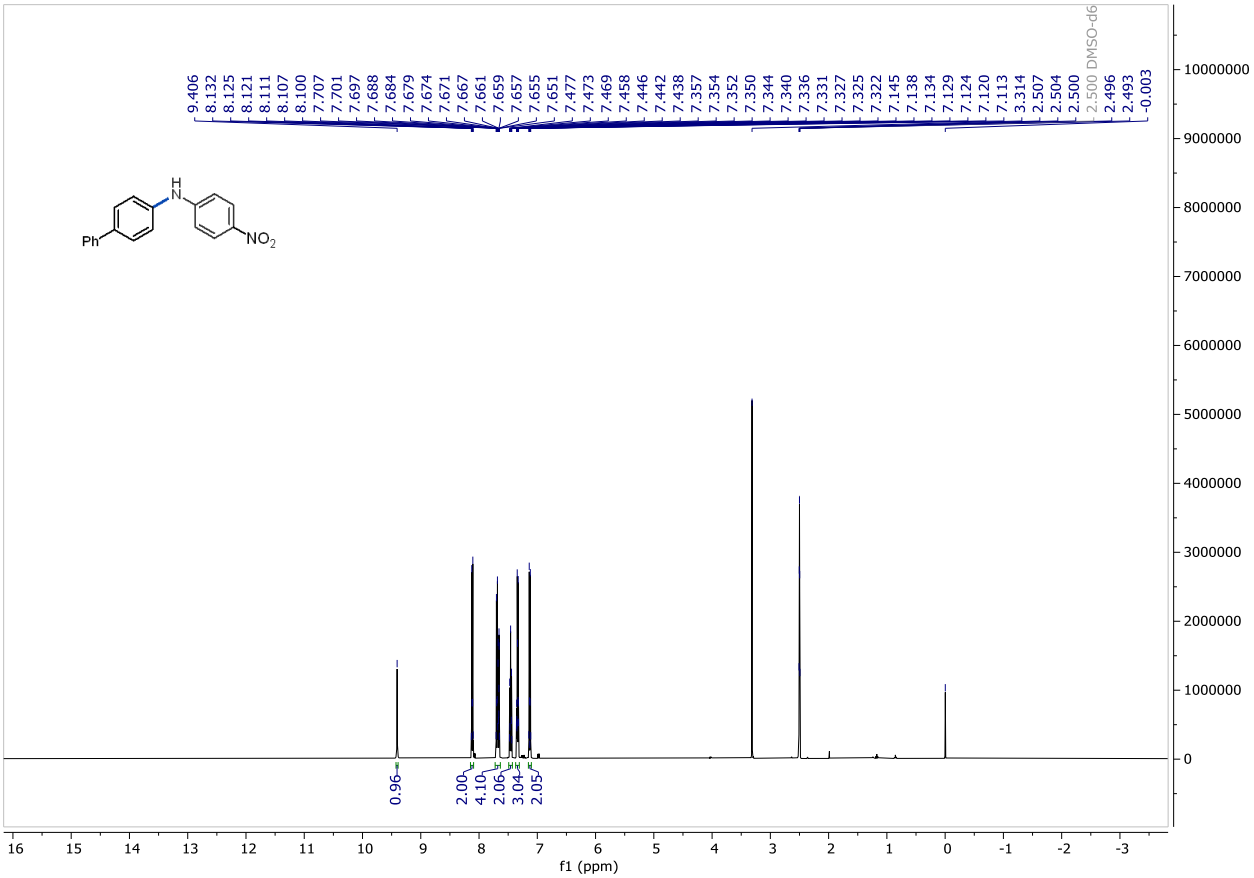

Figure S49. ^{1}H NMR (500 MHz, DMSO-d_6) of **2**.

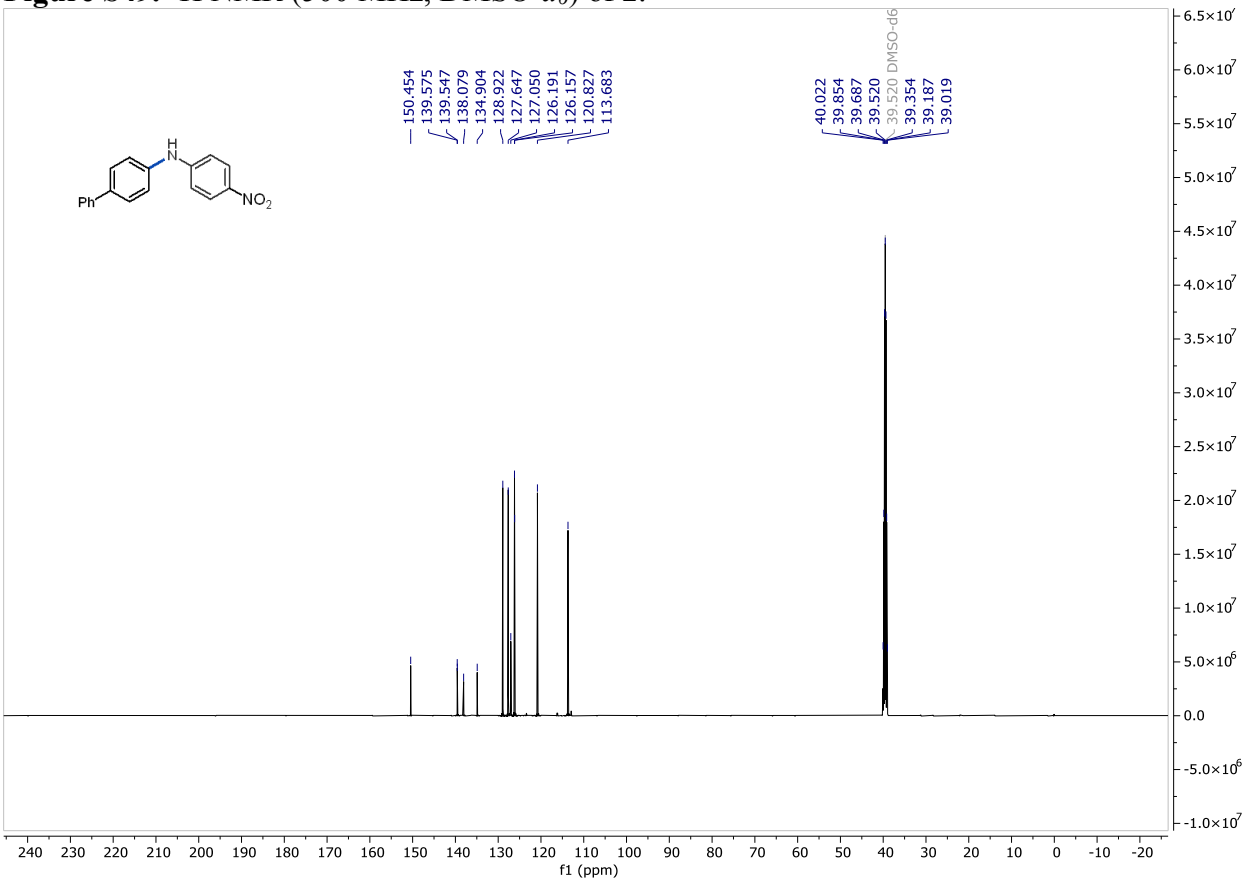

Figure S50. ^{13}C{^{1}H} NMR (126 MHz, DMSO-d_6) of **2**.

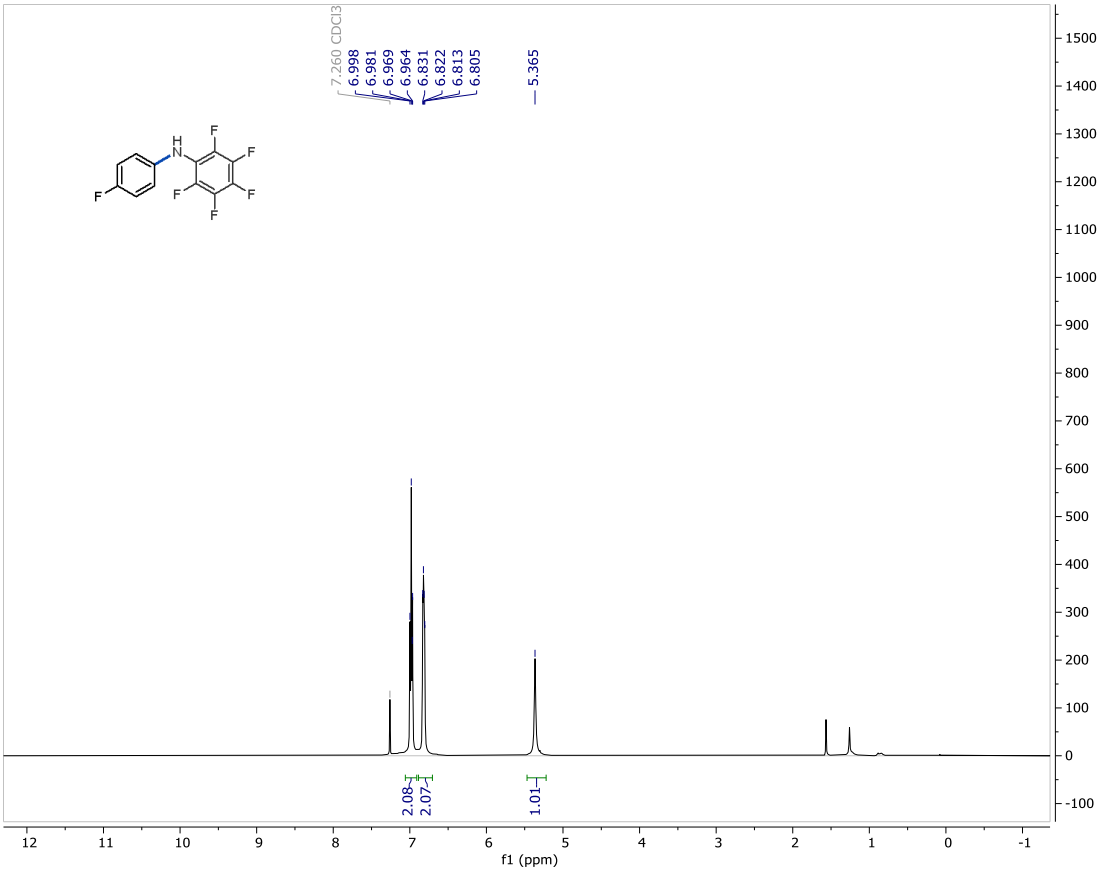

Figure S51. ^{1}H NMR (500 MHz, $CDCl_3$) of **4**.

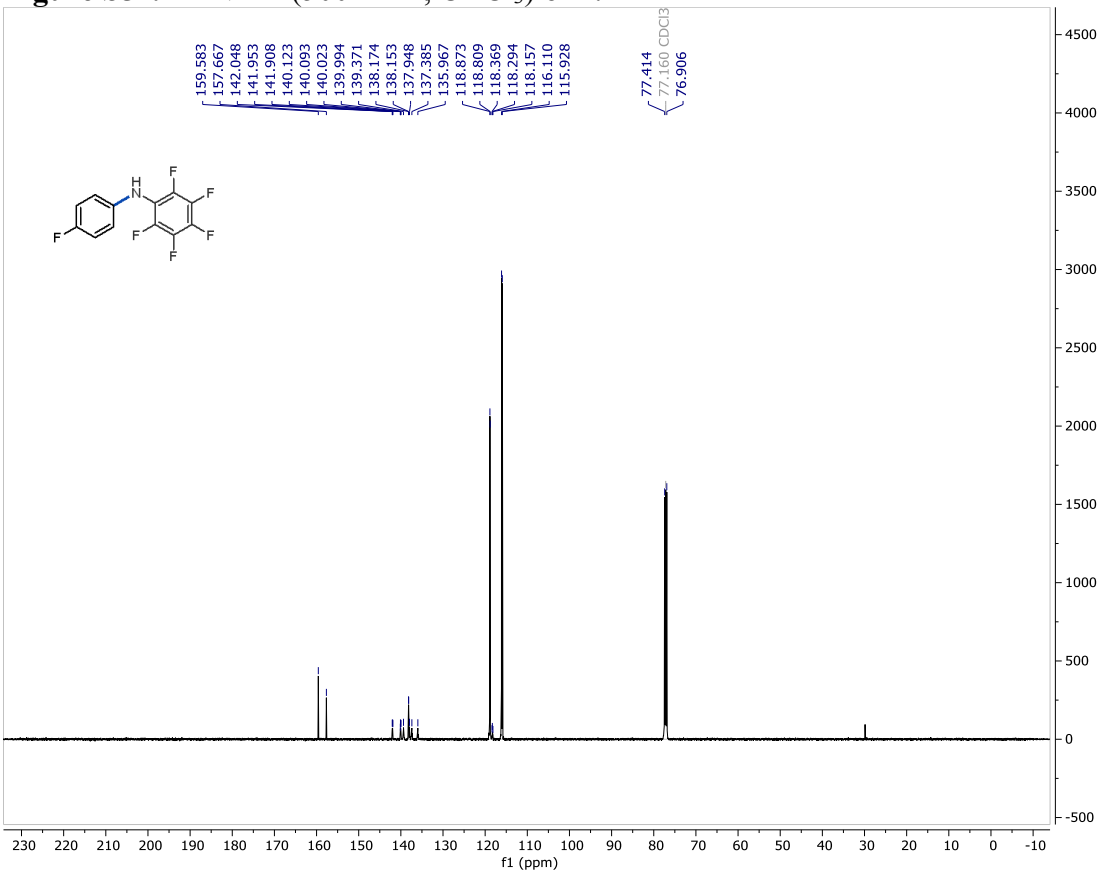

Figure S52. ^{13}C NMR (126 MHz, $CDCl_3$) of **4**.

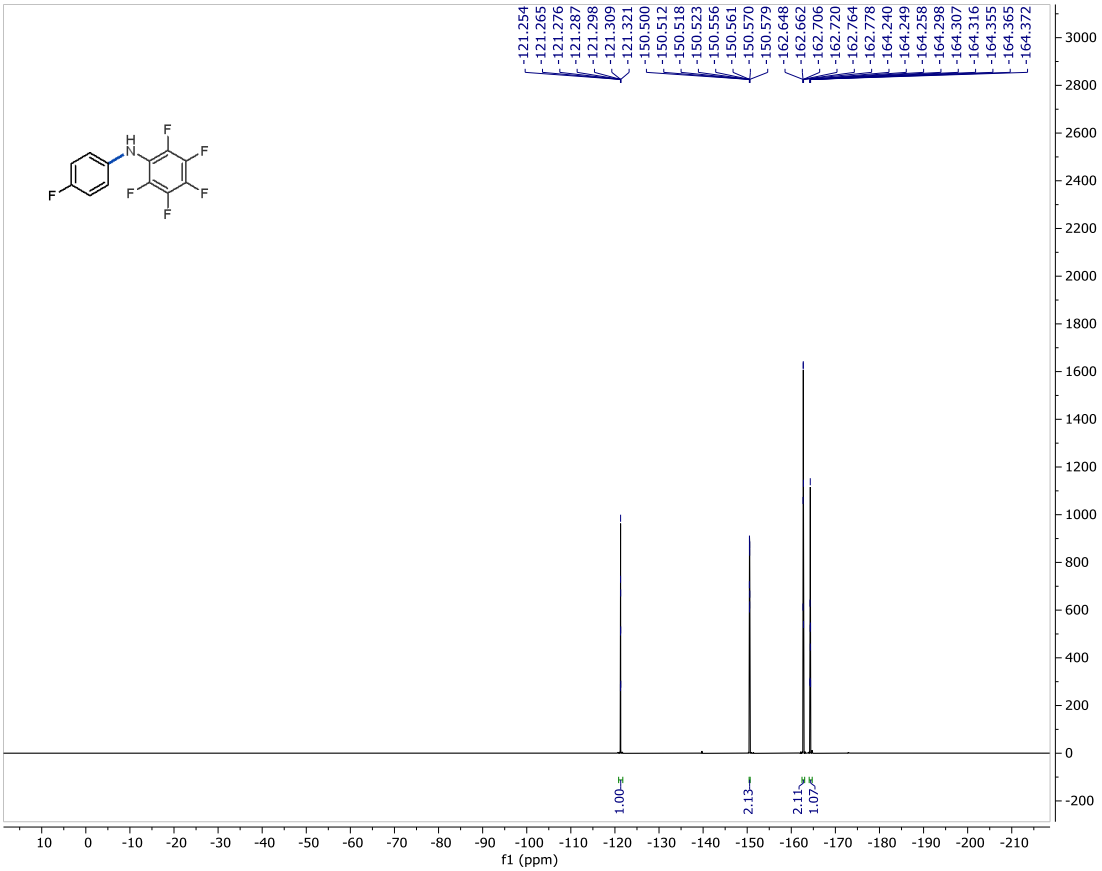

Figure S53. ^{19}F NMR (376 MHz, $CDCl_3$) of **4**.

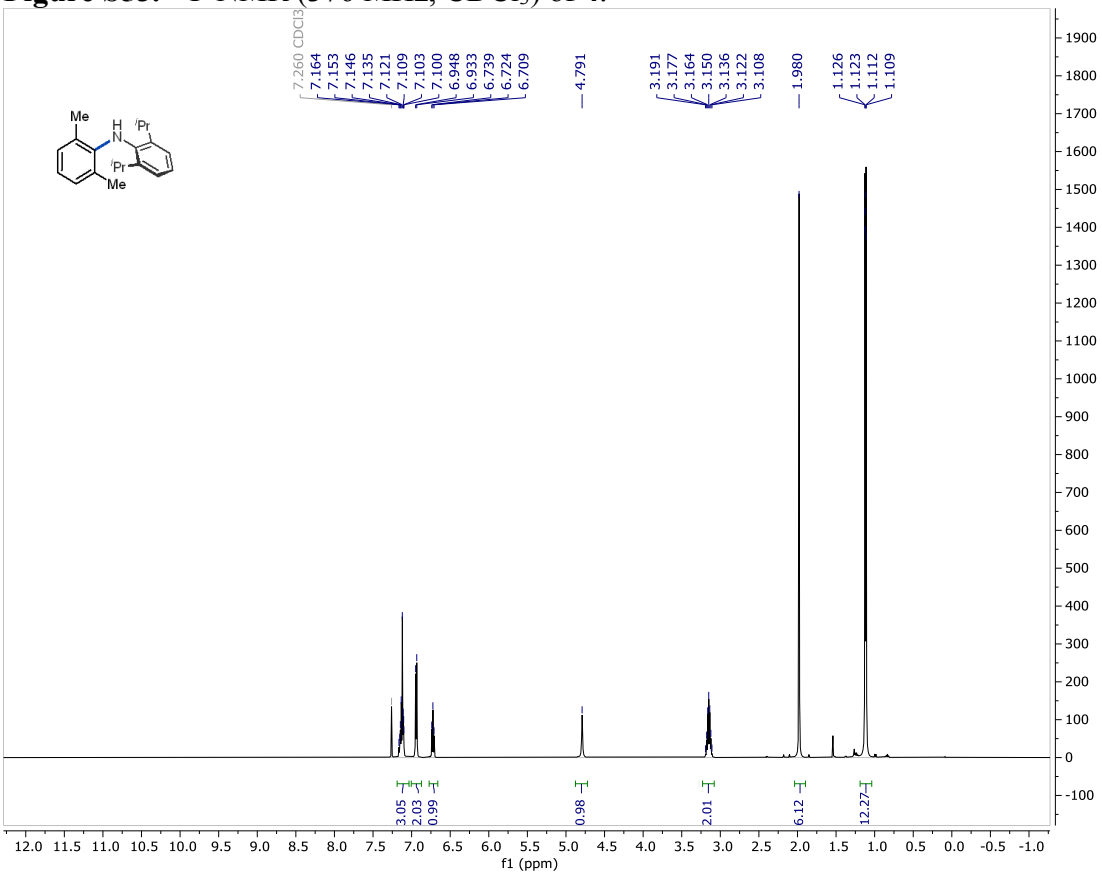

Figure S54. ^{1}H NMR (500 MHz, $CDCl_3$) of **5**.

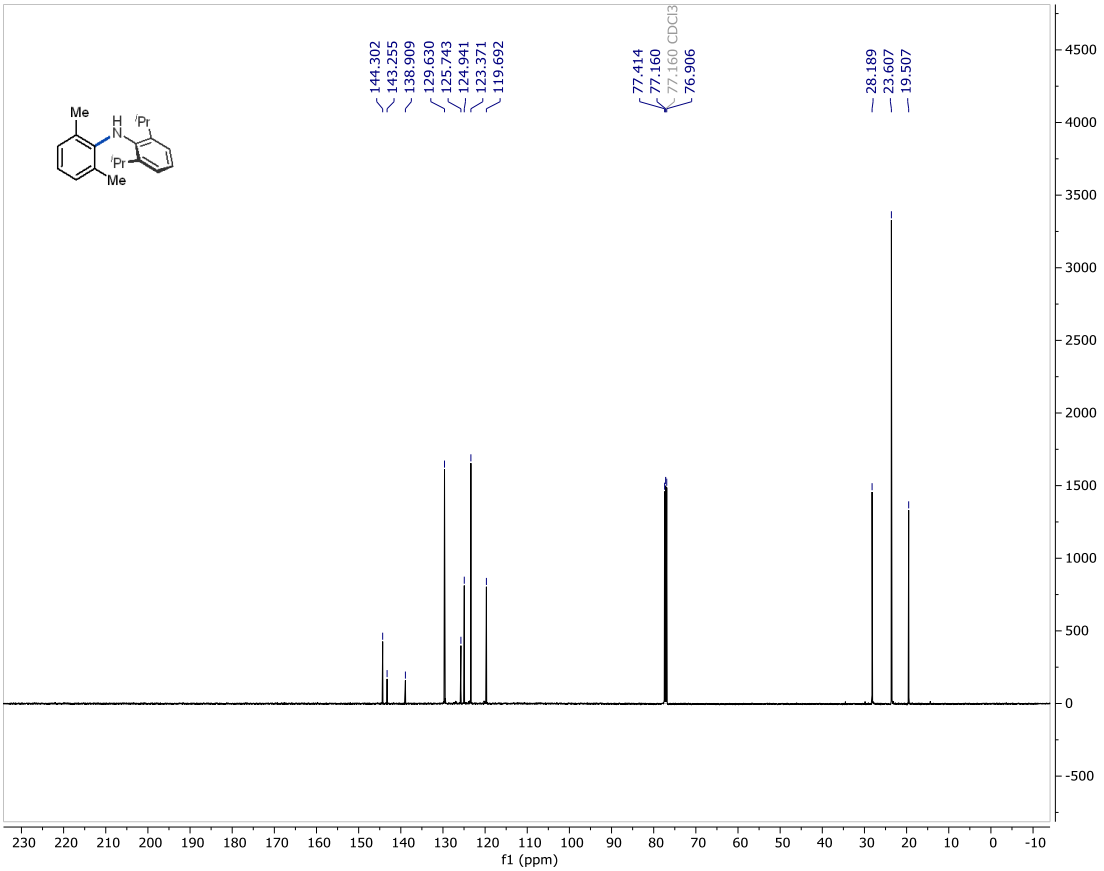

Figure S55. ^{13}C NMR (126 MHz, CDCl3) of **5**.

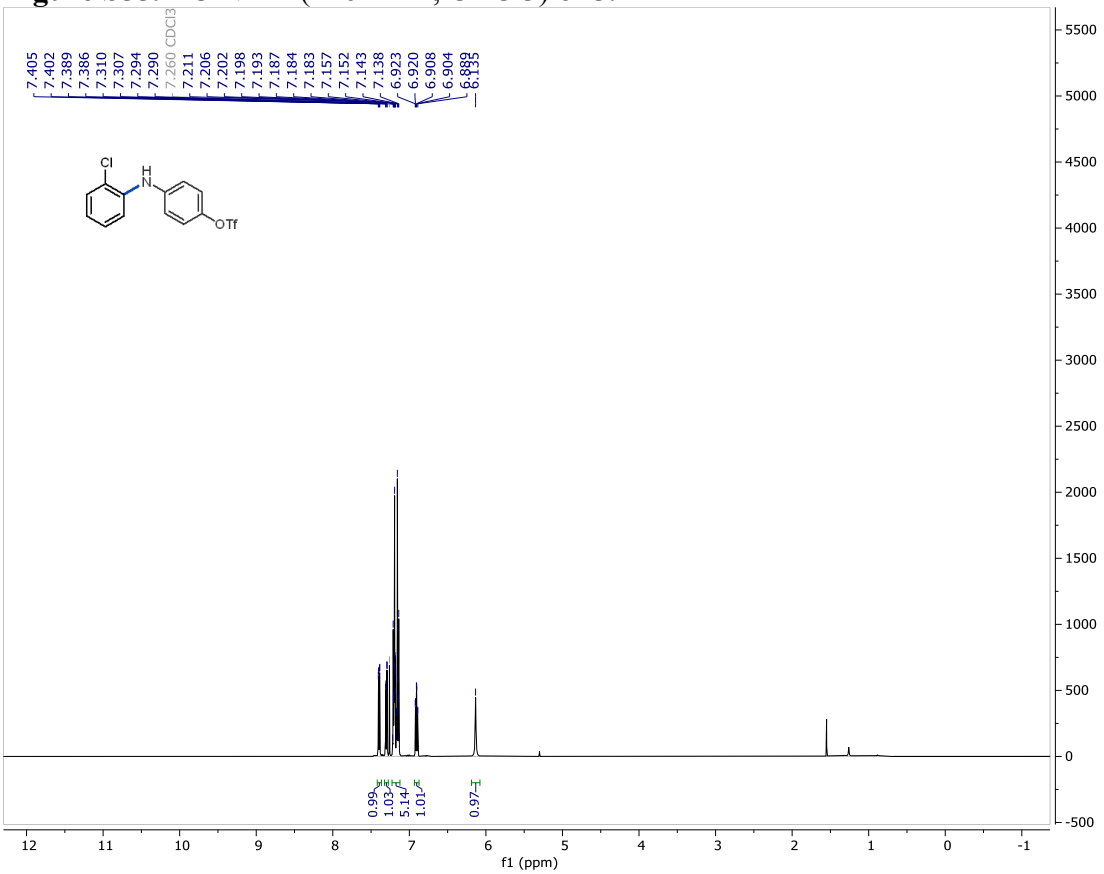

Figure S56. ^{1}H NMR (500 MHz, $CDCl_3$) of **6**.

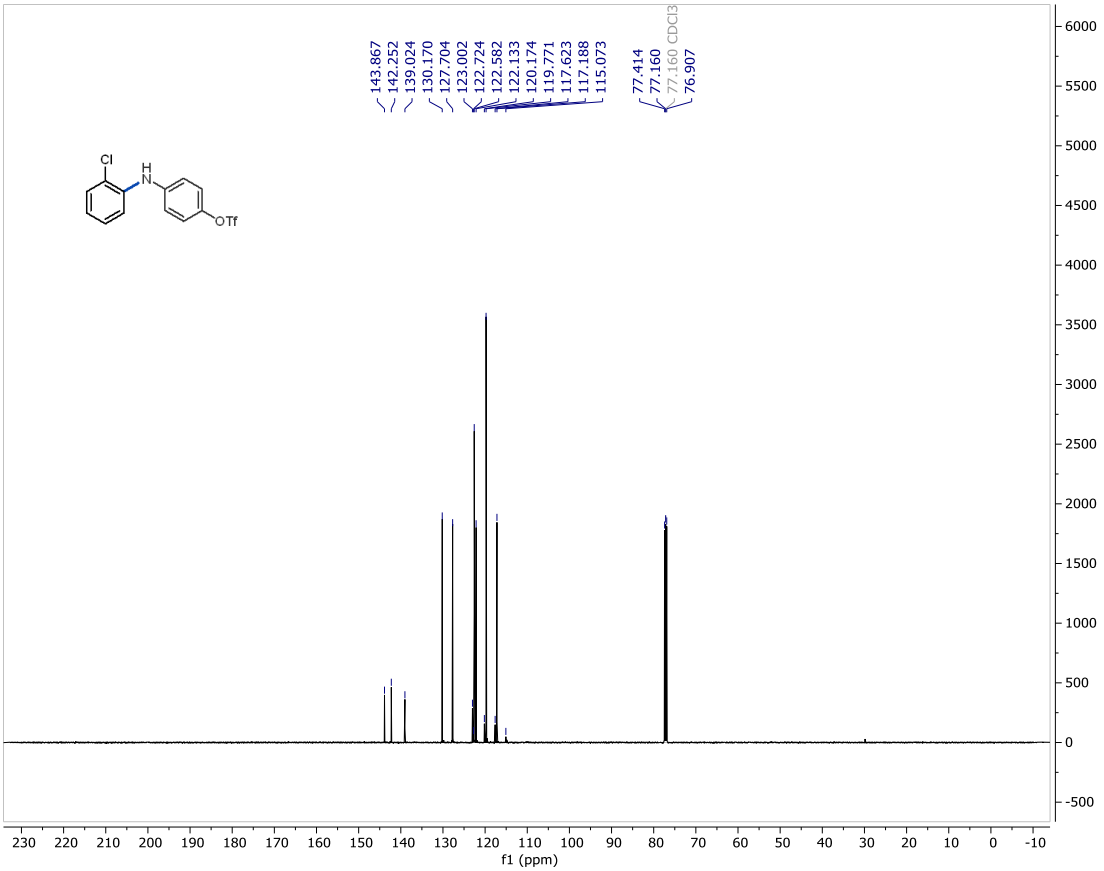

Figure S57. ^{13}C NMR (126 MHz, $CDCl_3$) of **6**.

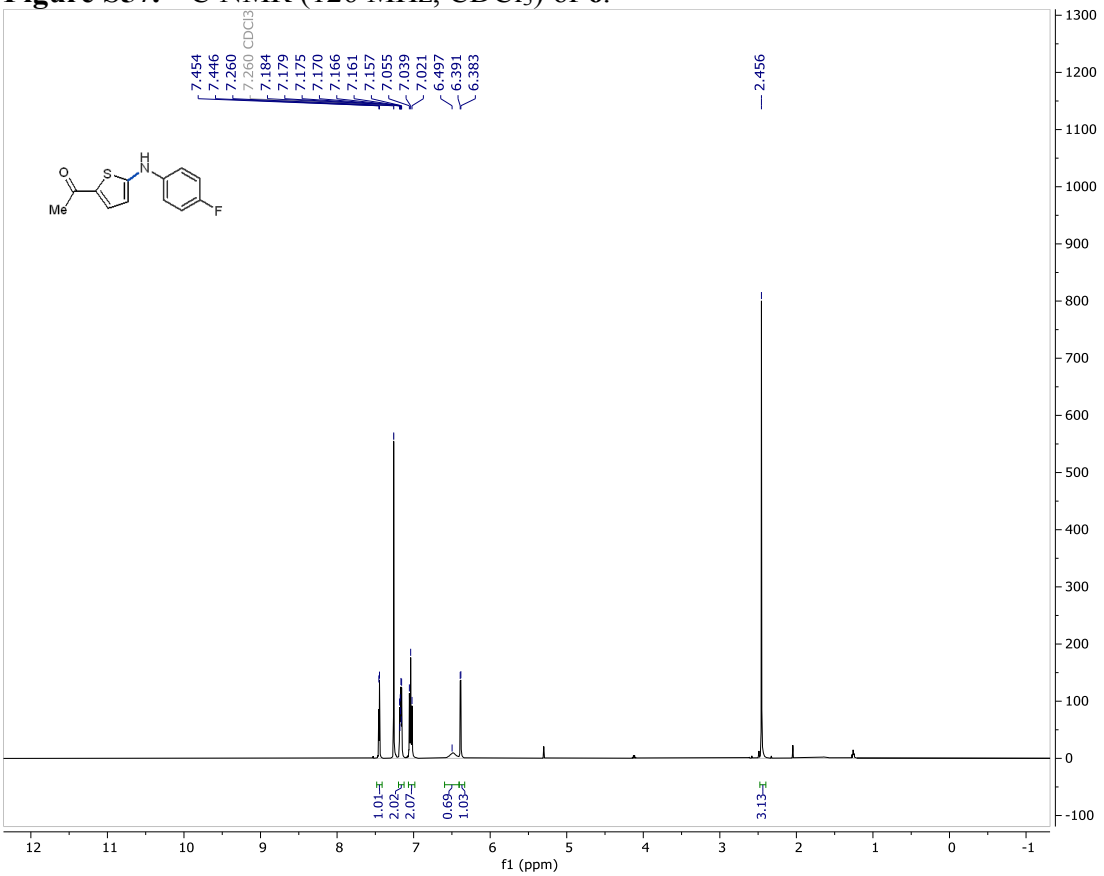

Figure S58. ^{1}H NMR (500 MHz, $CDCl_3$) of **7**.

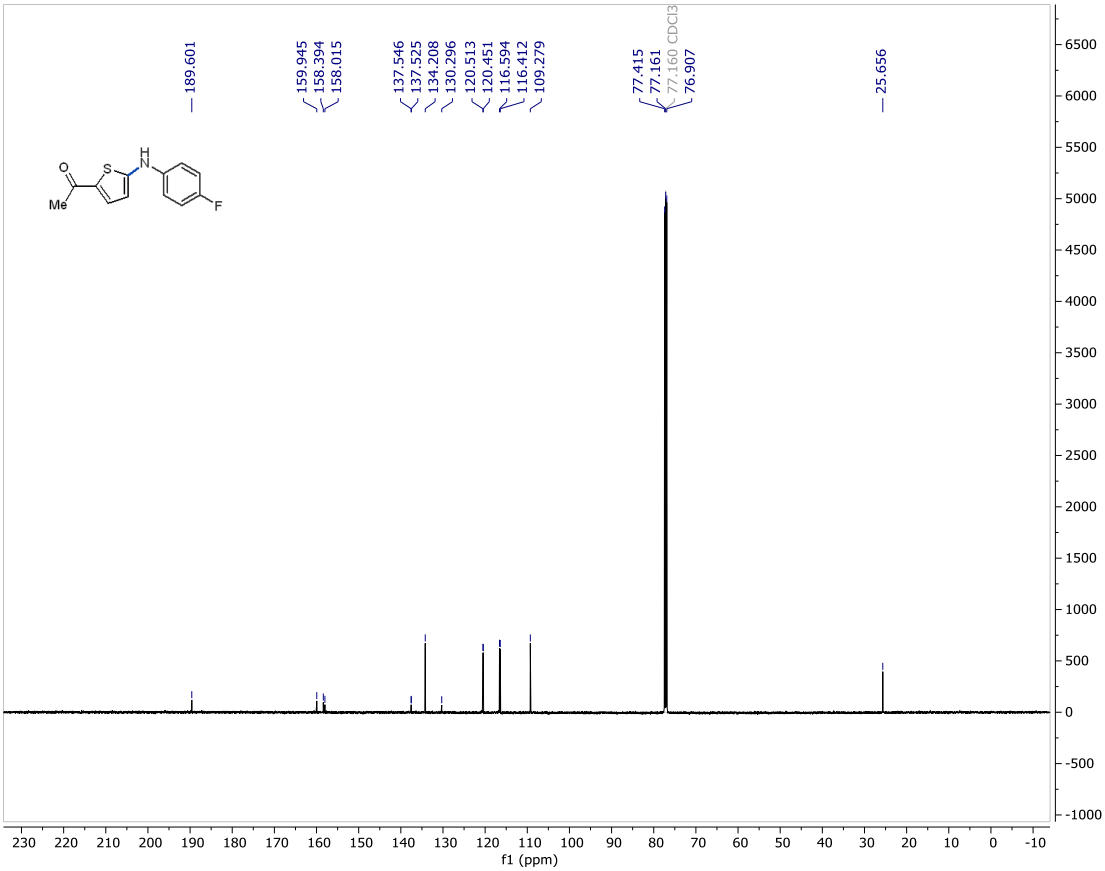

Figure S59. ^{13}C NMR (126 MHz, $CDCl_3$) of **7**.

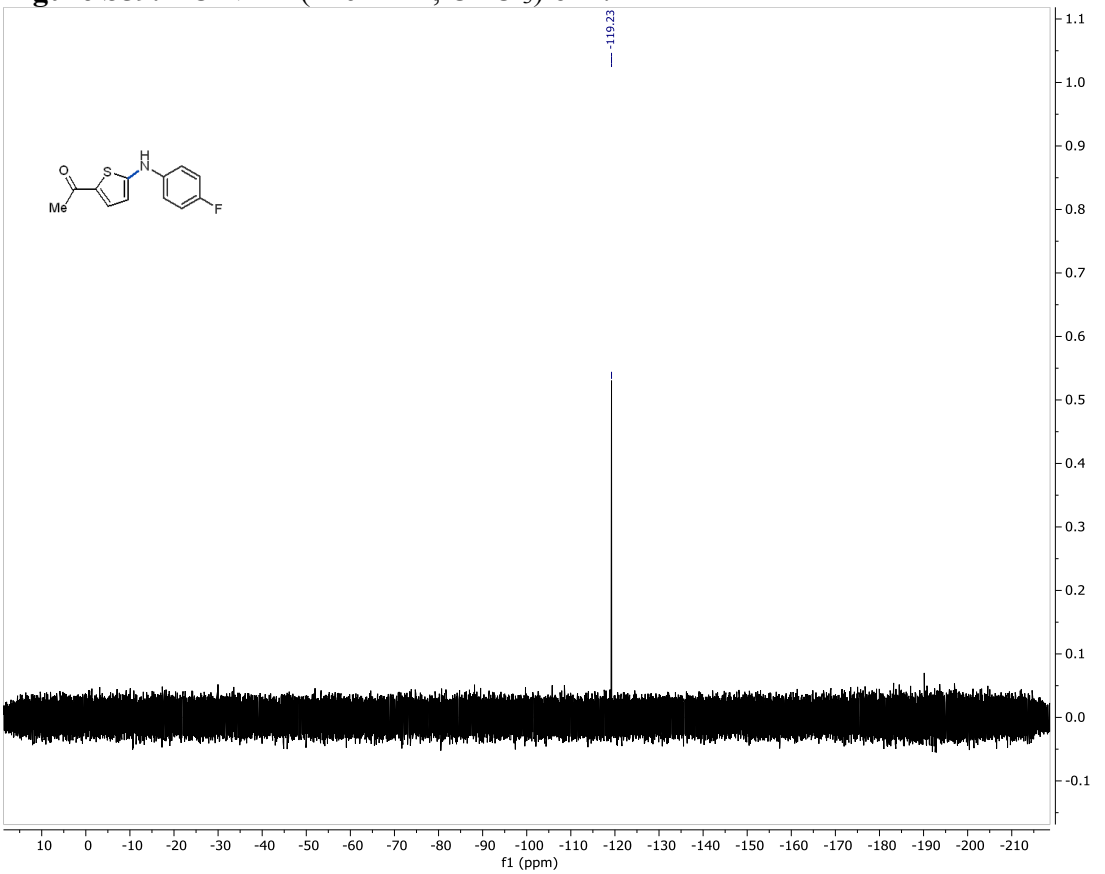

Figure S60. ^{19}F NMR (376 MHz, $CDCl_3$) of **7**.

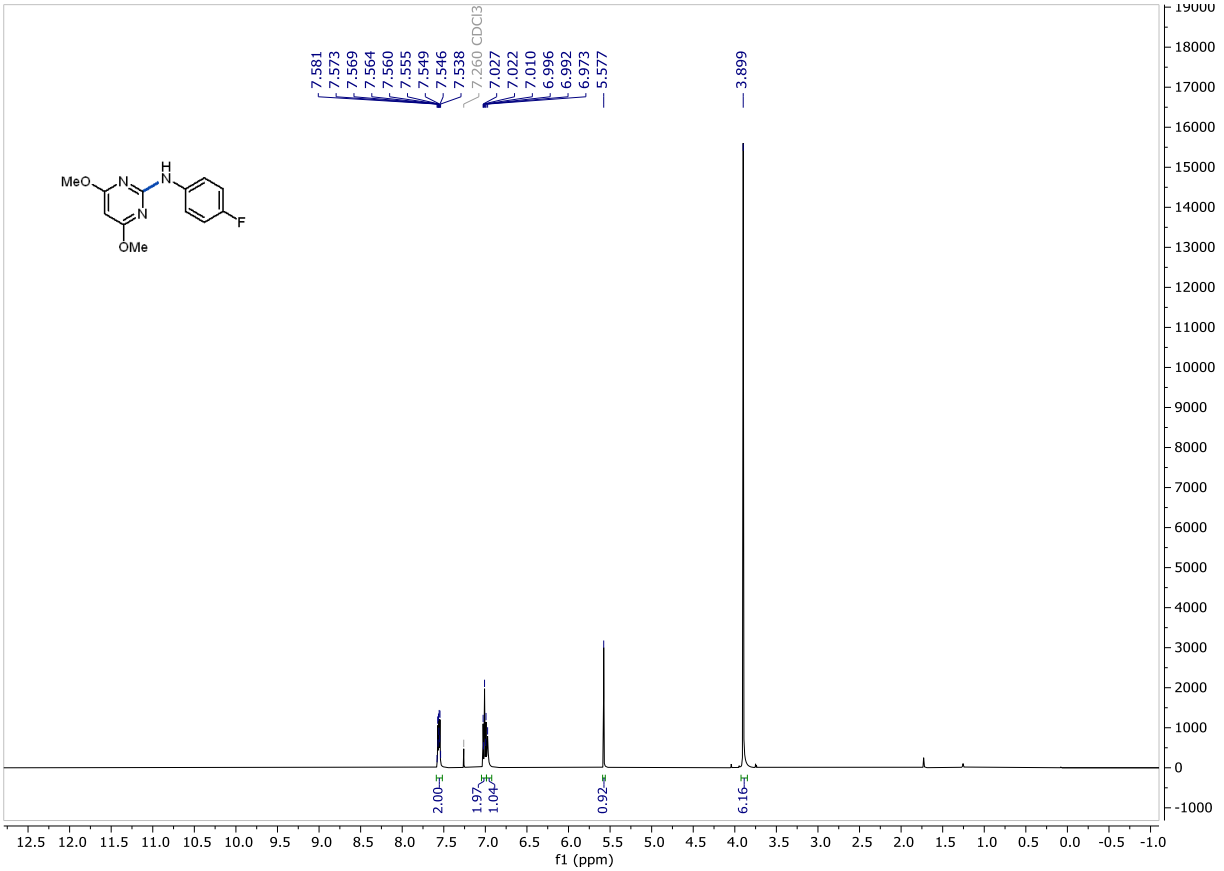

Figure S61. ^{1}H NMR (500 MHz, $CDCl_3$) of **8**.

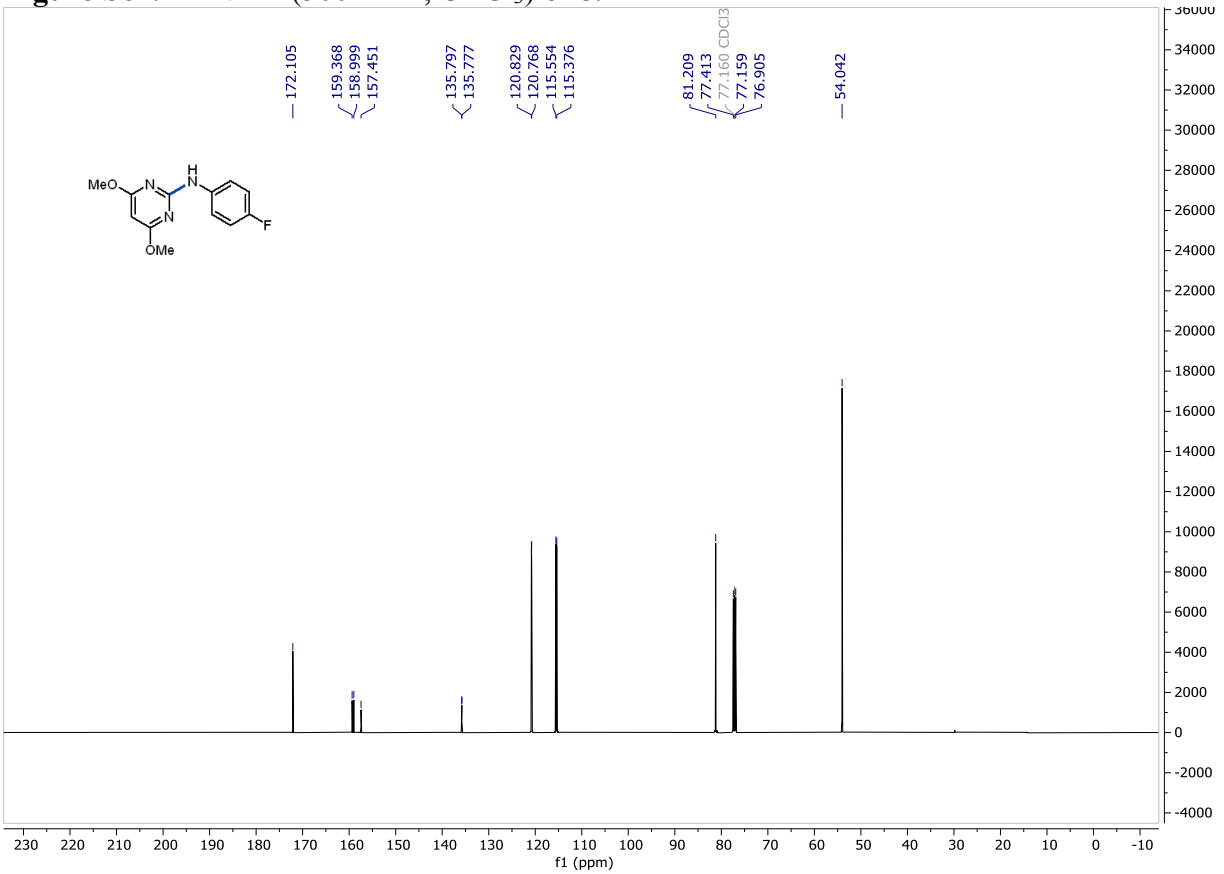

Figure S62. ^{13}C NMR (126 MHz, $CDCl_3$) of **8**.

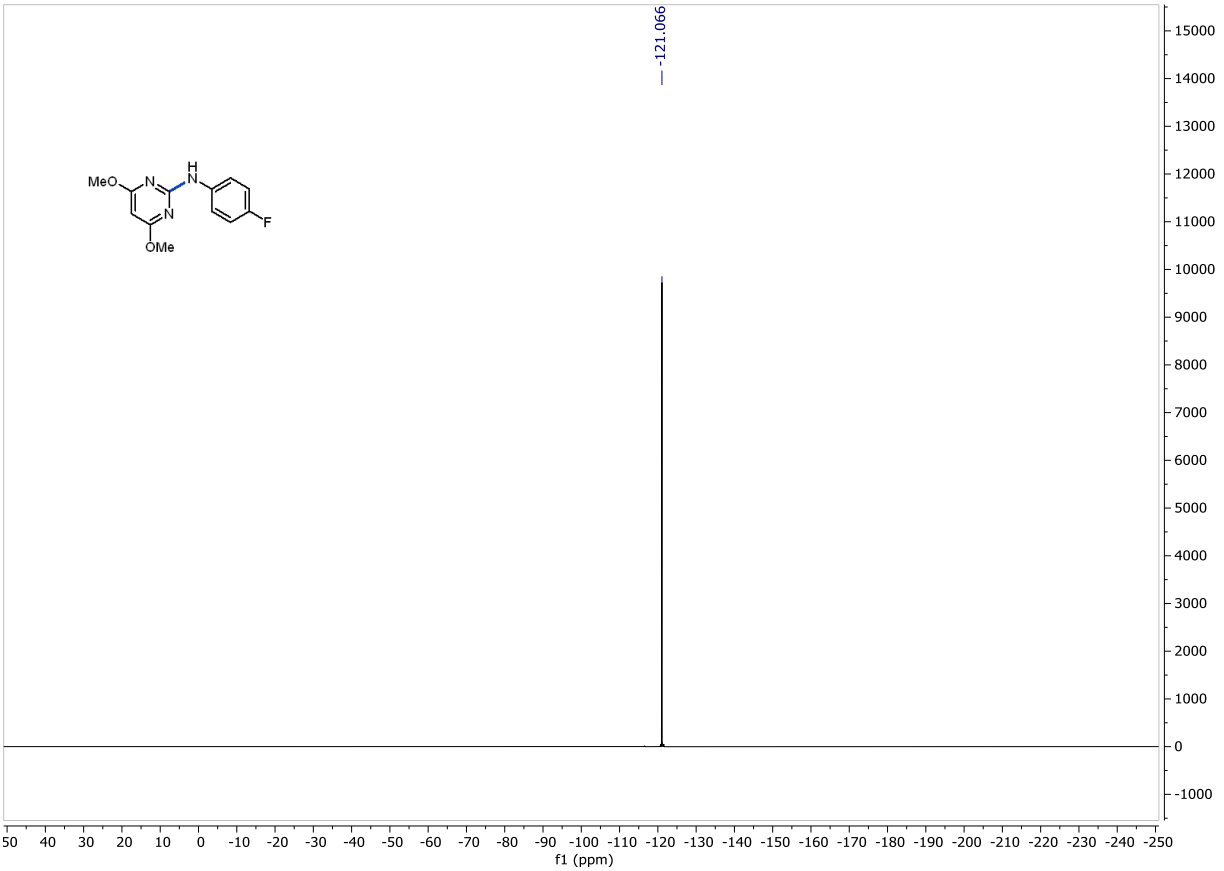

Figure S63. ^{19}F NMR (282 MHz, $CDCl_3$) of **8**.

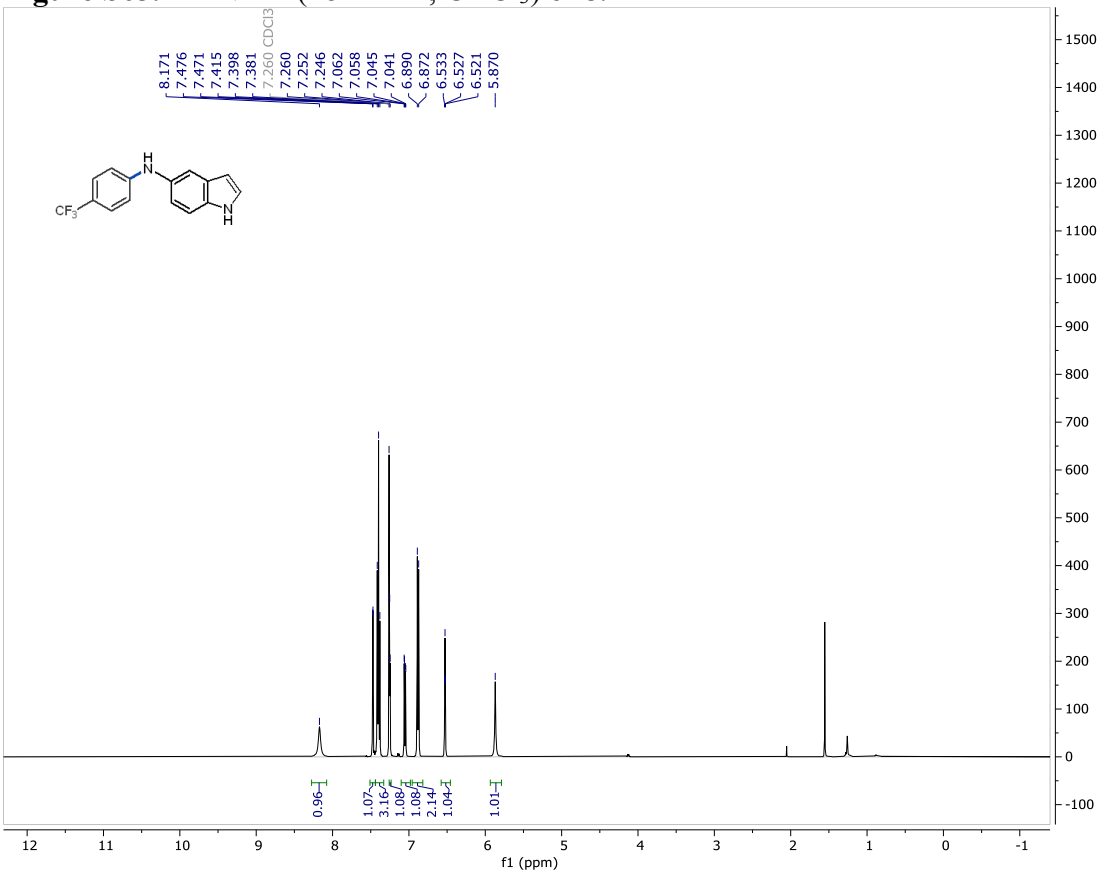

Figure S64. ^{1}H NMR (500 MHz, $CDCl_3$) of **9**.

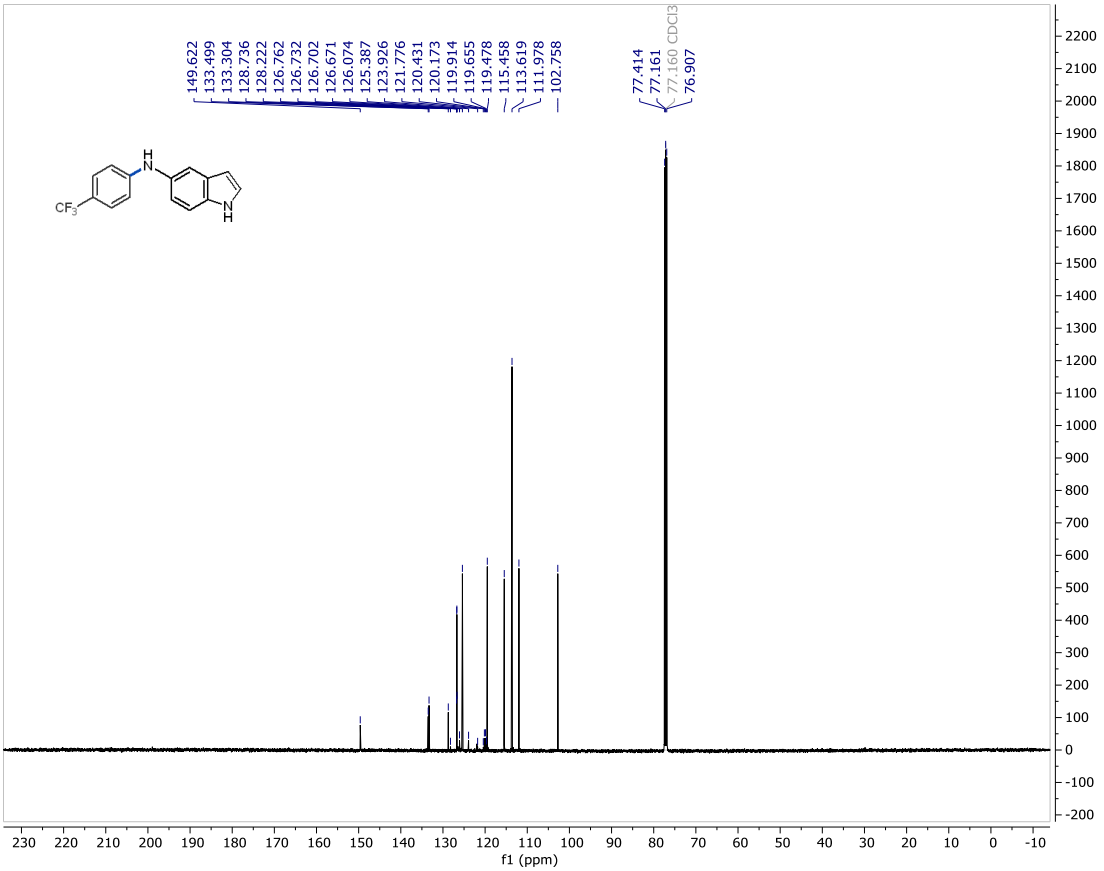

Figure S65. ^{13}C NMR (126 MHz, $CDCl_3$) of **9**.

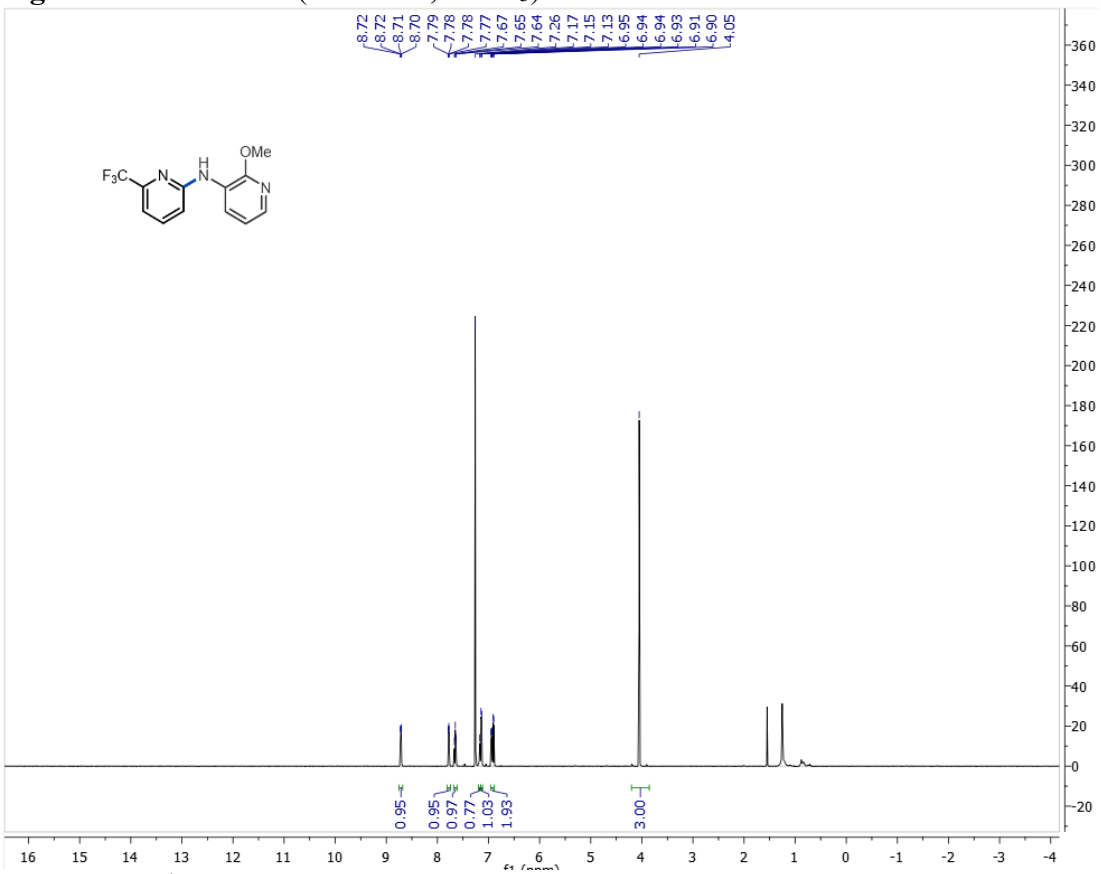

Figure S66. ^{1}H NMR (500 MHz, $CDCl_3$) of **10**.

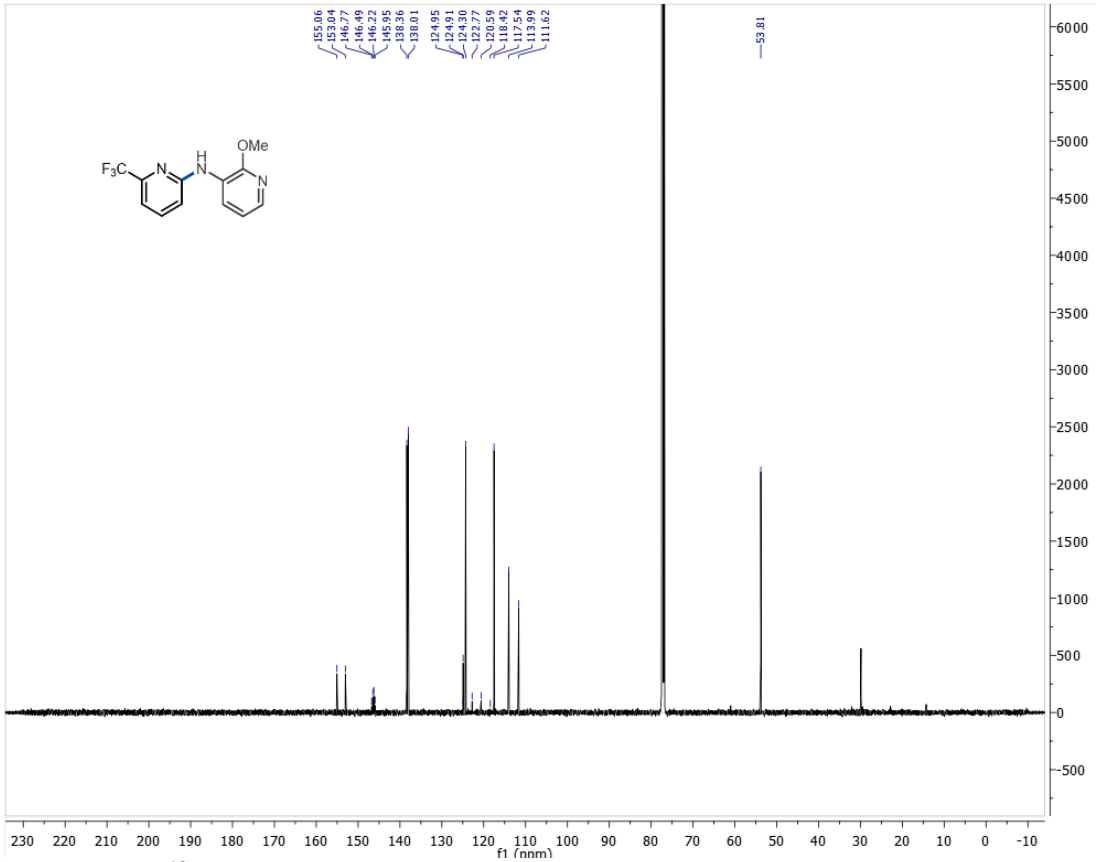

Figure S67. ^{13}C NMR (126 MHz, $CDCl_3$) of **10**.

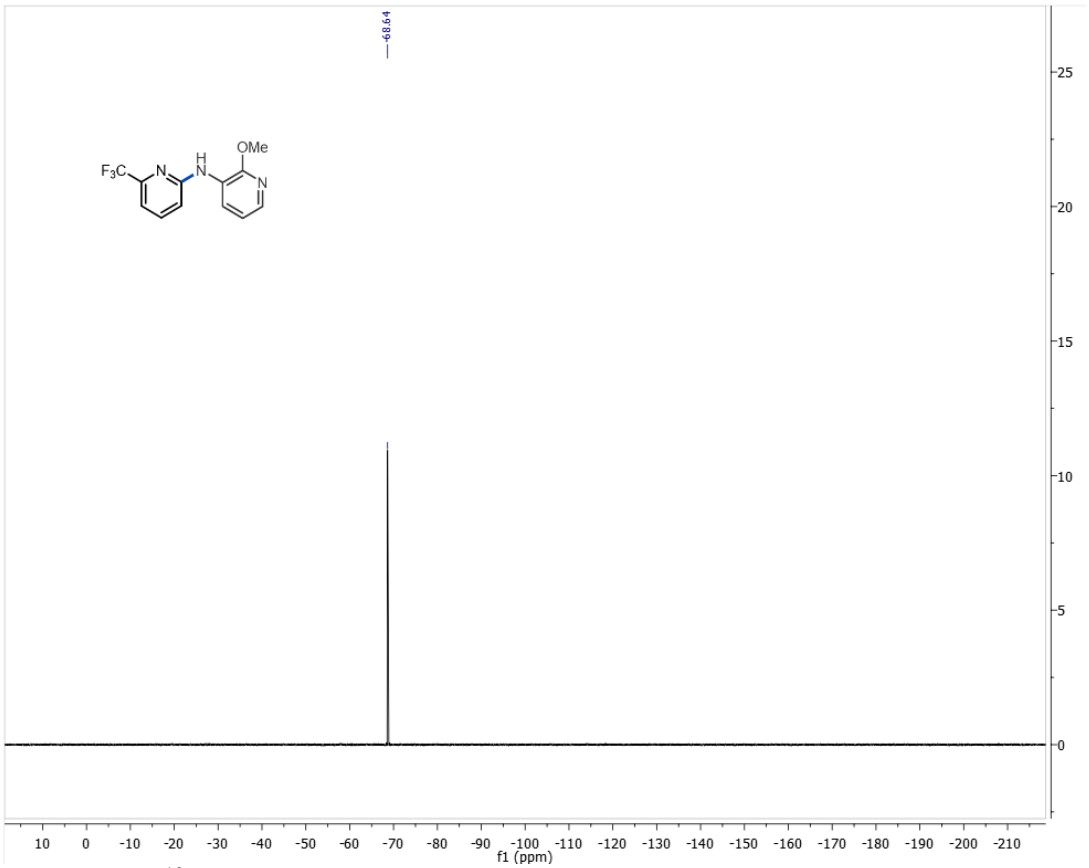

Figure S68. ^{19}F NMR (376 MHz, $CDCl_3$) of **10**.

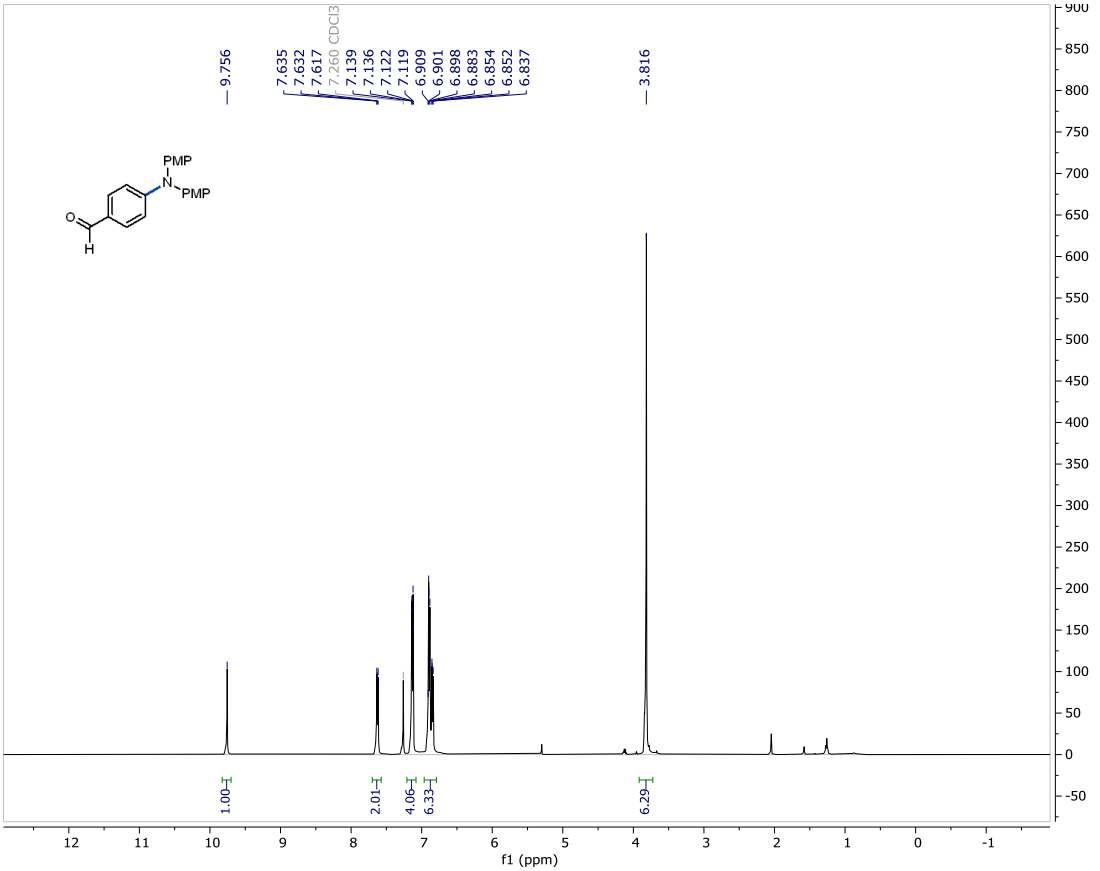

Figure S69. ^{1}H NMR (500 MHz, $CDCl_3$) of **11**.

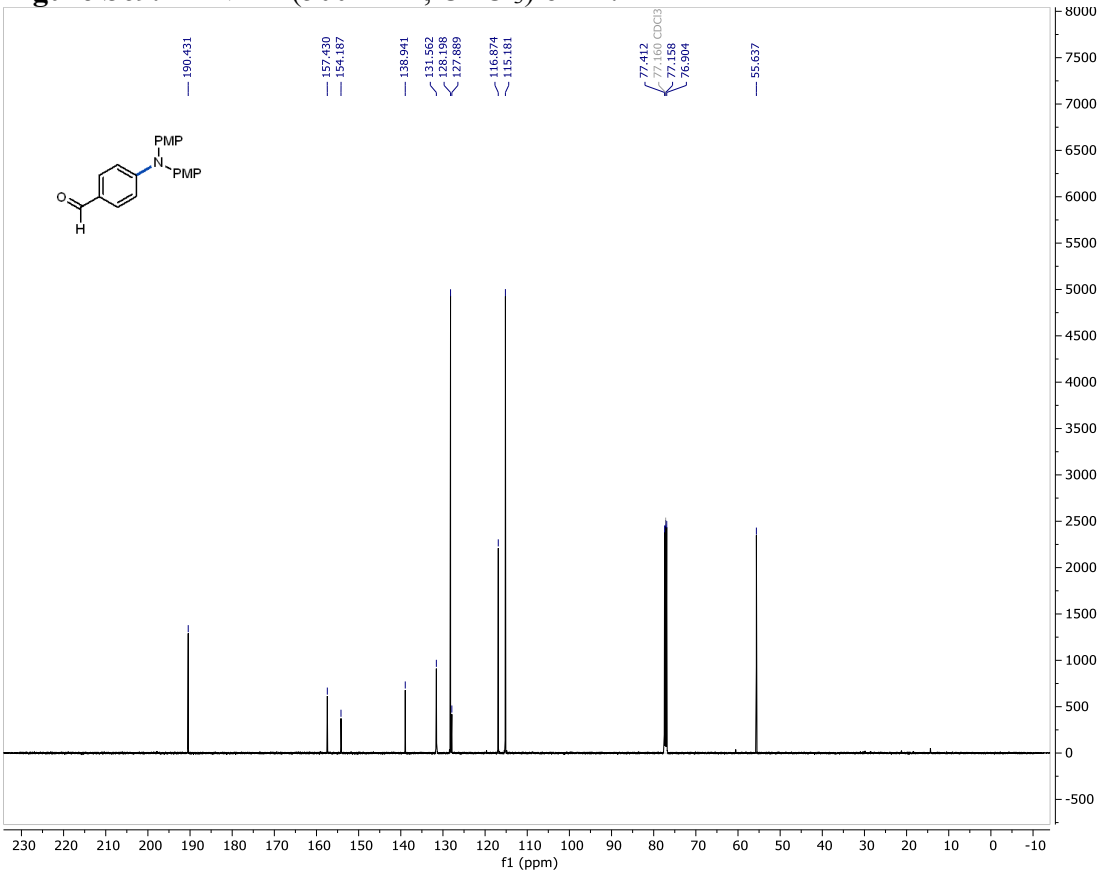

Figure S70. ^{13}C NMR (126 MHz, $CDCl_3$) of **11**.

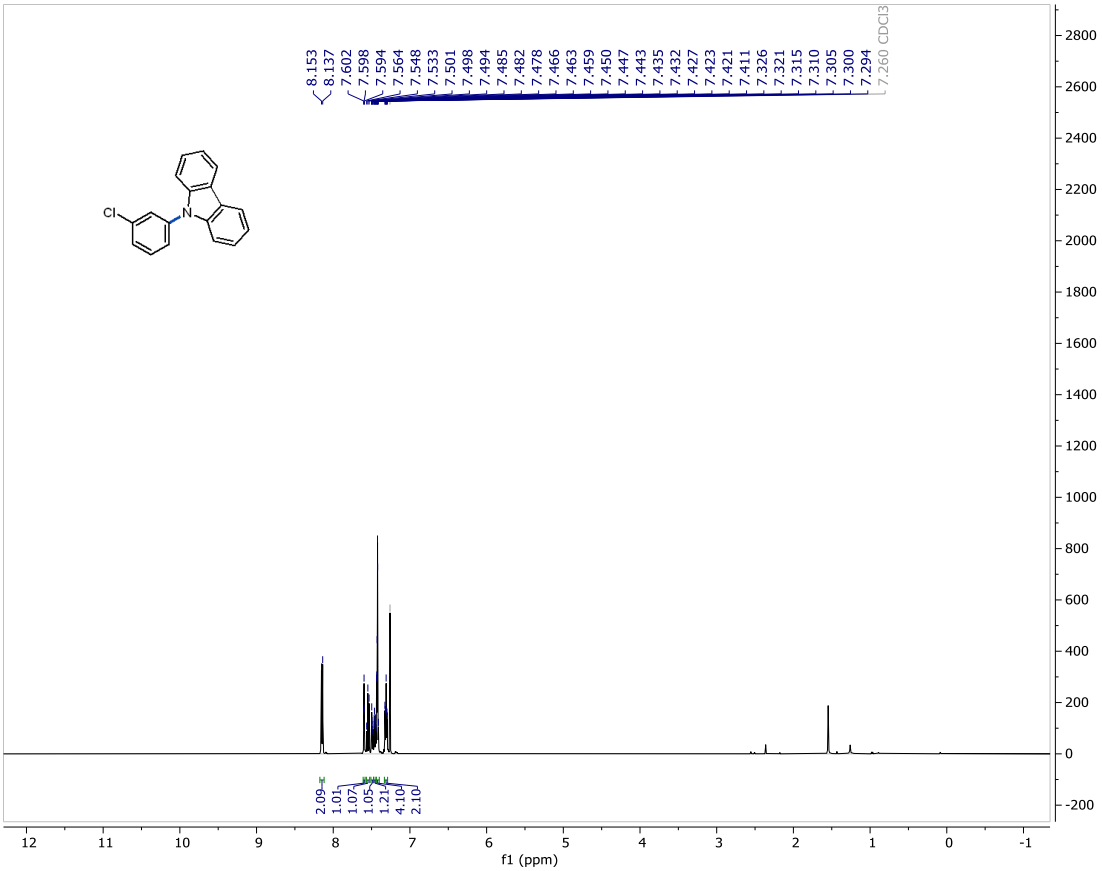

Figure S71. ^{1}H NMR (500 MHz, $CDCl_3$) of **12**.

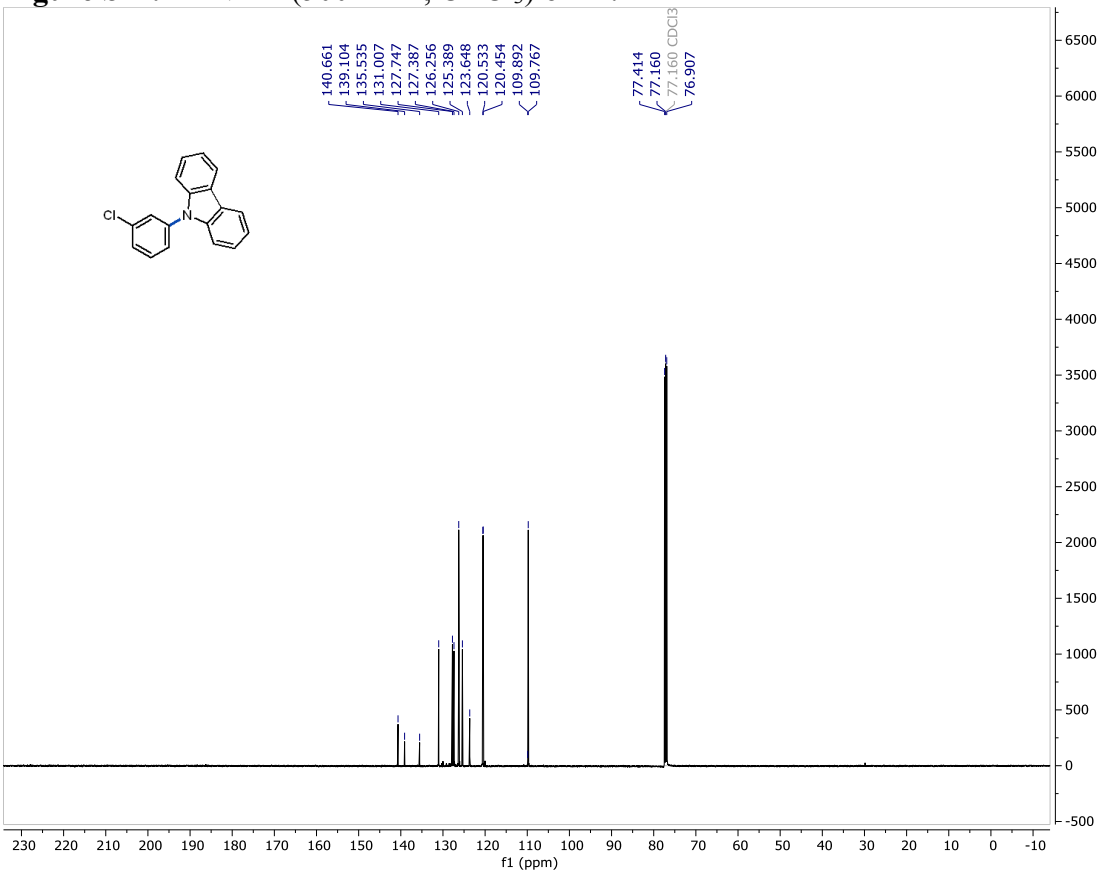

Figure S72. ^{13}C NMR (126 MHz, $CDCl_3$) of **12**.

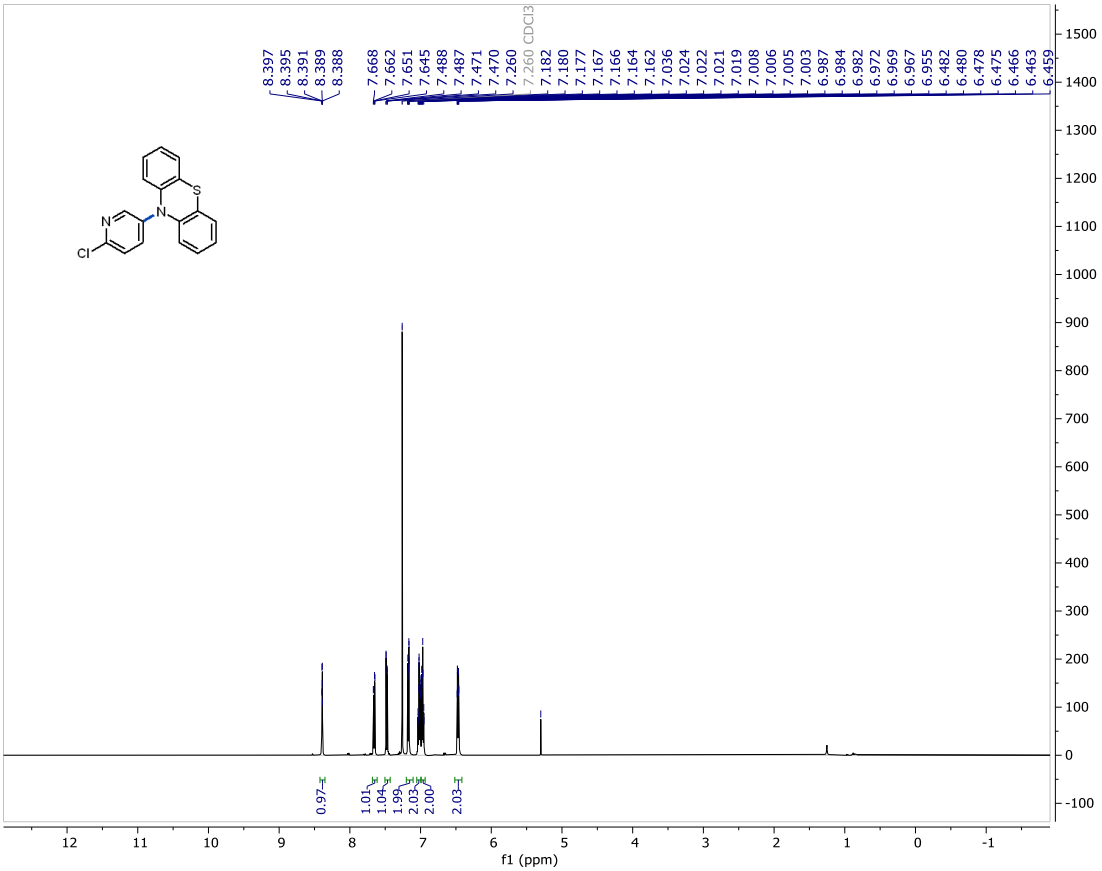

Figure S73. ^{1}H NMR (500 MHz, $CDCl_3$) of **13**.

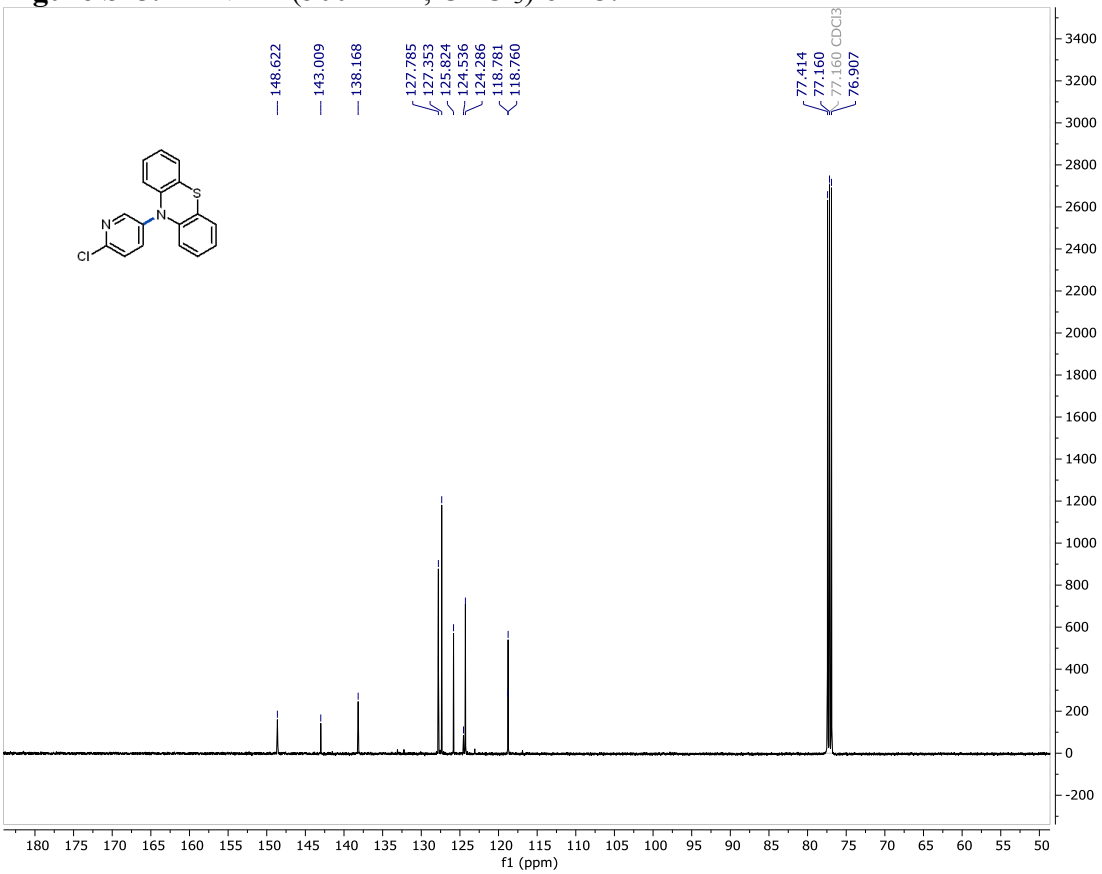

Figure S74. ^{13}C NMR (126 MHz, $CDCl_3$) of **13**.

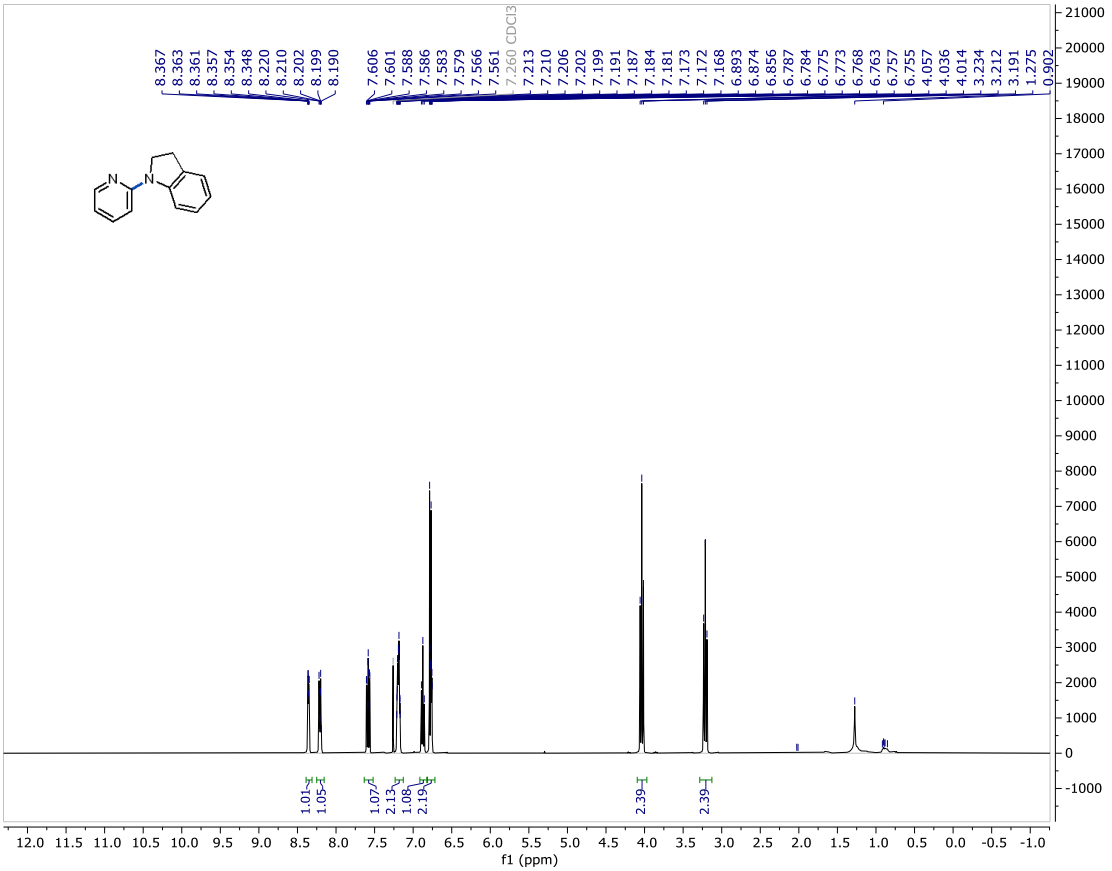

Figure S75. ^{1}H NMR (500 MHz, $CDCl_3$) of **14**.

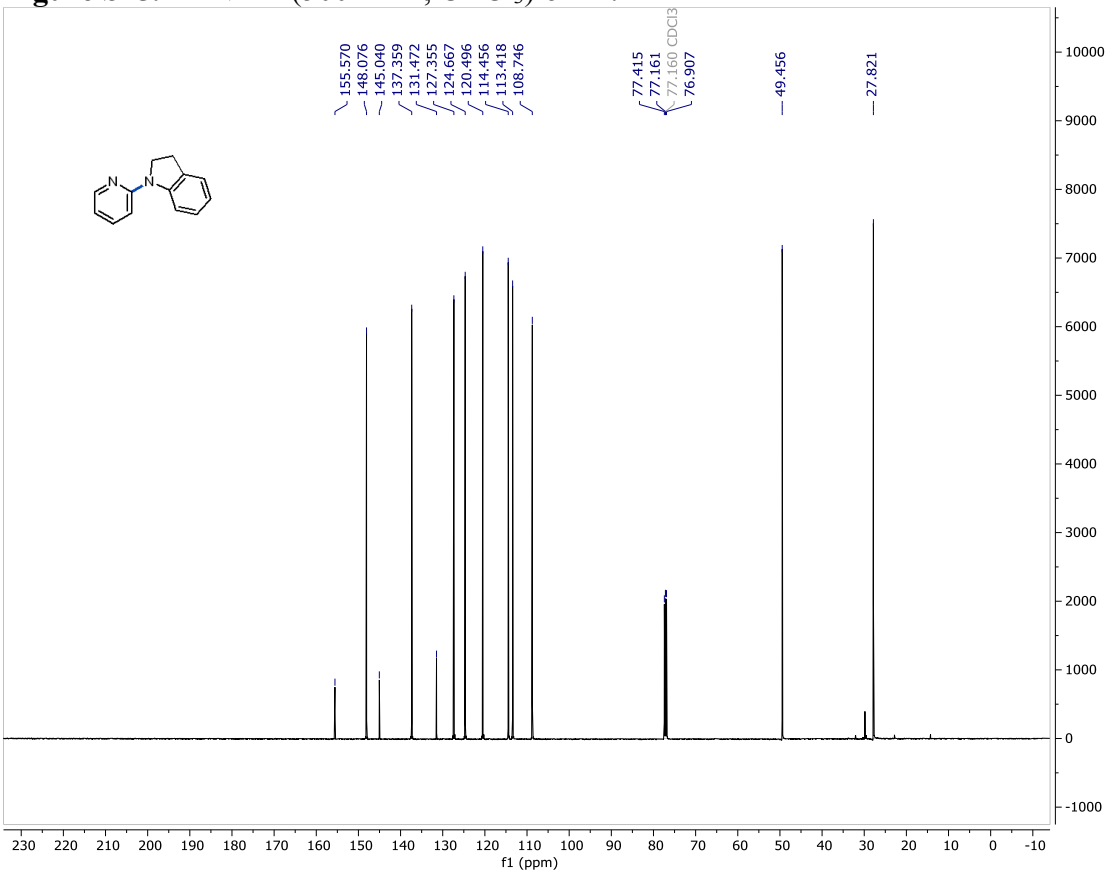

Figure S76. ^{13}C NMR (126 MHz, $CDCl_3$) of **14**.

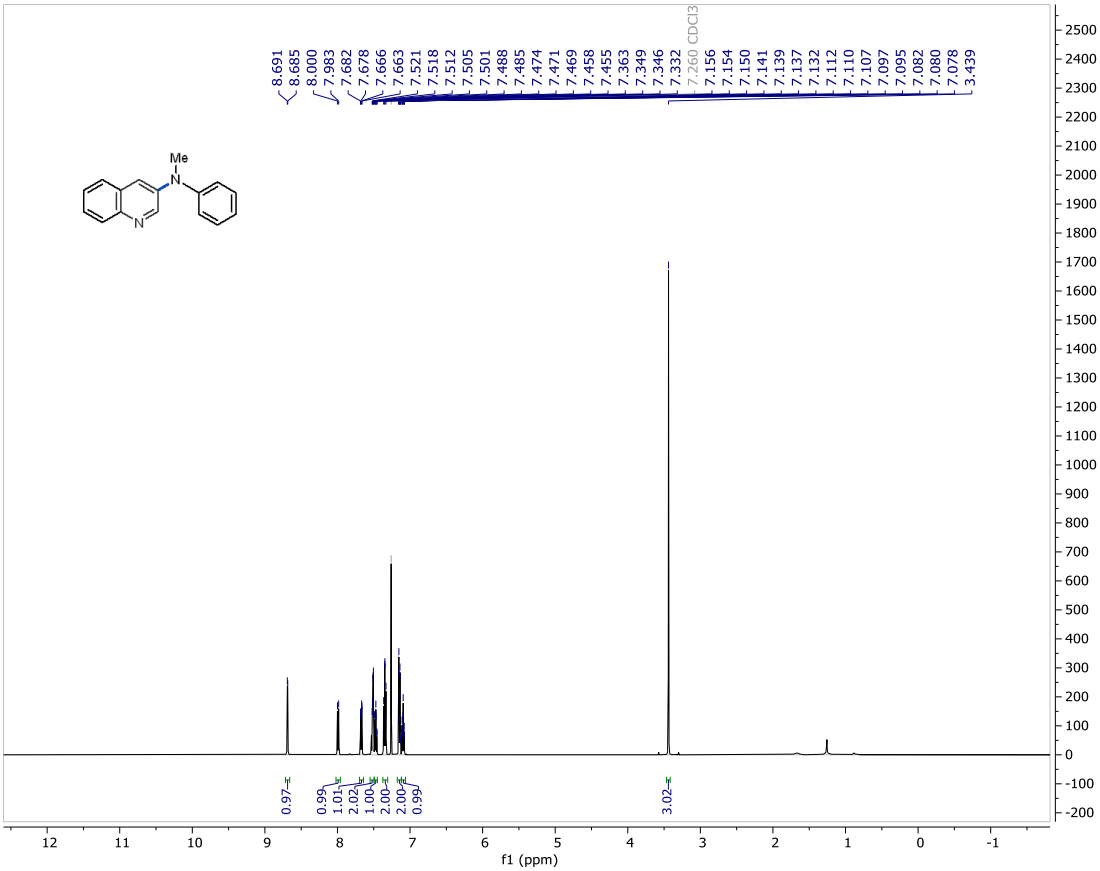

Figure S77. ^{1}H NMR (500 MHz, $CDCl_3$) of **15**.

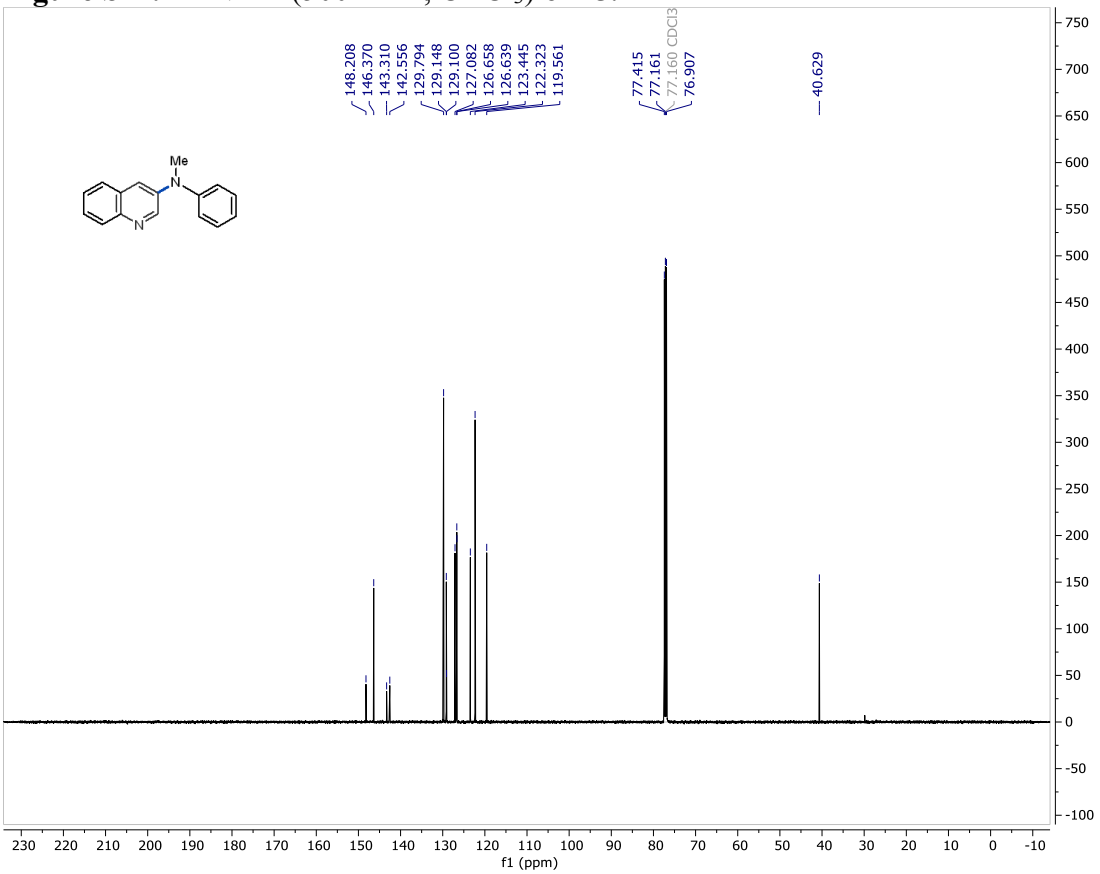

Figure S78. ^{13}C NMR (126 MHz, $CDCl_3$) of **15**.

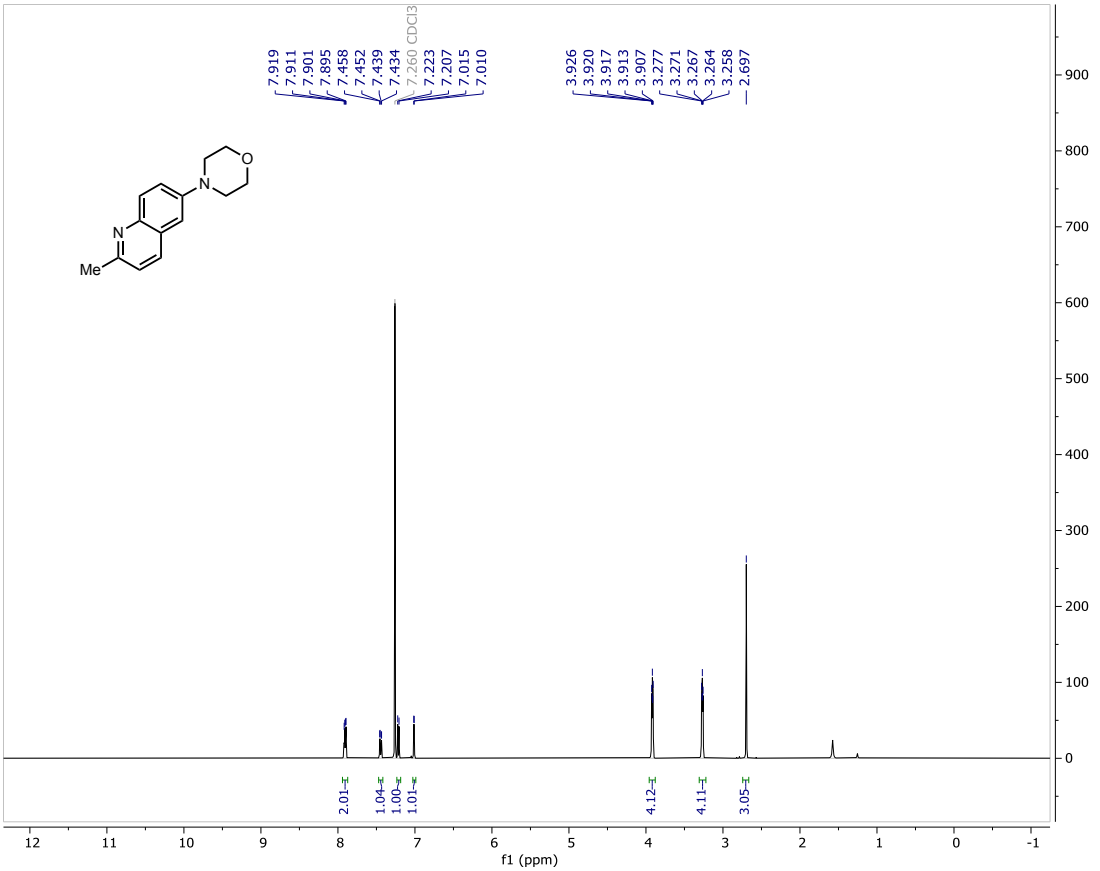

Figure S79. ^{1}H NMR (500 MHz, $CDCl_3$) of **16**.

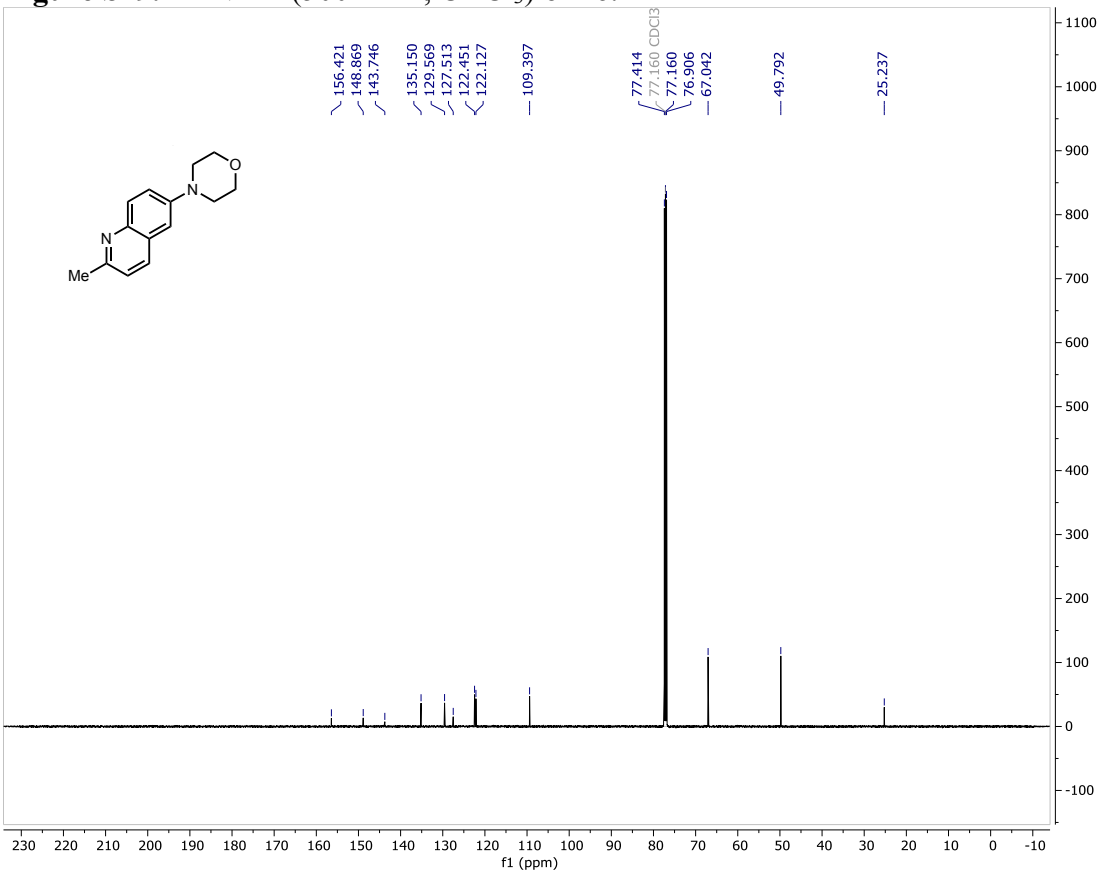

Figure S80. ^{13}C NMR (126 MHz, $CDCl_3$) of **16**.

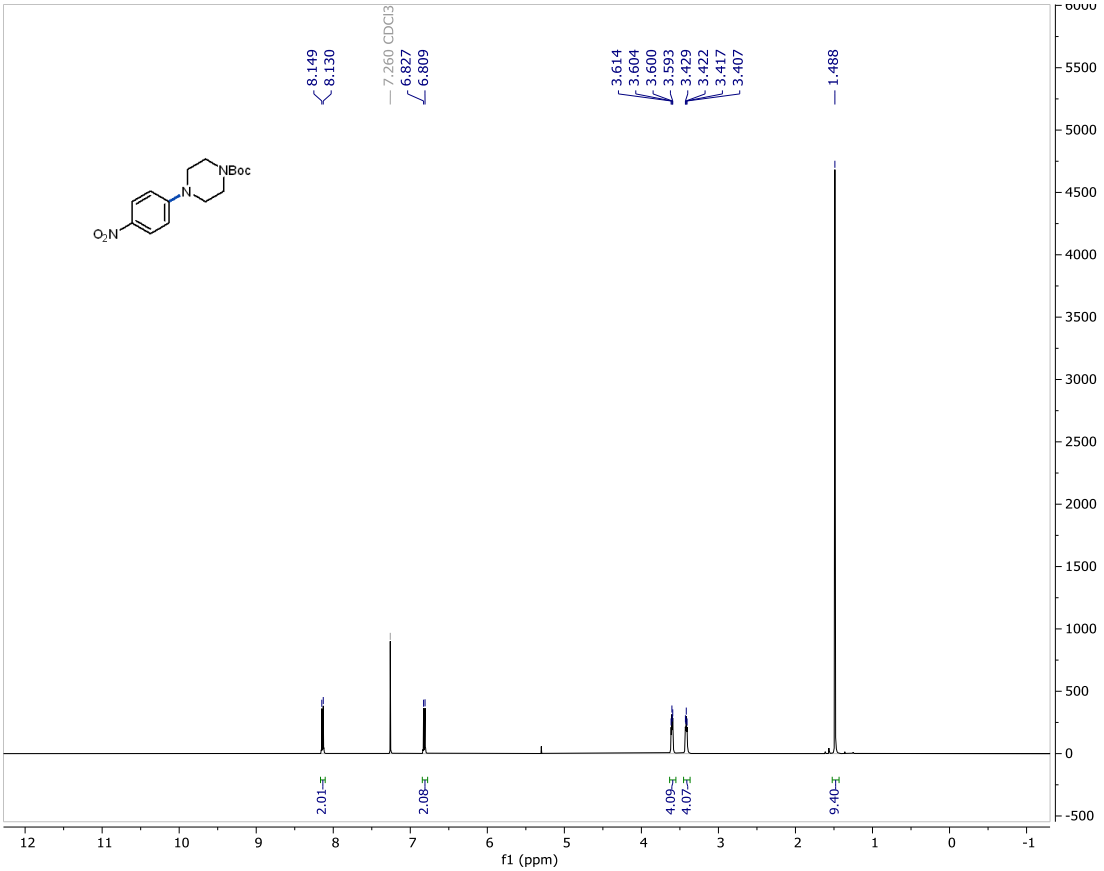

Figure S81. ^{1}H NMR (500 MHz, $CDCl_3$) of **17**.

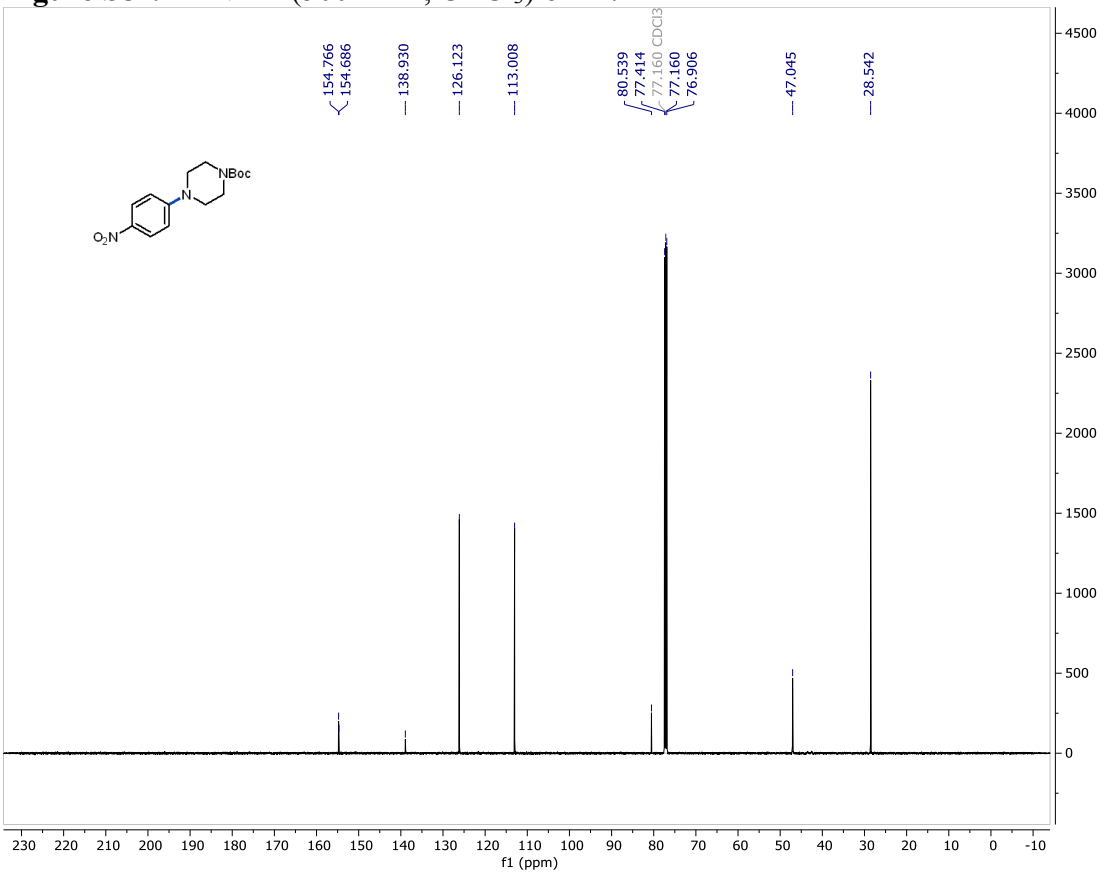

Figure S82. ^{13}C NMR (126 MHz, $CDCl_3$) of **17**.

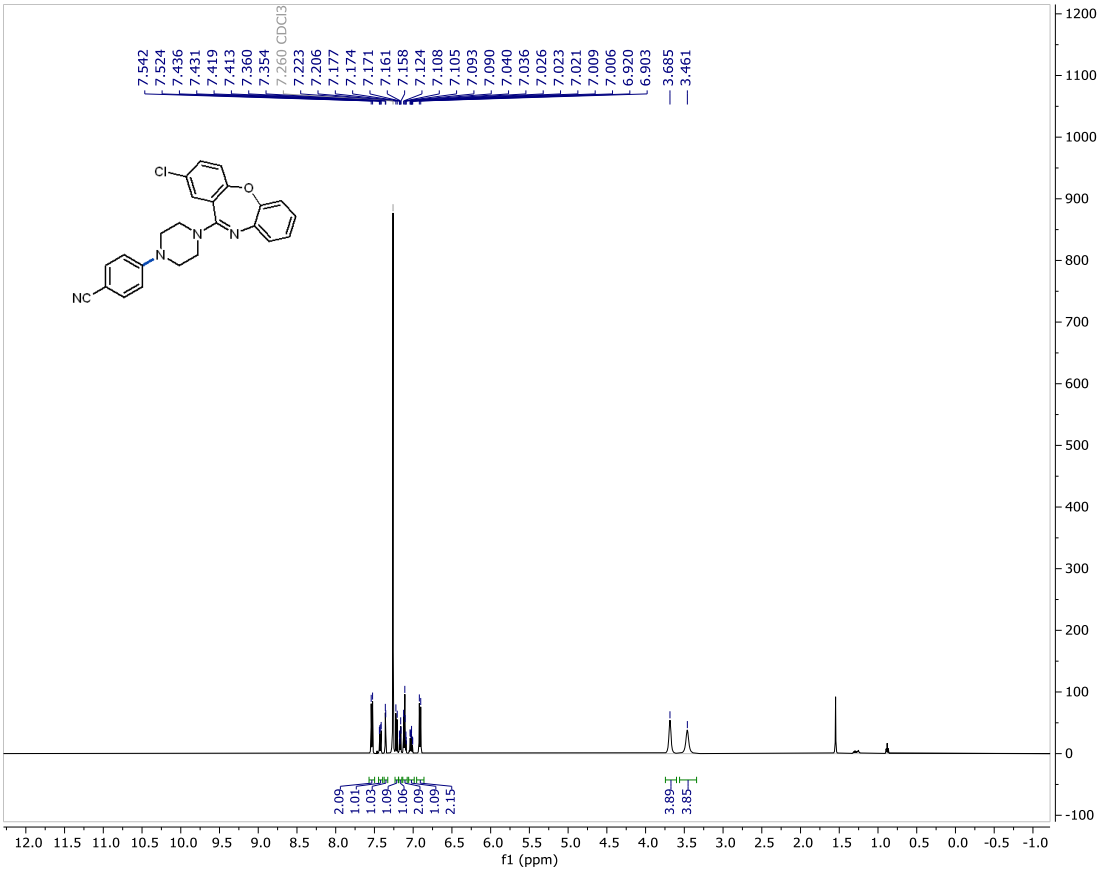

Figure S83. ^{1}H NMR (500 MHz, $CDCl_3$) of **18**.

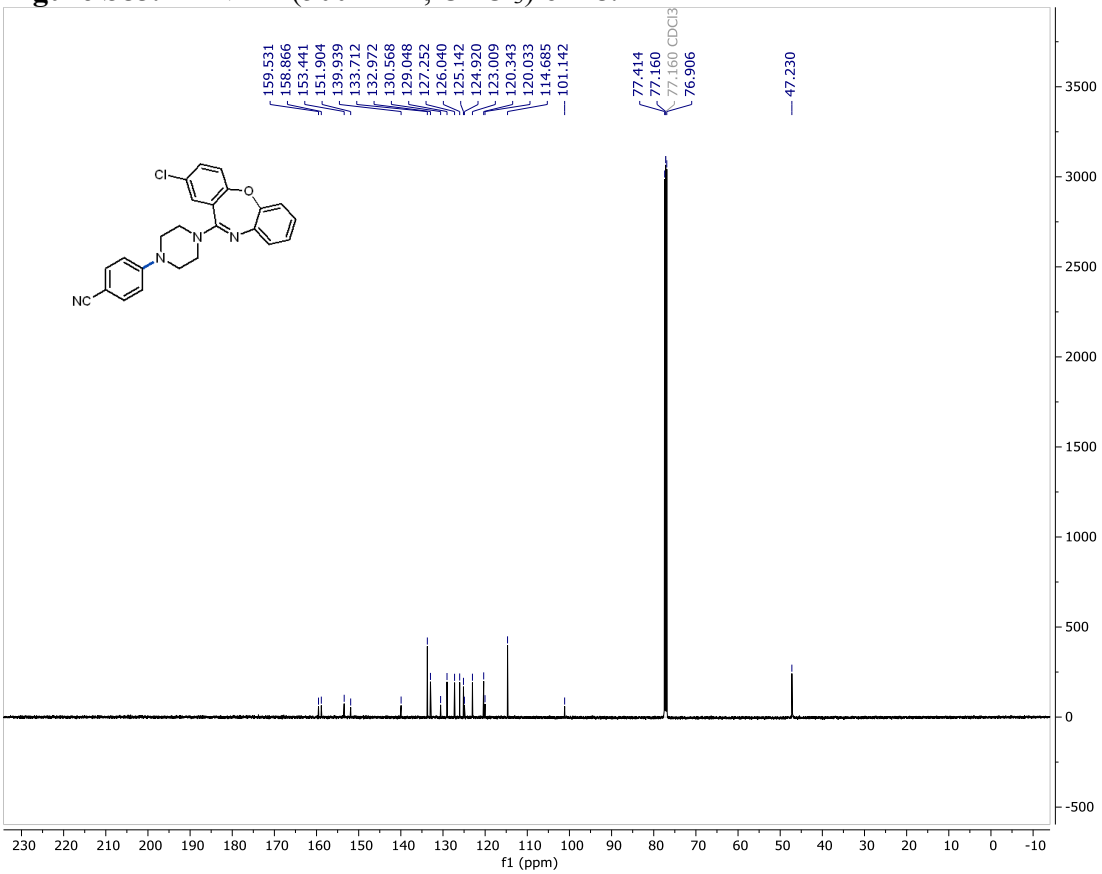

Figure S84. ^{13}C NMR (126 MHz, $CDCl_3$) of **18**.

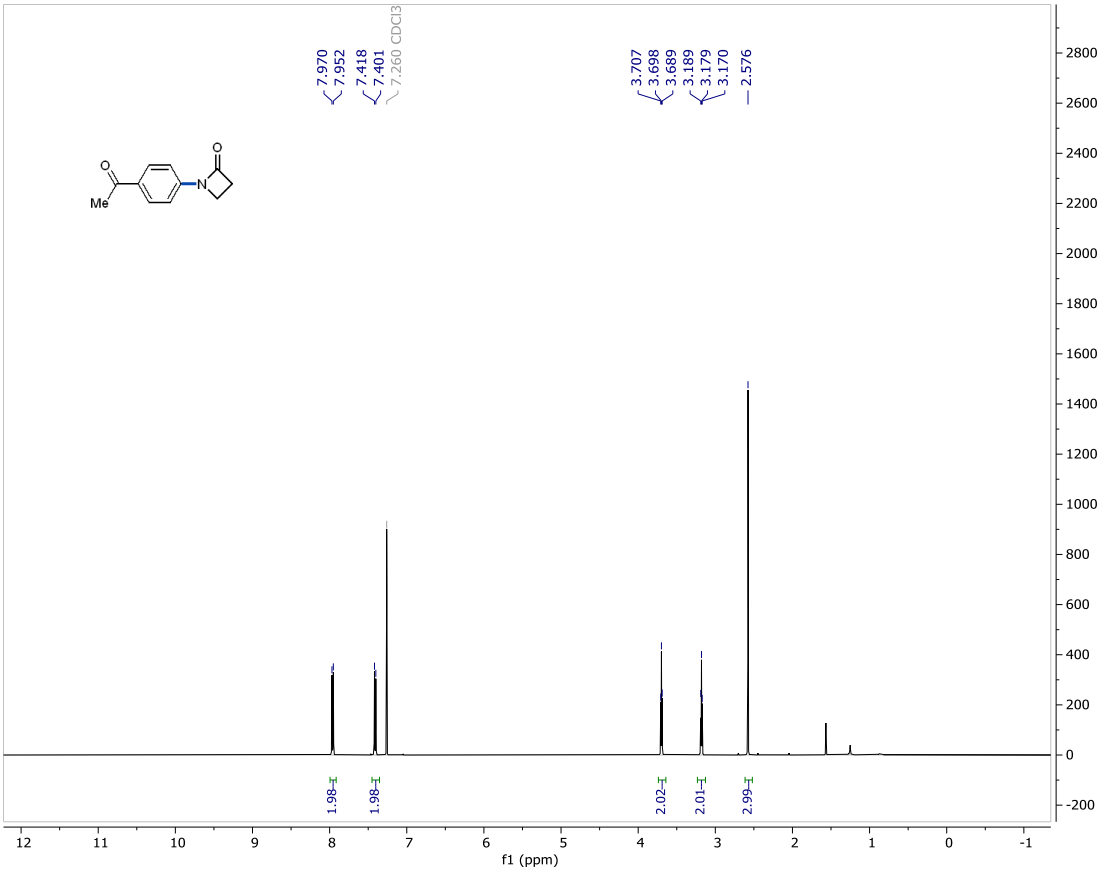

Figure S85. ^{1}H NMR (500 MHz, $CDCl_3$) of **19**.

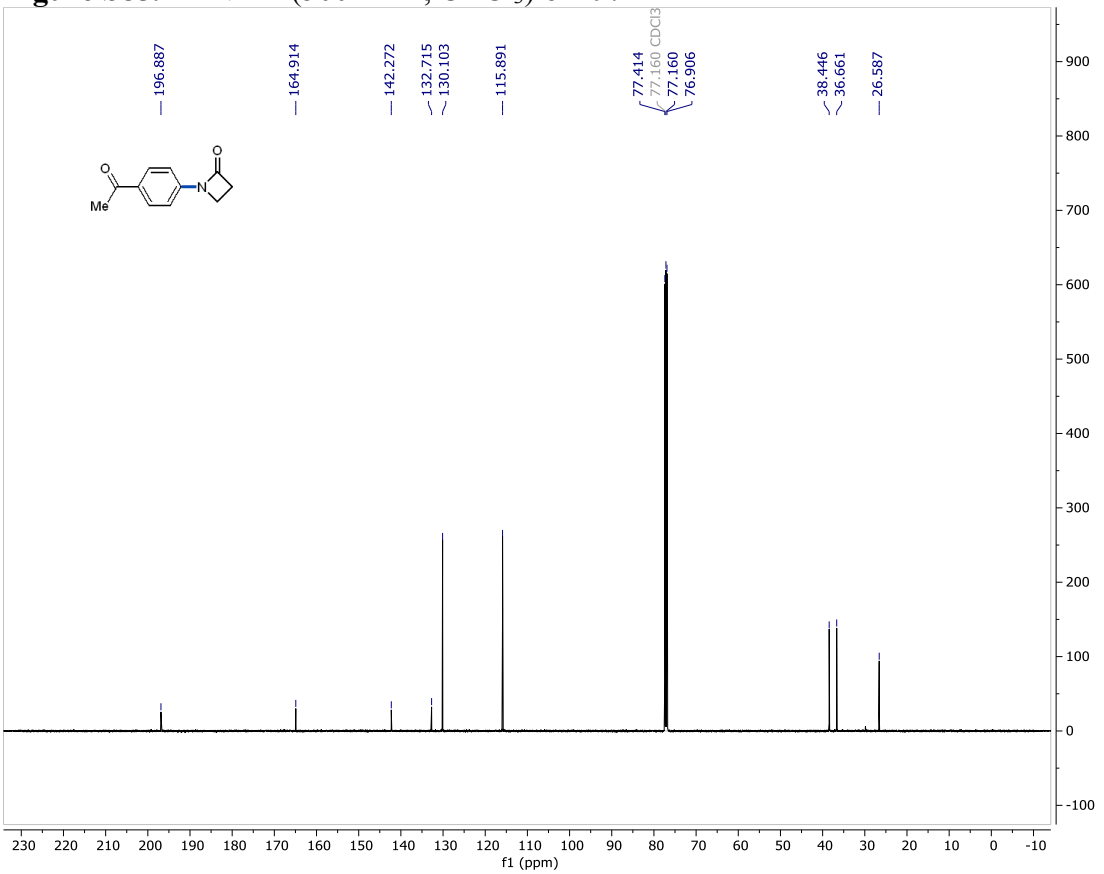

Figure S86. ^{13}C NMR (126 MHz, $CDCl_3$) of **19**.

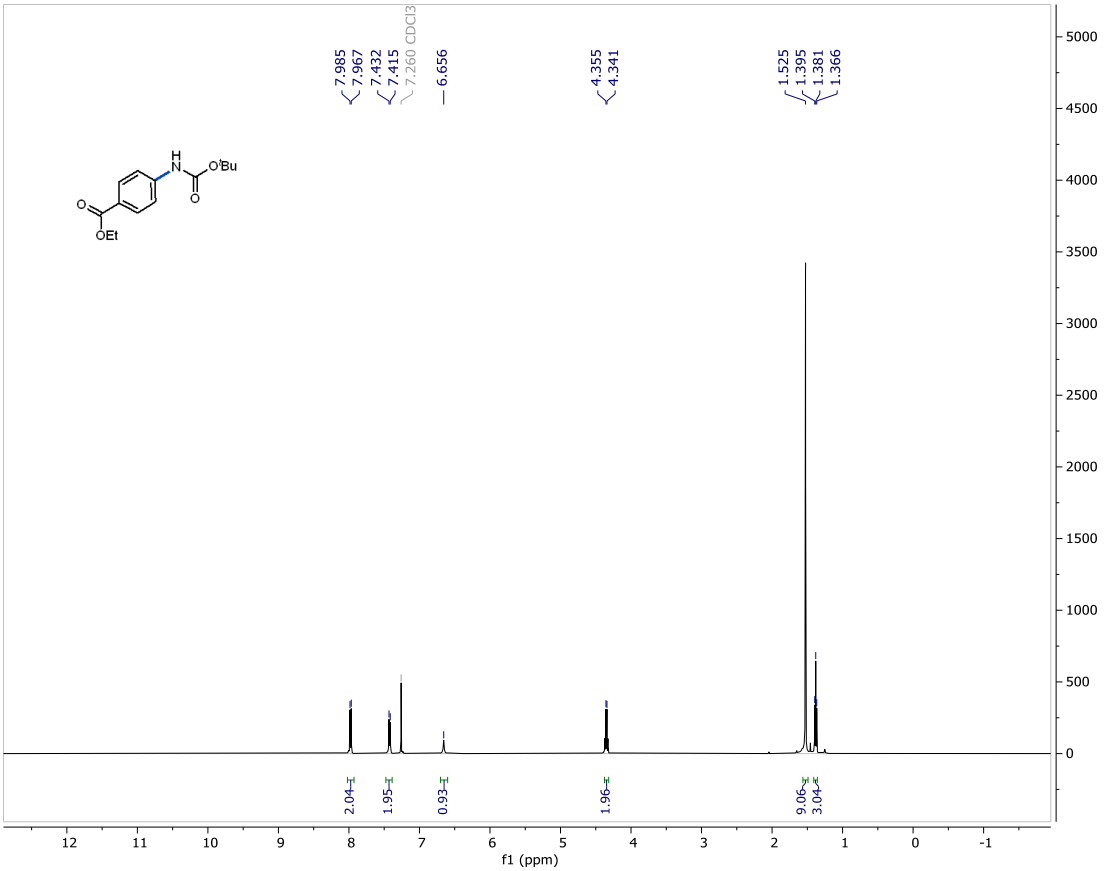

Figure S87. ^{1}H NMR (500 MHz, $CDCl_3$) of **20**.

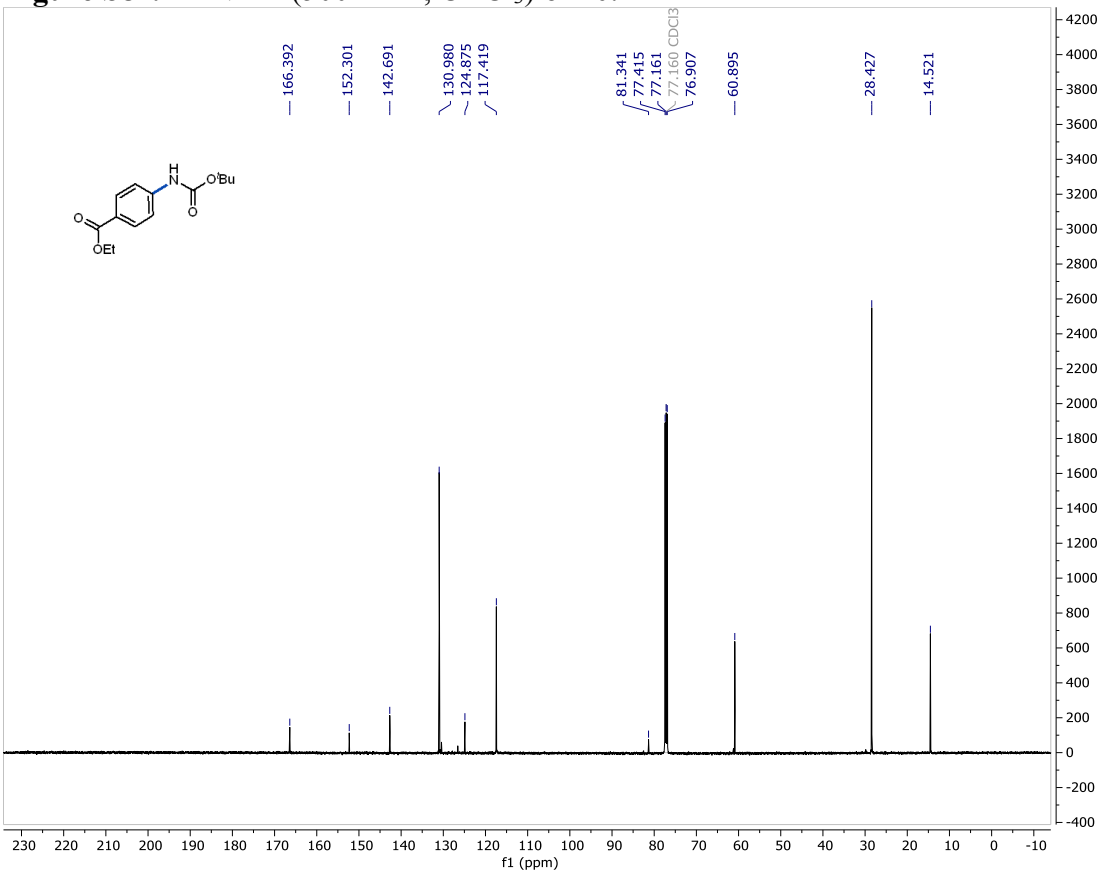

Figure S88. ^{13}C NMR (126 MHz, $CDCl_3$) of **20**.

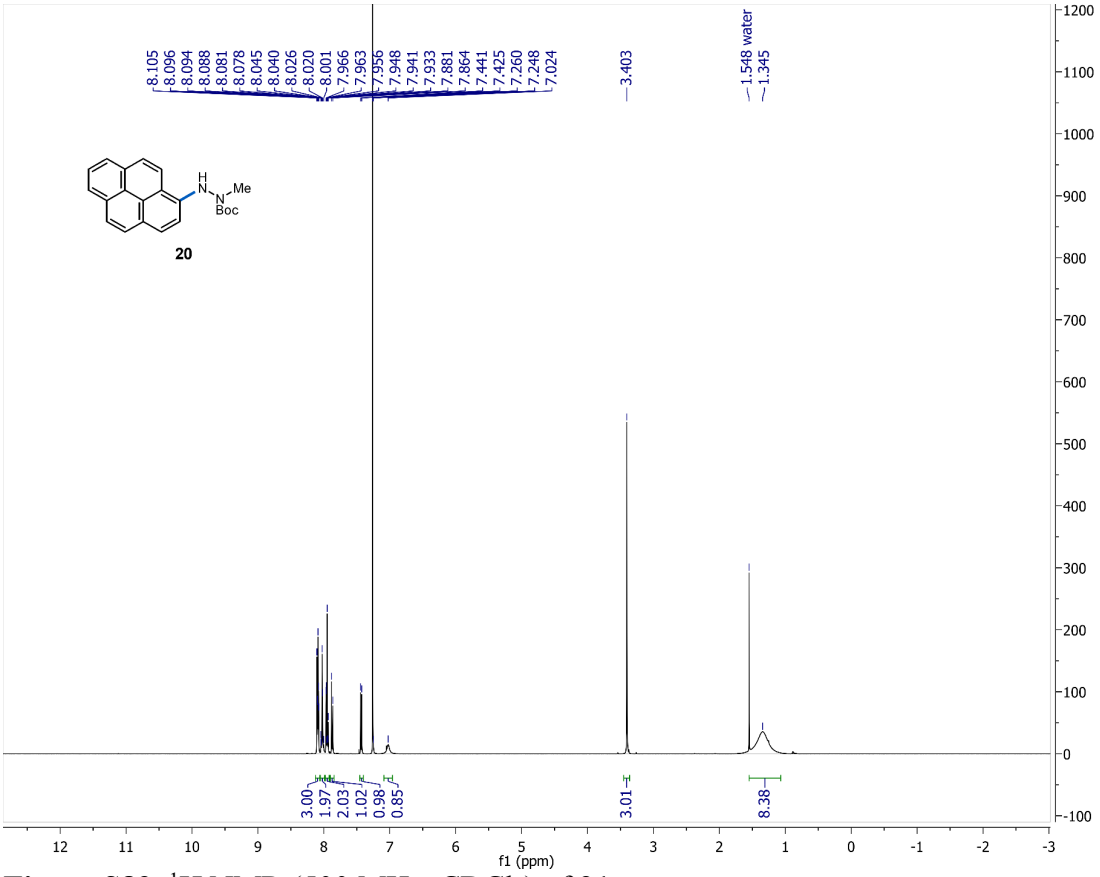

Figure S89. ^{1}H NMR (500 MHz, $CDCl_3$) of **21**.

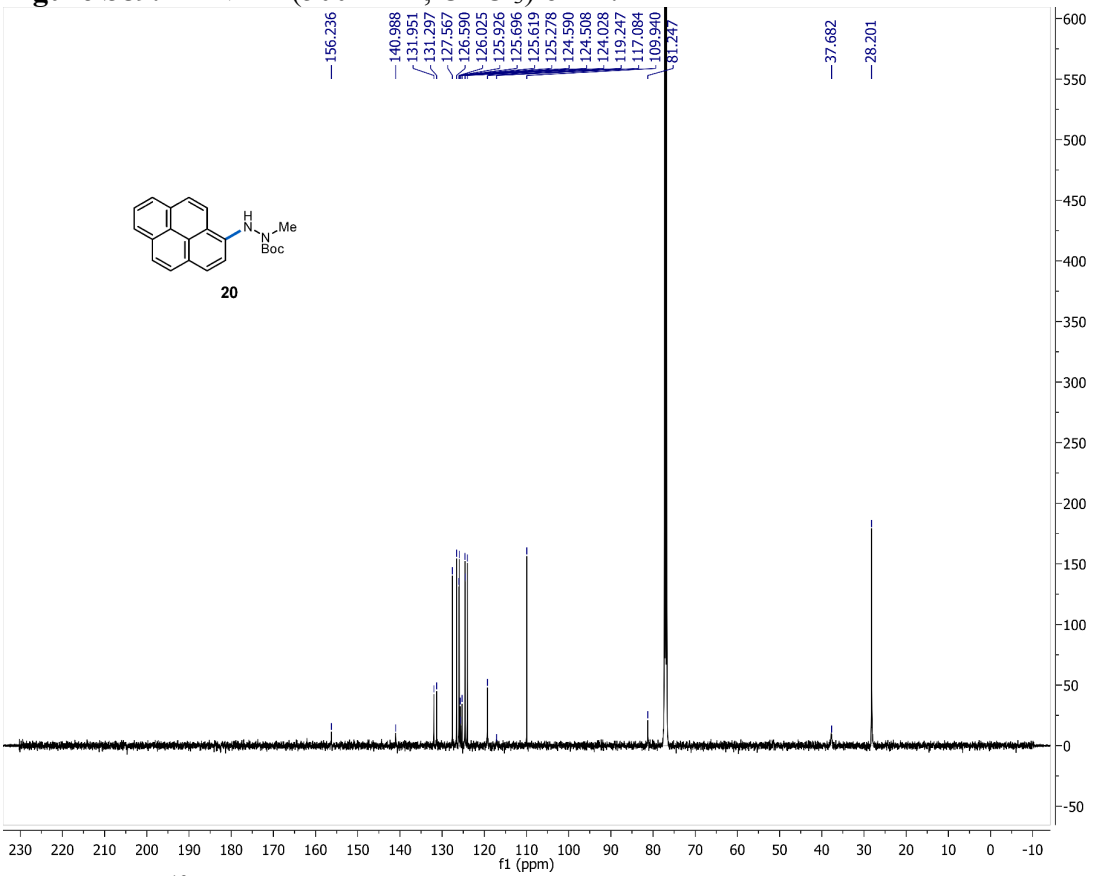

Figure S90. ^{13}C NMR (126 MHz, $CDCl_3$) of **21**.

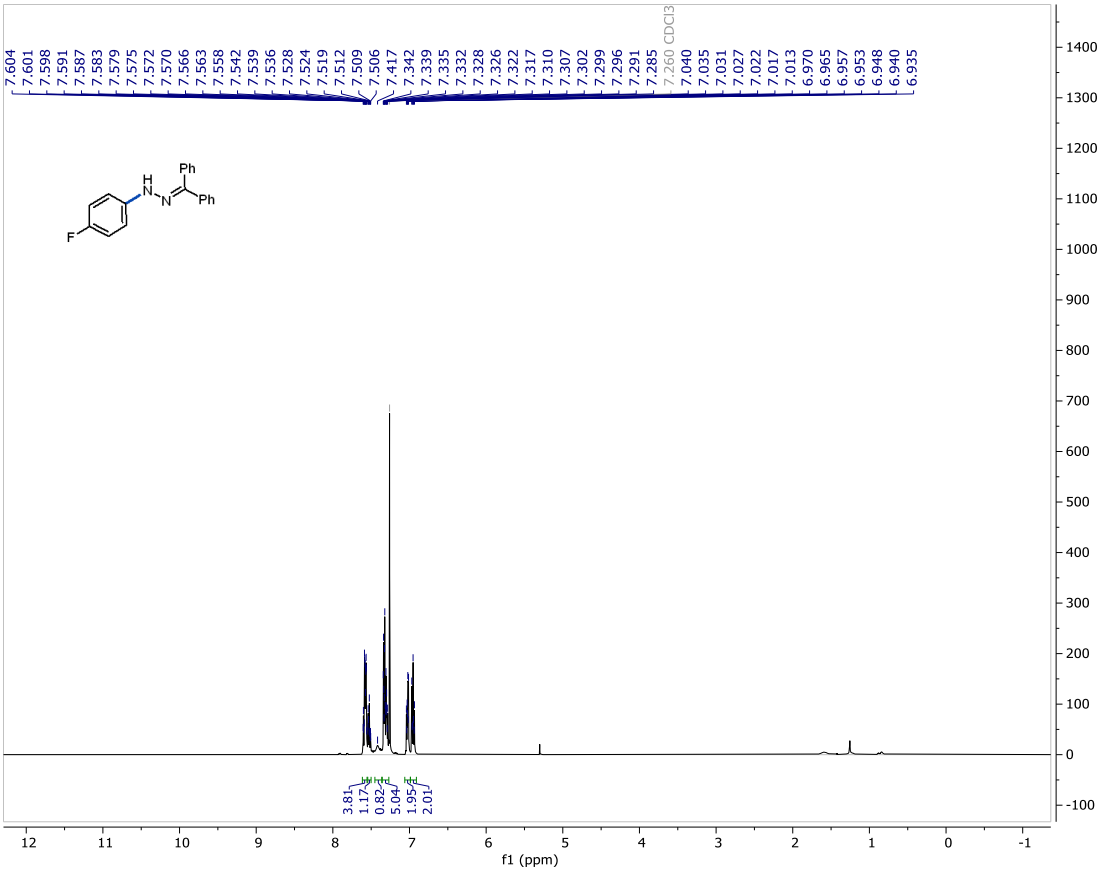

Figure S91. ^{1}H NMR (500 MHz, $CDCl_3$) of **22**.

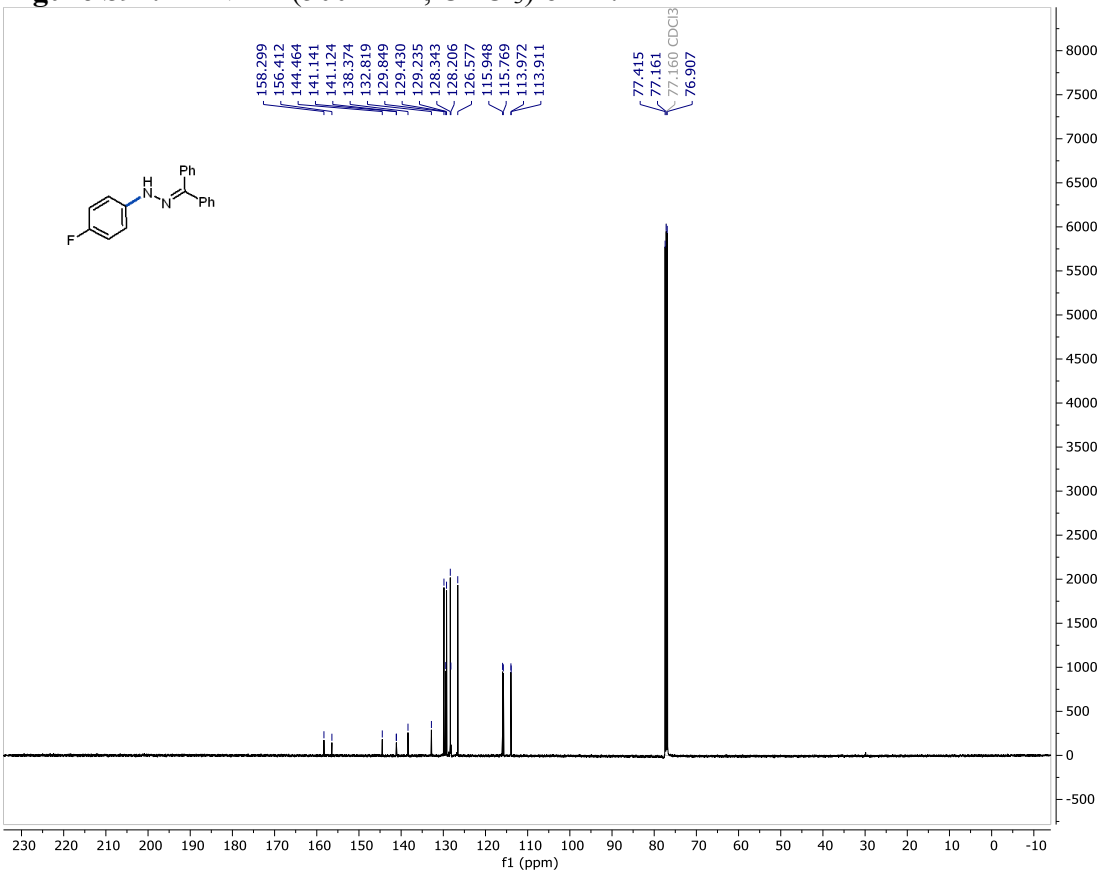

Figure S92. ^{13}C NMR (126 MHz, $CDCl_3$) of **22**.

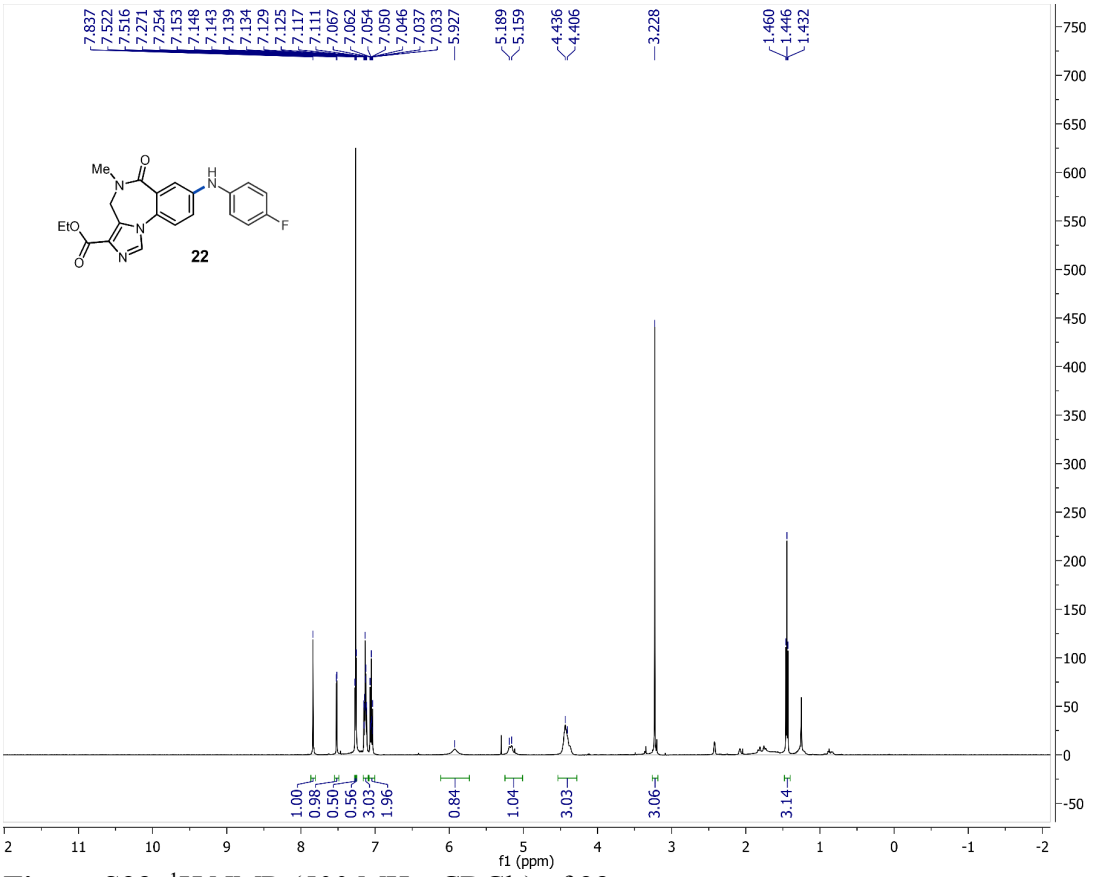

Figure S93. ^{1}H NMR (500 MHz, $CDCl_3$) of **23**.

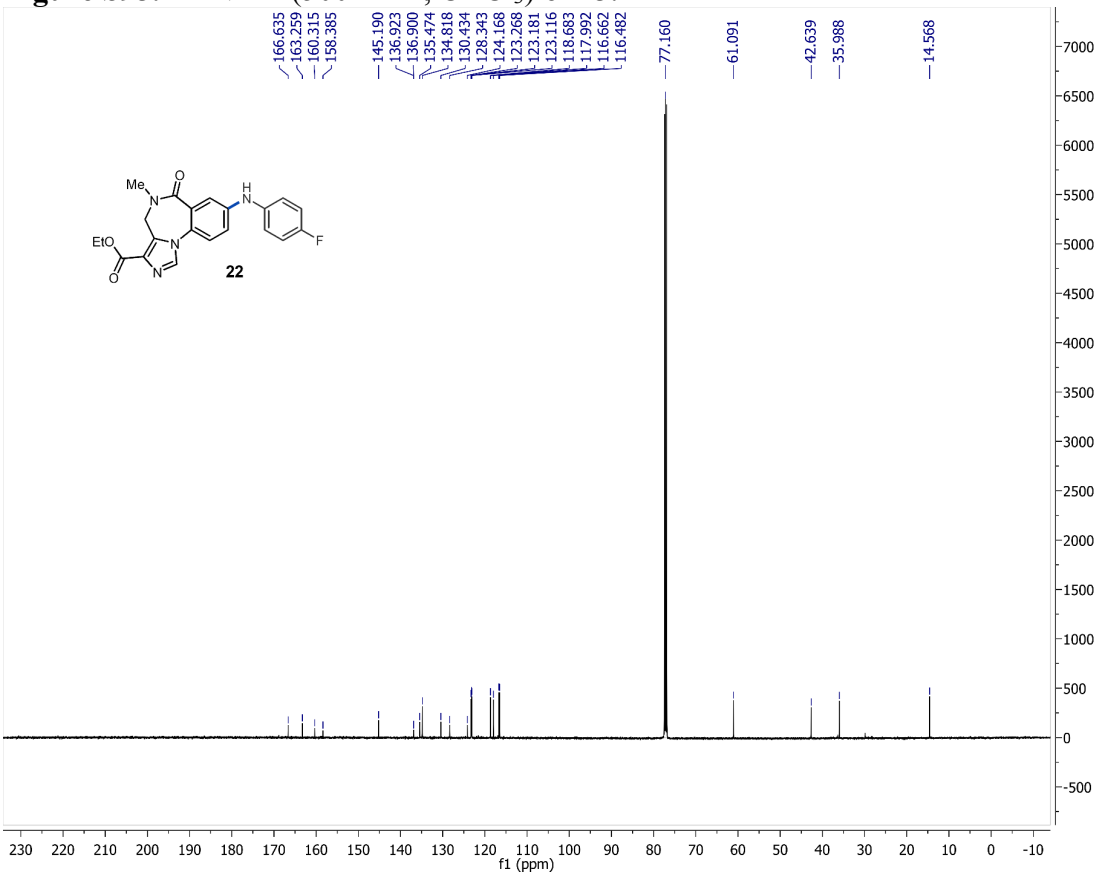

Figure S94. ^{13}C NMR (126 MHz, $CDCl_3$) of **23**.

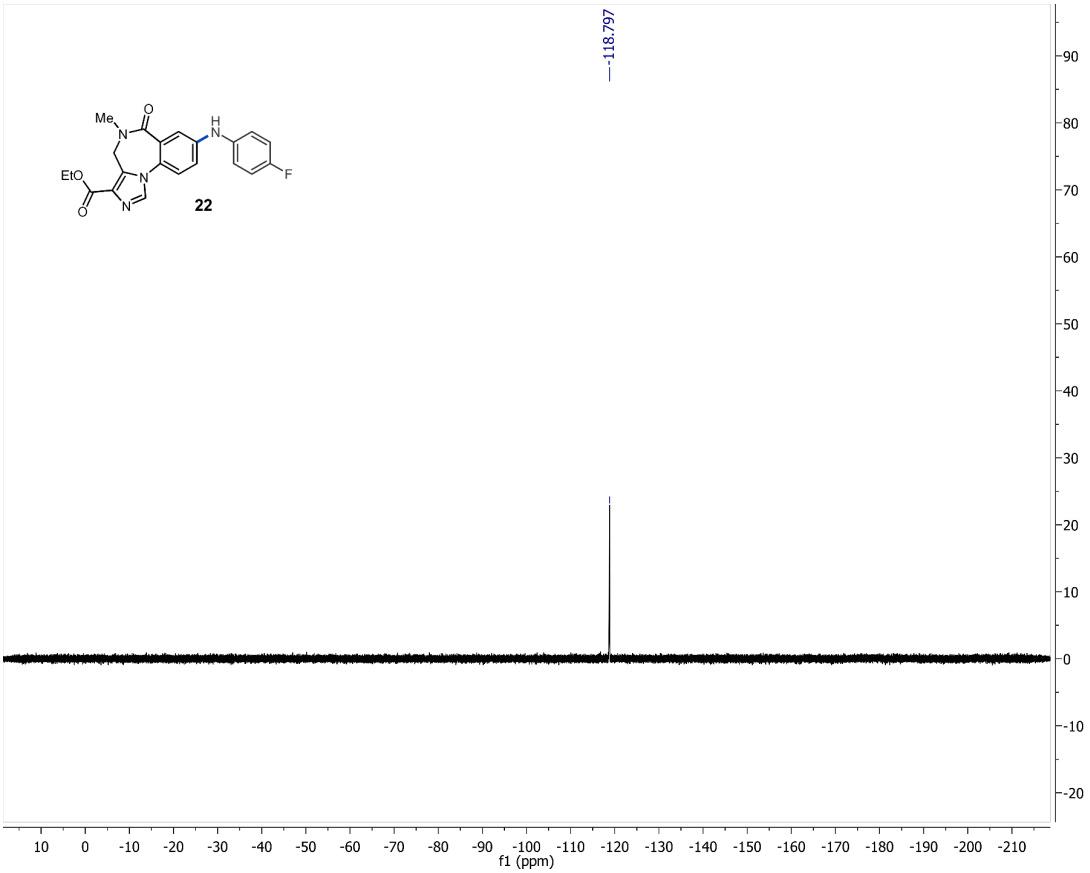

Figure S95. ^{19}F NMR (376 MHz, $CDCl_3$) of **23**.

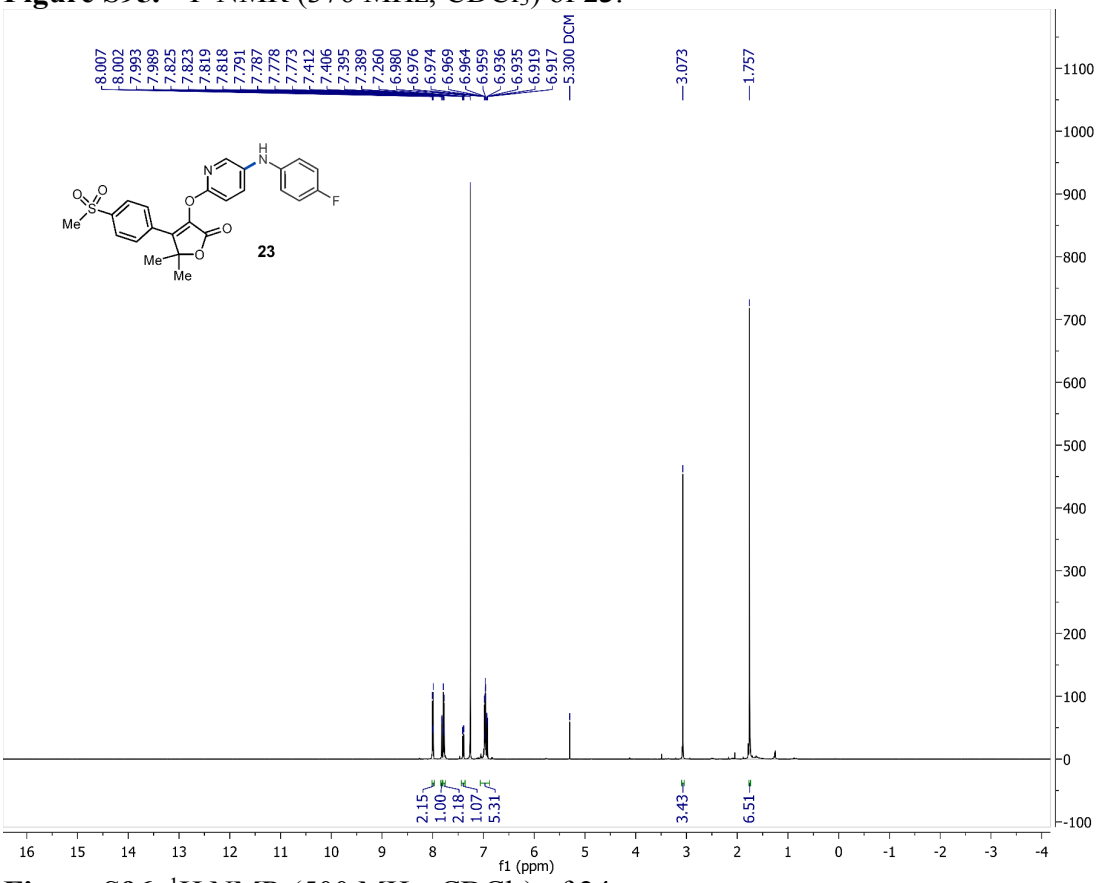

Figure S96. ^{1}H NMR (500 MHz, $CDCl_3$) of **24**.

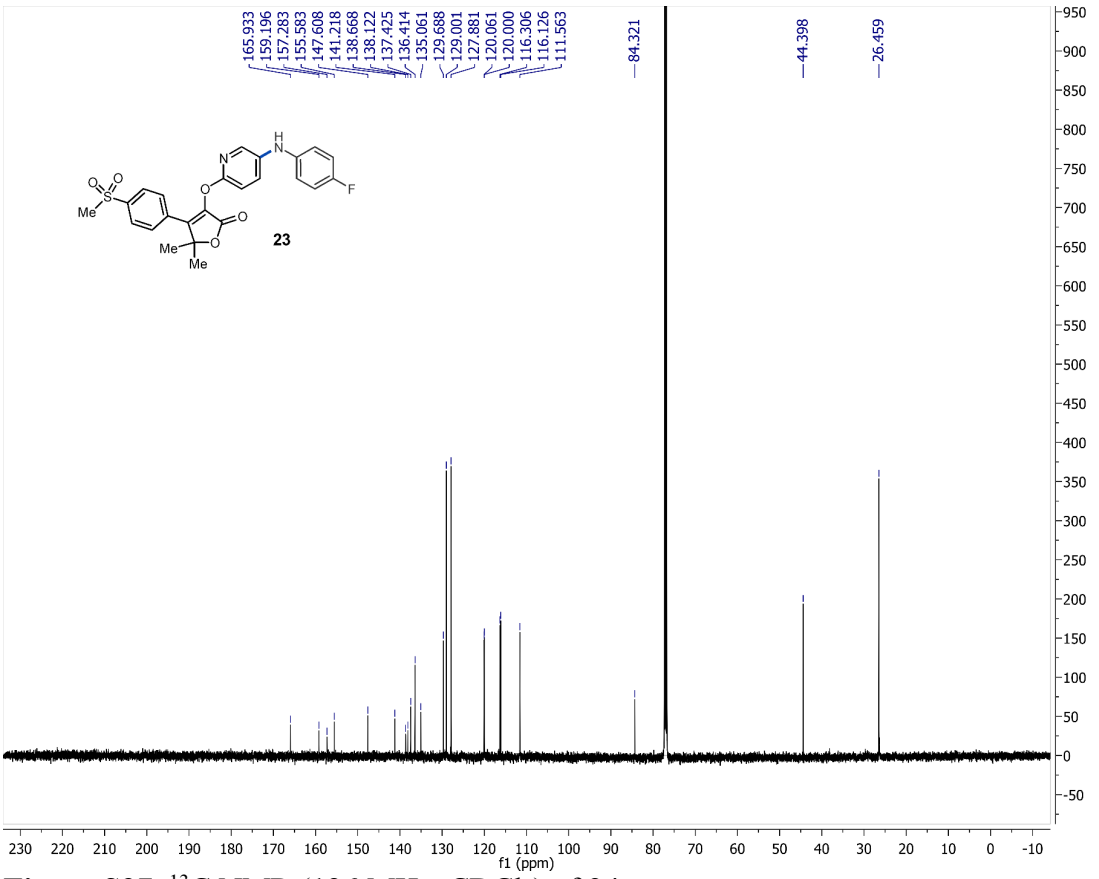

Figure S97. ^{13}C NMR (126 MHz, $CDCl_3$) of **24**.

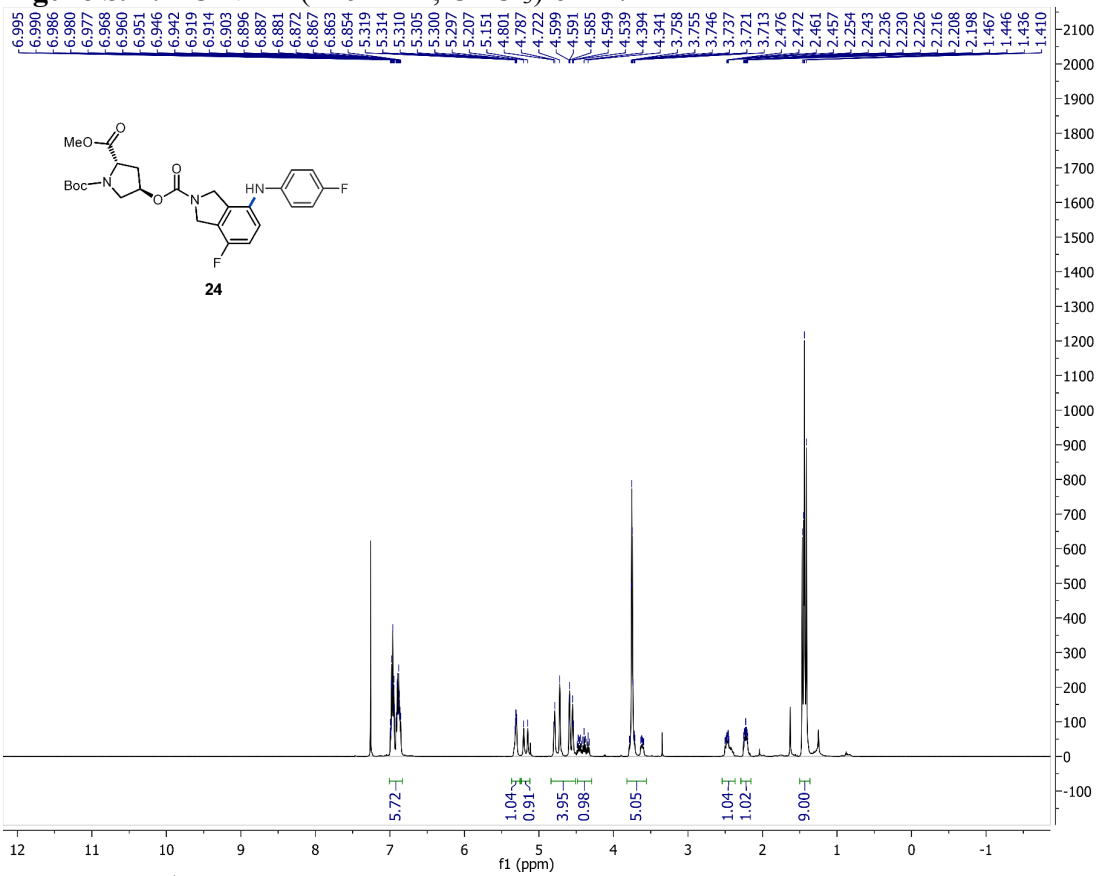

Figure S98. ^{1}H NMR (500 MHz, $CDCl_3$) of **25**.

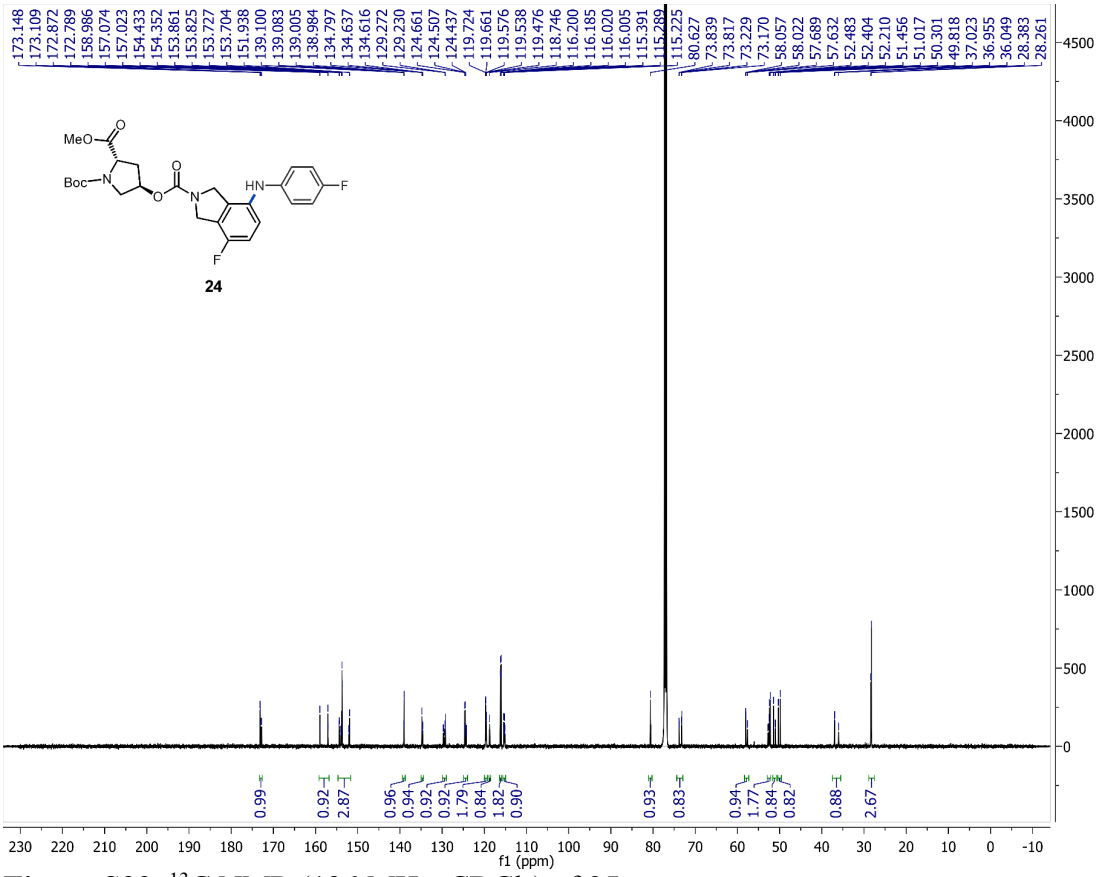

Figure S99. ^{13}C NMR (126 MHz, $CDCl_3$) of **25**.

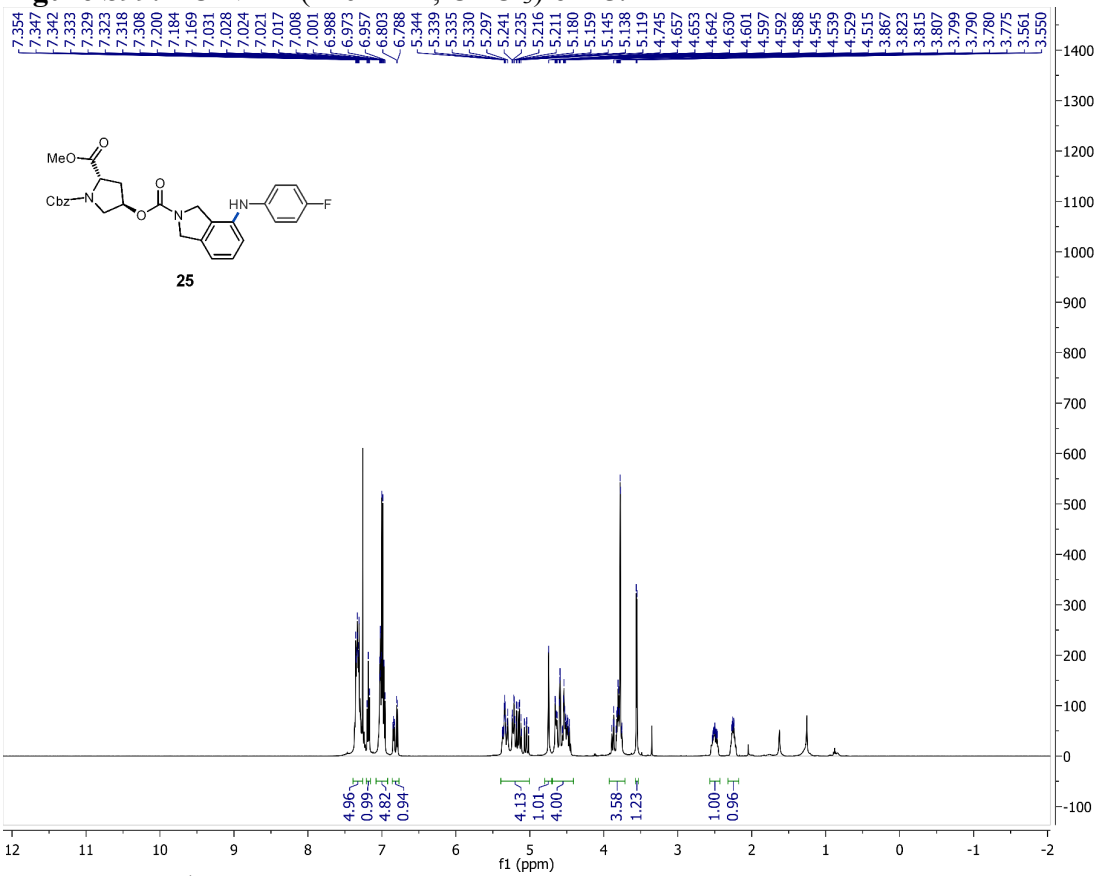

Figure S100. ^{1}H NMR (500 MHz, $CDCl_3$) of **26**.

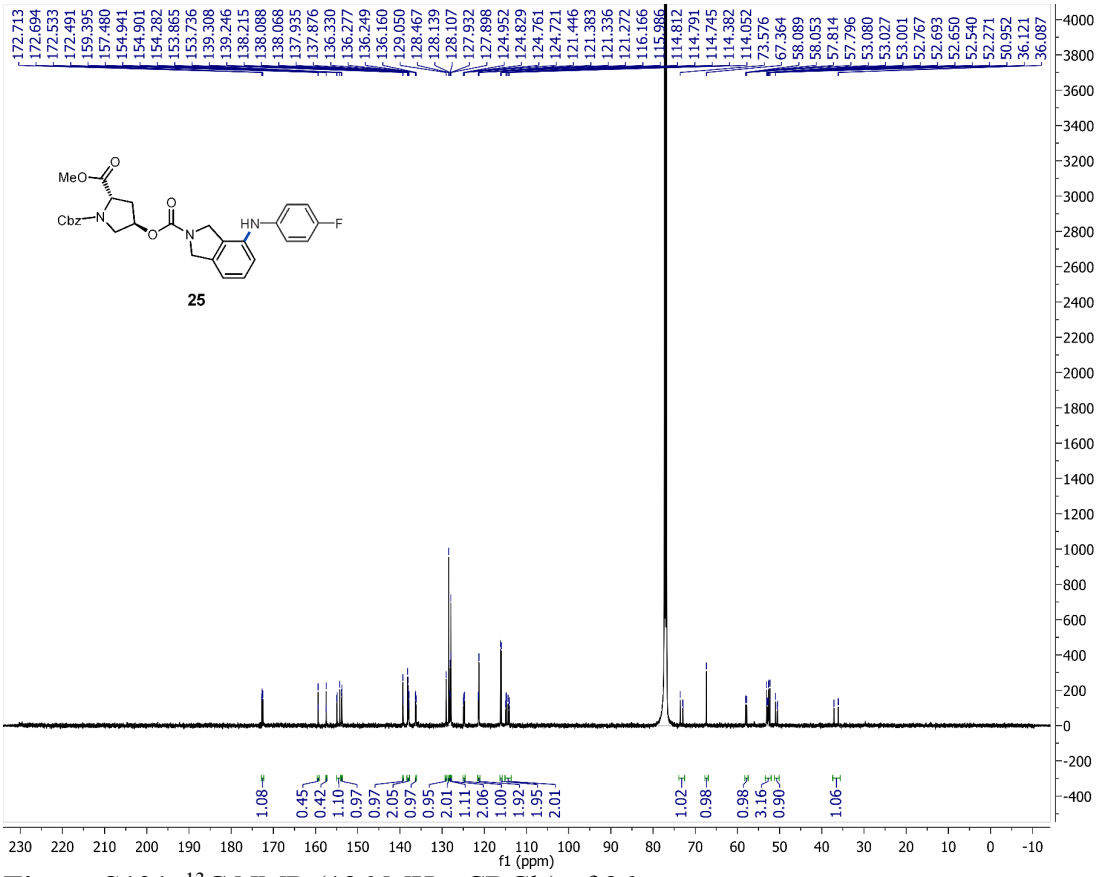

Figure S101. ^{13}C NMR (126 MHz, $CDCl_3$) of **26**.

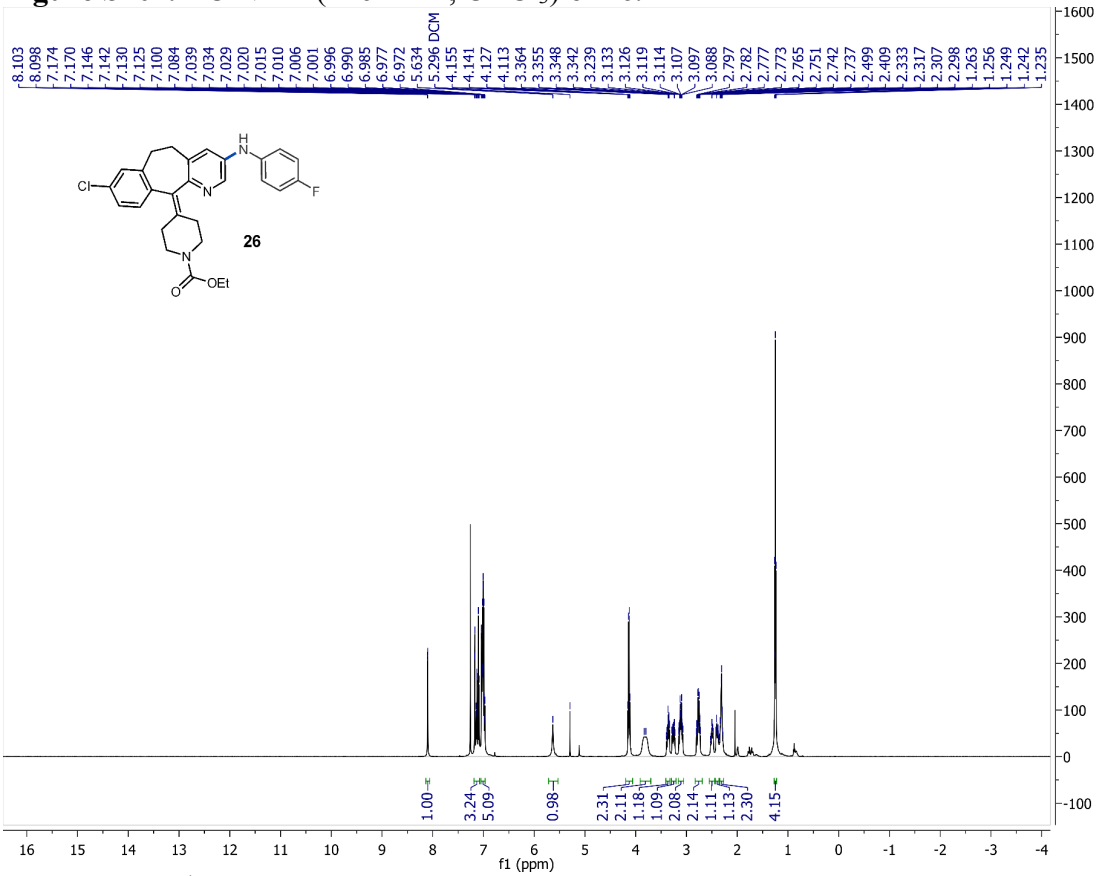

Figure S102. ^{1}H NMR (500 MHz, $CDCl_3$) of **27**.

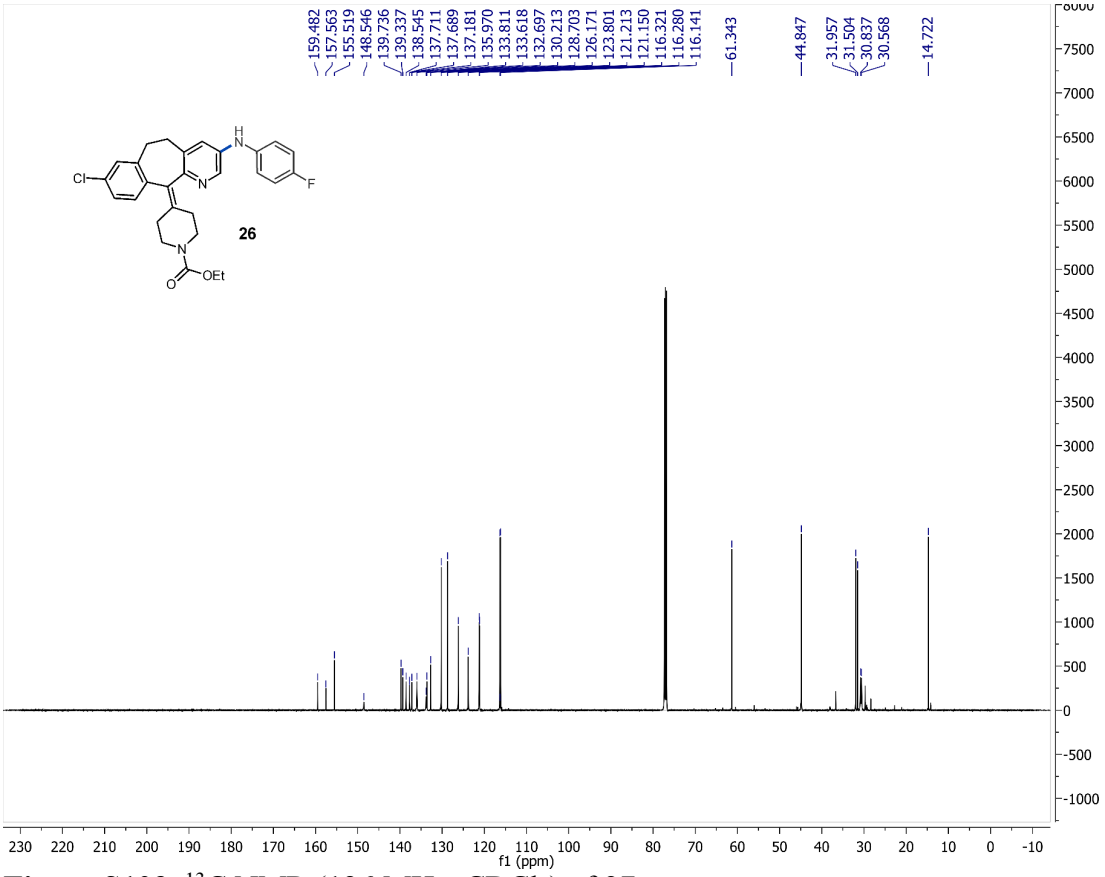

Figure S103. ^{13}C NMR (126 MHz, $CDCl_3$) of **27**.

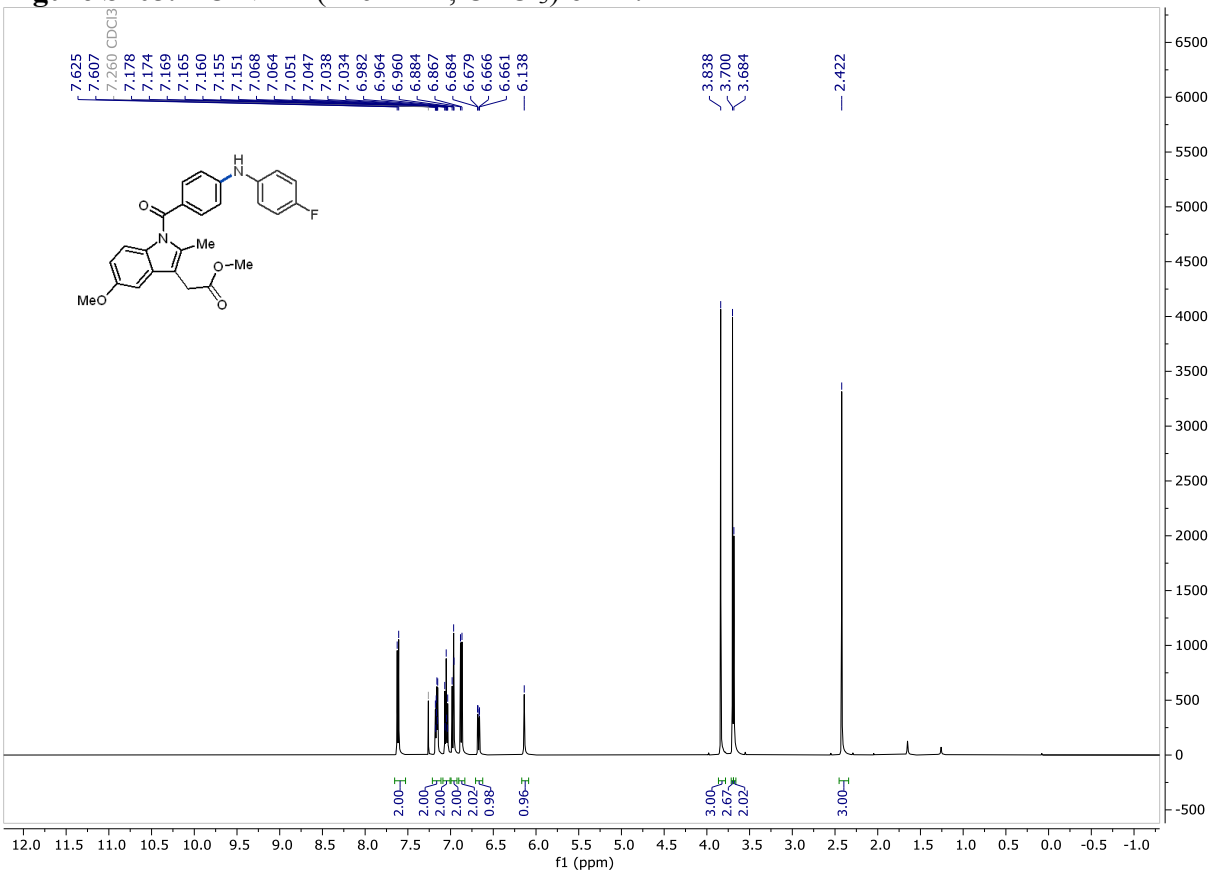

Figure S104. ^{1}H NMR (500 MHz, $CDCl_3$) of **28**.

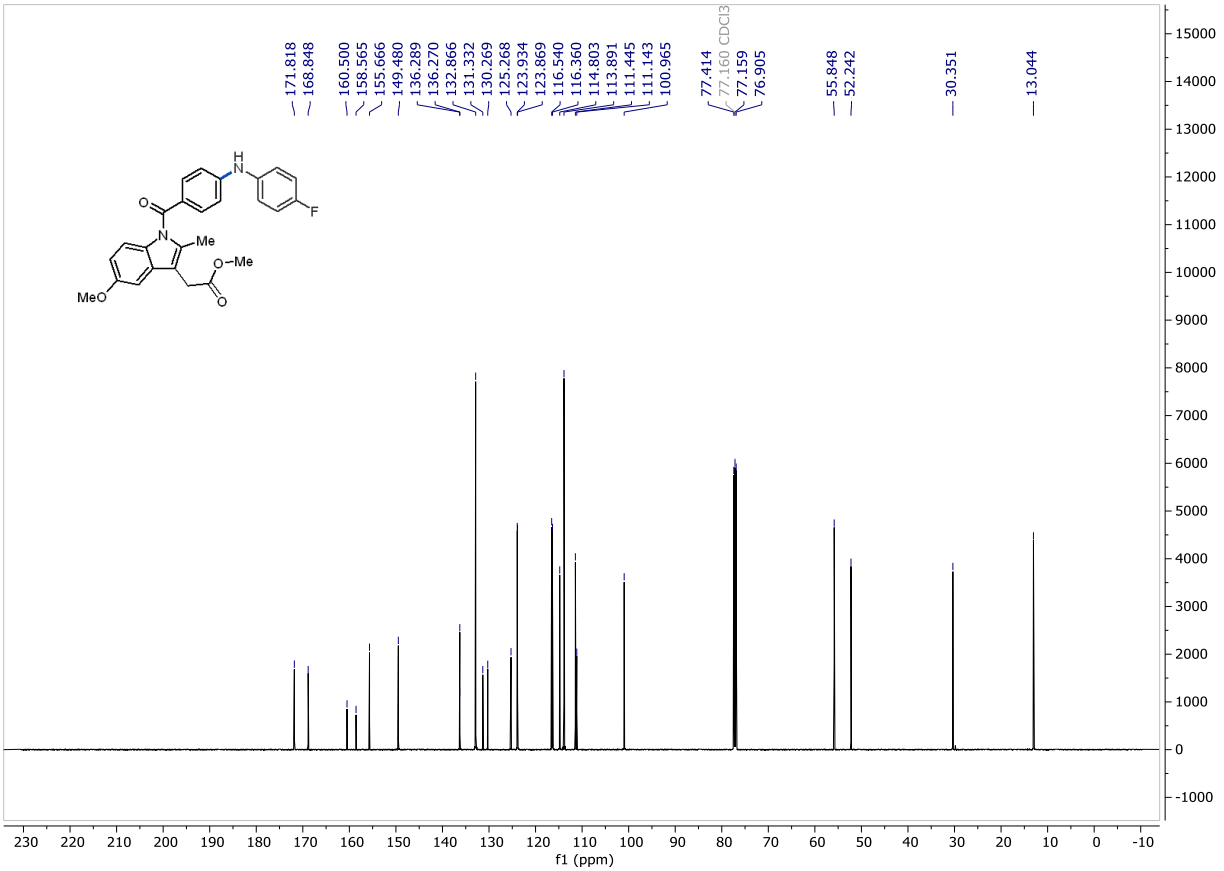

Figure S105. ^{13}C NMR (126 MHz, $CDCl_3$) of **28**.

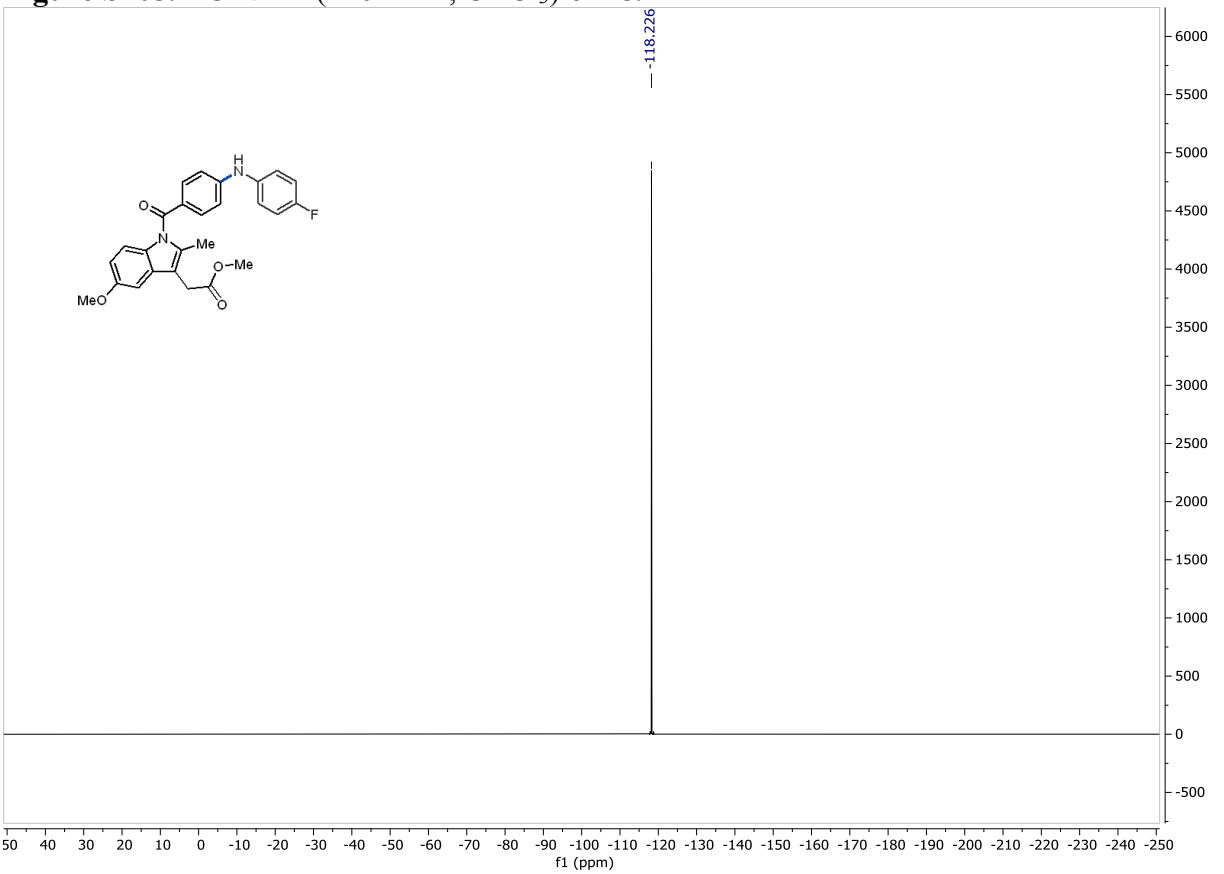

Figure S106. ^{19}F NMR (282 MHz, $CDCl_3$) of **28**.

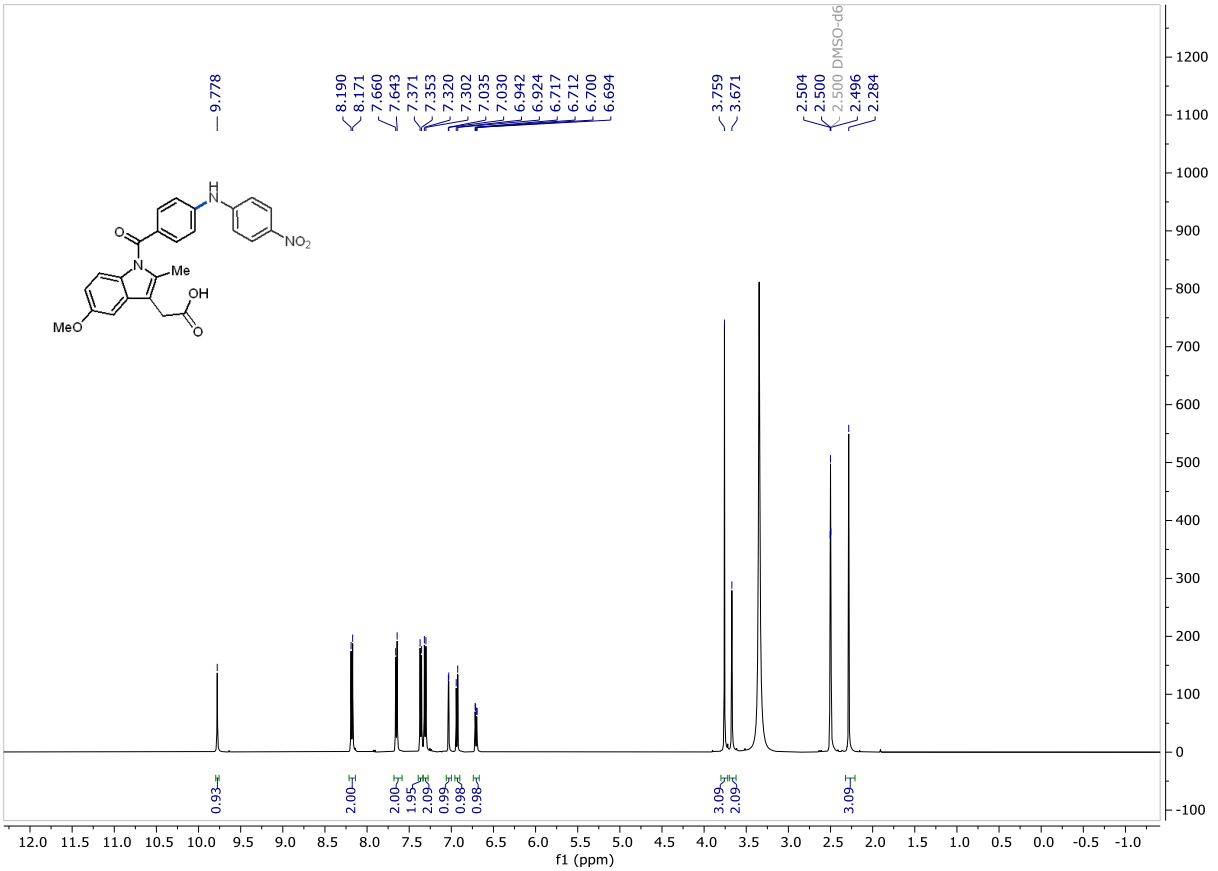

Figure S107. ^{1}H NMR (500 MHz, $CDCl_3$) of **29**.

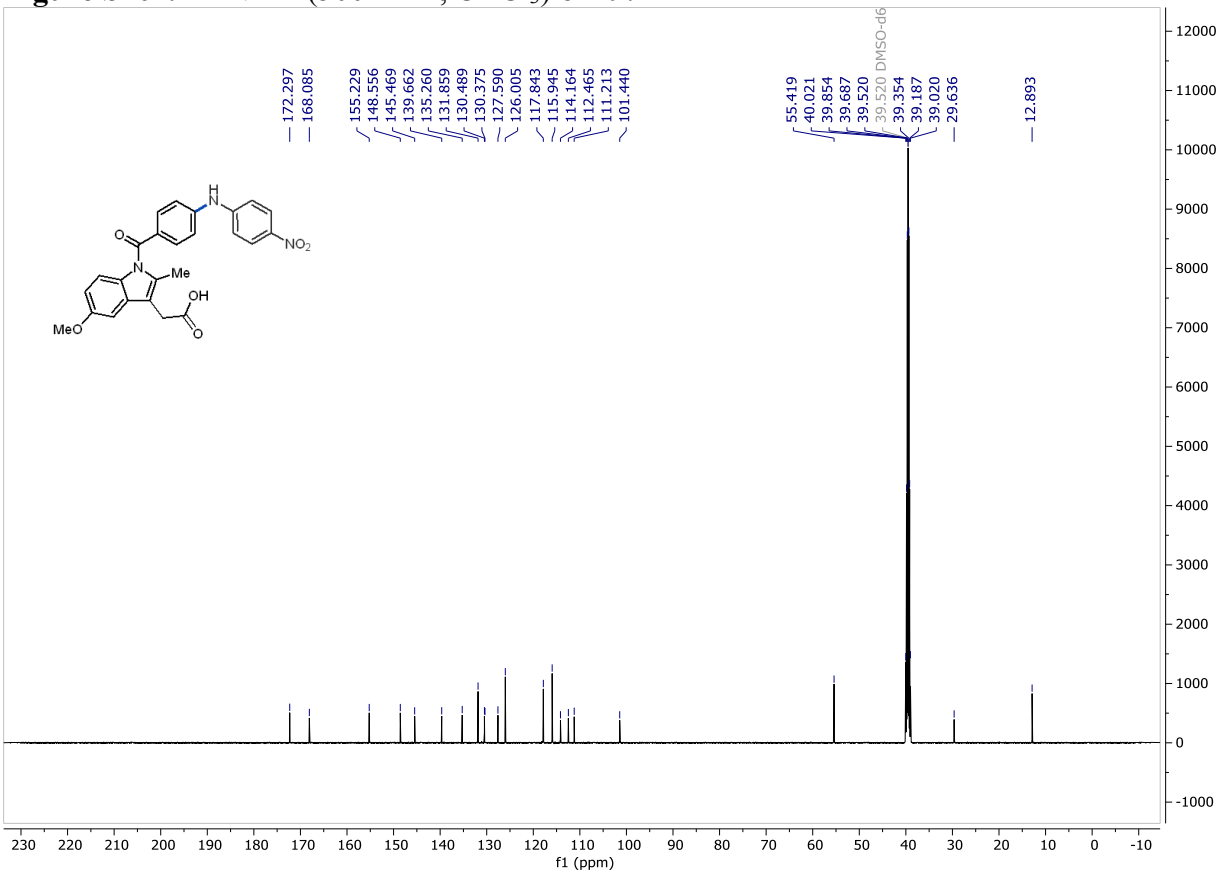

Figure S108. ^{13}C NMR (126 MHz, $CDCl_3$) of **29**.

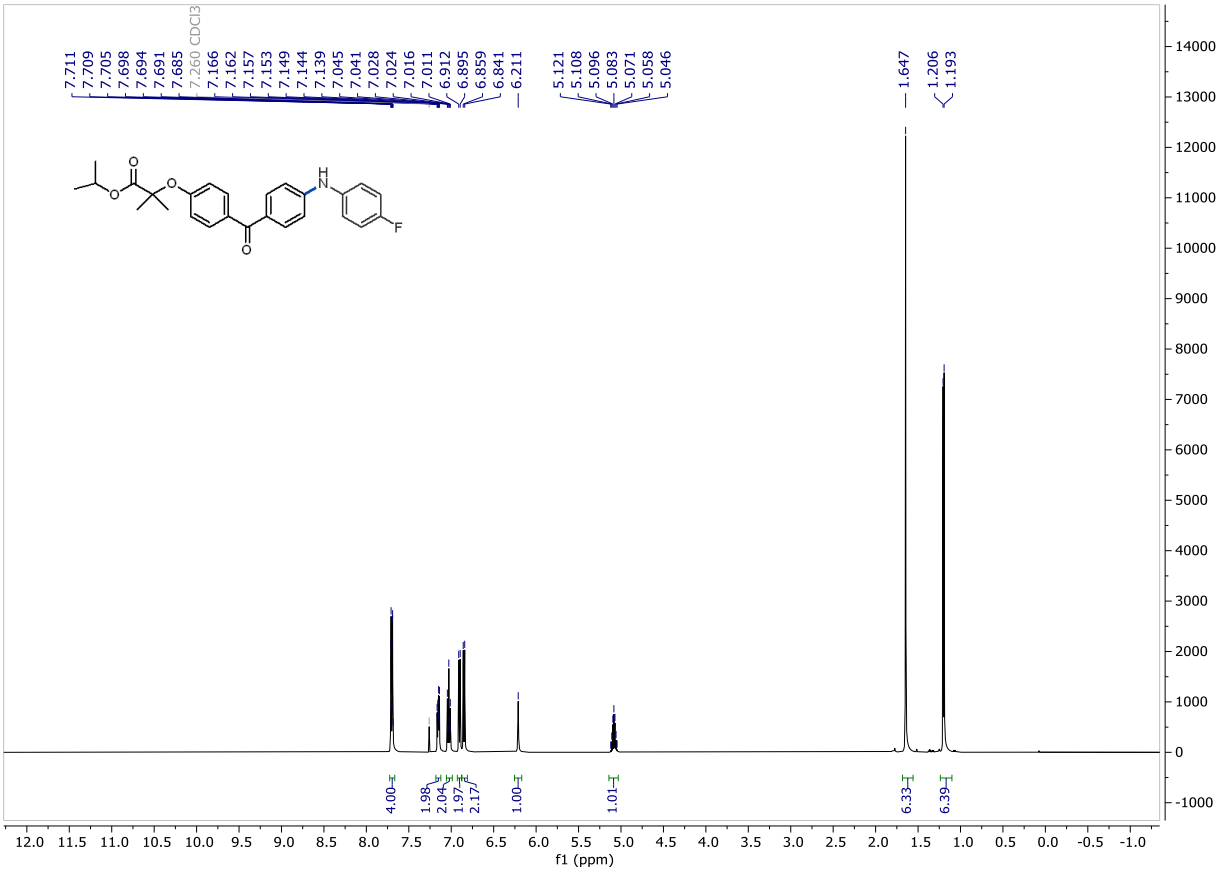

Figure S109. ^{1}H NMR (500 MHz, $CDCl_3$) of **30**.

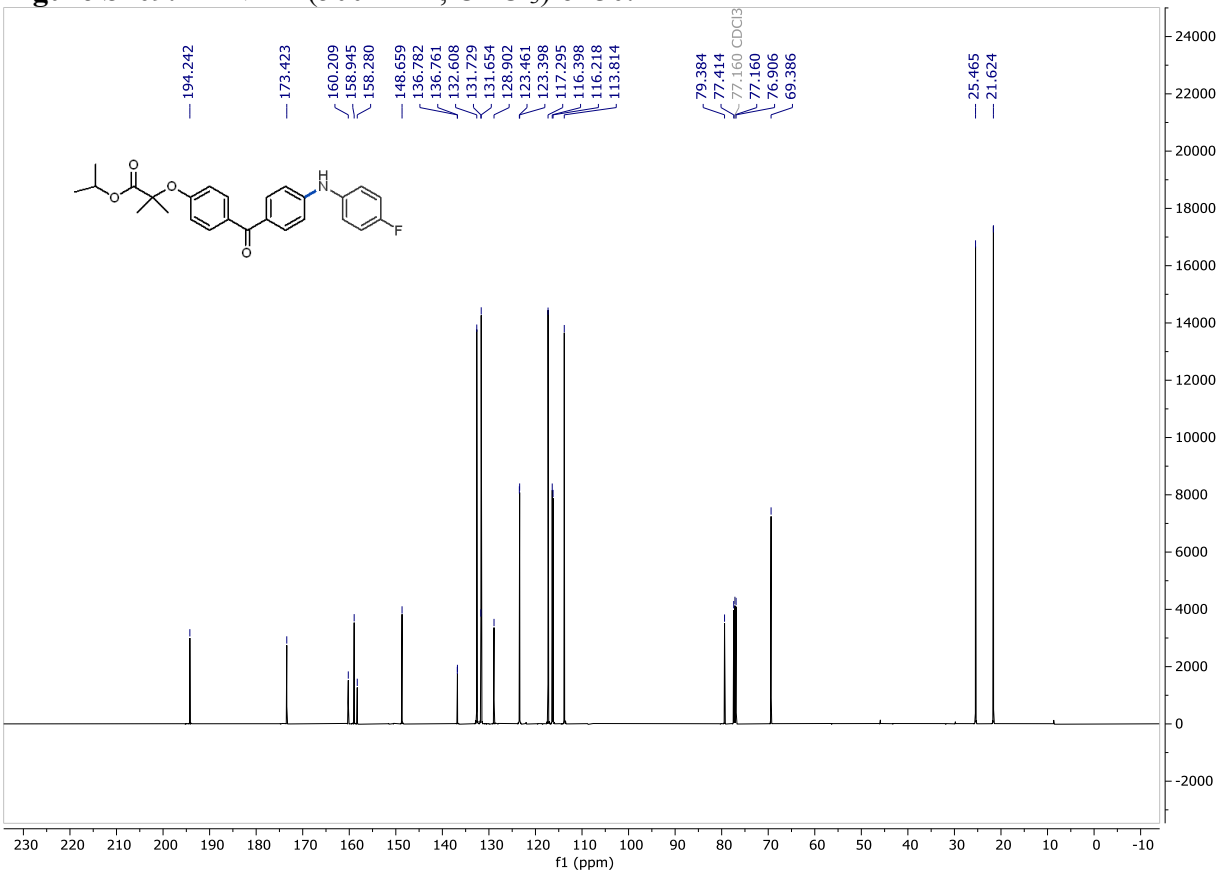

Figure S110. ^{13}C NMR (126 MHz, $CDCl_3$) of **30**.

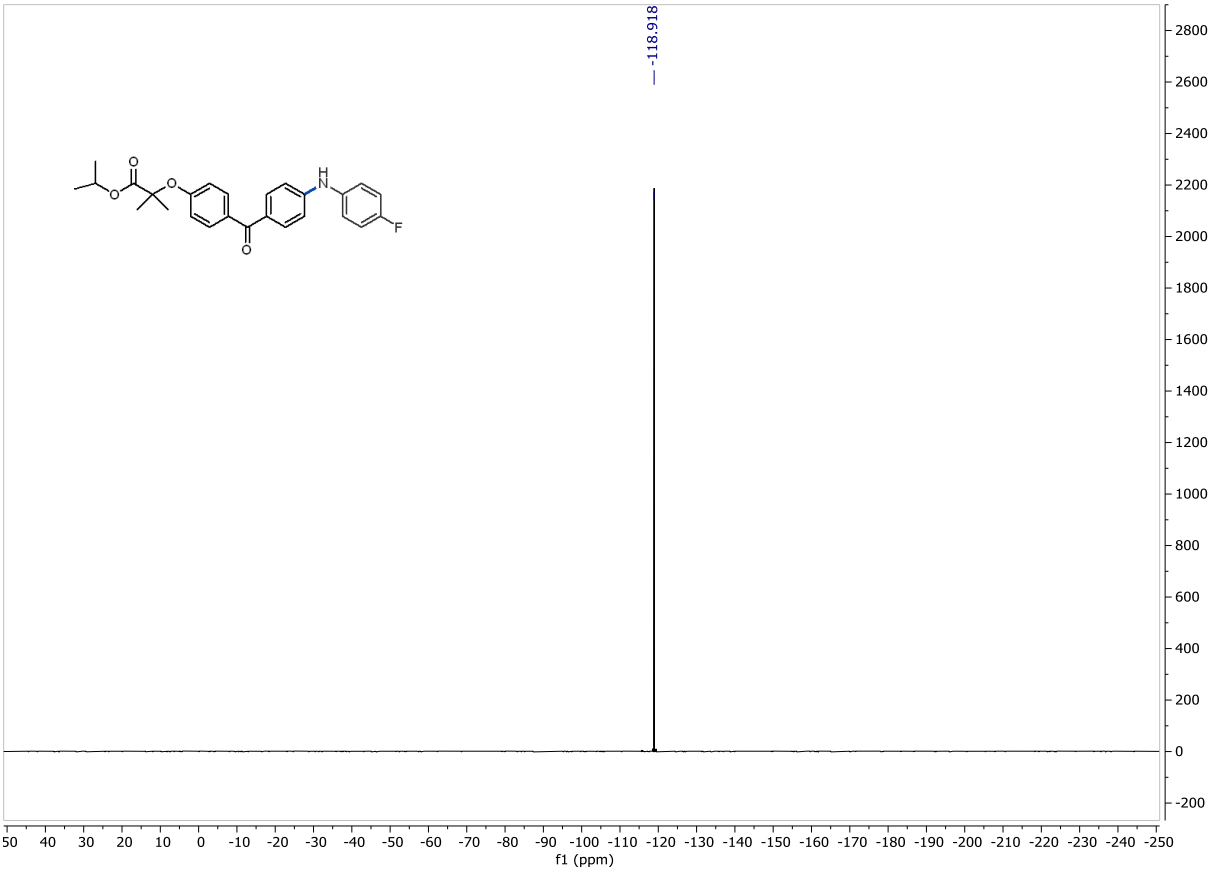

Figure S111. ^{19}F NMR (282 MHz, $CDCl_3$) of **30**.

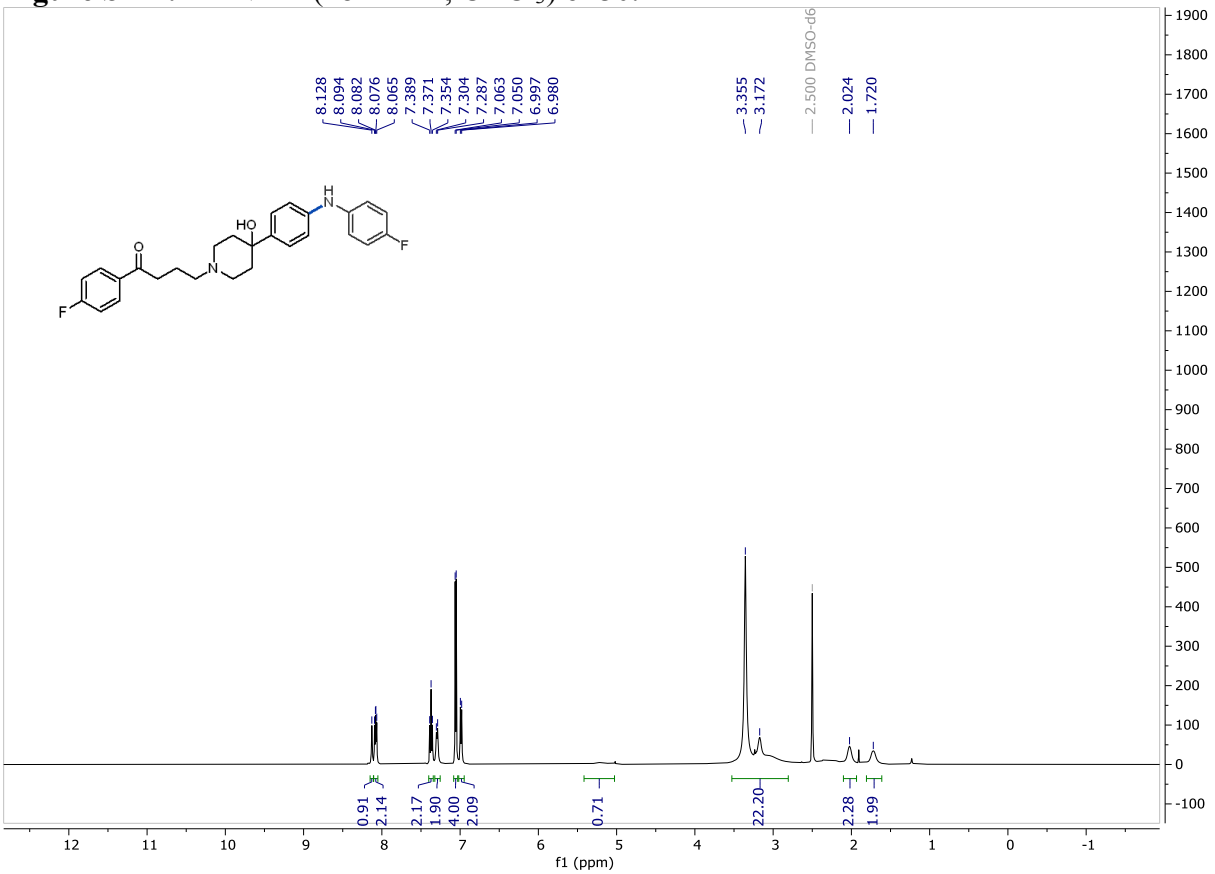

Figure S112. ^{1}H NMR (500 MHz, $CDCl_3$) of **31**.

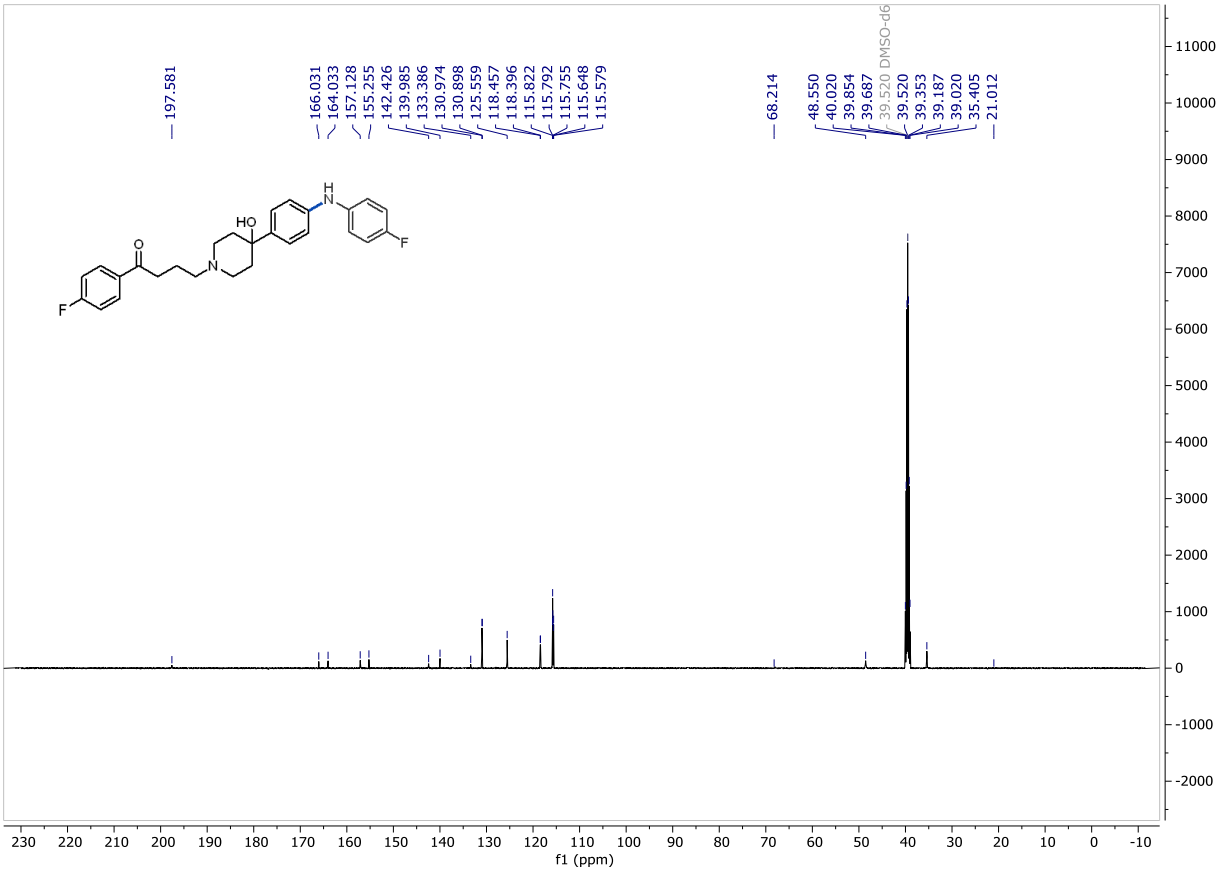

Figure S113. ^{13}C NMR (126MHz, $CDCl_3$) of **31**.

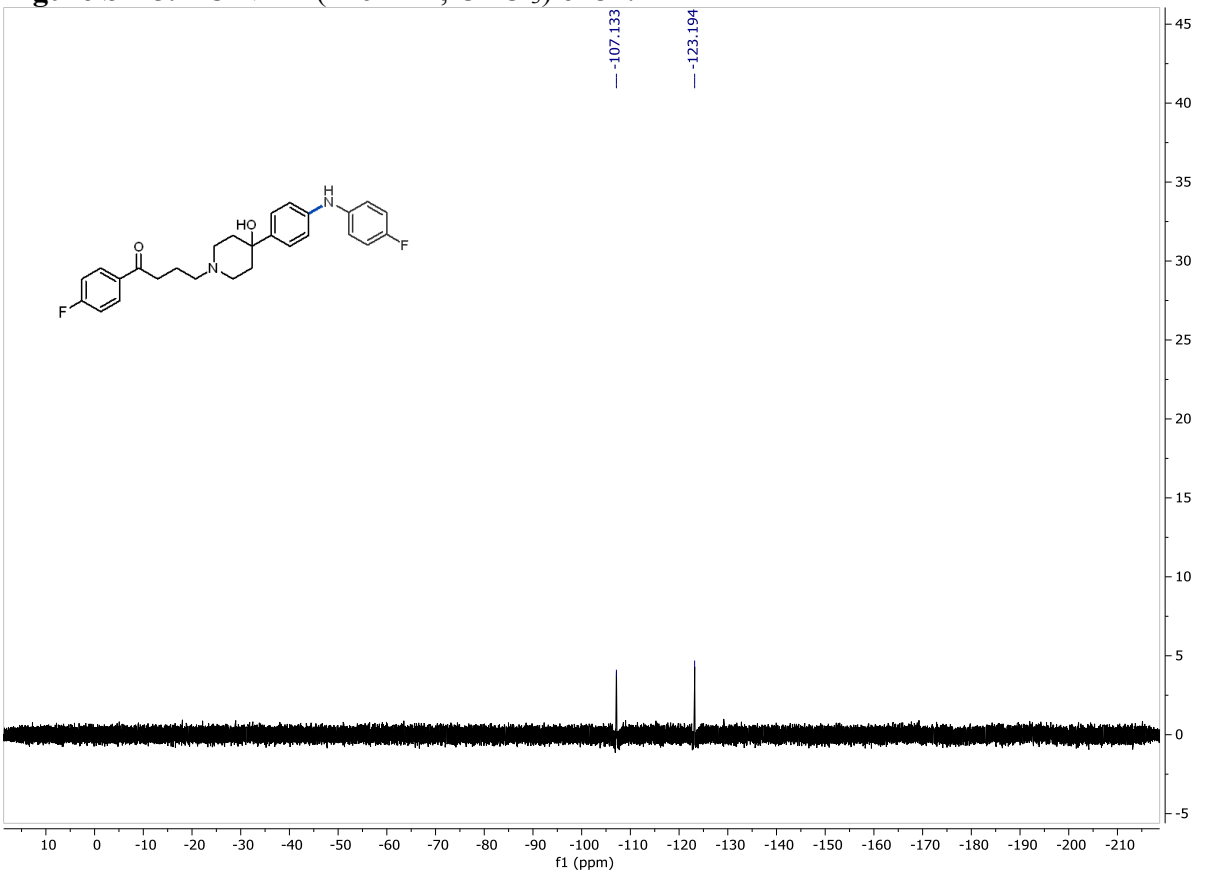

Figure S114. ^{19}F NMR (376 MHz, $CDCl_3$) of **31**.

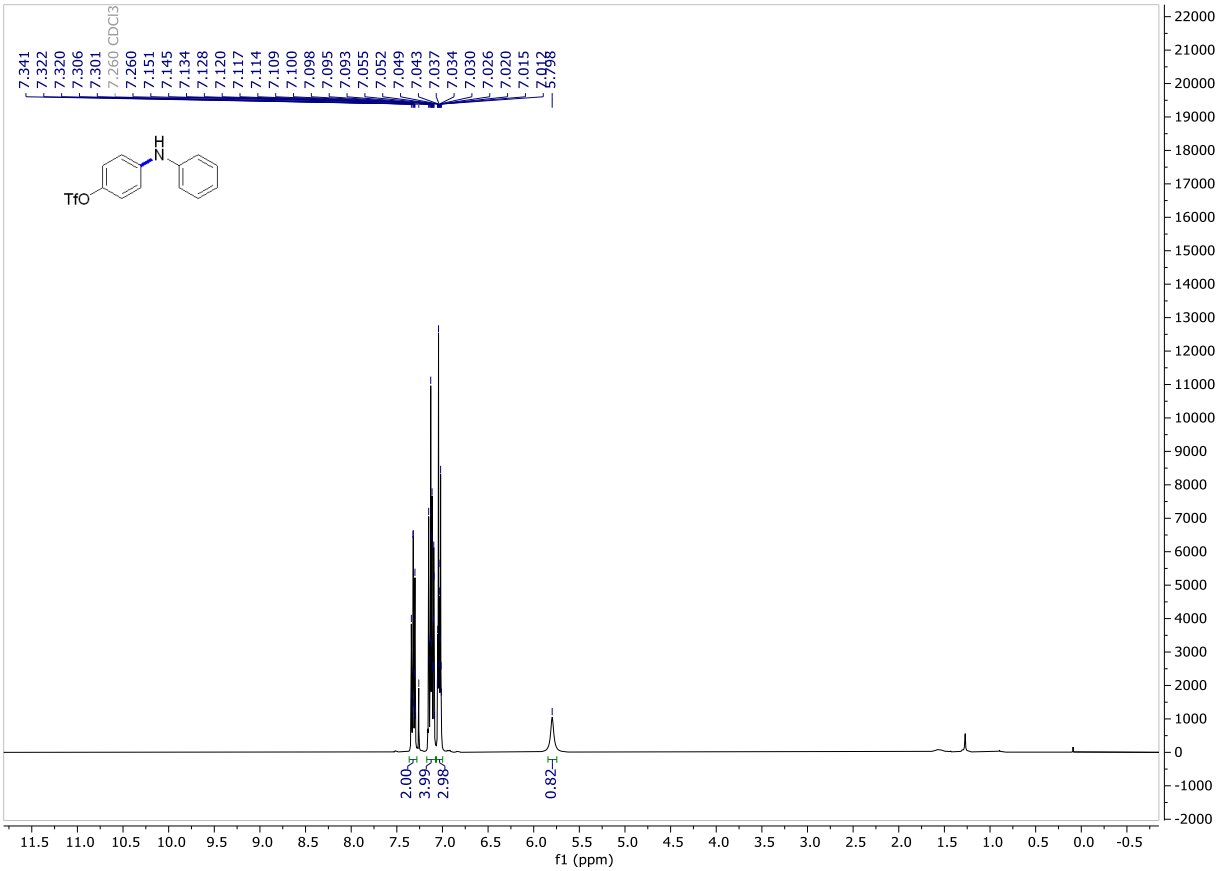

Figure S115. ^{1}F NMR (400 MHz, $CDCl_3$) of **S1**.

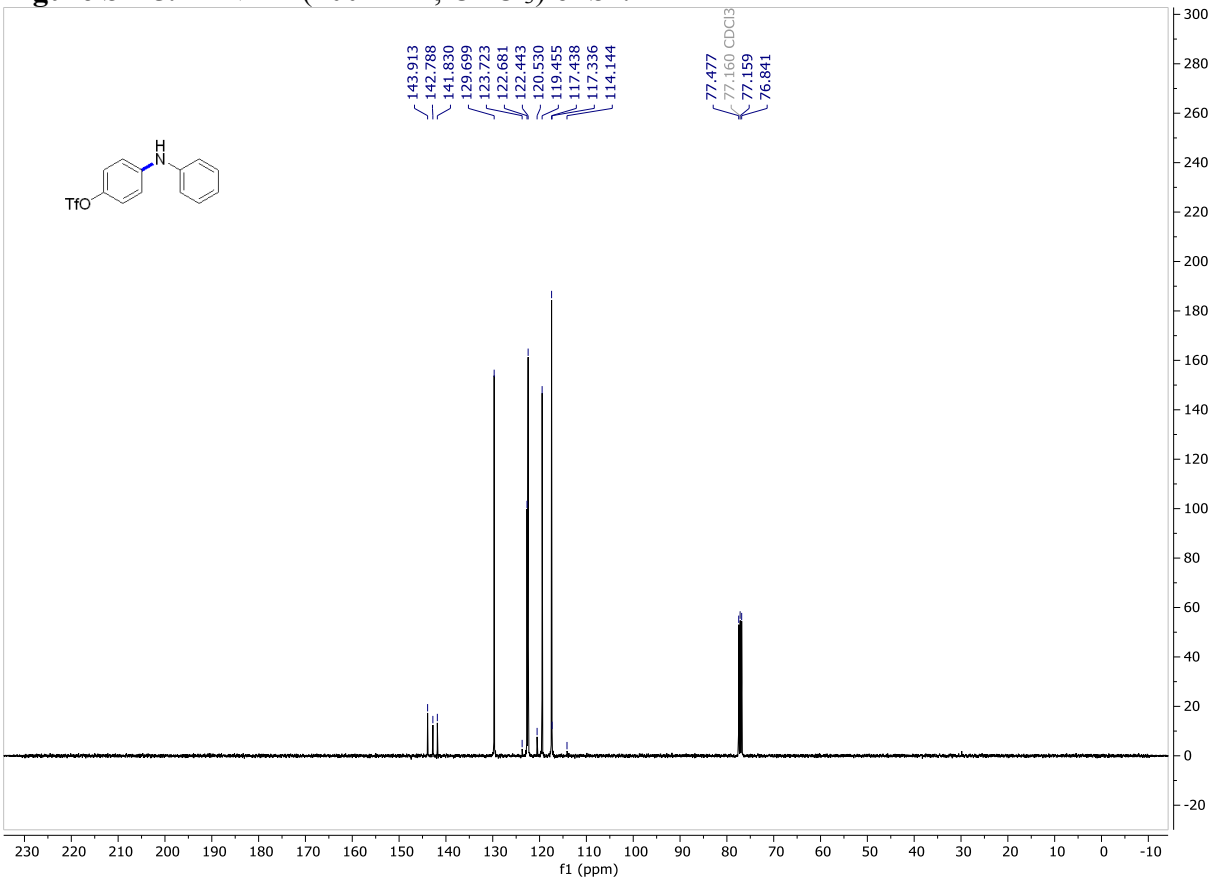

Figure S116. ^{13}C{^{1}H} NMR (101 MHz, $CDCl_3$) of **S1**.

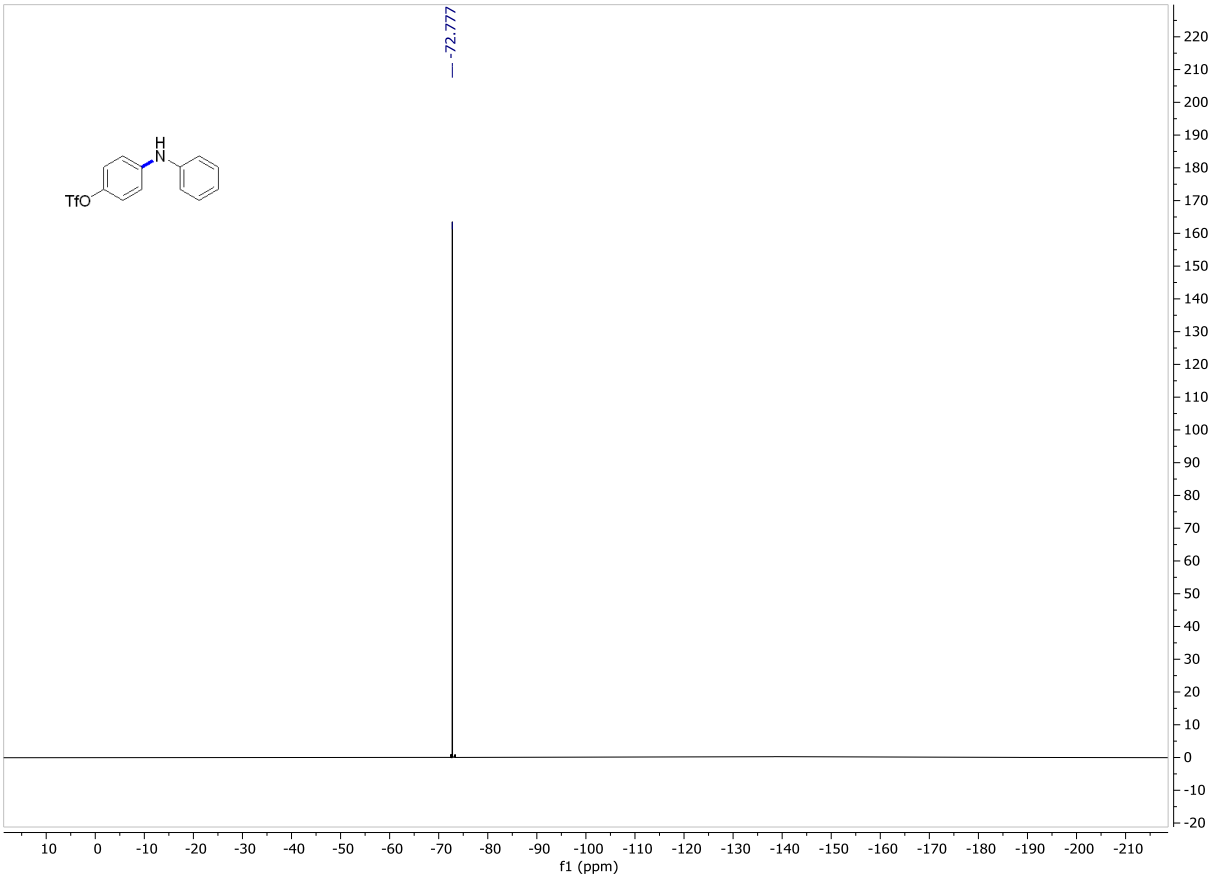

Figure S117. ^{19}F NMR (376 MHz, $CDCl_3$) of **S1**.

References

(1) Chen, L.; Ren, P.; Carrow, B. P. Tri(1-adamantyl)phosphine: Expanding the Boundary of Electron-Releasing Character Available to Organophosphorus Compounds. *J. Am. Chem. Soc.* **2016**, *138*, 6392-6395.

(2) Chen, L.; Francis, H.; Carrow, B. P. An "On-Cycle" Precatalyst Enables Room-Temperature Polyfluoroarylation Using Sensitive Boronic Acids. *ACS Catalysis* **2018**, *8*, 2989-2994.

(3) Chen, L.; Sanchez, D. R.; Zhang, B.; Carrow, B. P. "Cationic" Suzuki–Miyaura Coupling with Acutely Base-Sensitive Boronic Acids. *J. Am. Chem. Soc.* **2017**, *139*, 12418-12421.

(4) Fulmer, G. R.; Miller, A. J. M.; Sherden, N. H.; Gottlieb, H. E.; Nudelman, A.; Stoltz, B. M.; Bercaw, J. E.; Goldberg, K. I. NMR Chemical Shifts of Trace Impurities: Common Laboratory Solvents, Organics, and Gases in Deuterated Solvents Relevant to the Organometallic Chemist. *Organometallics* **2010**, *29*, 2176-2179.

(5) Nykaza, T. V.; Yang, J.; Radosevich, A. T. PEt3-mediated deoxygenative CN coupling of nitroarenes and boronic acids. *Tetrahedron* **2019**, *75*, 3248-3252.

(6) (a) Stambuli, J. P.; Kuwano, R.; Hartwig, J. F. Unparalleled rates for the activation of aryl chlorides and bromides: coupling with amines and boronic acids in minutes at room temperature. *Angew. Chem., Int. Ed.* **2002**, *41*, 4746-4748; (b) Marion, N.; Navarro, O.; Mei, J.; Stevens, E. D.; Scott, N. M.; Nolan, S. P. Modified (NHC)Pd(allyl)Cl (NHC = N-Heterocyclic Carbene) Complexes for Room-Temperature Suzuki-Miyaura and Buchwald-Hartwig Reactions. *J. Am. Chem. Soc.* **2006**, *128*, 4101-4111; (c) Beutner, G. L.; Coombs, J. R.; Green, R. A.; Inankur, B.; Lin, D.; Qiu, J.; Roberts, F.; Simmons, E. M.; Wisniewski, S. R. Palladium-Catalyzed Amidation and Amination of (Hetero)aryl Chlorides under Homogeneous Conditions Enabled by a Soluble DBU/NaTFA Dual-Base System. *Org. Process Res. Dev.* **2019**, *23*, 1529-1537; (d) Kashani, S. K.; Jessiman, J. E.; Newman, S. G. Exploring Homogeneous Conditions for Mild Buchwald–Hartwig Amination in Batch and Flow. *Org. Process Res. Dev.* **2020**.

(7) Burés, J. Variable Time Normalization Analysis: General Graphical Elucidation of Reaction Orders from Concentration Profiles. *Angew. Chem. Int. Ed.* **2016**, *55*, 16084-16087.

(8) (a) Bastug, G.; Nolan, S. P. [Pd(IPr*OMe)(cin)Cl] (cin = Cinnamyl): A Versatile Catalyst for C–N and C–C Bond Formation. *Organometallics* **2014**, *33*, 1253-1258; (b) Akram, M. O.; Das, A.; Chakrabarty, I.; Patil, N. T. Ligand-Enabled Gold-Catalyzed C(sp2)–N Cross-Coupling Reactions of Aryl Iodides with Amines. *Org. Lett.* **2019**, *21*, 8101-8105; (c) Kampmann, S. S.; Sobolev, A. N.; Koutsantonis, G. A.; Stewart, S. G. Stable Nickel(0) Phosphites as Catalysts for C–N Cross-Coupling Reactions. *Adv. Synth. Catal.* **2014**, *356*, 1967-1973; (d) Kudisch, M.; Lim, C.-H.; Thordarson, P.; Miyake, G. M. Energy Transfer to Ni-Amine Complexes in Dual Catalytic, Light-Driven C–N Cross-Coupling Reactions. *J. Am. Chem. Soc.* **2019**, *141*, 19479-19486.

(9) Hammett, L. P. The Effect of Structure upon the Reactions of Organic Compounds. Benzene Derivatives. *J. Am. Chem. Soc.* **1937**, *59*, 96-103.

(10) (a) Kitamura, M.; Suga, S.; Oka, H.; Noyori, R. Quantitative Analysis of the Chiral Amplification in the Amino Alcohol-Promoted Asymmetric Alkylation of Aldehydes with Dialkylzincs. *J. Am. Chem. Soc.* **1998**, *120*, 9800-9809; (b) Rosner, T.; Le Bars, J.; Pfaltz, A.; Blackmond, D. G. Kinetic Studies of Heck Coupling Reactions Using Palladacycle Catalysts: Experimental and Kinetic Modeling of the Role of Dimer Species. *J. Am. Chem. Soc.* **2001**, *123*, 1848-1855; (c) Kina, A.; Iwamura, H.; Hayashi, T. A Kinetic Study on Rh/Binap-Catalyzed 1,4-Addition of Phenylboronic Acid to Enones: Negative Nonlinear Effect Caused by Predominant Homochiral Dimer Contribution. *J. Am. Chem. Soc.* **2006**, *128*, 3904-3905.

(11) (a) Polynski, M. V.; Ananikov, V. P. Modeling Key Pathways Proposed for the Formation and Evolution of "Cocktail"-Type Systems in Pd-Catalyzed Reactions Involving ArX Reagents. *ACS Catal.* **2019**, *9*, 3991-4005; (b) Carrow, B. P.; Hartwig, J. F. Ligandless, Anionic, Arylpalladium Halide Intermediates in the Heck Reaction. *J. Am. Chem. Soc.* **2010**, *132*, 79-81; (c) Kolter, M.; Böck, K.; Karaghiosoff, K.; Koszinowski, K. Anionic Palladium(0) and Palladium(II) Ate Complexes. *Angew. Chem., Int. Ed.* **2017**, *56*, 13244-13248.